Tomato Shade Avoidance: Unraveling Internode Elongation and Hormonal Harmony

Linge Li

Tomato Shade Avoidance: Unraveling Internode Elongation and Hormonal Harmony

Linge Li

ISBN: 978-94-6483-864-0
Cover design: Youyang Hu huyyoo@outlook.com
Lay-out design: Parntawan | www.ridderprint.nl
Print: Ridderprint | www.ridderprint.nl

Tomato Shade Avoidance

Unraveling Internode Elongation and Hormonal Harmony

Het ontwijken van schaduw in tomaten planten: Het ontrafelen van de hormonale regulatie achter de strekking van stengels
(met een samenvatting in het Nederlands)

番茄的避阴反应：探索节间伸长和激素协调的奥秘
（内附中文摘要）

Proefschrift

ter verkrijging van de graad van doctor aan de
Universiteit Utrecht
op gezag van de
rector magnificus, prof. dr. H.R.B.M. Kummeling,
ingevolge het besluit van het college voor promoties
in het openbaar te verdedigen op

woensdag 27 maart 2024 des ochtends te 10.15 uur

door

Linge Li

geboren op 12 november 1993
te Province Liaoning, City Dalian, China

Promotor:
Prof. dr. R. Pierik

Copromotor:
Dr. K. Kajala

Beoordelingscommissie:
Dr. R.B. Karlova
Prof. dr. R. Offringa
Prof. dr. ir. C.M.J. Pieterse
Prof. dr. I. Rieu
Prof. dr. R. Sasidharan

Dit proefschrift werd (mede) mogelijk gemaakt met financiële steun van China Scholarship Council (CSC)(No.201807720067).

TABLE OF CONTENTS

GENERAL INTRODUCTION

This PhD thesis reports studies on the effects of supplemental far-red light on tomato growth and development. The background information for the research questions examined in the coming chapters will be provided in this introductory chapter. This introduction provides an overview of the historical significance and cultivation practices of the model plant, tomato. It subsequently draws a comparison between two model tomato cultivars. The narrative then introduces the key phenotypes in the shade avoidance response, shedding light on how these responses are regulated by photoreceptors. The intricate interplay of hormones in shade avoidance is then explored. Lastly, the discussion delves into the involvement of stem structure in the study of shade avoidance.

1.1 TOMATO

1.1.1 History of tomato cultivation

Tomato (*Solanum lycopersicum*) has a unique position in the botanical and culinary realms, tracing its origins to western South America, Mexico, and Central America (Naika et al., 2005). The journey of this versatile fruit, commonly recognized as a vegetable in culinary usage, spans centuries and continents, leaving an indelible mark on global agriculture.

With its botanical roots firmly embedded in the Andes region of South America, the tomato found its way into human cultivation and culinary practices through the ingenious efforts of indigenous people in Mexico (Naika et al., 2005). These early cultivators recognized the potential of this fruit, and it became an integral part of their cuisine long before the arrival of Spanish explorers. The transformative encounter between the Spanish conquistadors and the Aztec Empire during the 16th century brought the tomato to Europe as part of the monumental Columbian exchange. The culinary traditions of Europe were forever altered by this novel addition, as tomatoes found their place in a wide array of dishes, sauces, and culinary concoctions (Musselman, 2002; 2005).

Despite its fruit classification from a botanical standpoint, the tomato is predominantly utilized as a vegetable in culinary applications. Its rich umami flavour profile, when consumed raw or cooked, lends itself to an extensive range of culinary creations worldwide. From fresh salads to hearty sauces and refreshing beverages, the tomato continues to captivate the global dinning plates (Musselman, 2002).

Today, tomato production remains a vital component of global agriculture, with diverse varieties cultivated in temperate climates across continents but still reach a 39.2 million metric Ton (Dillon, 2022). For the reason that tomato is a crop with low maintenance and

high yield, and also a short life cycle, the economic value makes growing it attractive to breeders and farmers (Naika et al., 2005). Advancements in greenhouse technology enable year-round cultivation, making tomatoes an accessible crop regardless of season. The plant's growth characteristics, such as its sprawling vine-like nature and support requirements, further contribute to its cultivation practices.

1.1.2 Tomato growth habit

Tomato (*Solanum lycopersicum*) is a highly versatile plant that reaches impressive heights exceeding two meters. With careful maintenance, tomato plants can be harvested consecutively for multiple years, offering prolonged productivity. The first harvest typically occurs within a span of 45-55 days after flowering (Naika et al., 2005). In our experimental set-up, tomatoes flower at 35-42 days. Among the diverse tomato cultivars, two main categories can be distinguished: cultivars for fresh consumption and cultivars for processing. We selected a cultivar from each category as our experimental models, Moneymaker (MM) and M82, respectively.

Moneymaker stands out as an exceptional greenhouse variety renowned for its abundant yield, delightful bright red fruits, and smooth texture, making it an ideal choice for fresh consumption. This particular cultivar thrives in hot and humid climates, demonstrating its adaptability both outdoors and within greenhouse environments. MM, while not a current choice for large-scale greenhouse farming due to the availability of more modern varieties in recent years, it still remains a greenhouse variety favored by home gardeners. Originating from England, Moneymaker exhibits vigorous vine growth, necessitating proper staking to optimize results (Marks, 2010). M82 is a processing tomato, suited for field growth and machine harvest. M82 plants typically reach a height of 1.5 to 2 meters and have a bushy growth habit. The fruits are typically red when fully ripe, with a smooth skin and a juicy, flavorful flesh but comparing to MM, the fruits are less oval.

In our greenhouse set-up, we noticed M82 and Moneymaker (MM) have very similar life cycle and flowering time within 5-6 weeks, similar height with around 1.5 m. To distinguish these two species (Figure 1.1), we can use the first true leaf. The first true leaf of M82 and MM has a distinguishable pattern as shown in Figure 1.2. M82 usually has smaller main leaf lamina more similar to a simple leaf, whereas MM has a leaf pattern more similar to later true leaves with clear separation of each leaflet.

1.1.3 Tomato genomic resources

Recent advances in genomic research have significantly contributed to our understanding of the tomato species. The initial tomato genome was derived from the Heinz cultivar (Sato et al., 2012). Leveraging the existing *S. lycopersicum* cv. Heinz genome as a reference, and with extensive sequencing, and incorporating additional single-nucleotide polymorphisms (SNPs), this ultimately culminated in the final M82 genome (Bolger et al., 2014). Notably, the genome of *Solanum lycopersicum* cv. M82 was meticulously sequenced in conjunction with the *Solanum pennellii* genome, The 950-Mb tomato genome exhibits a distinct structure, comprising gene-rich euchromatin and gene-poor pericentromeric heterochromatin (Michaelson et al., 1991; Barone et al., 2008). Given the challenge of sequencing the heterochromatic fraction with its repetitive sequences, the initial strategy focused on sequencing the euchromatic portion, estimated to constitute one-quarter (220 Mb) of the tomato genomic sequence, encompassing over 90% of the genes. Various tools have been developed for the Tomato Genome Sequencing Project, (Sherman and Stack, 1995; Todesco et al., 2008; Mueller et al., 2009; Sato et al., 2012; Bolger et al., 2014). *S. lycopersicum* cv. M82's genetic information has provided valuable insights into the molecular mechanisms underlying various traits in tomatoes. M82 tomatoes are widely used in comparison to *S. pennellii* in drought resistance study, fruit development, and genetic comparison in stress (Gong et al., 2010; Ikeda et al., 2017; Liu et al., 2018; Reynoso et al., 2019; Watanabe et al., 2021). For example, the wild tomato relative *Solanum pennellii* shows a strong response to shade and in contrast, the domestic tomato *S. lycopersicum*, which has been bred for production in field conditions, shows a milder response (Bush et al., 2015). However, the Shade Avoidance Syndrome (SAS) mechanisms within the different tomato species are not fully characterized, and we set out to explore the significant changes of commercial tomato plants in stem elongation.

1.1.4 Summary

Tomato is an economically important crop, renowned as a well-established stress study model and offers distinctive genetic resources. Despite not having received the same level of attention as Arabidopsis, recent research has delved into the molecular and physiological aspects of SAS in tomato. The uniqueness of tomatoes, with their specific growth patterns, hormonal dynamics, and stem structures, using tomato as a model adds an intriguing layer to our understanding of adaptive strategies under varied light conditions.

Figure 1.1. Model plants of M82 (left) vs Moneymaker (right).

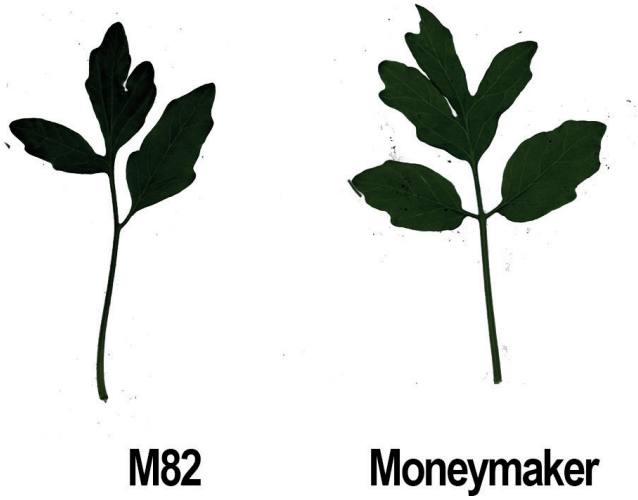

Figure 1.2. Examples of first true leaves of M82 vs Moneymaker.

1.2 SHADE AVOIDANCE RESPONSE

The shade avoidance syndrome (SAS) is a plant's acclimation reaction to changes in light that signal impending shade. SAS describes a suite of morphological and physiological changes that occur when plants perceive neighbours, typically through a reduction in the ratio of red: far-red (R:FR) light caused by reflection of far-red light from neighbouring leaves (Smith and Whitelam, 1997). Common shade avoidance responses include hyponasty (upward leaf movement), petiole elongation, stem elongation, and accelerated flowering time (Woodward and Bartel, 2005). Studying SAS unveils crucial insights into plant growth strategies with implications for agriculture and horticulture.

1.2.1. Shade avoidance and neighbour detection for farming

Light serves as a fundamental driver of plant growth and development, fuelling photosynthesis, through which plants convert light energy into chemical energy. Plants engage in a struggle for light and adapt their growth patterns to secure optimal light capture in the future. The quality and quantity of light received by plants exert a profound influence on various physiological and developmental processes, including seed germination, stem elongation, leaf development, flowering, and tuber formation. SAS enables plants to elongate stems and adjust leaf angles in an attempt to maximize light capture and mitigate the negative effects of shading (Pantazopoulou et al., 2017). Of particular importance is the ratio of red to far-red (R:FR) light (Osborne, 1991; Franklin, 2008; Ballaré and Pierik, 2017), which acts as a crucial signaling mechanism, conveying information about neighbouring plants and redirecting resource availability into growth, for example, at the cost of seed production (Smith and Whitelam, 1997; Hewitt, 1998; Yang and Li, 2017).

Smallholder farmers worldwide often confront common challenges, including constraints on resources, food insecurity, and heightened vulnerability to the impacts of climate change. These issues have been reported in various regions, such as Sub-Saharan Africa (Ariom et al., 2022), South Asia (Cerling et al., 1997), Southeast Asia (Nor Diana et al., 2022), and East Africa (Ndoli, 2018). In these areas, the reduction of fallow periods or continuous cropping practices, driven by population pressure, has led to soil erosion, diminished soil organic matter, and nutrient depletion without adequate replenishment. Consequently, agricultural productivity has been negatively affected, exacerbating the problem of food shortages. Addressing these challenges necessitates the adoption of sustainable agricultural practices and innovative solutions that consider the shade avoidance responses of crops to ensure the resilience and well-being of smallholder farmers globally.

1.2.2 Shade signal detection

Canopies formed by plants typically have decreased photosynthetically active radiation (PAR) compared to direct sunlight. Therefore, many plants will adjust their photosynthetic activity and growth (Lichtenthaler et al., 1981; Casal, 2013). Plants absorb photosynthetically active wavelengths (380 nm – 750 nm), including red (R) light (750 nm) and blue (B) light (450 nm). They hardly absorb far-red light (FR, >750 nm) light, and hence the reflected and transmitted light is enriched in FR wavelengths (Figure 1.3). In a situation where there are multiple plants in dense vegetation, FR light

will be reflected whereas the red light will be absorbed, increasing the amount of FR light in the canopy relative to other wavelengths, especially red (R). This difference in the light spectrum is detected by the plant, enabling it to perceive their neighbours and (impending) shade (Beall et al., 1996). In short, the shade consists of light spectrum change and lower light level, and in our experiments, we particularly focus on the signals perceived by plants through low R:FR light ratios.

In order to outcompete the neighbouring plants, shade-avoiding plants will adopt the SAS (Ballaré and Pierik, 2017), which involves a number of phenotypic changes that generally make the plant taller and more erect. One of the most significant phenotypic SAS changes observed is stem and petiole elongation. This phenomenon was originally identified to be associated with far-red light transmission in tobacco canopies in the 1970s (Kasperbauer, 1971): the stem elongated more with a lower R:FR light ratio in the canopy than in the daylight. This phenomenon has been observed in many species. For example, in Arabidopsis, both hypocotyl and petiole elongate (Reed et al., 1993; Devlin et al., 1996) and the elongation of the petiole can be induced especially by an end-of-day FR light treatment (Reed et al., 1993). In Arabidopsis, petiole elongation can also be induced by far-red treatment to the leaf tip only (Pantazopoulou et al., 2017). In *Brassica rapa*, FR light sensing in the cotyledon leads to the elongation of the hypocotyl (Procko et al., 2014). In tomato, significant stem elongation and leaf architecture differences have been observed (Chitwood et al., 2015; Maloof, 2015). Suppression of branching was also found in tomato (cv. Amberley Cross) by end-of-day FR-treatment (Tucker, 1975). In soybean (*Glycine max*), far-red light perceived on nodes can reduce the fruit production on the very same branch (Green-Tracewicz et al., 2011).

Plants detect light with various molecules. Photoreceptors are specialized proteins that absorb specific wavelengths of light, enabling plants to sense changes in light quality and quantity. Cryptochromes respond to blue and ultraviolet-A light and are involved in regulating plant growth, circadian rhythms, and photoperiodic flowering (Lin, 2002). Phototropins perceive blue light and are responsible for phototropism (bending toward light) and stomatal opening (Briggs and Christie, 2002). UVR8 is a photoreceptor that detects ultraviolet-B (UV-B) light and mediates UV-B responses, such as stress protection and regulation of pigmentation (Jenkins, 2017). Phytochromes detect red and far-red light and are involved in various processes such as seed germination, shade avoidance, and flowering (Reed et al., 1994). Phytochromes are 120-kD soluble proteins that have a covalently linked linear tetrapyrrole chromophore. They exist in two photointerconvertible forms, Pr and Pfr. Pr is the red light-absorbing form, which can be

converted to Pfr (the far-red light-absorbing form) by the red light. Pfr is the active form of phytochrome, and can be converted back to Pr by far-red light. Consequently, red light-induced positive phototropism mediated by phytochromes are typically reversible by far-red light (Reed et al., 1993; Kiss et al., 2003). Among all the phytochromes, phyB is essential for mediating SAS (Taiz et al., 2010); phyA can be activated by far-red light and therefore can antagonize phyB-meditated responses in light-grown seedlings (Sheerin and Hiltbrunner, 2017).

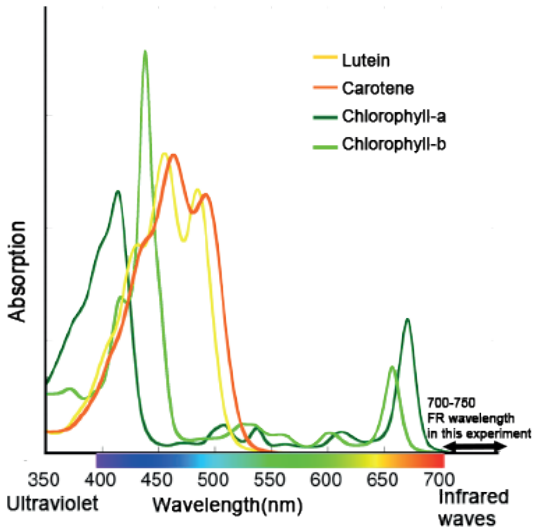

Figure 1.3. Light absorption graph of pigments in plants, adapted from literature (Glenn, 2022; Domenici et al., 2014).

The molecular changes accompanying this photoconversion have a significant impact on signal transduction pathways, leading to adjustments in developmental responses based on the prevailing light environment (Bischoff et al., 2001). In the presence of sunlight, phytochrome becomes active and translocates from the cytosol into the nucleus. Within the nucleus, it interacts with PHYTOCHROME INTERACTING FACTORS (PIFs) and facilitates their inactivation and degradation. PIFs are growth-promoting factors involved in various physiological processes (Shin et al., 1997; Ruberti et al., 2012; Yang and Li, 2017). The family of basic helix-loop-helix (bHLH) transcription factors, which PIFs belong to, serves as the central hub in a signaling cascade that promotes cell elongation. These bHLH factors play a crucial role in coordinating and regulating the processes involved in cell elongation (Oh et al., 2014). In response to low R:FR light conditions, the active pool of phytochrome decreases, leading to the

accumulation of specific phytochrome-interacting factors (PIFs) such as PIF4, PIF5, and PIF7. These PIFs activate growth-promoting genes containing E-box and G-box motifs. This activation stimulates various processes involved in the biosynthesis and transport of important plant hormones like auxin, gibberellins, brassinosteroids, cytokinins, and ethylene (Ueoka-Nakanishi et al., 2011; Casal, 2012; Ruberti et al., 2012; Pantazopoulou et al., 2017; Küpers et al., 2018). Specifically, auxin modulates cell wall remodeling and cell elongation via regulation of expansins and xyloglucan endotransglucosylase/hydrolases (XTHs) (Fry, 2004; Sasidharan et al., 2010; Sasidharan et al., 2014; de Wit et al., 2015).

1.2.3 Phenotypic response in shade avoidance

1.2.3.1 Hyponasty

Hyponasty is the upward bending of leaves or petioles. Hyponastic growth allows plants to reorient their leaves towards available light sources, thereby enhancing light interception and photosynthetic efficiency (Pierik and De Wit, 2014; Pantazopoulou et al., 2017). In recent years, extensive research has shed light on the molecular and physiological mechanisms underlying hyponasty in Arabidopsis in the context of shade avoidance.

Studies have revealed the central role of phytohormones, particularly auxins, in regulating hyponasty. Auxins act as key signaling molecules: they are synthesized in the leaf blade in response to FR and transported into the petiole where they induce a hyponastic response specifically localized to the leaf perceiving the FR signal (Michaud et al., 2017). Auxins promote cell elongation and influence the directionality of leaf and petiole bending in response to shade-induced stress (Yang and Li, 2017). The dynamic changes in auxin distribution and transport, mediated by the auxin efflux carriers and signaling pathways, orchestrate the precise adjustments in cell expansion and tissue growth required for hyponasty. The involvement of other phytohormones such as gibberellins and brassinosteroids has been recognized in modulating hyponastic responses. The interplay between these enable plants to fine-tune their growth patterns and optimize resource allocation in response to shade conditions (Bou-Torrent et al., 2014; Pantazopoulou et al., 2017; Yang and Li, 2017; Küpers et al., 2018; Küpers et al., 2023).

1.2.3.2 Elongation

When plants are subjected to shading conditions, they exhibit a remarkable ability to elongate their stems, petioles, and hypocotyls to reach and capture more light with their leaves.

In Arabidopsis, shade-induced elongation is regulated by a complex interplay of hormonal signaling pathways. Elongation of the petiole in Arabidopsis involves multiple hormone signaling pathways, including gibberellins, auxins, brassinosteroids, and ethylene. These hormones collectively coordinate cell division, cell elongation, and cell wall modifications to promote elongation in response to shading (Djakovic-Petrovic et al., 2007; Müller-Moulé et al., 2016). Similarly, in tomato, stems elongate in SAS (Figure 1.4) and this process potentially involves key regulators such as gibberellins, auxins, and ethylene, which are have been implicated to play a role (Courbier et al., 2021). Low red/far-red ratios (R:FR) stimulate stem growth-related gene expression and concurrently reduce the expression of genes associated with flavonoid synthesis, isoprenoid metabolism, and photosynthesis. This results in decreased levels of flavonoids and isoprenoid derivatives, alongside a reduction in stem jasmonate levels and photosynthetic capacity. While this model partially explains shade-avoidance responses, further understanding of the complex links between shade and auxin networks is needed. (Cagnola et al., 2012; Iglesias et al., 2018; Schrager-Lavelle et al., 2019; Courbier et al., 2021). However, the intricacies of shade-induced elongation in tomato, particularly the specific molecular mechanisms and signaling components, remain areas that require further investigation.

Other dicot plants, such as soybean (*Glycine max*) and sunflower (*Helianthus annuus*) also display significant elongation responses in SAS response to shade cues (Green-Tracewicz et al., 2011; Page et al., 2011; Tang and Liesche, 2017; Lyu et al., 2021). The underlying hormonal and molecular mechanisms regulating elongation in these plants are similar to those observed in tomato and Arabidopsis and involve gibberellin and auxin.

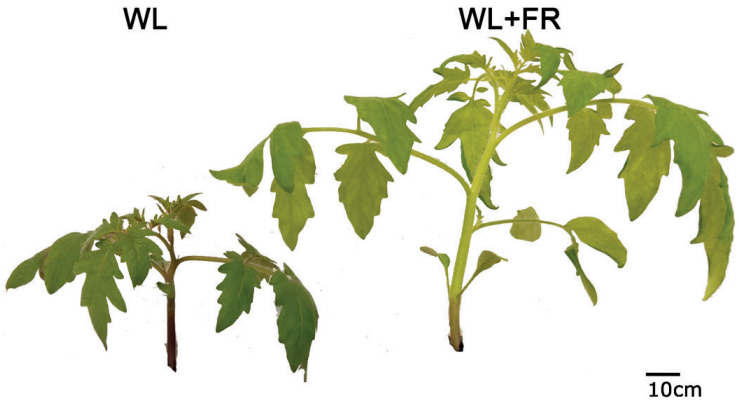

Figure 1.4. Shade avoidance response leads to a significant elongation response in tomato. Comparison of 21-day-old Moneymaker plants grown in white light (WL) vs far-red light treatment (WL+FR) for 14 days.

1.2.3.3 Leaf morphology

In Arabidopsis, research has been done on lamina blade traits in rosette stage of development. Far-red light signals lead to a blade area reduction coupled with curling (Reed et al., 1993; Devlin et al., 1999; Cagnola et al., 2012). Chitwood and colleagues performed a meta-analysis on the morphological consequences of short-term or long-term exposure to shade in tomato (Chitwood et al., 2012; Chitwood et al., 2015). They found that leaf area, stomatal density, and chlorophyll abundance were changed in shade, and that alteration of leaf shape under shade is dictated by the expression of *KNOX* and other indeterminacy genes in tomato (Chitwood et al., 2012; Chitwood et al., 2015). A SAS study in maize *(Zea mays)* indicated that decline in biomass and leaf area growth during competition against weeds are likely occurring via low R:FR signaling from weeds to maize (Page et al., 2009). Woody species such as *Populus, Acer,* and *Betula* had faster growth rates in response to supplemental FR if they were late succession species in comparison to early succession species (weedy, fugitive) (Gilbert et al., 2001). In densely populated communities, the competition for living space among plants is influenced by leaf morphology and size within the canopy, impacting the generation of proximity signals and the ability to tolerate shade (Gilbert et al., 2001).

1.2.3.4 Root system architecture

In shade avoidance response, plants undergo significant alterations in root morphology and architecture to acclimate to low light conditions and optimize their resource acquisition. Several studies have provided insights into the root modifications observed during shade avoidance.

Shade has well-documented effects on above-ground plant tissues, yet understanding its impact on root development remains limited (Gundel et al., 2014). Applying FR-enriched light to whole seedlings is known to reduce main root length and lateral roots (LRs) (Salisbury et al., 2007; van Gelderen et al., 2018). However, the influence of shoot R:FR signaling on root development and the underlying mechanisms are unclear. Root growth is traditionally regulated by auxin transport and signalling (Bhalerao et al., 2002), with auxin playing a role in responses to various stimuli (Baster et al., 2013; Galvan-Ampudia et al., 2013; Zhang et al., 2013). It is plausible that auxin dynamics associated with shoot shade avoidance responses impact root auxin levels, thereby influencing root development. Light signalling further influences auxin transport by regulating auxin-transporter proteins (PINs), demonstrating its intricate impact on root development (Van Gelderen et al., 2018). The dynamic changes in root structure and function during shade avoidance demonstrate the plant's ability to acclimated to shaded conditions and ensure optimal resource acquisition for sustained growth and development.

Overall, phenotypic traits linked with SAS are understood in Arabidopsis while the molecular mechanisms are still being resolved. However, not all plants share the rosette growth habit of Arabidopsis. Understanding the regulation of SAS traits in alternative model plants and other dicots will advance our understanding of the SAS for various traits, and reveal how much of the signalling networks and gene regulatory pathways are shared between different species and growth habits.

1.2.4 Hormonal regulation pathways in shade avoidance

Shade avoidance regulation is widely studied in Arabidopsis and various crops, and these studies have identified a network of hormones translating light information into developmental responses (Figure 1.5). In crops, responses to shade involve altered growth patterns and physiological changes, affecting both above-ground and below-ground structures. Different tissues, such as stems, leaves, and roots, exhibit specific responses to shade conditions. Hormones, such as auxin, gibberellin and brassinosteroid. The interplay of these hormones in the network of shade avoidance responses varies among crops and tissues, contributing to the adaptability of plants to light availability.

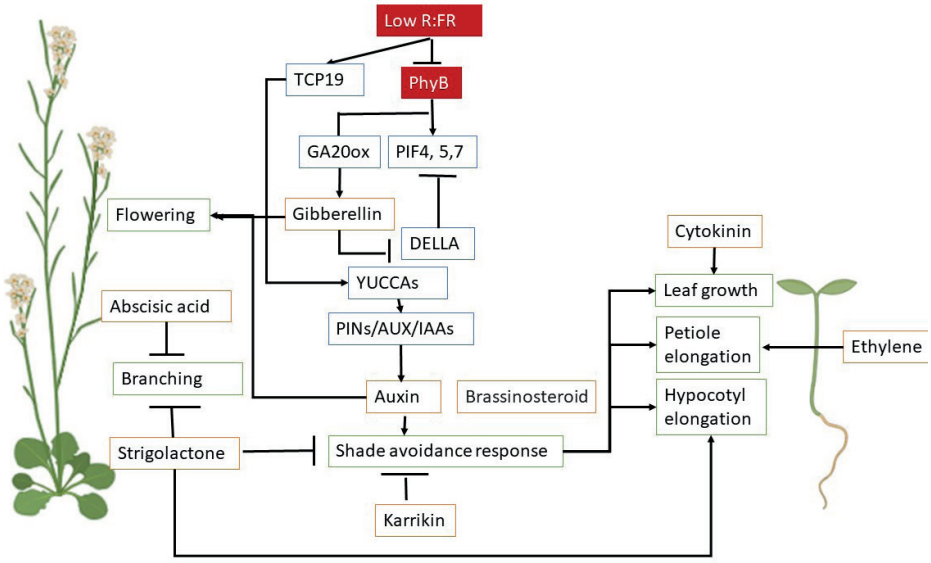

Figure 1.5. Arabidopsis SAS hormone regulation scheme adapted from literature (Yang and Li, 2017; Wang et al., 2020). Arabidopsis picture adapted from Biorender.com.

1.2.4.1 Role of Auxins in SAS

Auxins are a class of phytohormones that are essential for plant growth and development. Auxin is synthesized in the shoot apical meristem and young leaves, and transported to other parts of the plant through polar transport (Woodward and Bartel, 2005) Auxin biosynthesis is regulated by a family of genes known as *YUCCAs* (*YUC*), which encode flavin-containing monooxygenases that catalyze the rate-limiting step in auxin biosynthesis (Zhao, 2010). In Arabidopsis, there are 11 *YUC* genes, and their expression is regulated by light (Sato et al., 2015). *YUCs* have also been identified in other species such as tomato (Expósito-Rodríguez et al., 2011) and soybean (Wang et al., 2017).

Auxin signaling is mediated by a family of transcription factors, known as *AUXIN RESPONSE FACTOR*s (*ARF*s), which bind to auxin-responsive elements (AuxREs) in the promoters of target genes (Woodward and Bartel, 2005). Auxin is sensed by a family of F-box proteins known as TIR1/AFB that function as auxin receptors (Kepinski and Leyser, 2005). *ARF*s have the ability to bind tandem repeat AuxRE sequences either as homodimers, in conjunction with other *ARF*s, or in combination with repressive Aux/IAA proteins. In the absence of auxin, the function of *ARF*s is inhibited by Aux/IAA proteins, which form dimers with *ARF*s to prevent their activity (Woodward and Bartel, 2005; Li et al., 2016). Upon binding of auxin to its receptors, this complex can now interact with AUX/IAA proteins and facilitate their ubiquitination and subsequent degradation. This allows *ARF*s to homodimerize and regulate auxin-dependent gene expression.

Light-dependent interactions of cryptochrome 1 (CRY1) and phytochrome B with AUX/IAA proteins leads to the stabilization of AUX/IAAs, resulting in the inhibition of auxin signaling (Luo et al., 2018; Xu et al., 2018). When auxin levels increase, auxin binds to TIR1/AFB proteins, causing the degradation of AUX/IAA proteins and the activation of *ARF*-mediated gene expression (Stacey et al., 2016). As a consequence, hypocotyl elongation is stimulated. This elongation is also regulated by the *ARF7* and *ARF19* transcription factors, which are induced by low R:FR ratios (Nozue et al., 2015). *ARF7* and *ARF19* activate the expression of a number of downstream genes, including several encoding cell wall-modifying enzymes, which promote cell elongation (Okushima et al., 2007). It has been shown that auxin primarily acts in the hypocotyl epidermis to regulate low R:FR-induced hypocoyl elongation in Arabidopsis SAS (Keuskamp et al., 2010b; Procko et al., 2016).

Extensive investigation into auxin signaling in SAS has been conducted primarily in Arabidopsis, prompting a broader examination to assess the conservation of auxin signaling across different contexts. The role of auxin in the shade avoidance response in

legumes has been studied in several species. In soybean, for example, low R:FR condition has been shown to induce the expression of several auxin biosynthesis and transport genes, including *GmYUCCA1*, and *GmPIN1a*, thought to be involved in promoting stem elongation (Wang et al., 2017; Zhang et al., 2022).

1.2.4.2 Role of Gibberellins in SAS

Gibberellins (GAs) play a significant role in regulating the shade avoidance response in plants. Under low R:FR conditions, the accumulation of phytochrome-interacting factors (PIFs), modulate the expression of genes involved in GA biosynthesis and signaling pathways, and promote GA levels. Elevated GA levels results in a dynamic distribution of GA in organs, and further stimulate stem and petiole elongation (Djakovic-Petrovic et al., 2007; Casal, 2013; Küpers et al., 2018; Lyu et al., 2021). GA destabilizes DELLA proteins, which are suppressors of PIF action, thus providing a direct SAS modulation mechanism (Djakovic-Petrovic et al., 2007; Feng et al., 2008; De Lucas et al., 2008). Moreover, GAs are also involved in the regulation of other shade-induced responses, such as hyponasty, leaf expansion and reduced branching (Kurepin et al., 2007; Ueoka-Nakanishi et al., 2011; Küpers et al., 2023).

1.2.4.3 Role of Strigolactones in SAS

Another aspect of the shade avoidance hormonal network is the role of strigolactones, a class of plant hormones that have been shown to regulate shoot branching and plant architecture in response to environmental cues (Agusti et al., 2011; Siddiqi and Husen, 2017). In Arabidopsis, the transcription factors FAR-RED ELONGATED HYPOCOTYLS3 (FHY3) and FAR-RED IMPAIRED RESPONSE1 (FAR1), integral to phytochrome A-mediated light signaling, act with strigolactone pathway repressors, SUPPRESSORS OF MAX2 1-LIKE (SMXL6/7/8). This alliance directly inhibits SQUAMOSA PROMOTER BINDING PROTEIN-LIKE 9, 15 (SPL9 and SPL15), suppressing their activation *of BRANCHED 1* (*BRC1*), a pivotal branching repressor. FHY3 and FAR1 not only modulate SMXL6/7/8 but also directly up-regulate their expression, accentuating the central role of strigolactone in orchestrating branching. Under simulated shade conditions, reduced FHY3 accumulation results in elevated *BRC1* expression, limiting branching. This integrated model underscores how light and strigolactone intricately regulate branching through concerted actions on the *BRC1* promoter (Xie et al., 2020). Recent studies have suggested that strigolactones may also play a role in the shade avoidance response in legumes by regulating the balance between shoot and root growth (Siddiqi and Husen, 2017). In

pea (*Pisum sativum*), exposure to low R:FR conditions has been shown to increase the production of strigolactones, which in turn promote the growth of lateral roots and suppress shoot branching (Dun et al., 2013). In rice, strigolactone has been proven to promote tiller architecture (Zha et al., 2022).

1.3 STEM GROWTH

1.3.1 Comparison of stem and petiole

The stem is a support and transport organ in vascular plants. Plant stems have nodes from which they grow leaves, aerial roots, and flowers, and the sections of stem between nodes are called internodes. The conjunctive tissue that extends from the stem to the leaf lamina is the petiole (Mauseth, 2003). Petioles are generated from leaf primordium, and petiole activities are regulated by hormones and light (Sasidharan et al., 2010; Pierik and De Wit, 2014; Bravo et al., 2016). Both petioles and stem show elongation in SAS. Regarding their cellular morphology (Figure 1.6), both of them have epidermis, parenchyma and vascular bundles, and the vascular bundles in the petiole usually show multiple shapes, different from the mostly circular shape in stems (Ergen Akçin et al., 2011; Ragheb et al., 2019).

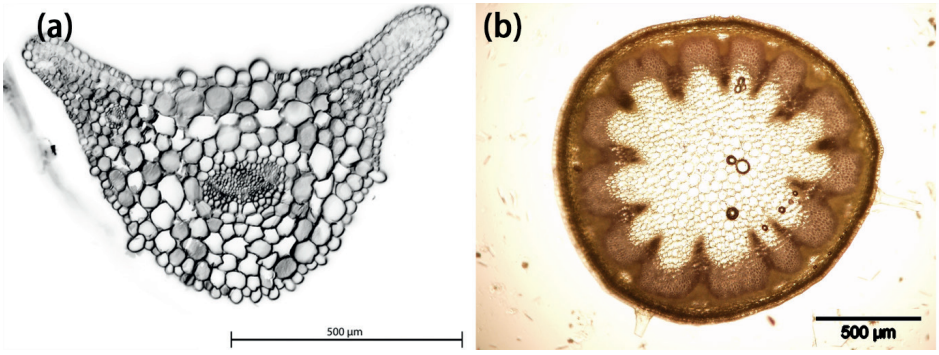

Figure 1.6. Petiole and inflorescence stem cross sections of Arabidopsis. (a) Cross section of the petiole, provided by Sanne Matton. (b) Cross section of the inflorescence stem.

1.3.2 Primary growth and secondary growth

Plant growth is categorized into primary growth, which increases the length or height of the plant, and secondary growth, which augments the plant's diameter. Secondary growth is facilitated by lateral meristems, specifically the vascular cambium and cork cambium (Etchells and Turner, 2010). The cork cambium forms the outer ring of the stem, giving

rise to phellem (cork) externally and phelloderm (secondary cortex) internally. The initiation of fibers and production of xylem indicates the start of secondary growth in hypocotyls (Taiz et al., 2010; Shana Kerr, 2017; Ragni and Greb, 2018). Vascular cambium, a closed ring of lateral meristematic tissue, is present in both roots and shoots, albeit with morphological differences. For instance, interfascicular cambium exists in shoots but is absent in roots, defined as cambium fusing to create a continuous ring in plant stems through a change in cell identity (Ragni and Greb, 2018).

In plant development, primary growth, occurring in apical meristems, propels the vertical elongation of shoots and roots, contributing to an increase in height and the development of primary tissues like the epidermis, cortex, and vascular bundles. On the other hand, secondary growth, occurring in lateral meristems such as the vascular cambium and cork cambium, leads to the thickening of stems and roots. This process adds layers of secondary xylem and phloem, contributing to wood formation in dicots and enhancing mechanical support, water transport, and nutrient distribution. While primary growth facilitates upward and downward extension, secondary growth fortifies structural strength and adaptability, collectively shaping the overall form and function of plants.

1.3.3 Tomato stem structure identification in this thesis

Tomato stems at four weeks of age are multi-layered structures that serve as a scaffold for plant growth and support (Figure 1.7). The stem consists of outer epidermis (light green layer), hypodermis (purple layer), 1-3 layers of collenchyma cells (blue-green layer), 1-3 layers of parenchyma cells (light orange layers), pith (yellow layer) and a vascular bundle and interfascicular cambium composed of tightly connected tiny cells (red layer). The outer epidermis layer provides a protective barrier against external stresses, while the hypodermis layer provides structural support to the stem. The collenchyma cells offer flexible support for the stem to grow and move, while the parenchyma cells are involved in photosynthesis, storage of water and nutrients, and transport of metabolites. The pith serves as storage tissue for water and nutrients, and the vascular bundle and interfascicular cambium provide the stem with transport tissue for water and nutrients. The tomato stem structure plays a crucial role in the overall growth and development of the plant (Esau, 1953; Evert and Esau, 2006).

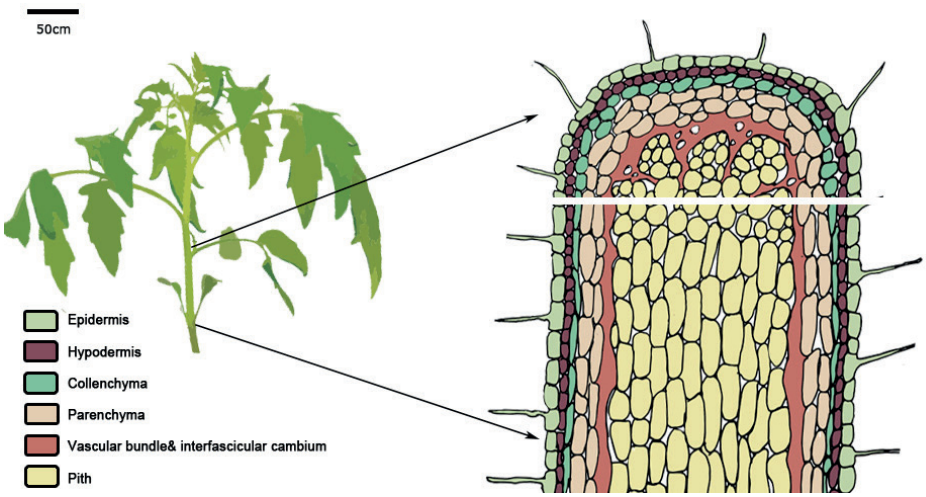

Figure 1.7. The cell types of tomato stem. The diagram shows combined cross section and longitudinal section, both taken from the middle of the first internode.

In SAS research, some attention has been on how cellular morphology changes in response to shade or low R:FR. The most well-known hypothesis is epidermal growth-control: the epidermal layer is controlled by the tension and stress coming from the expansion of the inner layers of the hypocotyl in the stage of unidirectional growth (Kutschera and Niklas, 2007; Robinson and Kuhlemeier, 2018). Epidermis cell numbers and cell length increase in the petiole in response to shade, as found in *Trifolium repens* (Huber et al., 2008). In a soybean study, pith cell elongation in particular was related to internode elongation, as well as cell division of all cell types was enhanced to result in internode elongation (Beall et al., 1996). However, there is only limited results from tomato: the cellular morphology changes of stem in SAS have not been characterized previously.

1.4 GENERAL SUMMARY AND OUTLOOKS

In this general introduction, it was discussed what are the intricate regulation networks that contribute to the regulation of plant architecture as part of SAS, and the coordination of hormone interplay in shade avoidance in multiple crop species and Arabidopsis was explored. In this thesis, we explore the shade avoidance responses of tomato and other dicots, focusing on stems and the hormonal regulation of internode elongation, involving different cell layers.

Chapter 2 of this thesis is a comprehensive phenotyping analysis of two tomato cultivars under different lighting- white light control and white light that is supplemented with far-red light as the treatment. We report various phenotypic traits, including stem and petiole length, leaf area, leaf thickness, chlorophyll content, and cellular level analysis of stem morphology using microscopy. These detailed phenotyping data form the basis for further investigations at the molecular level, focusing specifically on internode 1.

Building upon the phenotypic findings, in **Chapter 3** we delve into a molecular analysis of internode 1 using time series transcriptomics. This approach allowed for a deeper understanding of the regulatory pathways involved in early-stage elongation, preceding visible changes in plant growth. By examining gene expression patterns over time, we identified several intriguing transcription factors (TFs) including a bZIP finger TF, a *GATA* TF, and a *TCP* (*TEOSINTE BRANCHED1/CYCLOIDEA/PROLIFERATING*) TF for further exploration.

In **Chapter 4,** we unravel the roles of auxin, gibberellin and brassinosteroids in the tomato SAS. Manipulating hormone levels, we aimed to further understand the elongation and cellular changes observed under far-red enrichment. A better understanding of their contribution to SAS was obtained, shedding light on the molecular mechanisms underlying tomato responses to shading.

Expanding the investigation outwards in **Chapter 5,** our study broadened its scope to include multiple dicot species. We aimed to investigate the conservation of pith cell responses in SAS and the conservation of FR-responsiveness of our target TFs across different plants, providing insights into the evolution of this adaptive response. **Chapter 6** then brings the discoveries in the experimental chapters together for a general discussion.

Through a multidisciplinary approach encompassing phenotyping, transcriptomic analysis, hormone manipulation, and cross-species comparisons, this research thesis unravels the intricate mechanisms of shade avoidance responses in dicots beyond the usual model plant Arabidopsis. Here, we have discussed the rationale behind choosing tomato as the focal point of investigation. This choice may be underscored by the unique characteristics of tomato growth patterns and responses that deviate from established models, thus warranting dedicated exploration. Moreover, the experimental design should be contextualized within the existing gaps in knowledge, emphasizing what remains unknown, particularly in the context of the role of hormones in SAS tomato shade avoidance.

CELLULAR ANATOMY OF TOMATO STEMS IN RESPONSE TO FAR-RED LIGHT

Linge Li, Ticho Helming, Ronald Pierik, Kaisa Kajala

ABSTRACT

Food scarcity is a pressing global concern, particularly as the world's population is projected to increase. With limited agricultural land available, the demand for higher crop yields forces dense planting and intensifies competition for limited resources. One crucial resource that becomes scarce in dense canopies is light, prompting some plants to elongate to search for light and to counter shading. This adaptive behavior is known as the shade avoidance syndrome (SAS).

This study focuses on two tomato (*Solanum lycopersicum*) cultivars, M82 and Moneymaker, serving as representative models. Our investigation delves into how M82 and Moneymaker, cultivated in the field and greenhouse respectively, acclimate to light cues of shade. Our objective was to characterize the tomatoes' cellular developmental plasticity in response to far-red light, a common cue for detecting neighboring plants. We evaluated cellular phenotypic traits in white light versus far-red supplemented white light conditions that simulate shading or light reflection by green leaves. Using statistical analyses, we identified the most notable responses among the measured traits. Furthermore, we conducted microscopy-based quantification of cell types of the stem in the first internode where we had observed increased elongation under far-red treatment compared to white light. We found significant cellular anatomy responses in pith and interfascicular cambium, paving the way for an in-depth exploration of these cell types in subsequent chapters (3-5).

2.1 INTRODUCTION

With the increasing population and shortage of land area, the huge need for food, fuel, and fiber from field crops cannot be fully satisfied by current agricultural production. Hence, plants are farmed in dense vegetation to increase the yield from the available land area. However, this will not necessarily lead to an increase in yield per plant. On the contrary, dense vegetation increases plant competition for limited resources, one of which is light. When the light captured by the plant is not able to meet the growth demand, plant growth will decrease. The competition for light between neighboring plants is usually triggered by impending shade. Shade from vegetation is a light condition that is characterized by the relative enrichment of far-red (FR) light and overall low light density. FR light is already increased in canopies before true shading occurs by the reflection of light from neighboring plants, and FR enrichment alone can trigger a set of developmental responses known as the shade avoidance syndrome (SAS). Plants that face shade stress can either survive through tolerance to low light, or avoid future shade by SAS; a set of morphological changes to grow away from unfavorable growth condition (Smith and Whitelam, 1997).

Plants adapt their growth and photosynthetic activity in response to changes in light conditions, particularly the ratio of red (R) to far-red (FR) light, but also the depletion of blue light. This shift in the light spectrum, which occurs in dense plant canopies, triggers SAS in plants, most commonly making them taller and more erect. Key photoreceptors, such as phytochromes and cryptochromes, play pivotal roles in perceiving these light signals. Phytochromes exist in two forms, Pr (red-absorbing) and Pfr (far-red-absorbing), with Pfr being the active form responsible for mediating SAS. The shade-induced changes, including stem elongation and altered leaf architecture, have been observed across various plant species, such as Arabidopsis, *Brassica rapa*, and tomato (Osborne, 1991; Pierik and De Wit, 2014; Ballaré and Pierik, 2017; Courbier et al., 2021).

While stem elongation is a prominent feature of SAS, the cellular mechanisms underlying these changes have not been extensively studied in tomato. The response to shade varies among tomato species, with some showing a stronger SAS than others. Notably, *Solanum pennellii* exhibits a robust SAS, while cultivated tomato species like *Solanum lycopersicum* display a milder reaction. However, the specific SAS mechanisms within different tomato species remain less understood (Bush et al., 2015)

In SAS, both stems and petioles undergo elongation, and these tissues share similarities in function and cellular morphology. Cellular changes in response to shade, particularly in the epidermal layer, have been documented in other plant species. For instance,

epidermal cell numbers and lengths increase in response to shade, contributing to stem and petiole elongation. While these cellular responses have been observed in *Trifolium repens* and soybean (Weijschedé et al., 2008; Lyu et al., 2021), similar investigations in tomato are scarce (Courbier et al., 2021).

In this chapter, we measured various architectural traits in response to low R:FR in two commercial tomato cultivars: M82 and Moneymaker. M82 is a model for field-grown processing tomatoes. M82 has medium-sized oval fruit, originates from the USA, and has been used for many gene function studies (Brooks et al., 2014; Xu et al., 2015; Gupta and Van Eck, 2016; Kajala et al., 2021). Moneymaker is a greenhouse crop from the UK, cultivated for more than 80 years worldwide, and is a typical model for greenhouse tomatoes in research (https://www.ufseeds.com/product/moneymaker-tomato-seeds/TOMO.html; Courbier et al., 2021).As these two cultivars have differences in usage and growth environment, we chose to compare them in this study to provide a more comprehensive understanding of the SAS among tomato cultivars. After the architectural traits, we used microscopy to characterize the cellular anatomy SAS of the first internode and identified the most significantly responding cell types,

2.2 RESULTS

2.2.1 FR promotes hypocotyl length, but has no effect on root growth in tomato seedlings

In SAS studies of Arabidopsis, many responses at seedling stages are of interest, including hypocotyl elongation, hyponasty (increased leaf angle), and changes in root system architecture (Kasperbauer, 1971; Pierik et al., 2004; Bou-Torrent et al., 2014; Pantazopoulou et al., 2017; van Gelderen et al., 2018). Arabidopsis seedlings root system responds to FR enrichment with decreased lateral root density (van Gelderen et al., 2018; Kang, 2018). We wanted to see how Arabidopsis knowledge translates to a crop species, so we set out to characterize phenotypes of tomato seedlings in white light supplemented with far-red (WL+FR) compared to white light (WL) control. First, we conducted seedling characterization. We grew *S. lycopersicum* cv. Moneymaker seedlings on plates for 5 dag (days after germination) and then treated them with supplementary FR or continued with control WL for 7 days. At this point, the cotyledons had emerged but the seedlings did not yet have true leaves (Figure 2.1). We measured hypocotyl length (Figure 2.2a), primary root length (Figure 2.2b), lateral root length (Figure 2.2c), total lateral root length (Figure 2.2d), lateral root number (Figure 2.2e), and calculated the lateral root density as lateral root number divided by primary root length (Figure 2.2f).

Moneymaker hypocotyls were two times longer (1.9cm compared to 3.9 cm) in WL+FR treatment compared to WL control (Figure 2.4a). However, unlike hypocotyl elongation, main root length, lateral root length, lateral root number and density did not respond to WL+FR treatment (Figure 2.4).

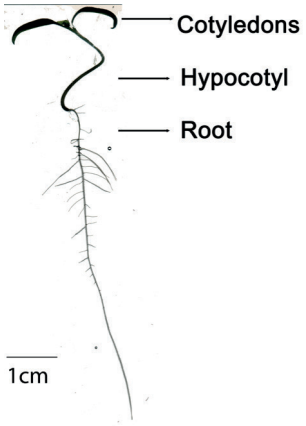

Figure 2.1. Seedling stage of Moneymaker grown on a plate for 10 days.

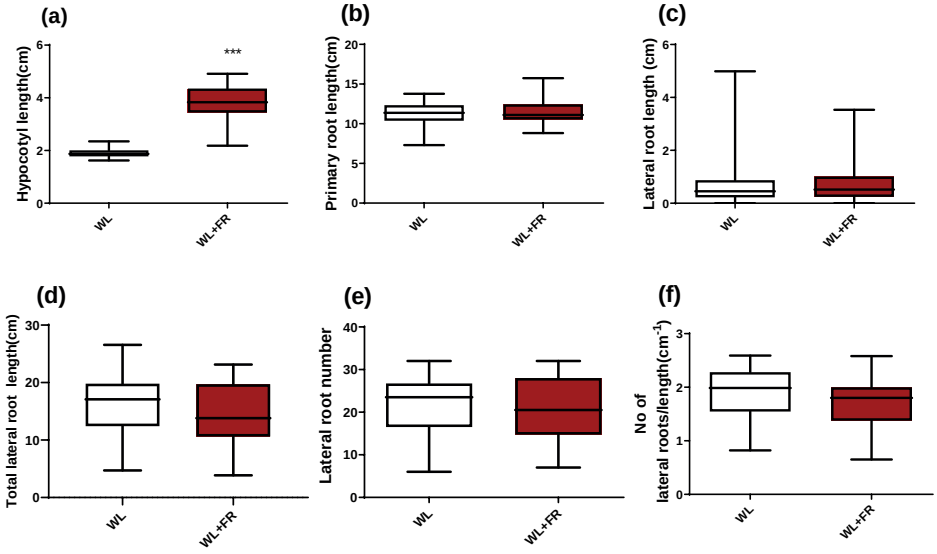

Figure 2.2. Hypocotyl and root traits in WL and WL+FR for tomato cultivar Moneymaker. Two independent biological experiments were conducted (n=15). The data includes measurements of (a) hypocotyl length, (b) primary root length, (c) lateral root length, (d) total lateral root length, (e) lateral root number and (f) lateral root density (e divided by b). Asterisks indicate significance between WL and WL+FR as follows: *** $p \leq 0.001$.

2.2.2 Stem elongates in response to FR in M82 and Moneymaker

Based on the seedling experiment, we chose to focus on shoot responses, with the intention of expanding our research to encompass tomatoes that were bred for two distinct cultivation systems, M82 and Moneymaker (MM). We wanted to conduct phenotyping on young plants to investigate more aspects of stem and leaf responses and zoom in also at the cellular level. We transplanted germinated seedlings into soil and let them recover for a week before 7-day light treatments (WL+FR or WL). We collected phenotypic data of MM and M82 at 21 dag (see Figure 2.3). In general, the stems elongated more and leaves were paler green in both cultivars when they were grown in WL+FR light as compared to WL.

Figure 2.3. Comparison of *S. lycopersicum* cultivars M82 and Moneymaker 24-day-old young plants in WL (left) vs FR+WL (right). This picture was taken at 10 days of treatment to illustrate the different phenotypes between WL and FR+WL.

We conducted shoot architecture phenotyping which included measuring the following traits: stem length, hypocotyl length, internode lengths, stem diameters, petiole lengths, rachis lengths, and leaf areas. Length and diameter measurements were taken by caliper and measured traits are shown in Figure 2.4. Leaf area was measured from scanned images using ImageJ. The major finding from the phenotyping is that FR significantly enhances stem and internode length in both varieties (Figure 2.5).

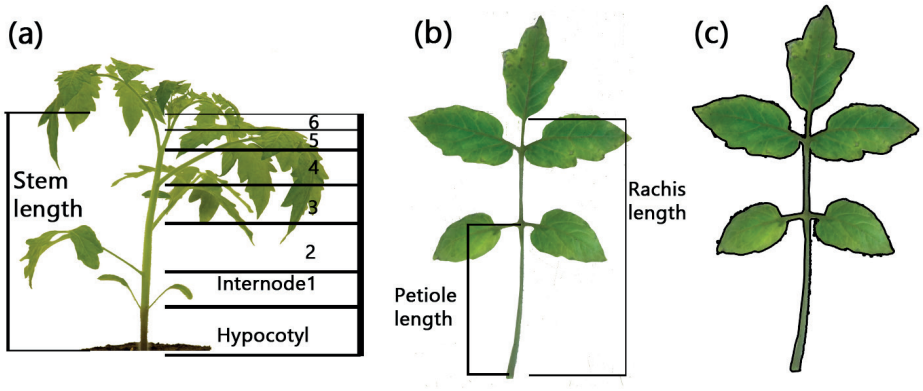

Figure 2.4. Traits measured for shoot architecture phenotyping of *S. lycopersicum* plants at 21 dag. The picture is an illustration of (a) stem length and internodes, (b) petiole length and rachis length, and (c) leaf area is highlighted in black outline.

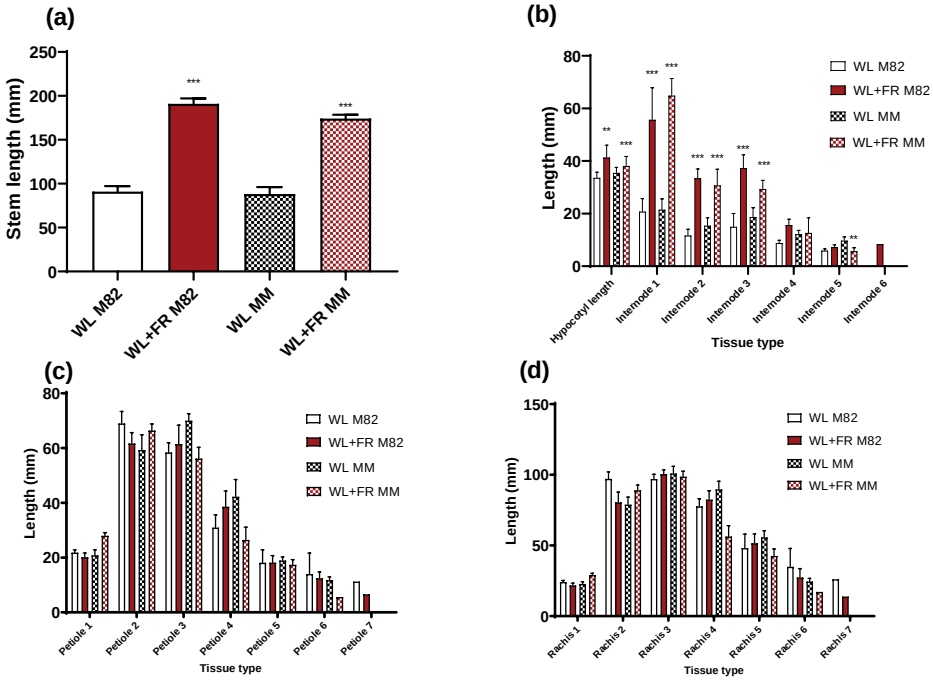

Figure 2.5. Stem and petiole lengths of three-week-old M82 and Moneymaker plants after seven-day WL and FR+WL treatments. The data include measurements of (a) stem length, (b) internode length, (c) petiole length, (d) rachis length. Asterisks indicate significance between WL and WL+FR as followed: * $p \leq 0.05$; ** $p \leq 0.01$, *** $p \leq 0.001$. Biological replicates n=18, the experiment was repeated three times.

In addition to these measurements, we also assessed stem diameter. Our observations revealed a notable increase in the diameter of internode 1 of M82 in response to FR+WL (Figure 2.6). This augmented diameter response could serve as a critical mechanism to bolster the tomato stems against potential breakage and prevent tomatoes from toppling over during rapid stem elongation. It indicates that there is not only longitudinal elongation in supplemental FR, but also radial expansion in M82, but not so much in MM.

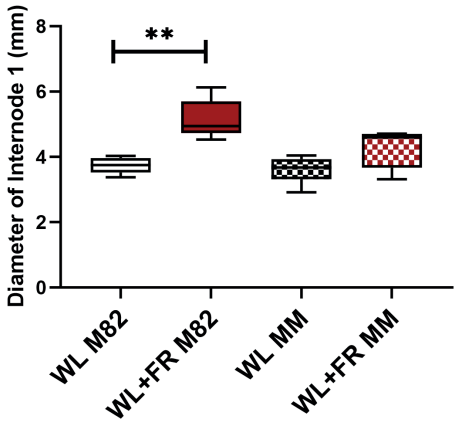

Figure 2.6. Stem diameter of internode 1 of three-week-old M82 and Moneymaker after seven-day WL and FR+WL treatments. Asterisks indicate significance between WL and WL+FR as follows: * p≤ 0.05; ** p≤0.01, *** p≤0.001. Biological replicates *n*=18, the experiment was repeated three times

In the literature, the effect of FR on leaf area is not always consistent. In Arabidopsis leaf area reduces in SAS (Keiller and Smith, 1989; Robson et al., 1993) while leaf area increases in *Trifolium repens* and tomato (Weijschedé et al., 2006; Chitwood et al., 2015). In our experiments (Figure 2.7), no obvious changes to the leaf area were observed. Building upon prior research that highlighted the pivotal role of phytochromes in redirecting carbon metabolism towards growth in Arabidopsis (Yang et al.), and given the limited knowledge about the specifics of leaf cell structural changes in tomato SAS (Courbier et al., 2021), the collection of fresh and dry leaf weights in shade avoidance experiments enables a deeper understanding of how plants adjust their resource allocation and biomass accumulation strategies in response to fluctuations in light conditions. We measured a series of leaves, starting from the bottom of the stem (oldest) to the shoot apex (youngest) through image analysis. Petiole and rachis were removed as much as possible from the image. We observed no significant responses of leaf area to WL+FR as compared to WL controls (Figure 2.7). Since the leaves looked more yellow in WL+FR than in WL, we assumed the cellular

aspects of leaflets might have changed, such as pigment composition or cellular structure. We first followed up with fresh and dry weight measurements of leaf discs of fixed area. Both the fresh weight and the dry weight decreased in response to FR in MM, with a similar trend in M82 (Figure 2.8). This indicates that the plants may have formed leaf area with reduced investment in carbon, thus making relatively cheaper leaves.

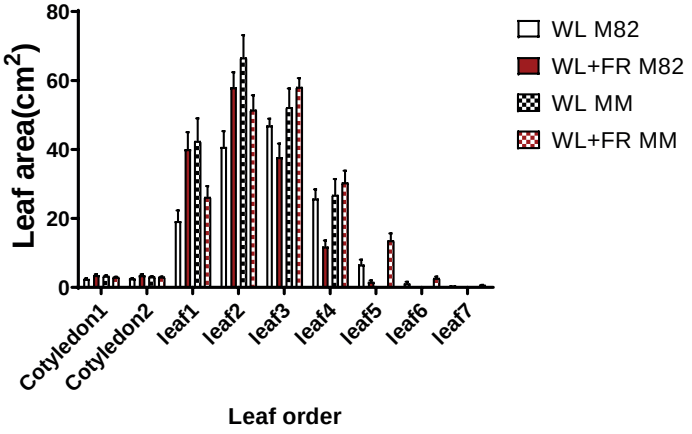

Figure 2.7. Leaf area of internode 1 of three-week-old M82 and Moneymaker after seven-day WL and FR+WL treatments. No significant differences were found by student's t-test. Biological replicates *n*=18 and experiments were repeated for 3 times.

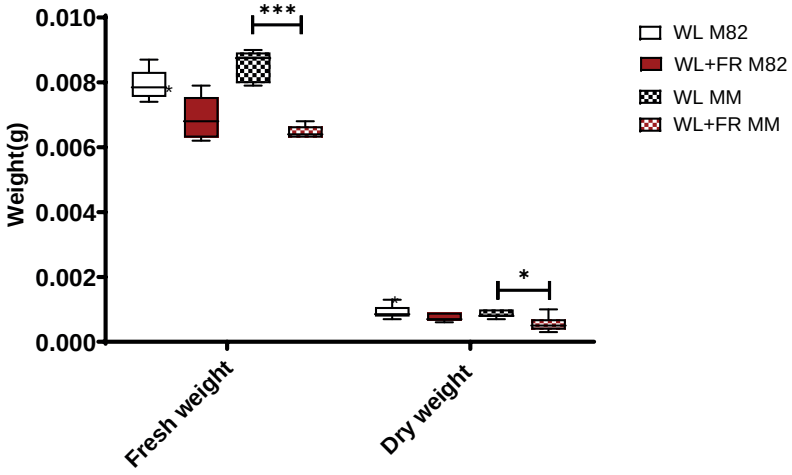

Figure 2.8. Leaf disc weight of three-week-old M82 and Moneymaker after seven-day WL and FR+WL treatments. Asterisks indicate significance between WL and WL+FR as follows: * $p \leq 0.05$; ** $p \leq 0.01$, *** $p \leq 0.001$. Biological replicates *n*=6 and experiments were repeated for 3 times.

The assessment of chlorophyll content within the context of SAS provides insights into the dynamics of a plant's photosynthetic processes and its capacity to acclimatize to fluctuations in light conditions. We carried out overall chlorophyll content measurement to quantify the leaf color changes seen in Figure 2.4. The chlorophyll content was lower in the FR treatment, which could indicate leaves acclimating to carry out less photosynthesis in shaded conditions (Figure 2.9).

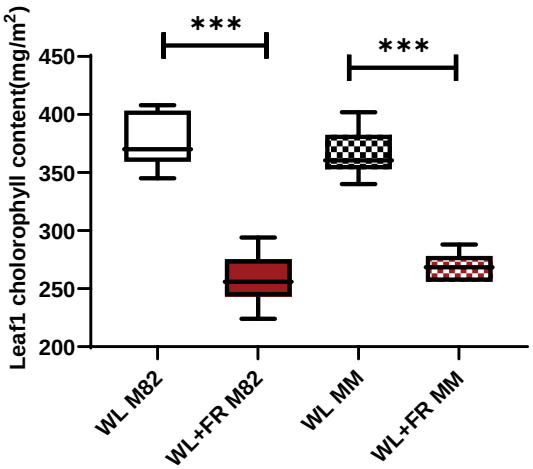

Figure 2.9. Chlorophyll content of three-week-old M82 and Moneymaker after seven-day WL and FR+WL treatments. Asterisks indicate significance between WL and WL+FR as follows: *** $p \leq 0.001$. Biological replicates $n=6$ and experiments were repeated for 3 times.

2.2.3 Stem elongation and diameter increase negatively correlated with R:FR

Since we did not see a significant internode diameter response in MM to FR enrichment, we wondered if it was due to the R:FR not being low enough at R:FR=0.28. So, we further tested R:FR ratio=0.21 and 0.11. We observed that reduced R:FR ratios could increase the internode 1 elongation and diameter thickening in MM (Figure 2.10). Also, we were able to confirm that in the FR-induced response, stem elongation and diameter increase, are positively correlated with each other (Figure 2.10).

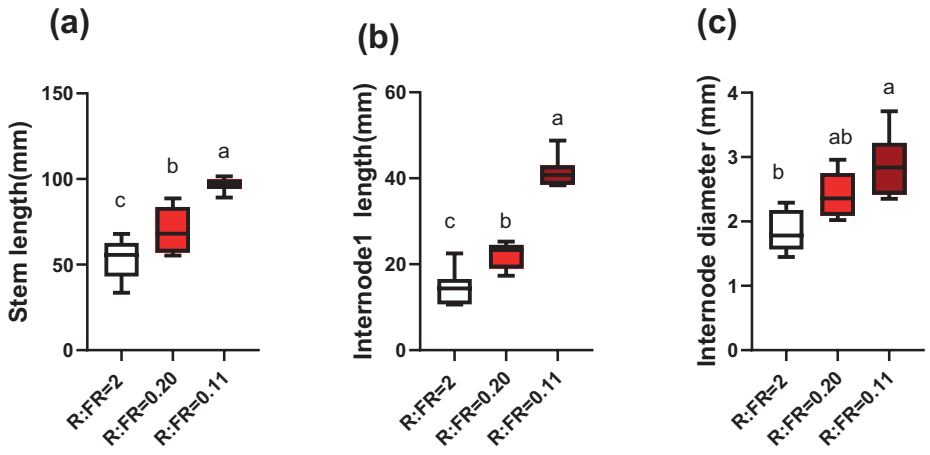

Figure 2.10. **Moneymaker responses to different R:FR ratios**. The data includes measurements of (a) stem length, (b) internode 1 length, and (c) internode 1 diameter. The data are presented as mean ± SEM, and different letters indicate significant differences between treatments based on ANOVA analysis with Tukey's post hoc test ($P<0.05$). There were 18 plants per local treatment, and the experiment was repeated three times.

2.2.4 FR induced responses in multiple cell types in the stem

We found that supplemental FR induced many phenotypic responses, and the stem elongation was the most striking one. However, how the cellular anatomy changes during the FR-induced stem elongation has not been previously fully characterized and we wanted to address this gap in knowledge. We selected the first internode for cellular anatomy phenotyping because it was the only internode that was present at the start of the FR light day treatment, 14 days after sowing, and it had the most significant response among all internodes: it had the lowest p-value and it contributed most to the elongation in stem (Figure 2.5b). We prepared cross and longitudinal sections at the halfway point of the internode. Cell types (Figure 2.11) were characterized according to the descriptions by Taiz et al. (2010) and plant anatomy website (https://www.kbg.fpvai.ukf.sk/studium_materialy/morfologia_rastlin/index.html), summarized as: 1) Epidermis: the outermost one layer of stem; 2) hypodermis: the layer beneath epidermis with a relatively similar structure as epidermis (Murray, 1983); 3) Collenchyma: the thicker, secondarily formed cell layer next to the epidermis and hypodermis; 4) Parenchyma: elongated spongy cells with regular shape between interfascicular cambium and collenchyma; 5) Interfascicular cambium: cells linking the vascular bundles with remarkably thicker cell walls; 7) Pith: big spongy and round cells in the middle of the stem. In the vasculature we measured the two main tissues: 8) Xylem: complex tissues that consists of different types of cells,

most characterized are tracheary elements and vessel; 9) Phloem: the principal sugar conducting tissue that connected to xylem. We numbered the layers of each cell type starting from the outermost layer as the first layer in the cross section. At this stage of tomato growth, there is 1 layer of epidermis, 1-3 layers of collenchyma, 1-3 layers of parenchyma, and more than 5 layers of pith. We measured cell layer numbers, cell areas, cell lengths, and cell widths to characterize cell-level anatomical responses to FR. We measured cell layer number, cell diameter, and cell area for individual cell types from cross sections, whereas cell length was measured from longitudinal sections (Figure 2.12). The xylem and phloem were characterized with a different staining method later in this chapter.

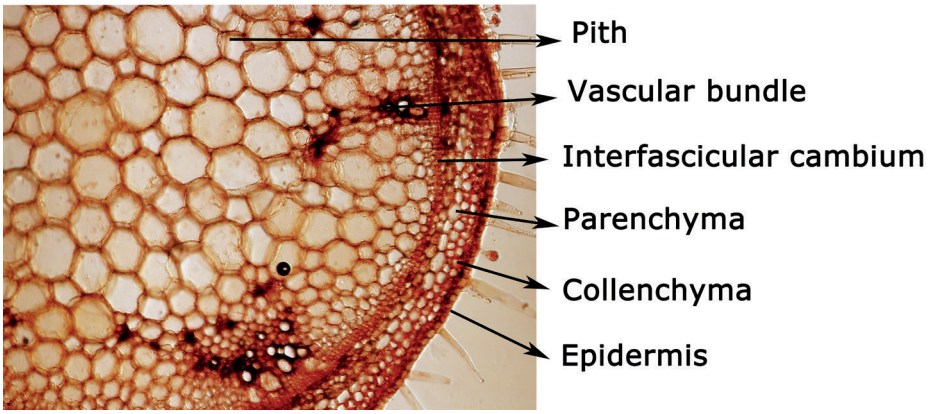

Figure 2.11. Cell types in M82 internode 1 cross section

We first tested if there was an effect of the cultivar or the treatment on the data (Figure 2.12a) and concluded that the cultivars should be treated separately for analysis. We calculated the log fold change of the traits as WL+FR divided by WL, therefore, the result above 0 indicates an increase, below 0 indicates a decrease in the heatmap we plotted with all of the parameters (Figure 2.12b). Among all the selected parameters, the ones that show significance ($p<0.05$ in WL vs WL+FR, Figure 2.12c) are Interfascicular cambium thickness, Pith layer, Middle pith length, Pith thickness, Parenchyma layer, Collenchyma layer, Collenchyma cell area and Epidermis cell length.

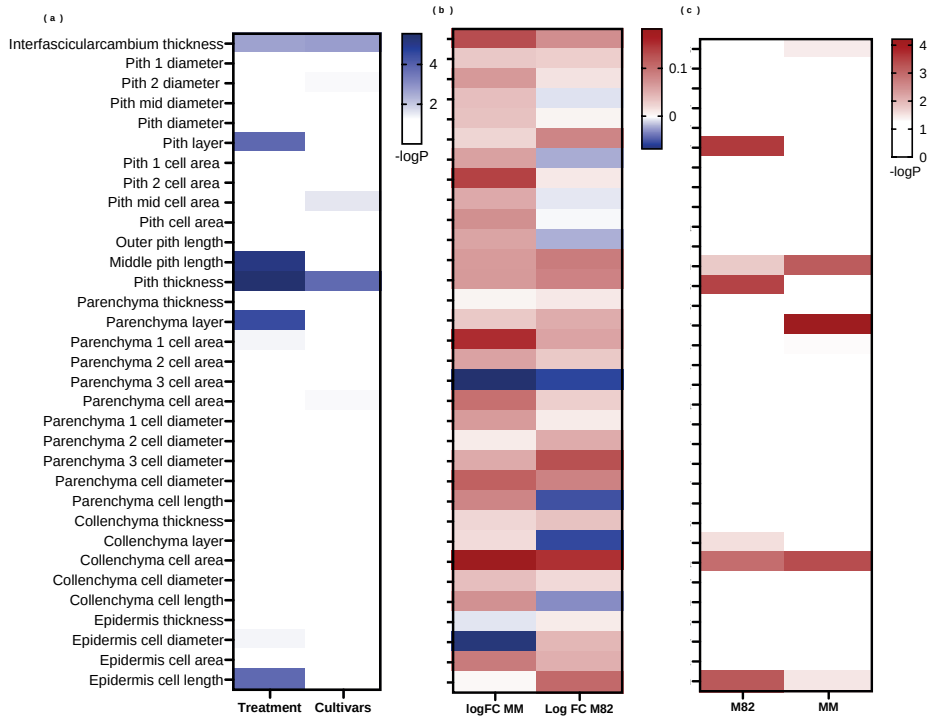

Figure 2.12. Summary of FR responses on cellular parameters characterized from internode 1 sections. (a) Significance of treatment, cultivar shown as -log p-value. (b) Logarithm of fold-change for each trait comparing FR to WL. (c) Significance of FR-responses in each cultivar shown as -log p-value for each trait. The layer number of each cell type are indicated from the outmost layer (1) moving inwards (2, 3). The interfascicular cambium thickness was measured in regions without vascular bundles. In panels (a) and (c), -log Pval=-log0.05 are set to white that indicate no significance. In panel (b), logFC=0 is set to white indicate no fold change, upregulation is indicated with red color, while down regulation is indicated by blue.

2.2.5 Interfascicular cambium thickness increases in response to FR

Vascular tissues transport water, nutrients, and hormones in the plant stems (Scarpella and Meijer, 2004; Sieburth and Deyholos, 2006). To create these transportive tissues, plant stems rely on fascicular cambium (primary meristem) and interfascicular cambium (secondary/lateral meristem), which function in generating radial growth through cell division and patterning these cells into xylem and phloem in vascular bundles of dicots (Lachaud et al., 1999; Helariutta, 2007). Interfascicular cambium is a sign of secondary growth of the stem (Parra et al., 2010). Therefore, we interpreted the interfascicular cambium thickness increase resulting from FR treatment to be an

indication of increased secondary growth in SAS (Figure 2.13) and we wanted to explore the radial growth and the cambium thickness change in more detail.

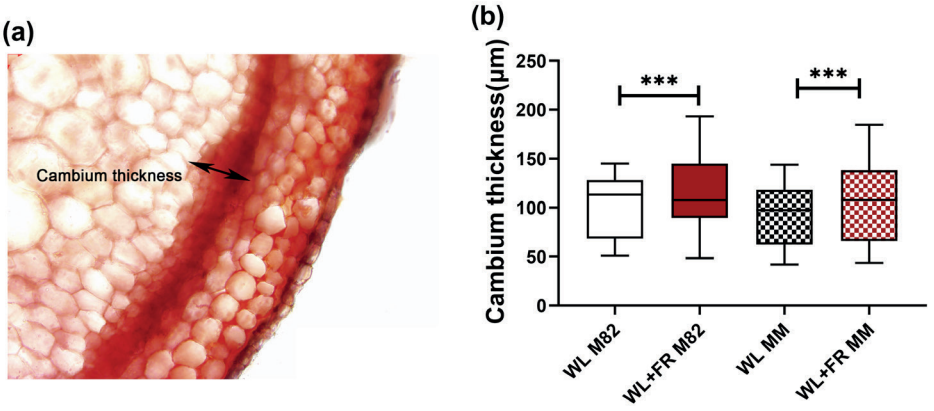

Figure 2.13. Cambium thickness in WL and WL+FR. (a) Tomato internode 1 section indicating where the measurement was taken. (b) Cambium thickness of three-week-old M82 and Moneymaker after seven-day WL and FR+WL treatments. Data are presented as mean ± SEM, Significance between WL and WL+FR is denoted by asterisks (*** $p \leq 0.001$). Error bars represent ± SE. There are 18 biological replicates, and the experiment was repeated 3 times.

In the 7-day FR treatment, both M82 and Moneymaker internode 1 developed more interfascicular cambium (Figure 2.13). This could be a sign that stem secondary growth was promoted after the FR treatment was applied. We hypothesized that the radial growth is activated by FR to provide support for the upcoming stem elongation. So, we wanted to explore the relationships of stem elongation with radial growth and interfascicular cambium thickness. We found that cambium was thicker in WL+FR in an age-dependent fashion (Figure 2.14). We compared also how internode 1 length correlated with cambium thickness with data from various time points (Figure 2.15) and tried to resolve the relationship with statistics. The regression lines show the linear linkage between internode 1 length and cambium thickness, which indicates there is a potential relationship. In the WL+FR, the stem growth was promoted as was cambium thickness compared to WL, but overall the WL+FR internodes had much thinner cambium than WL internodes of comparable length.

We had observed development of M82 and Moneymaker and seen that M82 in general grows quicker than MM in stem elongation, flowering, and aging (see Chapter 1, section 1.1.2). The increase in cambium thickness in M82 is also quicker than in Moneymaker (Figure 2.14), which reflects the cultivar-specific differences.

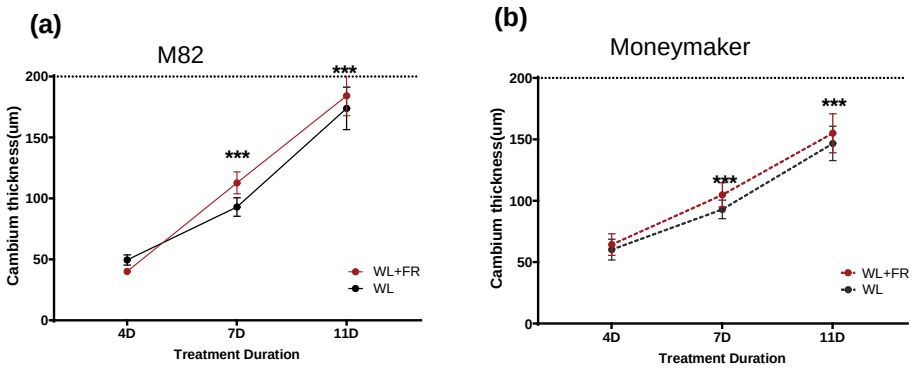

Figure 2.14. Cambium thickness of three-week-old (a) M82 and (b) Moneymaker in WL and FR+WL at different durations of treatment. Significance between WL and WL+FR is denoted by asterisks (* p≤0.05, ** p≤0.01). Error bars represent ± SE. There are 12 biological replicates, and the experiment was repeated twice.

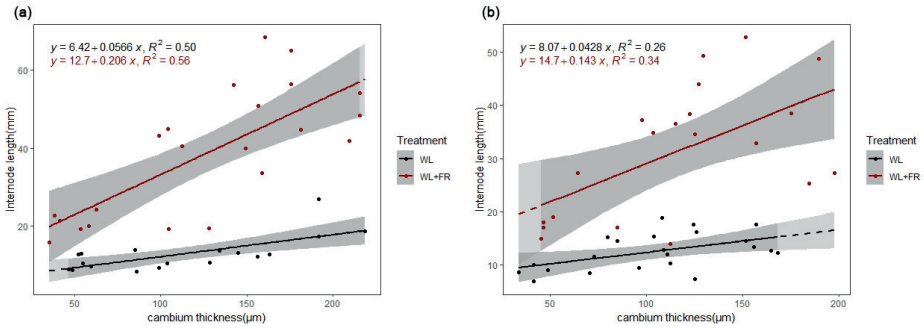

Figure 2.15. Internode 1 length against cambium thickness in (a) M82 and (b) Moneymaker. We combined phenotyping data (internode 1 length) and microscopy data (cambium thickness) from 4D, 7D and 10D FR treated 14-day-old tomatoes, and plotted the regression relationship with R.

2.2.6 Internode 1 has more pith layers and longer pith cells in FR than in WL

We measured pith cell layer number, diameter, and area from cross sections (Figure 2.16). The pith cell lengths were calculated from longitudinal sections. Figure 2.8 showed that far-red enrichment induced larger diameter in the internode 1, which could be explained by the pith (Figure 2.16) and cambium increases. Furthermore, pith layers were increased in WL+FR, but only significantly in M82 and not in Moneymaker. The ratio of pith thickness to diameter in M82 increased by 7%.

We further measured cell lengths for 60 cells per cell type in each biological replicate from five independent sets of internode samples (Figure 2.17). We found that pith cells located in the middle of the stem ("Pith-middle") elongated significantly, and so did epidermis. To follow up, we used dental paste to make imprints of the epidermis, allowing us to measure cell lengths along internode 1 (Figure 2.18). More than 200 cells were analyzed in this method. We found that MM and M82 display differences: the MM basal epidermis cells (close to the cotyledons) were not significantly different between the treatments, while all the other comparisons showed significantly increased epidermis lengths in the WL+FR.

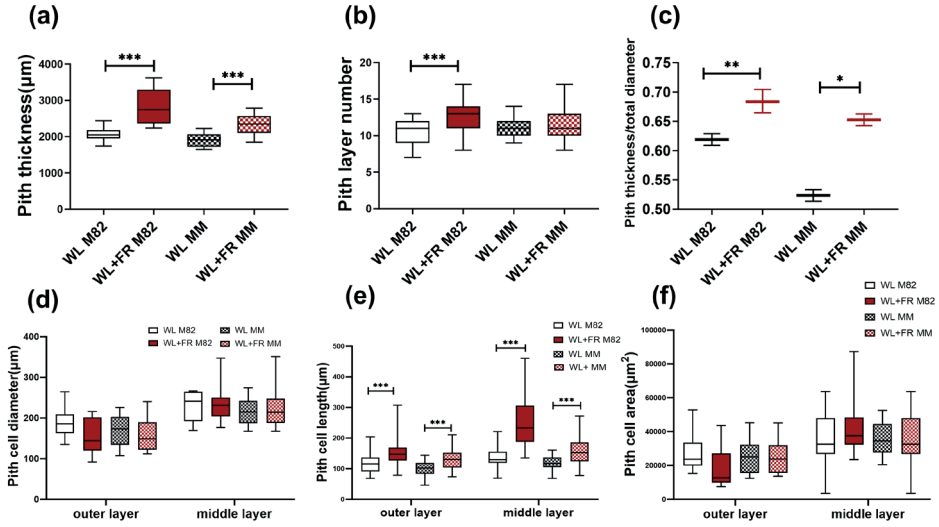

Figure 2.16. Pith cell parameters of M82 and Moneymaker in WL and WL+FR. The data includes measurements of (a) pith thickness, (b) pith layer number, (c) pith radial ratio (pith thickness divided by stem diameter), (d) pith cell diameter, (e) pith cell length, and (f) pith cell area. Data are presented as mean ± SEM, Significance between WL and WL+FR is denoted by asterisks (* $p \leq 0.05$; ** $p \leq 0.01$, *** $p \leq 0.001$). Error bars represent ± SE. There are 18 biological replicates, and the experiment was repeated 3 times.

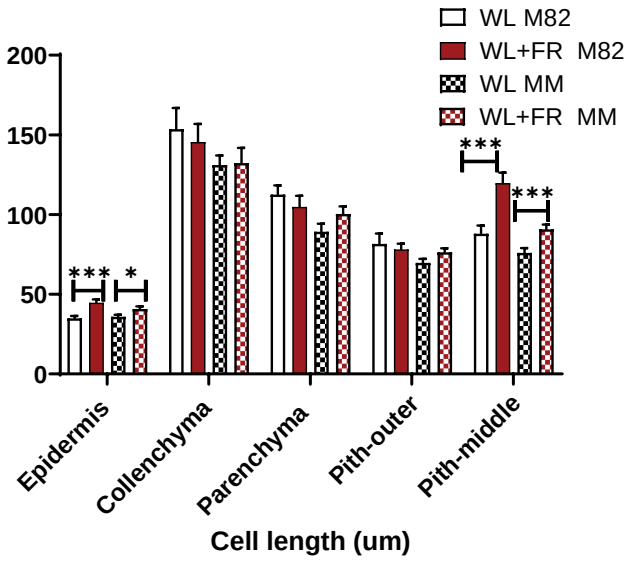

Figure 2.17. Cell lengths in M82 and Moneymaker in WL and WL+FR. Data are presented as mean ± SEM, Significance between WL and WL+FR is denoted by asterisks (* p≤ 0.05; ** p≤0.01, *** p≤0.001, **** p≤0.0001). Error bars represent ± SE. There are 18 biological replicates, and the experiment was repeated 3 times.

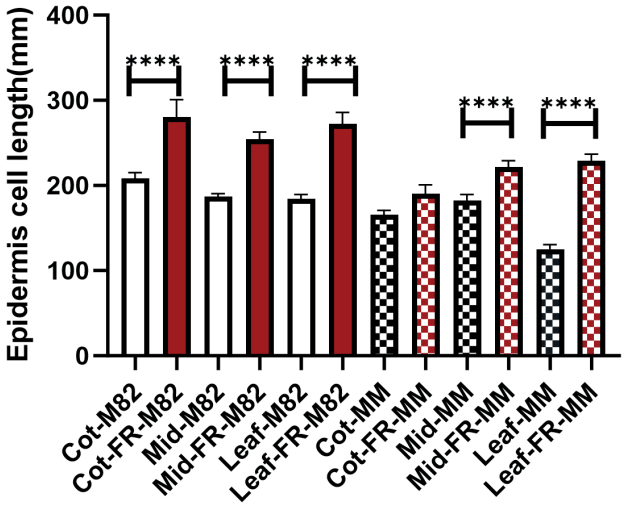

Figure 2.18. Epidermis cell lengths of M82 and Moneymaker in different locations along the internode 1 in WL and WL+FR. Cot means epidermis cell close to cotyledons, leaf means epidermis cell close to leaf 1, and mid means the cells at the mid-point of the internode 1. Asterisks indicate significant differences between WL and WL+FR as follows: * p≤ 0.05; ** p≤0.01, *** p≤0.001, **** p≤0.0001. n≈200.

2.2.7 No vascular bundle responses to FR were found

The effects of WL+FR treatment on the vascular bundle structure was also investigated. Cross sections of the stem of plants grown in WL and WL+FR were made. These sections were stained using 0.02% Toluidine and 3% Phloroglucinol and imaged using a light microscope (Figure 2.19). In both tomato cultivars, far-red enrichment did not lead to an increase or decrease in the percentage that xylem contributes to the vascular bundles (Figure 2.19).

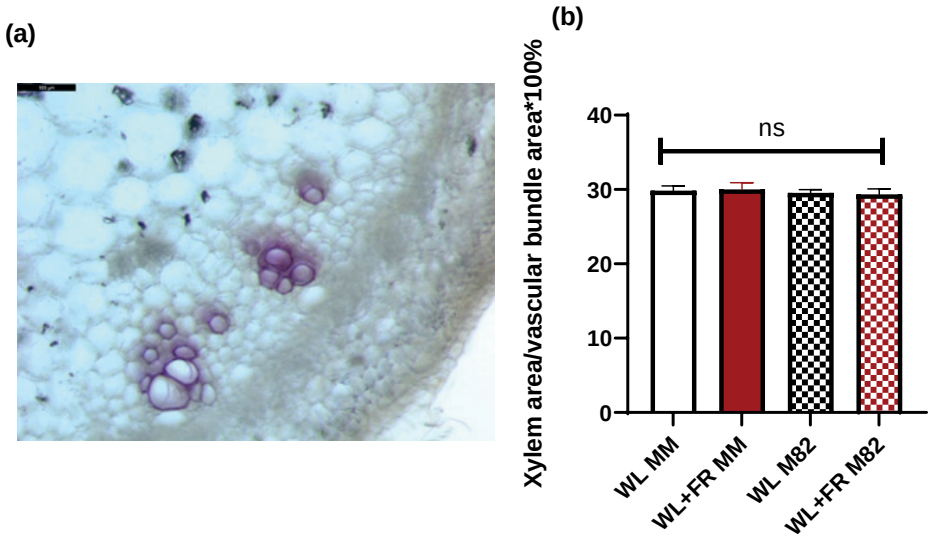

Figure 2.19. Quantification of vascular bundles of the first internode after 7D of treatment. (a) Illustration of xylem under microscopy. Xylem stains purple at the center of the bundle while the phloem cells are on the outward edge of the vascular bundle. (b) Percentage of xylem in the vascular bundles. Both tomato cultivars were treated with WL or WL+FR for 7 days. Error bars represent SEM (n=8). Different letters indicate a significant difference between means ($p < 0.05$).

2.3 DISCUSSION

Crops often develop in resource-limited environments, and one common limiting resource is light at high planting densities. The SAS (shade avoidance syndrome) is a common response, and there are many commercial crops such as raspberry, apples and corn (Maughan et al., 2017) that suffer from light shortage-related yield loss. And tomato is one of these plants. In the earlier study conducted by Bush and colleagues(Bush et al., 2015), the stem elongation phenotype was clearly observed, but a comprehensive analysis of cellular anatomy was not carried out. To address this gap,

we conducted a microscopy-based examination of internode 1 elongation at the cellular level. Our findings indicate that, during the far-red (FR)-responsive stem elongation in tomatoes, the most pronounced cellular changes involve the elongation of pith cells and the generation of pith layers. Interestingly, our cross-sectional analysis revealed no alterations in the pith cell area, indicating that pith cells expanded exclusively in the longitudinal direction. We characterised in detail the FR-induced changes on juvenile tomato plants.

2.3.1 Cultivar-specific variations in leaf area changes under low R:FR

Overall, our characterization of tomato aligns with the generally expected SAS phenotype. Previous reports on tomato SAS are limited, but a preceeding study on tomato cultivar Moneymaker in older growth stages (5-6 weeks) also demonstrated the FR-responsive stem elongation and leaf thickness changes (Courbier et al., 2021). Our phenotyping data on stem length and leaf thickness confirmed these findings. Secondly, a previous report (Bush et al., 2015) showed leaf area increases and leaf edge changes in FR. We observed a FR-responsive leaf area increase only in M82 and not Moneymaker. Therefore, leaf area response in SAS might be a cultivar-specific feature. More cultivars are needed to studied for a better conclusion of how the leaf areas change in SAS.

2.3.2 Cell elongation in SAS occurs predominantly in the pith in tomato

SAS has been characterized in great detail in Arabidopsis, with elongation phenotypes for hypocotyl and petiole that show resemblance to the response observed in tomato. Investigations into SAS have revealed a key phenomenon in Arabidopsis: XTH (XYLOGLUCAN ENDOTRANSGLUCOSYLASE/HYDROLASE) cell wall-modifying proteins play a role in relaxing the cell wall, facilitating cell expansion in response to shading (Sasidharan et al., 2010; Sasidharan et al., 2014). This process plays a pivotal role in facilitating petiole elongation under FR light (Sasidharan et al., 2010). In addition, epidermis cells of hypocotyl (18d) (Procko et al., 2016) and petiole (28d) (Pantazopoulou et al., 2017) in Arabidopsis were found to elongate in FR light treatment. However, the Arabidopsis and tomato have different tissue morphologies and growth habits. Hence, direct comparison between species is difficult. This leads us to ask the question: how do these different cell types play a role in stem elongation,

and how are these developmental changes regulated at the molecular level? What is the uniqueness of pith cell compared to the collenchyma and parenchyma? What is the similarity between pith and epidermis in cell elongation activities? We are going to further explore this questions in following chapters.

The comparison of our results to the well-charaterized Arabidopsis petiole SAS is complicated by the cell types present. The cellular morphology of Arabidopsis petiole and tomato stem are different in that petiole does not have pith cells, and the only structure of Arabidopsis containing pith cells is the inflorescence stem. Pith cells are spongy parenchyma cells, which provide support and nutrient storage for the stem and root (Abercrombie et al., 1968; Gallego-Giraldo et al., 2016; Yang et al., 2016). According to literature, the extensibility of outer layers is less than that of pith. The low water potential in the xylem has the effect of diminishing the transmission of tensile forces by compressed cells in the stem cortex to the epidermis, which is believed to be the critical cell layer for controlling extension growth. As the xylem water potential decreases, cells in the cortex undergo a reduction in turgor pressure (Brown et al., 1995a), and epidermis acts as a signal receptor to promote and restrict growth of the entire shoot (Savaldi-Goldstein and Chory, 2008). In this chapter, we show that the pith was very responsive to FR enrichment: more pith cell layers were generated and the pith cells elongated in response to FR enrichment. The epidermis cells elongated as well but less significantly compared to pith, while the other cell types in the internode 1 did not show FR-responsive elongation. Therefore, how did these cell types receive the SAS signals and mediate the SAS elongation response is worth investigation. Therefore, we continued to look into transcriptomic changes to understand the regulation of FR-responsive internode elongation in tomato.

Another thing about pith is that this tissue is not present in all dicot and monocot species. Pith conducts progressive programmed cell death in many species including tomato (Esau, 1953; Fujimoto et al., 2018). This raises many questions for us about the role of pith in in FR-responsive internode elongation. If pith elongation consistently occurs during SAS elongation, what distinguishes it from elongation in other cell types? Do species with pith share this feature? Do species without pith elongate through different mechanisms? Some of these questions are explored further in the later chapters of this thesis.

2.3.3 Shade avoidance affects both primary and secondary growth, but the relationship between these two processes remains unknown.

The correlation of secondary growth, measured *via* interfascicular cambium thickening, with internode 1 elongation in SAS is another new insight. Plant growth is divided into primary growth (increases the length or height of the plant) and secondary growth (increases the diameter of the plant). Secondary growth is formed by lateral meristems; vascular cambium and cork cambium (Etchells & Turner, 2009). Vascular cambium is a closed ring of lateral meristematic tissue in the stem. Vascular cambium is composed of cells which proliferate and then based on location, differentiate to xylem on the inside or to phloem on the outside of the cambium (Etchells & Turner, 2009). Proliferation and differentiation of the vascular cambium lead to formation of secondary phloem and xylem (Mazur et al., 2014). However, in our data, we were not able to distinguish a significant difference in the xylem proportion of the vascular bundle.

Interfascicular cambium is defined as cambium that fuses to form a continuous ring in the stem (Ragni and Greb, 2018; Etchells et al., 2019). In our study, we observed an increase in interfascicular cambium thickness under the supplemental FR treatment, indicating its active proliferation; however, we did not observe additional xylem development, suggesting that differentiation into xylem is inhibited at this stage. This inhibition of cambium differentiation activity has been reported by recent research in Arabidopsis (Ghosh et al., 2022). The authors proposed a model in which dark conditions lead to the accumulation of PIFs (PHYTOCHROME INTERACTING FACTORs), resulting in the inhibition of vascular differentiation and secondary cell wall deposition through the activation of CLE44 (CLAVATA3/ESR-RELATED 44). Conversely, the presence of light rapidly deactivates PIFs, consequently reducing CLE44 transcription and promoting xylem differentiation (Ghosh et al., 2022).

Botterweg-Paredes et al. (2020) showed that tomato, dill, and carrot exhibit significant hypocotyl elongation when exposed to white light supplemented with FR. This response is accompanied by changes in vascular organization and the development of larger tracheary elements in tomato and carrot plants. However, not all shade-responsive species, such as dill, display an increase in tracheary elements (Botterweg-Paredes et al., 2020). There are currently no reports of how stem elongation (primary growth) and interfascicular cambium activity (secondary growth) relate to each other. Literature on how secondary growth links with pith is also very scarce, and as we observed a radial thickening coming from increased pith thickness, we are interested to learn how pith is associated with secondary growth in SAS.

Overall, this chapter explored the relationship between primary and secondary plant growth, with a focus on interfascicular cambium's connection with stem elongation. While FR treatment led to increased interfascicular cambium thickness, indicating active proliferation, it didn't significantly affect xylem development. This aligns with prior research showing that dark conditions, which similarly are signalled through phytochromes and PIFs, can hinder vascular differentiation, highlighting the interplay between light and xylem differentiation in plant growth. We also highlighted the need for a deeper understanding of the connection between secondary growth and pith with stem elongation.

2.3.4 Summary

In our investigation of tomato, we observed a SAS phenotype consistent with expectations, although prior studies on tomato SAS are limited. We further explored the relationship between primary and secondary plant growth, including pith cell elongation and interfascicular cambium in stem elongation. This chapter highlights the intricate relationship between primary and secondary growth in tomato response to supplemental far-red light, emphasizing the need for further research to understand the dynamics in SAS.

2.4 MATERIAL AND METHODS

2.4.1 Light treatments

Plants were grown in long day conditions (8 h of darkness and 16 h of light) under natural spectrum of 190-200 μmol m–2 s–1 photosynthetically active radiation (PAR), far-red spectrum of 0 μmol and a R/FR ratio of 2,000. They were grown with white light HPI lamps with a temperature of 25°C at day and 20°C at night, with humidity of 70%. To simulate canopy shade, FR LEDs (730nm, Philips GreenPower) were used to apply supplemental FR light and to change R:FR ratio to 0.3 (Figure 2.20).

For experiment of epidermis imprint, vascular bundle structure quantification, and R/FR ratio test, plants were grown in light condition shown in Figure 2.21. Majority of the experiment was carried out with R:FR ratio 0.2, and a few experiments were conducted with R:FR=0.11.

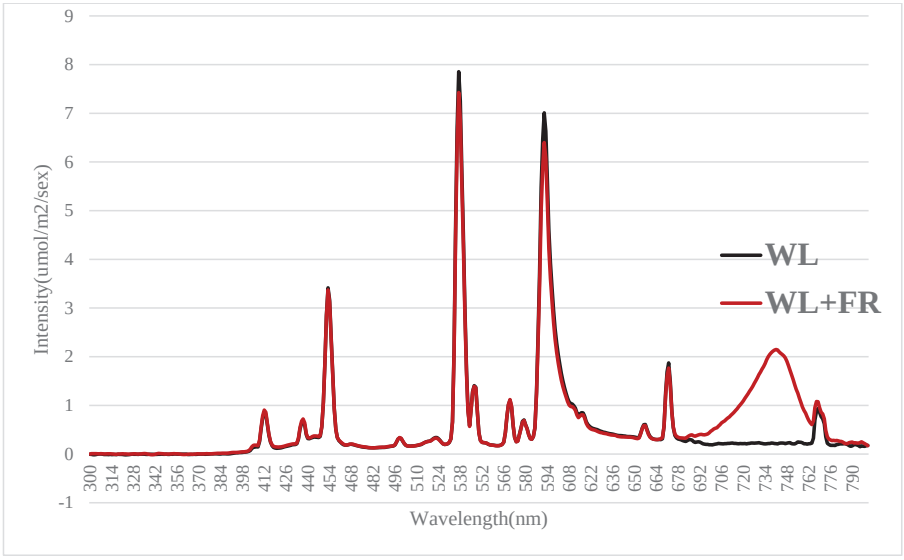

Figure 2.20. The light spectrum composition in white light (WL) and white light + far-red (WL+FR) light conditions using in this chapter. The figure shows two light spectra, photosynthetic photon flux density (PPFD) plotted against wavelength. The black line in the light spectrum represents the white light (WL) conditions and the red line represents the white light + far red (WL+FR) conditions.

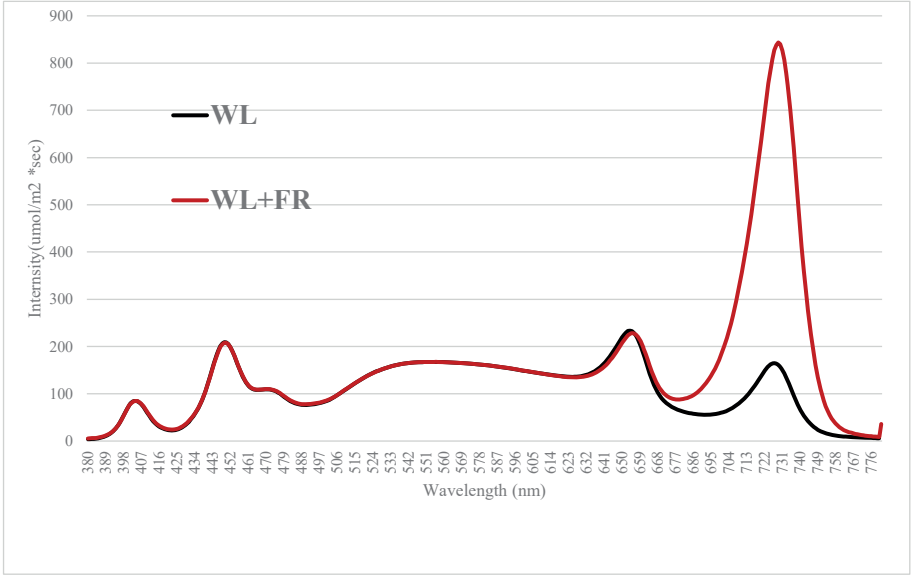

Figure 2.21. The light spectrum composition in white light and white light + far-red light conditions using in epidermis imprint and xylem quantification experiments.

2.4.2 Plant growth conditions

2.4.2.1 Root growth

Solanum lycopersicum (cv Moneymaker) (Obtained from Intratuin B.V.) seeds were washed with 70% ethanol for 1 min and then washed for 20 minutes with ½ Glorix bleach. We continued to wash with MQ until no scent of bleach remained. Fifty seeds were sown on 12.5 cm square petri dishes containing MS medium (Murashige and Skoog medium (Duchefa Biochmie),) 1 g L^{-1} MES hydrate (Sigma-Aldrich), 0.8% agar w/v; pH =5.8, and germinated for 5 days. The seedlings were measured for current root length (starting length), and then 5 seedlings per plate were transferred to the 24 cm square agar plates with MS media. Seedlings were grown vertically under white light + far-red (WL+FR) or white light (WL) for one week, and then imaged with a plate scanner.

2.4.2.2 Seedling growth

Tomato seeds (*S. lycopersicum* cv. Moneymaker and M82 (Obtained from Tomato Genetics Resource Center)) were sown in Agra® vermiculite or wetted tissue paper in a box for 1 week for germination, then transplanted to medium sized (8 cm * 8 cm) pot with Primasta® soil. The pots were all sprayed with entonem (Koppert®) for biological pest control. Seedlings were grown in a phytotron (long day, 22°C, 65% humidity) for a week. One week after transplanting, tomato plants were treated in low R:FR condition for **3, 7** or **10** days. With 6 biological replicates per experiment, each phenotyping experiment was repeated at least 3 times.

2.4.3 Phenotyping

2.4.3.1 Root measurements

In order to quantify root system architecture, image analysis was used. Petri dishes with seedlings were scanned with the Epson Perfection V800 Photo scanner using WinRhizo software (Regent Instruments Inc.) We adopted SmartRoot plugin (Lobet et al., 2011) embedded in Image J FUJI (Schindelin et al., 2012) to identify main root, lateral root and measure the length.

2.4.3.2 Plant architecture measurement

After the light treatment, we took out plants at 11am to measure the whole stem length, hypocotyl length, internode lengths and the leaves' petiole lengths, and the diameter of the first internode at the midpoint. For all the leaves, we dissected all the leaflets from the stem and

petiole, and scanned them with the Epson Perfection V800 Photo scanner using WinRhizo software (Regent Instruments Inc.) For each treatment, we used at least 6 replicates for each independent biological replicate, and this experiment was repeated for at least three times.

2.4.3.3 Leaf weight measurement

To understand the changes in leaf anatomy, we measured the leaf weight. The leaf discs were taken as shown in Figure 2.22. We took 6 leaf discs from the third true leaf (avoiding main veins and the largest side veins). We measured the fresh weight of and the dry weight. They were taken from the third true leaf avoiding the main veins. The fresh weight was measured with digital scales, and then all the leaf discs were put into a drying oven at 30°C and dried for 4 days. We used the same digital scales with to measure the dry weight.

Figure 2.22. Leaf disc sampling from the third leaf.

2.4.3.4 Chlorophyll content measurements

The chlorophyll content was measured with, the living plants by FLIR A655sc high-resolution science grade LWIR camera on the third leaf. The LWIR camera clip was clicked to the big leaflet of the third leaf for 3 seconds until the reading was obtained. We measured 8 plants for each treatment.

2.4.3.5 Vascular bundle microscopy

The 14-day old tomato plants of both cultivars were treated with either WL or WL+FR for 7 days. After the 7 days, hand cross sections were made of the mid-region of the first internode and stored in 70% ethanol. The sections were stained using a 0.02% (w/v) Toluidine blue solution for 5 minutes (Pradhan Mitra and Loqué, 2014). After staining, the samples were rinsed with 70% ethanol and stored in 4°C for later analysis. The samples were mounted on a microscope slide and treated with a droplet of 3% (w/v) phloroglucinol solution (Pradhan Mitra et al., 2014). After application of the phloroglucinol, the sections were imaged with a light microscope. the pictures were acquired with Olympus BX50-WI microscope using 4X, 10X and 20X magnifications.

2.4.3.6 Microscopy analysis

The sections to visualize vascular bundles were cut with a vibratome with the section thickness 150 μm or with razor blade by hand. And all samples were fixed by 4% PFA (pH= 6.9) for minimum 4 hours, and washed by 30%, 50%, 70%, 95% series of ethanol washes for 20 min per step, and put back to 70% ethanol. Then they were stained for 2 minutes with 0.1% (w/v) safranin (sigma) and washed with MQ until water was clear. All the sections were mounted with 50% glycerol on microscope slides, the cover glass was sealed with nail polish, each sample was stored in 4°C.

2.4.3.7 Epidermis imprinting

After 7 days of WL or WL+FR treatment, the epidermis cell layers were peeled off from the whole internode, and using Present B.V. dental paste mix to fix them immediately. After the dental paste was fully dried, we used clear nail polish to imprint the structure. We imaged the imprints under Axioscope 2 Zeiss microscope.

2.4.4 Statistical analyses

2.4.4.1 Root measurements

To measure primary root length, number, hypocotyl length and length of lateral roots, ImageJ Smartroot plugin (Lobet et al., 2011) was used to analyse the pictures. The data were analysed by Graphpad prism 8, the significant differences between WL and FR+WL were calculated by student's t-test.

2.4.4.2 Phenotypic analysis

The phenotypic data were analysed and plotted with Graphpad prism 8. The significant differences between WL and FR+WL were calculated by student's t-test.

2.4.4.3 Microscope analysis

The measurements were done with analysis^D software (Olympus BX50-WI microscope compatible software) and FIJI Image J. The software Graphprism 8 was used to plot the data. The significant differences between WL and FR+WL were calculated by student's t-test. To summarize all the data from microscope analysis, custom R scripts (R Development Core Team, 2010) were used to visualize the data as a heatmap. After performing ANOVA analysis among Moneymaker vs M82, WL vs WL+FR and experiment repeats with R, -logP values were extracted from ANOVA and used for heatmap.

TRANSCRIPTOME CHANGES OF TOMATO INTERNODE ELONGATION INDUCED BY FAR-RED LIGHT

Linge Li, Ronald Pierik, Kaisa Kajala

ABSTRACT

Plants utilize especially red and blue light for the essential activity of photosynthesis. Also, the plant sensing mechanisms for light can detect these wavelengths: red by phytochrome, and blue by the cryptochromes and phototropins. Phytochrome can also sense far-red light (FR) as a signal for detecting light reflected from neighboring plants and leaves. Changes in the ratio of red and far-red light alter the ratio of phytochrome active and inactive forms, leading to stem elongation in tomato as described in Chapter 2. Despite being a well-known phenomenon for decades, the cellular level regulatory mechanisms in stem-forming plants have not been fully resolved. To address this, we designed a time series RNA-seq at a tissue-specific level in tomato. The transcriptome data indicated regulation of auxin during internode elongation in the first few hours which had a lasting effect on cell elongation. We also found that internode and pith cells exhibit a strong auxin response during the afternoon FR treatment timepoints. Moreover, through GO analysis, we observed indications for changes in cell division and elongation, including cell wall formation. The role of auxin and other hormones is followed up experimentally in Chapter 4. We also analyzed expression modules through WGCNA, which identified FR-responsive transcription factors (TFs) that are our putative key regulators. We reviewed the known roles for these TFs from the literature and selected three candidate TFs that may play a role in shade avoidance syndrome (SAS)-linked cell division in stem tissues for further study (Chapter 5). In conclusion, this chapter has successfully identified potential candidate TFs and highlighted the crucial role of auxin in the examined context.

3.1 INTRODUCTION

Shade is one of the most common environmental challenges plants come across throughout their development. Plants' morphology changes in response to neighbor cues, such as enrichment of far-red (FR) light in order to escape impending shade. This phenomenon, which is called shade avoidance syndrome (SAS), is observed in many plants and includes examples such as elongation of the petiole and the internodes in mustard (*Sinapis alba*) in response to local FR exposure (Child and Smith, 1987; Casal and Smith, 1988), and elongation of the hypocotyl in oil seed rape (*Brassica rapa*) in response to FR (Procko et al., 2014). In tomato (*Solanum lycopersicum* cultivars Moneymaker and M82), whole-plant FR treatment promotes shoot growth as described in Chapter 2 of this thesis.

Stem, the plant's support organ connecting leaves and flowers, functions in transportation of water, minerals, and other nutrients from roots to leaves, where they can be used for photosynthesis and plant growth (Esau, 1953). In dicotyledonous plants, the stem is the major vertical shoot which has maintenance, support, and nutrient transport functions. Generally, dicot stems support their longitudinal (primary) growth through radial (secondary) growth. Most dicots have two major transitions in stem growth. The first transition is from primary growth that mainly happens in shoot and root apical meristems to secondary growth which is driven by vascular (pro)cambium, a lateral meristem (Tonn and Greb, 2017) The second transition is from radial growth to extensive wood formation driven by another lateral meristem, cork cambium (Sanchez et al., 2012). During secondary growth, plants remodel the structures of their vascular tissues via vascular cambium (Savidge, 1983; Friml et al., 2002; Randall et al., 2015; Ragni and Greb, 2018)

Cell division, expansion, and differentiation in secondary growth are coordinated by a complex network of hormones and other signals. Woody plants usually have a hard stem that continues secondary growth every year, such as evergreen species and deciduous trees, leading to very thick stems. Some dicots undergo secondary growth but have a limited scope, for example, tomato (*Solanum lycopersicum*) (Figure 3.1), potato (*S. tuberosum*), and Brassicaceae such as Arabidopsis (Moazzeni et al., 2014; Hardwick and Elliott, 2016)

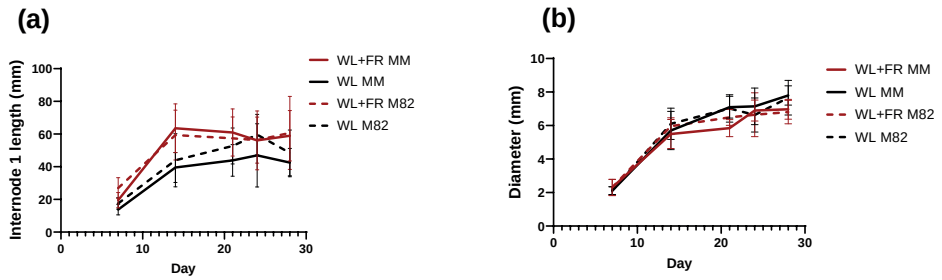

Figure 3.1. Tomato first internode length and diameter changes over time. (a) First internode length of tomato cultivars Moneymaker (MM) and M82 over 28 days of 7D supplemental far-red treatment. (b) Diameter of first internode of MM and M82 over 28 days of far-red treatment. WL = white light, WL+FR = white light supplemented with far-red.

As discussed in the previous chapter, plant stems are composed of various cell types. Each cell type has a unique structure and macromolecular composition that allows it to carry out specific functions. For instance, the cambium consists of undifferentiated meristem cells that produce new cells for specialized functions. The response of different cell types to environmental signals varies, and specific pathways are activated depending on the cell type (Miller Coyle, 2004). This knowledge is crucial in understanding the role of plant stems in growth and development, as well as in the response to external stimuli (Kutschera, 2001; Kozuka et al., 2010; Mack and Davis, 2015).

Stem growth is composed of various cell activities that lead to stem elongation and stem expansion. These pathways are modulated by multiple hormones, as shown in Figure 3.2, which demonstrates the interplay of different hormones in stem growth. In the earlier stage of primary growth, the shoot apical meristem is the major regulator of stem elongation. Therefore, genes such as *ARGO*s (*Auxin-Regulated Gene involved in Organ Size*) and *EBP1* (*Erbb-3 Binding Protein 1*) play key roles in maintaining meristematic competence regulated by sucrose, auxin, and cytokinin (Mizukami and Fischer, 2000; Hu et al., 2003; Horváth et al., 2006).

In the lateral growth of the stem, when the lateral meristem is involved, more complex signaling pathways are required. Auxin still dominates stem growth in secondary growth, but it is essential to have strigolactone signaling to mediate auxin function in secondary growth, and jasmonate positively regulates vascular cambium (Perrot-Rechenmann, 2010; Sehr et al., 2010; Agusti et al., 2011; Chandler and Werr, 2015; Ma and Li, 2019). In the cambium activities, WOX and CLAVATA are intensively studied in Arabidopsis (Hirakawa et al., 2010; Wang et al., 2018). In our model, tomato, clear secondary growth patterns were reported (Venning, 1949; Thompson and Heimsch, 1964). Auxin,

gibberellin, and brassinosteroids facilitate wood formation in stem and stem elongation in tomato (Lee et al., 2019; Schrager-Lavelle et al., 2019; Thompson & Jacobs, 1966). Auxin has also been reported to function in SAS stem elongation in older tomatoes (24 dag (days after germination)) (Cagnola et al., 2012; Courbier et al., 2020), but how auxin regulates younger plant signaling and the detailed regulatory pathway have not been fully resolved. In this chapter, we aim to contribute to stem-specific studies of developmental changes in the SAS and identify transcriptome patterns during supplemental FR-regulated shade avoidance in tomato.

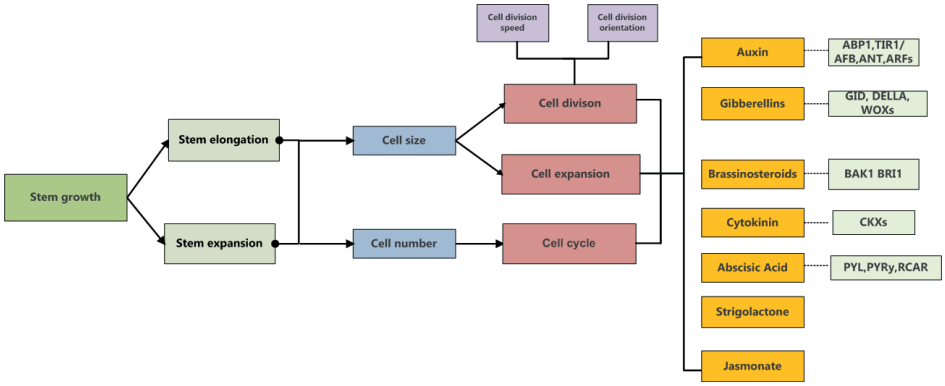

Figure 3.2. Stem growth on cellular level is regulated by hormones. This graph summarizes findings from arabidopsis. Genes colored in light green are some very well studied receptors or pathway genes that show a function in cell activities in stem growth. Adapted from (Greulach and Haesloop, 1958; Anastasiou et al., 2007; Dello Ioio et al., 2008; Perrot-Rechenmann, 2010; Oh et al., 2020).

Stem elongation and radial expansion have been studied for a century, but it still remains unresolved how each of the cell types exactly functions in both radial and longitudinal stem expansion. The interfascicular cambium (in red in Figure 1.5) in the vasculature can produce new vascular cells (Aichinger et al., 2012), but we also observed increased pith numbers in Chapter 2. Kraus in the 19th century raised the argument about the inner tissues, especially the pith, as the driving force for stem elongation, while the outer cell layers determine the rate of elongation by enforcing a mechanical constraint (Kraus, 1867; Kraus, 1869). Kutschera proposed the idea that the inner tissues (pith especially) provide the driving force by changing the turgor pressure, whereas the peripheral cell type(s) control the speed of stem elongation (Kutschera, 1992). This idea was further confirmed by Savaldi-Goldstein et al. by constructing epidermis-specific stabilized mutant protein of IAA17 in Arabidopsis (Savaldi-Goldstein et al., 2007). Concordant with this hypothesis, pith cell elongation was observed in SAS in bean (*Phaseolus*

vulgaris 'Kentucky Wonder') during the internode elongation (Beall et al., 1996). In Chapter 2, we also observed elongation and cell layer increase in pith, thickness increase in interfascicular cambium, and longer epidermis cells in response to FR.

Distinguishing gene expression in specific cell types is an effective way to reveal cell functions of individual cell types in plants without the noise from surrounding tissue. High-resolution gene expression profiling methods to understand SAS have been conducted in Arabidopsis and other models, including tomato (Li et al., 2012; Bolger et al., 2014; Bush et al., 2015; Kohnen et al., 2016a; Gommers et al., 2017; Pantazopoulou et al., 2017; Molina-Contreras et al., 2019; Courbier et al., 2020; Küpers et al., 2023). Profiling the cell type and organ-specific gene expression changes in the stem SAS would aid understanding the pith elongation, division, and expansion in secondary growth. In this chapter, we present time course transcriptomes from tomato first internode and its inner cylinder (pith & vasculature) for FR response. We found that in the young seedlings of 14 dag, auxin was the major growth regulation response, upregulated at our earliest timepoint of 6 hours of FR treatment. Auxin response was enriched in upregulated genes of both internode and pith, and however, no other hormonal regulation pathways were enriched in FR-responsive genes. Meanwhile, the metabolic changes such as amine metabolic process and catalytic activity were enriched in pith differentially expressed genes. These tissue-specific transcriptional signatures often predict previously unknown cell-type-specific functions, and the results could lead to the discovery of unknown pathways in tomato and unknown characteristic in pith.

3.2 RESULTS

3.2.1 First internode elongation was visible from the second day after the supplemental FR treatment started

In the previous chapter, we demonstrated that tomato first internode was significantly longer after 7-day whole-plant FR-treatment (WL+FR) compared to the control white light (WL) treatment. In this chapter, we set out to investigate the molecular mechanisms of elongation on tissue level in first internode by conducting a time course RNA seq analysis. Initially we investigated the elongation of first internode from the start of the FR exposure at 7 dag (Figure 3.3). At the start of FR supplementation, the first internode already existed, but was still very small and closely connected with the meristem. We observed that at 48 hours, the elongation of the first internode started to show increase in WL+FR compared to WL. This increase was observed for the elongation of the total stem as well. Both tomato cultivars MM and M82 show very similar response pattern for the duration we investigated.

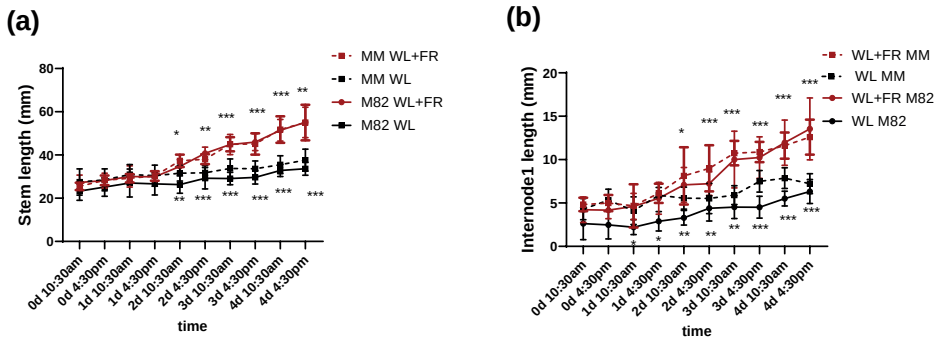

Figure 3.3. Stem and first internode length for 4 days in WL+FR treatment. (a) The stem length of MM and M82 in WL and WL+FR. (b) The first internode length of MM and M82 in WL and WL+FR. The seedlings were grown in WL for 1 week, and 0 day 10:30 am in the morning we started supplemental FR treatment, the lengths were measured at 0, 6, 24, 30, 48, 52, 64, 70, 94 hours that correspond to day 0 at 10:30am, day 0 at 4:30 pm, day 1 at 10:30 am, and so on. Asterisks indicate significance between WL and WL+FR as follows: $p \leq 0.05$,** $p \leq 0.01$, *** $p \leq 0.001$.Upper significance indicates comparison in MM, lower significance indicates comparison in M82.

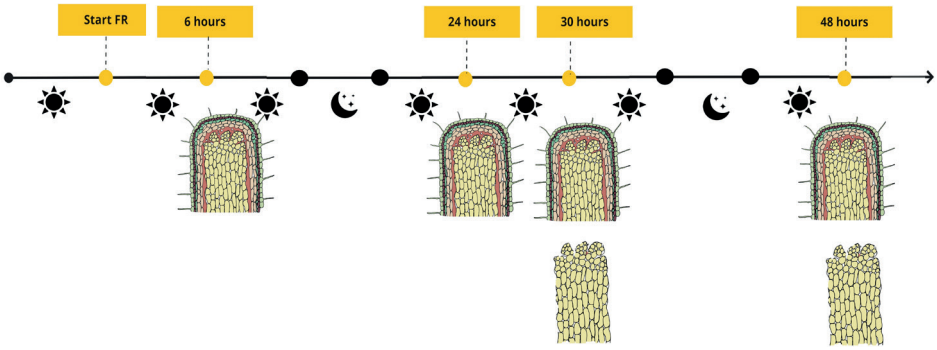

Figure 3.4. Experimental design for time series and tissue-specific RNA sequencing on tomato internode elongation in WL vs WL+FR treatment. Plants were grown for 7 days in WL before the WL+FR treatment. The whole internodes were harvested at all timepoints, and pith tissue only at the two latest timepoints.

In order to capture the early events in the first internode elongation, we designed the RNA-sequencing timepoints leading to the point where the elongation phenotype was observed, specifically: 6 hours (16:30 day 0), 24 hours (10:30 day 1), 30 hours (16:30 day 1), and 48 hours (10:30 day 2). The samples harvested were the first internode and the central cylinder (pith) of the first internode. The pith was only successfully sectioned at the two later timepoints (Figure 3.4) where the stem is thick enough for accurate dissection. The experiment consisted of two light treatments, two cultivars, two tissue

types and four timepoints, altogether 24 sample types, with 3-4 replicates each. The barcodes were assigned to each sample and separated in 4 individual lanes for sequencing. The samples were sequenced to the depth of at least 3 million raw reads and then mapped to SL4.0 tomato genome (https://solgenomics.net/) and ITAG4.1 annoqtation.

3.2.2 The two cultivars' gene expression profiles were similar

Before differential expression (DE) analysis, we firstly ran a quality check with samples using principal component analysis (PCA, Figure S3.1). From the PCA analysis, the samples from the two cultivars, MM and M82, did not separate from each other when compared to the other variables. DE analysis of MM vs M82 (Figure S3.2) shows no differentially expressed genes (DEGs) in WL at any timepoint, and the only distinguishable difference between the cultivars appeared at 6h WL+FR treatment. Combining with the phenotyping evidence from previous chapter and Figure 3.4, we assume these cultivars can be taken as replicates. Based on these data, we decided to put these two cultivars together in the following analysis, without no more considering cultivar differences.

3.2.3 Differential gene expression was induced already at our earliest FR timepoint

To identify DEGs, we utilized the limma voom package (Law et al., 2014; Ritchie et al., 2015) for comparing WL+FR transcriptomes to WL at each different timepoint and tissue type (Figure 3.5a). The most pronounced gene regulation emerged at the initial timepoint, after 6 hours of FR treatment, highlighting the rapid adjustment of gene expression within the stem due to FR light. Notably, the DEGs in first internode exhibited a gradual decline throughout the FR treatment duration. Pith showed comparable DEG numbers to internode 1 at 30h and 48h timepoints (Figure 3.5b), The overall number of DEGs remained modest, but pith and internode do present different DEGs (Figure 3.6).

Notably, FR treatment reveals a higher number of DEGs when comparing morning to afternoon, both upregulated and downregulated. This suggests that FR can augment diurnal changes (Figure 3.5 c).

The sectioning protocol was carefully carried out to remove all outer layers to ensure the precision of pith harvest. Notably, pith-specific expression, when compared to internode expression, demonstrated minimal upregulation (pith-enriched gene expression) and predominantly showcased downregulation (Figure S3.2b). This could indicate the role of pith being a "blank slate" without any outstanding specialized processes. Consequently, this pattern did not captivate our interest to a significant degree.

Additionally, our PCA analysis (Figure S3.1) unveiled a discernible contrast between morning and afternoon timepoints, indicating a robust response linked to the diurnal cycle, which was also reported in Arabidopsis (Franklin, 2020; Fraser et al., 2021).

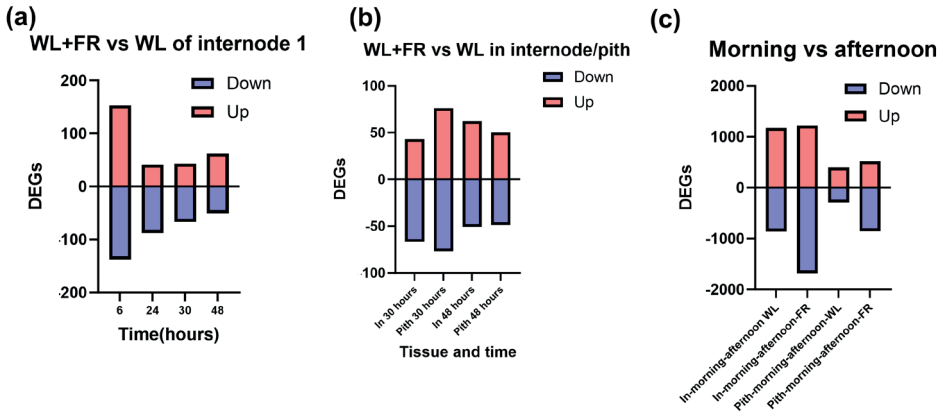

Figure 3.5. Differentially expressed genes (DEGs) upon FR treatment from RNA-seq on tomato SAS internode elongation. (a) First internode FR-responsive DEGs at the four timepoints. (b) First internode and pith FR-responsive DEGs at 30 and 48 hours of FR treatment. (c) Pith and internode diurnal-responsive DEGs, analysed by grouping the morning or afternoon timepoints.

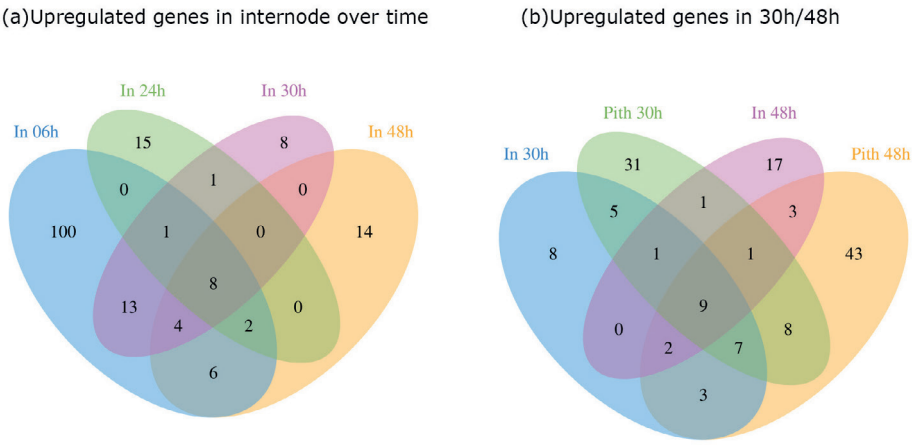

Figure 3.6. Overlap between DEGs. Venn diagram showing the overlap in FR-responsive DEGs in (a) first internode over time, and (b) in the two tissues, first internode or pith, at 30h and 48h.

To conduct a detailed examination of the DEGs, we looked at the overlap in upregulated genes in the internode over time (Figure 3.6). It's worth noting that at the 6-hour timepoint, a substantial number of DEGs are uniquely present. Additionally, when

comparing the DEGs in the pith and internode at both 30 and 48 hours, we observed that the pith exhibits a higher count of unique DEGs. These findings suggest a distinctive pattern of gene expression regulation in the pith, potentially highlighting its specialized role in SAS.

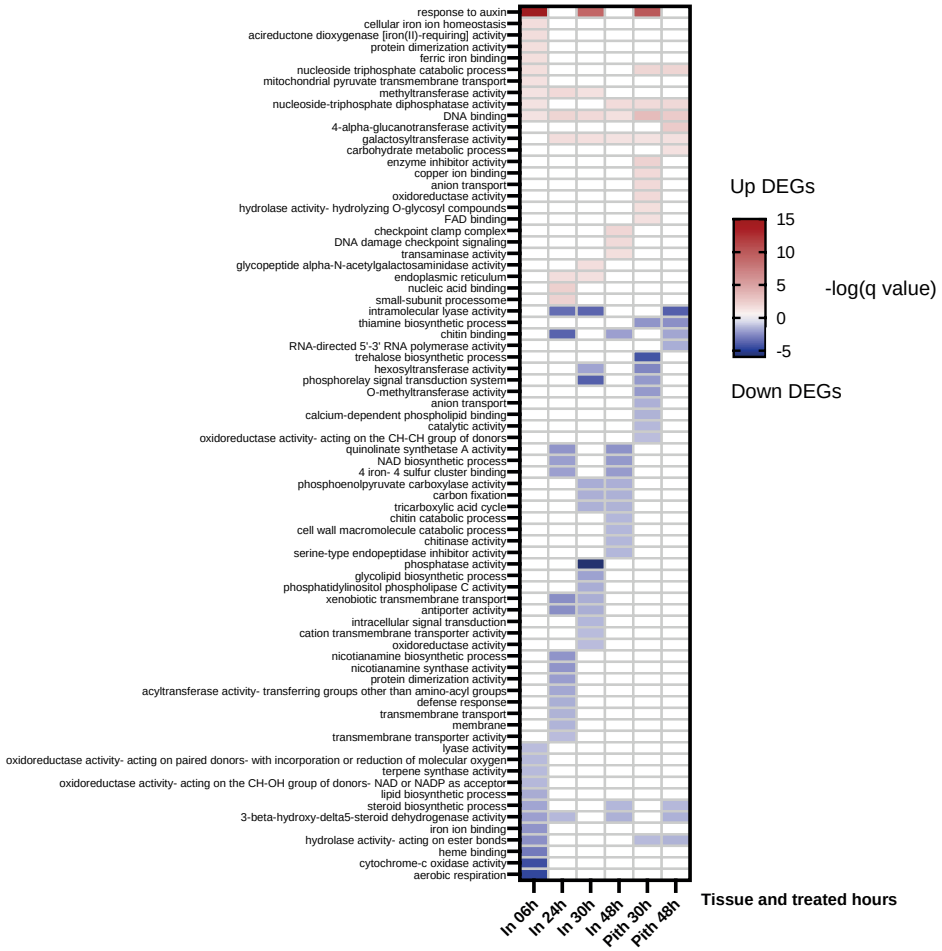

Figure 3.7. Gene ontology (GO) enrichment analysis of FR-responsive DEGs in whole internode or pith. Heatmap of the -log of adjusted p-values (q-value) for each enriched GO category. Red color scheme for upregulated DEGs, and blue for downregulated. The color scale is capped the at 15 to ensure clearer visualization of all GO details.

3.2.4 Auxin signalling showed strong upregulation in afternoon timepoints

To explore the response pathway governed by WL+FR treatment, we conducted a gene ontology (GO) enrichment analysis on up- and downregulated DEGs at different timepoints, utilizing ITAG 4.1 annotation data from Sol Genomics Network (solgenomics.net). We observed several enriched GO categories, with a notable concentration emerging at the 6-hour timepoint. Genes responsive to auxin exhibited a remarkable enrichment in upregulated genes, indicating a substantial 38-fold enrichment (Figure 3.7). What's particularly interesting is that this enrichment in auxin response was exclusively observed during the afternoon timepoints throughout the entire internode and pith. This implies a synchronized regulation of auxin across all cell types, particularly prominently in the pith, suggesting a diurnal-related effect, a phenomenon previously documented in Arabidopsis (Covington and Harmer, 2007).

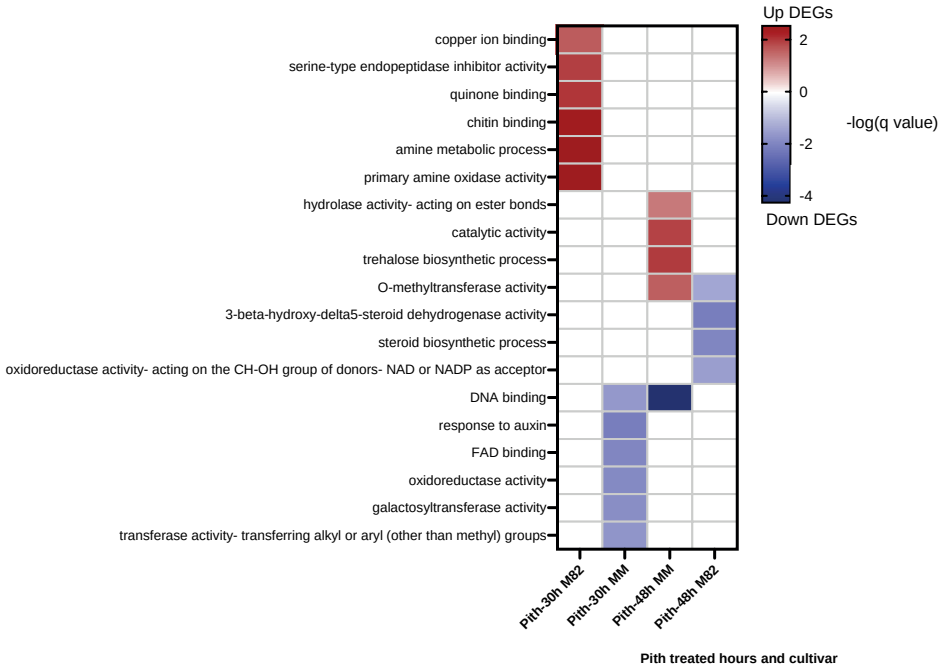

Figure 3.8. Gene ontology enrichment analysis of FR-responsive DEGs in pith of each cultivar. Heatmap of the -log of adjusted p-values (q-value) for each enriched GO category. Red color scheme for upregulated DEGs, and blue for downregulated. The DEG comparisons are made by comparing WL+FR to WL in a specific cultivar at a specific timepoint.

3.2.5 Internode data revealed an FR-effect on growth-related GO terms

To gain insight into the processes underpinning cell elongation and division that contribute to internode elongation, we focused on GO terms that could be associated with these processes. Firstly, we looked into GO term "nucleoside triphosphate catabolic process", which refers to ATP and GTP breakdown or hydrolysis into their respective nucleoside diphosphate forms or even further into nucleoside monophosphates (https://www.ebi.ac.uk/QuickGO/term/GO:0009143). This process typically involves the release of energy stored within the high-energy phosphate bonds of these triphosphate molecules. This GO term is enriched among the initially upregulated DEGs in whole internode, and at the later timepoints, it is enriched specifically in the pith FR response (Figure 3.7). Secondly, we observed an enrichment of pathways linked to carbohydrate metabolism within the FR-upregulated DEGs, specifically carbohydrate metabolic process, nucleoside triphosphate catabolic process, nucleoside-triphosphate diphosphatase activity. This collective enrichment is an indication of FR enhancing growth. Furthermore, this pattern appears intermittently across specific timepoints throughout the entire internode.

For cell division and enlargement to occur, it is imperative that cell walls undergo a loosening process. We noted that molecular components (GO terms: cellulose biosynthetic process, cellulose synthase (UDP-forming) activity, membrane, cell wall modification) linked with cell wall loosening are also enriched in FR-treated pith compared to whole internode (Figure 3.9). Similarly many transmembrane transport activities are enriched in FR-treated pith (Figure 3.9), potentially indicating changes in osmotic potential in pith.

3.2.6 At 6h FR treatment, energy exchanging activities were enriched

The GO enrichment analysis (Figure 3.7) unveiled a noteworthy energy exchange pattern. Specifically, after 6 hours of FR treatment, we observed an enrichment in aerobic respiration and cytochrome-c oxidase activity within the internode upregulated DEGs. This signal of increased metabolic activity could indicate a more rapid respiration process, thereby providing increased energy for internode growth in response to FR.

Furthermore, we identified enriched GO terms related to energy exchange activities essential for maintaining vital cell functions, including protein dimerization and pyruvate metabolism. In the context of protein dimerization, the synthesis of protein subunits demands energy, often in the form of ATP. However, the subsequent dimerization step

typically relies on energetically favourable non-covalent interactions (Dang, 2022). Pyruvate metabolism involves energy consumption: the input of energy in the form of ATP and NADH during the conversion of pyruvate to acetyl-CoA in the mitochondria (McCommis and Finck, 2015; Bispo and Vieira, 2022). These energy exchange activities are instrumental in sustaining vital cellular functions, such as energy storage and signalling processes (McCommis and Finck, 2015; Lim et al., 2017; Dang, 2022). This result is consistent with the previous finding in FR pre-treatment of 4-week-old tomato (Courbier et al., 2020), where it was observed that in WL there was a downregulation of genes associated with glucan-related structural processes, potentially indicating carbohydrate reallocation for energy production in response to a fungal pathogen.

3.2.7 Examining pith-specific expression in comparison to the whole internode under far-red light conditions

Delving into the significance of pith as a tissue understudied, we examined enriched GO categories to unravel its roles and functions. In all pith-specific GO enrichments (Figure 3.9), transmembrane transport was highly upregulated. This may indicate that the movement of nutrients and/or metabolites was active in pith cells, and it is a typical stress adaptive strategy in abiotic stress due to ionic balance and sugar supply change (Gill et al., 2021). At the same time, multiple photosynthesis-related GO terms were enriched in the downregulated DEGs at the beginning of FR treatment. From 6 hours until 48 hours, the sugar-related transfer pathway was enriched in the downregulated DEGs, with the most drastic response happening at 6 hours and gradually soothing down. Enriched GO categories highlighted the heightened activity of transmembrane transport in pith cells, suggesting an adaptive strategy in response to abiotic stress. Concurrently, the downregulation of photosynthesis-related GO terms and the sugar-related transfer pathway indicated dynamic shifts in cellular processes over the course of the far-red light treatment.

3.2.8 DNA-binding is enriched in FR-upregulated DEGs

The second most enriched pathway in upregulated DEGs, which consistently appeared at multiple timepoints in response to far-red light (FR), is associated with DNA binding (Figure 3.7). DNA-binding proteins include transcription factors, which control the expression of genes by binding to specific DNA sequences in the promoter region of genes, and chromatin-modifying enzymes, which modify the structure of the DNA molecule and its associated proteins to regulate gene expression (Luscombe et al., 2000). This DNA-

binding molecular response could also be indicated by the other GO categories, such as the protein dimerization activity, which includes enzyme activation that can be involved in DNA binding activities (Dang, 2022). Thus, looking into transcription factors in the DEGs will be interesting for our following analysis.

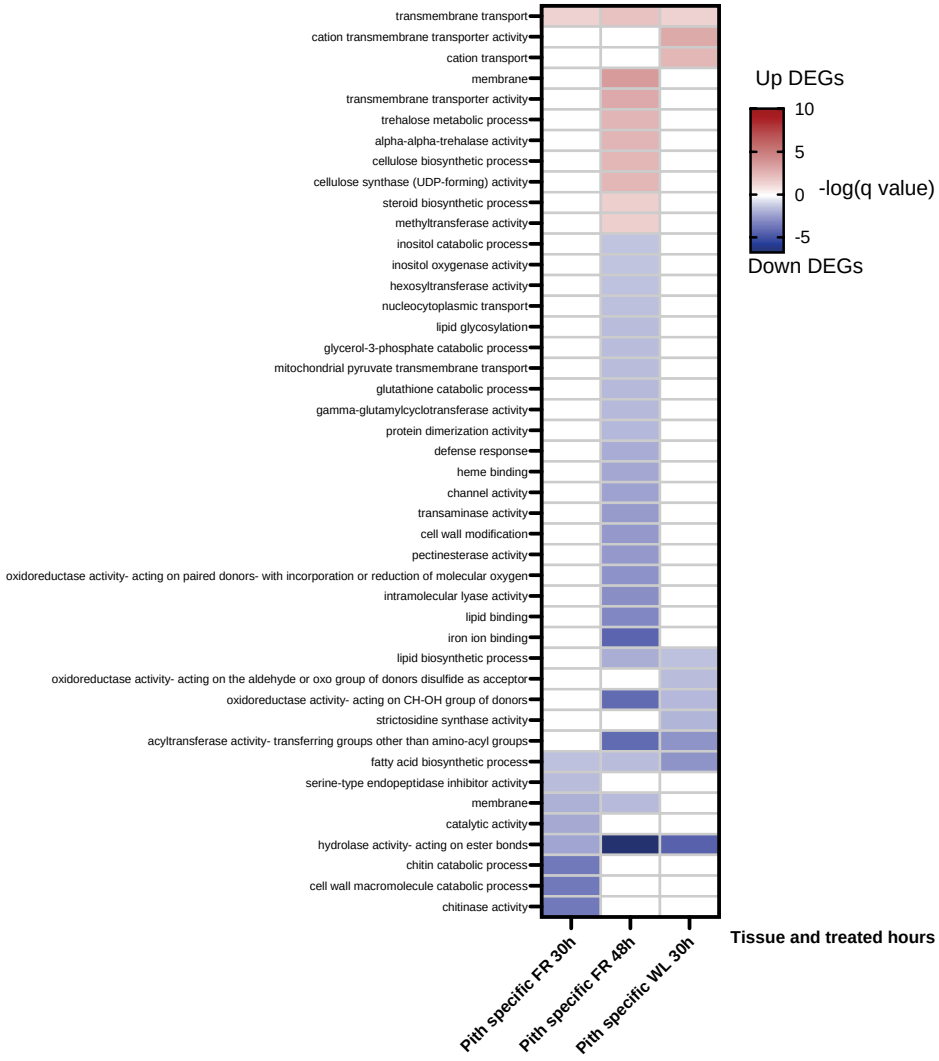

Figure 3.9. GO enrichment analysis of pith-specific DEGs (pith compared to whole internode). Heatmap of the -log of adjusted p-values (q-value) for each enriched GO category. Red color scheme for upregulated DEGs, and blue for downregulated.

The lyase activity is enriched in the downregulated FR-responsive DEGs (Figure 3.7) is attributed to genes *Solyc05g010320* and *Solyc05g052240*, both annotated to encode chalcone-flavanone isomerase (CHI) on Solgenomics.net. CHI is a crucial enzyme in plant biology, converting chalcones into flavanones, vital compounds in plants (Moustafa and Wong, 1967). CHI downregulation reduces flavonoid levels in plant tissues, impacting functions such as UV protection, pollinator attraction, and pathogen defence. Additionally, it can alter tissue pigmentation, potentially resulting in different colours and patterns (Ryan et al., 2002). This downregulation affects a plant's stress response and pathogen resistance, as flavonoids attribute in part to their antioxidative effects, involve the non-specific quenching of reactive oxygen species (ROS) generated by both the pathogens and the plant in response to infection and stress (Mierziak et al., 2014). There is an enrichment of hydrolase activity targeting ester bonds. Ester bonds are the connections that link a carboxylic acid group to an alcohol group, forming a molecule known as an ester. Hydrolases break these bonds apart, releasing the carboxylic acid and alcohol components. Alcohols, particularly ethanol, may contribute to defense mechanisms by participating in the synthesis of secondary metabolites like lignin and flavonoids, strengthening cell walls, and inducing stress-related genes. Additionally, alcohol accumulation can serve as an indicator of stress or pathogen attack (Bashir et al., 2022; Matsui et al., 2022).

In all pith FR-upregulated DEGs (Figure 3.7), there are two specific genes of interest: *Solyc06g008870* and *Solyc09g075680*, both annotated to encode the gibberellin receptor, GIBBERELLIN INSENSITIVE DWARF 1 (GID1) on Solgenomics.net. GID1 is involved in the plant's response to gibberellin hormones, regulating growth and development. The downregulation of GID1 in the pith may have various change on gibberellin pathway involving cell division and elongation (Ueguchi-Tanaka et al., 2007; Murase et al., 2008).

Downregulation of various pathways involved in the synthesis of compounds with diverse functions, such as the NAD biosynthetic process, carbon fixation (photosynthesis), and nicotianamine biosynthetic process, can have far-reaching effects. These pathways being downregulated in response to FR treatment suggests that the plants may be building up secondary metabolites, considered to be a stress hallmark. These pathways are reported to involved in many crucial functions such as defense mechanism which was reported in previous research (Courbier et al., 2020).

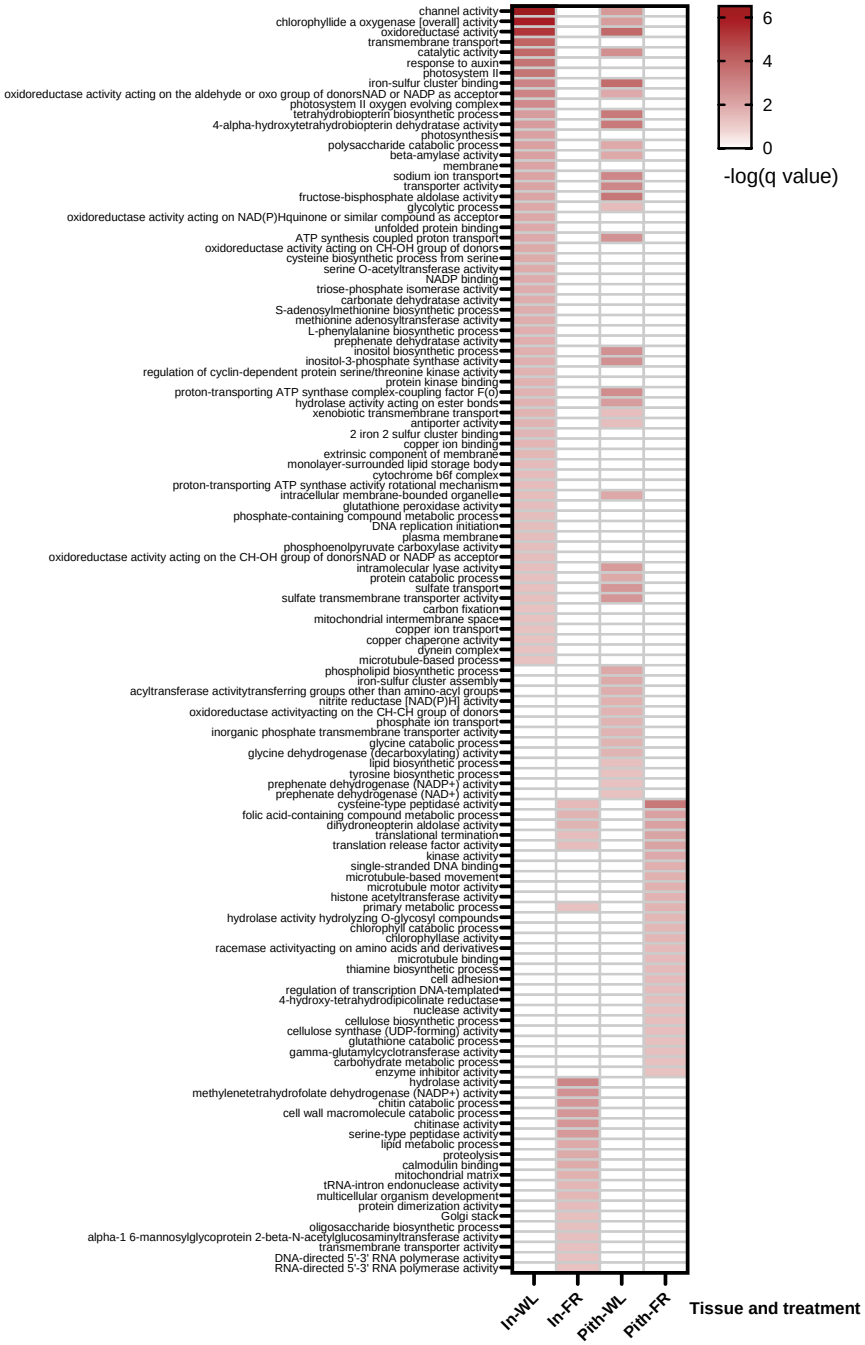

Figure 3.10. Gene ontology enrichment analysis of DEGs in pith or whole internode comparing morning timepoints to afternoon timepoints. Heatmap of the -log of adjusted p-values (q-values) for each enriched GO category. Red color scheme for upregulated DEG.

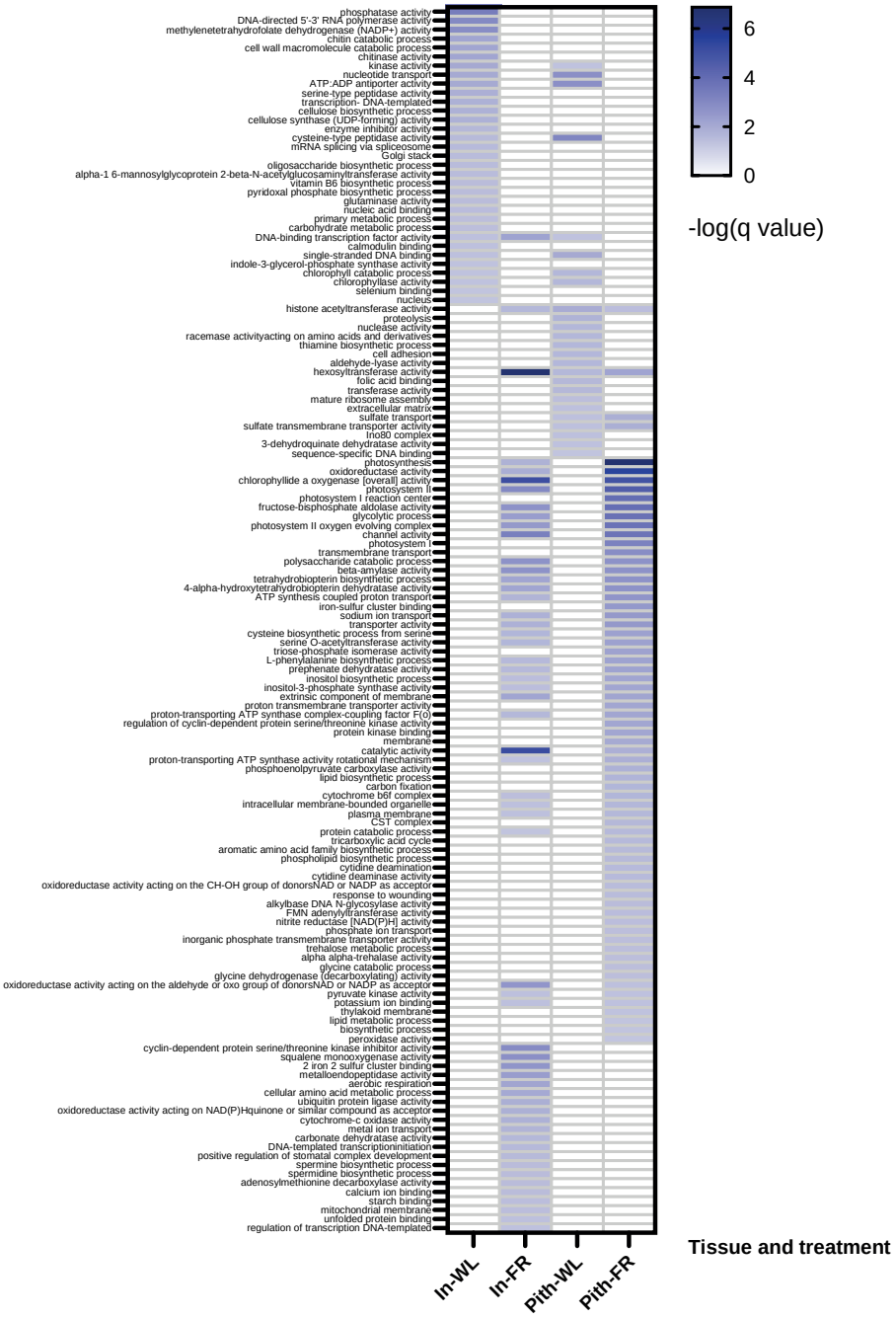

Figure 3.11 Gene ontology enrichment analysis of DEGs in pith or whole internode comparing morning timepoints to afternoon timepoints. Heatmap of the -log of adjusted p-values (q-value) for each enriched GO category. Blue color scheme for down regulated DEGs.

3.2.9 Diurnal expression patterns are associated with defence, light, and metabolism

In our data there is a clear pattern of diurnal rhythm. The morning (10am) timepoints (24h, 48h) and the afternoon (6h, 30h) timepoints cluster together in the PCA (Figure S3.1), and the afternoon 4 pm timepoints tend to show clearer FR-responses than the morning 10 am timepoints (Figure 3.7). In the afternoon, methyltransferase activity was enriched in the FR-upregulated DEGs (Figure 3.7) and trehalose biosynthetic process was enriched in FR-downregulated DEGs. We assume methyltransferase activity upregulation indicates significant molecular modifications, possibly involving epigenetic and protein-level changes. Simultaneously, the downregulation of genes associated with trehalose biosynthesis hints at a recalibration of stress protection mechanisms. While trehalose typically safeguards plants from environmental stresses, vascular plants like tomatoes have shifted towards regulating carbon assimilation and sugar status, indicating a divergence in stress response strategies (Grennan, 2007; Paul et al., 2010; Lunn et al., 2014). This strategic switch may prioritize growth over stress tolerance. Moreover, trehalose's involvement in signaling during interactions with microorganisms, responses to cold, salinity, and the regulation of stomatal conductance and water-use efficiency underscores its multifaceted role in plant biology. This interplay reflects the plant's adaptive response to shifting environmental conditions, enhancing our understanding of its intricate survival strategies (Finnegan and Kovac, 2000; Lunn et al., 2014).

To investigate which genes in our data followed diurnal regulation, we analysed the DEGs between morning and afternoon for each tissue and treatment, and carried out GO enrichment analyses (Figure 3.10 and Figure 3.11). In the internode WL conditions, we observe that auxin is enriched in afternoon up DEGs, while other treatments and tissues do not show the same response. Simultaneously, we see an increase in activities related to photosynthesis in internode WL in the morning.. Concurrently, the upregulation of polysaccharide catabolic processes indicates an increased energy demand to support DNA binding, translation and more. Morning downregulation of photosynthesis and DNA binding activities in both the whole internode and pith reflects the natural influence of the diurnal rhythm on shade avoidance (GO: DNA-binding transcription factor activity, histone acetyltransferase activity, sequence-specific DNA binding, photosynthesis, chlorophyllide a oxygenase [overall] activity, photosystem II).

Collectively, these responses signify the plant's adaptation to morning light conditions, allowing it to effectively capture and convert light energy into chemical energy for growth and maintenance. And light treatment did make a major change to diurnal cycle in general.

3.2.10 Utilizing WGCNA to illuminate the transcriptome dynamics in SAS

In order to explore the multi-factorial RNAseq data in more depth, we wanted to look for expression pattern trends. Therefore, we continued with WGCNA (Weighted Gene Co-expression Network Analysis) to identify interesting modules, functions and genes. To filter the input data to WGCNA, we selected the DEGs from any comparison previously tested ($p<0.05$) and used the quantile normalized expression data in WGCNA analysis. We used undirected analysis to identify the expression patterns among the genes. In total we were able to characterize 43 modules based on gene expression (Tables S3.1, S3.3 in the digital supplement). We conducted a GO enrichment on all these modules to infer their functions (Figure S3.3). We also visualized the gene expression patterns of these modules (Figures 3.12-3.14). In Figure 3.13, we constructed a heatmap based on the average normalized expression fold change comparing WL+FR vs WL in each tissue and treatment. Several modules consistently exhibited upregulation in response to FR: darkred, greenyellow, mediumpurplegrey3, red, and royal blue. These modules represent clusters of nodes that have grouped together due to shared attributes or connectivity patterns within the network (Figure 3.13). In Figure 3.13 we illustrate the modules in the network topology, denoted by different colors; the main modules that are clearly visible are the blue, green, grey, pink, orange, red, and yellow modules. Then, in Figure 3.14 we combined the log fold change data with the topology of gene modules to visualize the change over time across the network.

From these approaches, a number of modules stood out. The mediumpurplegrey3 module showed an increasing, high degree of upregulation over time, where the expression in the pith was significantly elevated. This module is primarily associated with chloroplast and translation activities (as shown in Figure S3.3), indicating a potential role in enhancing photosynthetic and protein synthesis processes.

Conversely, salmon and lightsteelblue1 modules demonstrated downregulation over time. The top function associated with the salmon module is the methionine metabolic process and methylenetetrahydrofolate reductase (NAD(P)H) activity, suggesting a potential shift in metabolic priorities. Meanwhile, the lightsteelblue1 module is related to vascular transfer processes, implying adjustments in the plant's transport mechanisms to adapt to changing environmental conditions. These findings collectively provide insights into the dynamic regulatory responses of different modules to FR light exposure and their functional implications in plant acclimation.

We observed a cluster of genes situated on the first chromosome within the turquoise module, indicating robust physical connection and heritability in response to the FR treatment (Figure 3.12, 3.13). The turquoise module is primarily characterized by downregulation in both internode and pith over time. These genes exhibit a wealth of functions related to ribosome, nucleosome, and photosystem I, all with central role in plant growth and maintenance. This discovery underscores the significance of apparently housekeeping genes within response pathways, and further exploration may unveil the mechanisms through which they influence a plant's response to environmental cues. This dynamic interplay between different modules further enhances our comprehension of intricate signaling networks in plant responses to environmental stimuli, offering potential targets for future genetic engineering endeavors aimed at enhancing crop yield and resilience.

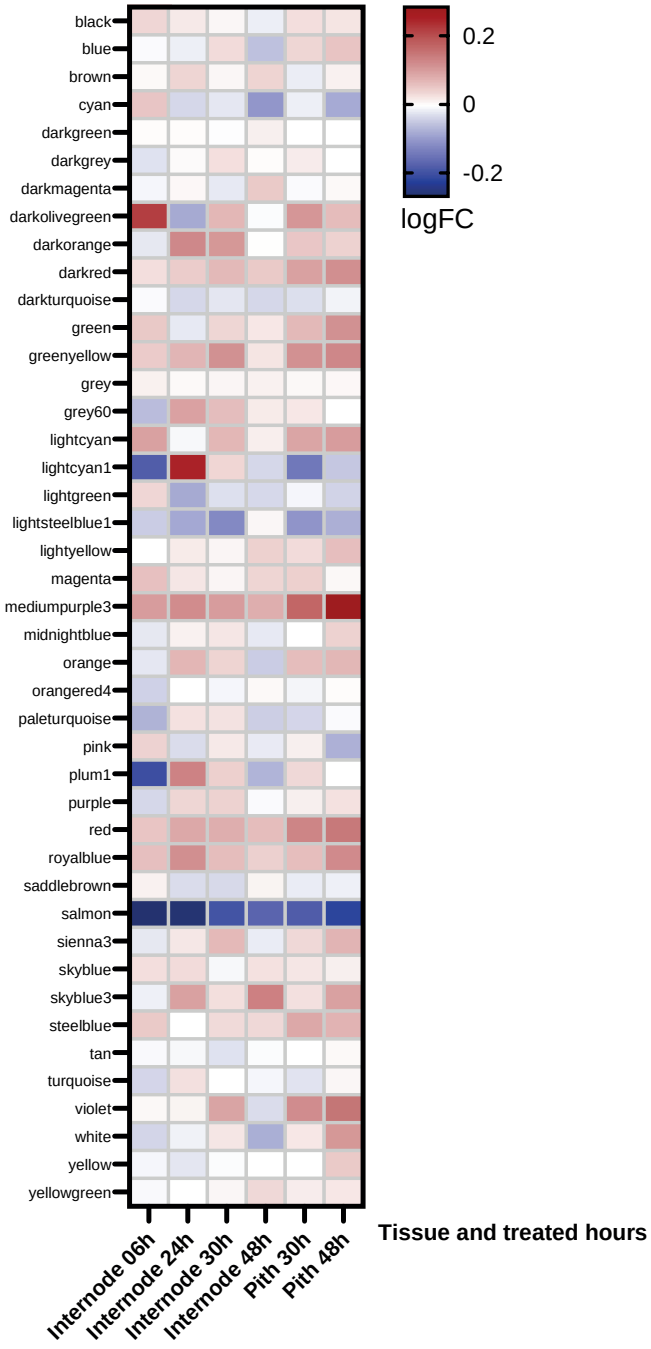

Figure 3.12. Visual representation of the FR-responsive expression patterns of each module. The heatmap color indicates average fold change in response to FR treatment, red indicating upregulation in FR and blue indicating downregulation.

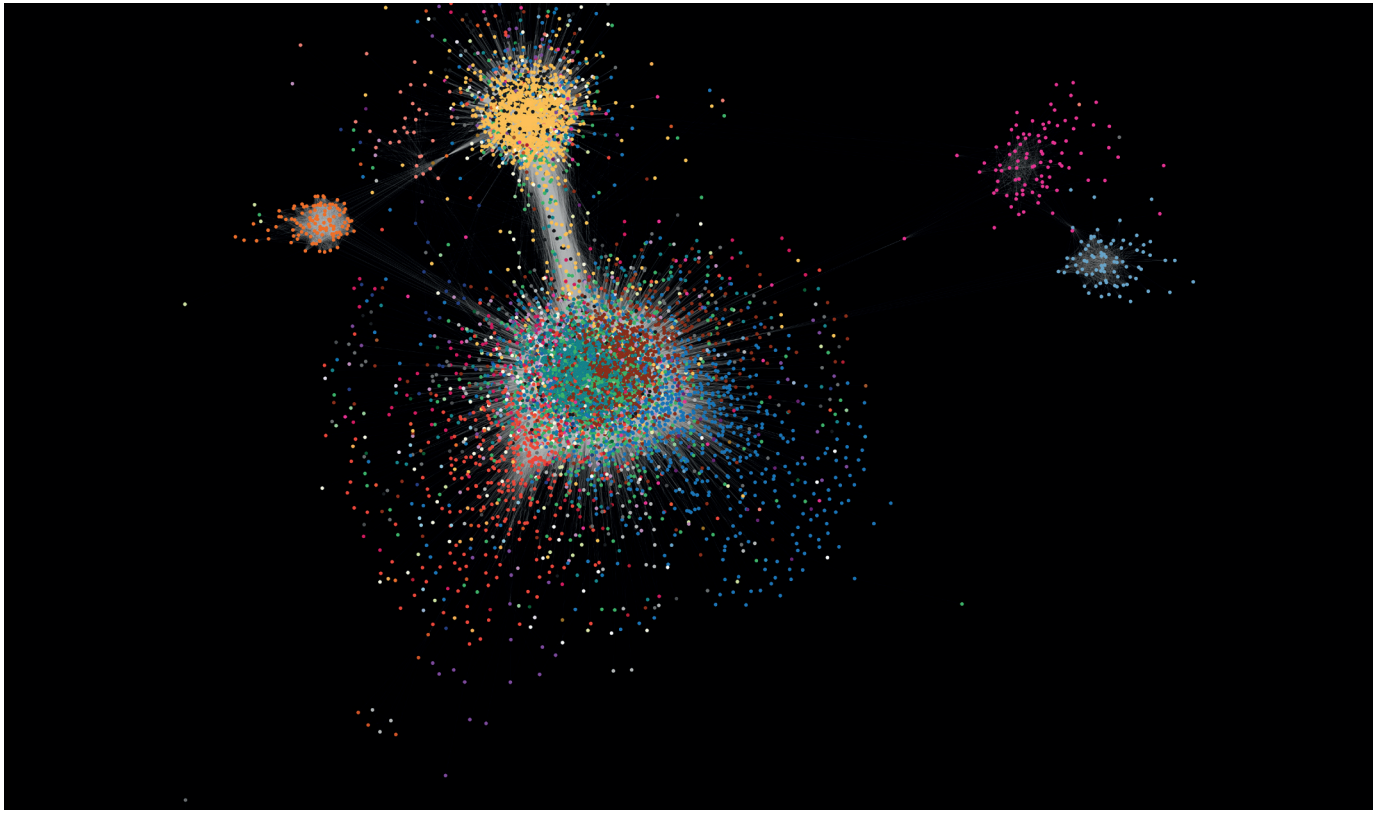

Figure 3.13. Inferred WGCNA network colored by the main co-expressed modules. Each expression pattern was assigned a specific color, same color indicates similar expression patterns over time, treatment, and tissue. Edges between nodes indicate the relationship between nodes (genes) in obtained from TOMsimilarity function. The higher weights indicate stronger connection or co-expression of genes. The soft threshold=0.06.

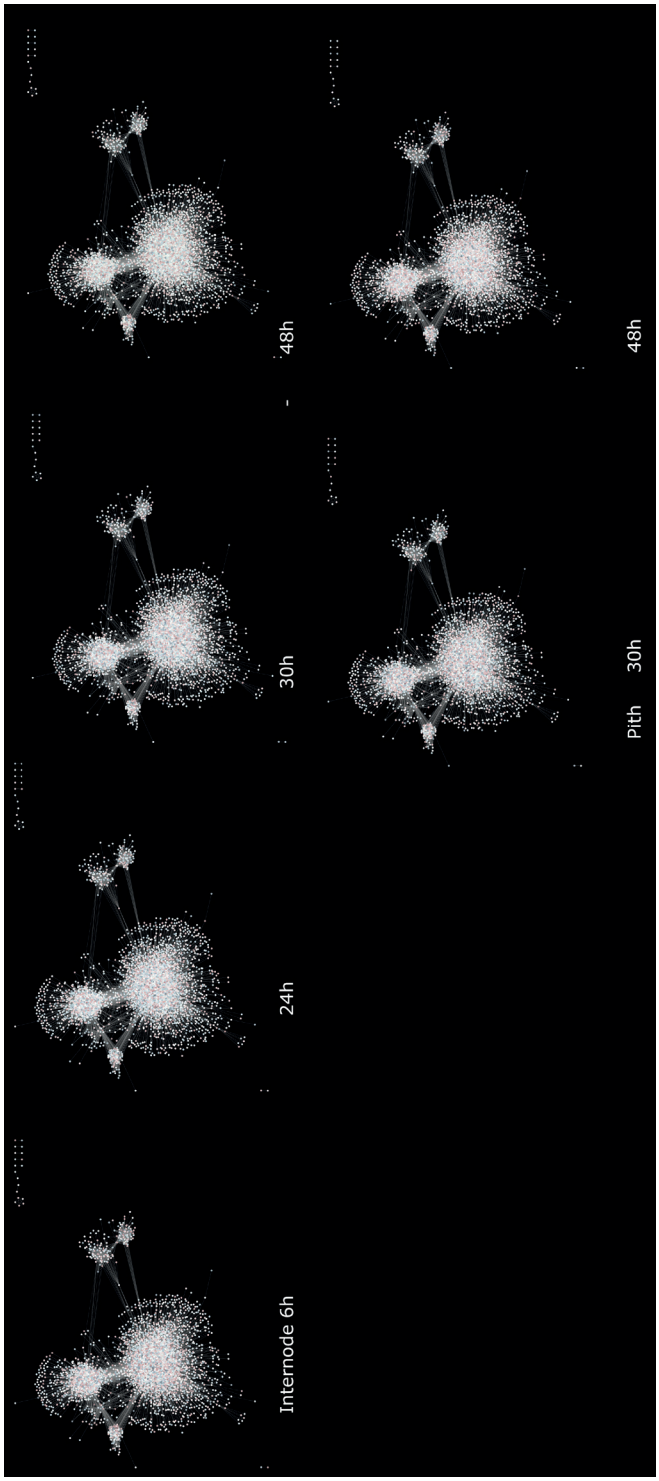

Figure 3.14. Changes in gene expression of overlaid with the co-expression gene network throughout time in internode and pith. Genes that are differentially expressed (adj.p < 0.05). The color scheme for the fold changes of FR-responsive DEGs: upregulation in red and downregulation in blue.

Next, we wanted to infer a gene regulatory network using our data. We used Maximum Clique Centrality (MCC) to calculate MCC, a centrality measure, to identify the most central or influential nodes (in this case, genes) in a network. It is based on the concept of cliques, which are subsets of nodes in a network that are fully connected to each other (i.e., all nodes within the subset are directly connected). A hub gene is a gene within a biological network (e.g., a gene interaction network or a protein-protein interaction network) that has a high degree of connectivity (Chin et al., 2014). We identified a set of central hub genes based on their connectivity and associated centrality scores (Figure 3.15, Table S3.4 in digital supplement).

We looked at the behavior of the hub genes in response to FR and observed a notable downregulation of several of them at 6h internode (Figure 3.16). Among these genes are *Solyc02g031900* (kinase family protein), *Solyc02g031970* (encoding 50S ribosomal protein L12-2 localized to the chloroplast), *Solyc03g118150* (Sec14-like), a gene potentially involved in cellular retinaldehyde-binding or triple function, *Solyc06g071370* (NHL repeat-containing protein-like gene), *Solyc07g041930*, (Adenylyl cyclase) and *Solyc10g005100* (Salt stress root protein RS1). The downregulated hub genes may play integral roles in the plant's response to FR light, potentially affecting processes related to kinase activity, ribosomal function, cellular retinaldehyde binding, and stress responses.

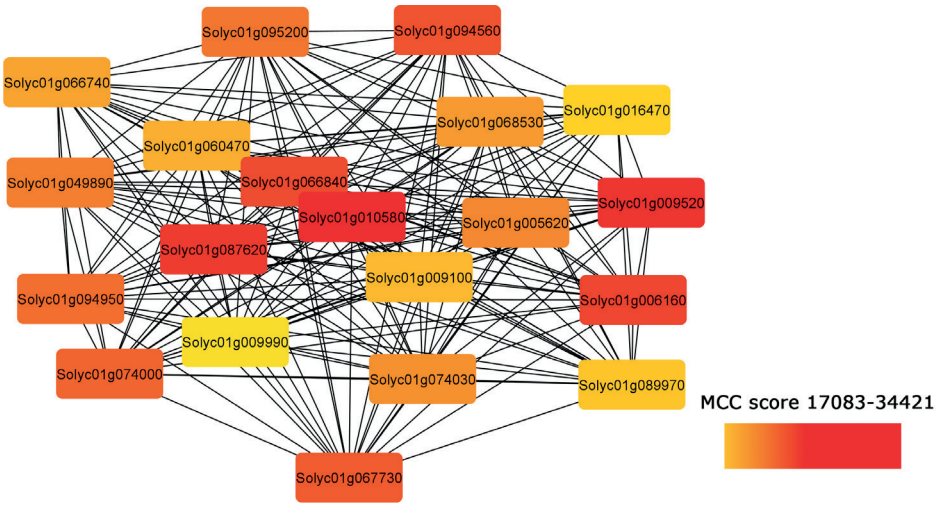

Figure 3.15. Hub genes and their centrality. The color gradient indicates the Maximum Clique Centrality (MCC) score. MCC calculates the size of the largest clique that a node belongs to and assigns a centrality score based on this. The score is indication of the centrality which is represented by the redness of the color.

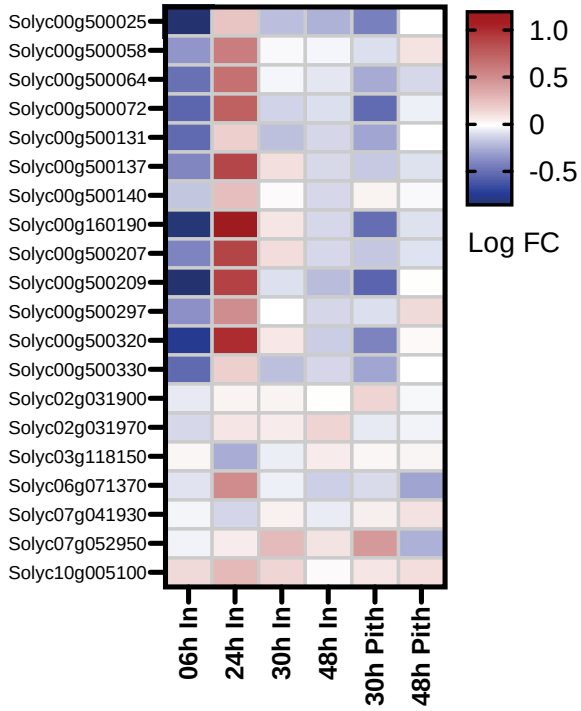

Figure 3.16. Hub gene expression heatmap. The heatmap colors indicate average fold change in response to FR treatment, red indicating upregulation in FR and blue indicating downregulation.

3.2.11 TF identification identified well-recognized motifs that regulate cell fate

Next, we wanted to explore the possible transcriptional regulators of the gene expression changes we observed. With a list of tomato transcription factors (ITAG 3.2 annotation) obtained from Plant Cistrome Database (http://neomorph.salk.edu/dap_web/pages/index.php)(O'Malley et al., 2016), we identified the DEGs which are TFs (Table S3.2). Then, we looked for TFs whose Arabidopsis orthologs had functional annotations related to cell size, cell elongation and cell expansion. Our primary focus moving forward was centered on the transcription factors (TFs) that have already been identified and are known for their functions in cell or organ elongation. Many of these TFs have previously been studied in Arabidopsis and Solanaceae roots under stress conditions, where they play a role in regulating e.g. epidermis cell functions and anthocyanin biosynthesis, including basic-helix-loop-helix (bHLH) *GLABRA3 (GL3)*, *ENHANCER OF GLABRA3 (EGL3)*,) and MYB transcription factors (such as *CAPRICE PAP1*, *PAP2*, *MYB113* or *MYB114* in Arabidopsis and *FER* in tomato). MYBs, such *AtMYB30* in Arabidopsis root

and *PHB/PHV-LIKE1* and *SlCNAL1* in tomato root xylem for instance, have a well-conserved function in cell type differentiation, such as in endodermis and xylem (Wada et al., 1997; Bernhardt et al., 2003; Feller et al., 2011; Zhao et al., 2012; Kim et al., 2014; Wang et al., 2015; Sakaoka et al., 2018; Nagao and Tominaga, 2020; Kajala et al., 2021).

Our specific objective was to investigate whether our FR-responsive DEGs share common regulatory motifs. To address this, we conducted motif enrichment analysis using the 500bp promoters of all FR-responsive upregulated DEGs and identified the presence of 5 enriched motifs with MEME suite (Motif based sequence analysis tool) (https://meme-suite.org/meme/index.html)(Figure 3.17). Then the enrichment was submitted again to TOMTOM to find Arabidopsis TFs according to the database (O'Malley et al., 2016). First motif was found in MYB17, 41, 49, 107, WRKY22, 27, 29 and motif 2 was found in TCPs (At1g72010, At1g72010, At5g08330, At5g08330, At1g69690, the third motif are found in TCPs, MYBs and BPCs (BASIC PENTACYSTEINES) in Figure 3.17. Homologs of five TFs belonging to our DEGs have been also identified in FR response in Arabidopsis from a yeast 1-hybrid screen (*Solyc10g079070* (*AT3G57800*), S*olyc06g083170* (*AT3G07340*), *Solyc01g109700* (*AT4G34530*), *Solyc04g005660* (*AT3G28857*), *Solyc07g056360* (*AT2G42870*)) (Buti, 2008).

In our list of 25 differentially expressed TFs in response to FR (Table S3.2), there are members of the TCP, MYB, and bHLH TF families that could be the candidates to bind the identified motifs (Figure 3.17). This can provide clues on FR regulatory elements and provide insight into the transcriptional dynamics orchestrated by FR light in plants.

3.2.12 Candidate TFs were selected for follow-up study

We further screened the DEG TF list based on the functions reported in literature, and selected three upregulated TFs for further analysis. These TFs are encoded by *Solyc08g080150*, *Solyc01g090760*, *Solyc07g053450*, which are all highly upregulated in FR (Figure 3.18). Full details can be found in Table S3.2, below are the descriptions of the selected TFs for further study:

Solyc01g090760, a GATA transcription factor from the zinc finger DNA binding protein family. This TF plays a crucial role in regulating transcription processes essential for development and cell differentiation (Gao et al., 2015). Additionally, BLAST results indicate that its homologs in Arabidopsis may be involved in elongation processes (Lu et al., 2021; Hou et al., 2022).

Solyc08g080150, also known as *SlTCP20*, is highlighted for its diverse functions observed in leaf development, regulation of flower symmetry, influence on shoot branching, and participation in senescence (Parapunova et al., 2014). TCP TFs are characterized by the TCP domain, featuring a non-canonical basic-helix-loop-helix (bHLH) structure, and are named after the first three characterized family members (Cubas et al., 1999).

Solyc07g053450, a bZIP transcription factor, is identified as playing a pivotal role in various biological processes, particularly in responding to abiotic stresses (Liu et al., 2023a). This TF is a member of the BZIP transcription factor family.

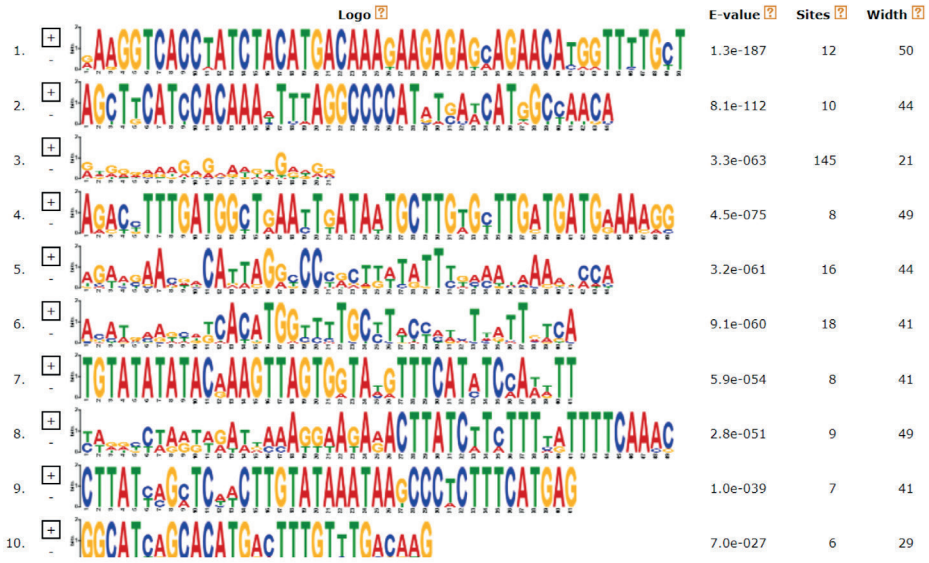

Figure 3.17. Motif enrichment of the upregulated FR-responsive DEGs' 500bp promoters. Promoters are obtained 500bp upstream of TSS from Phytozome v13 (Goodstein et al., 2012), motif enrichment was carried out with MEME suite.

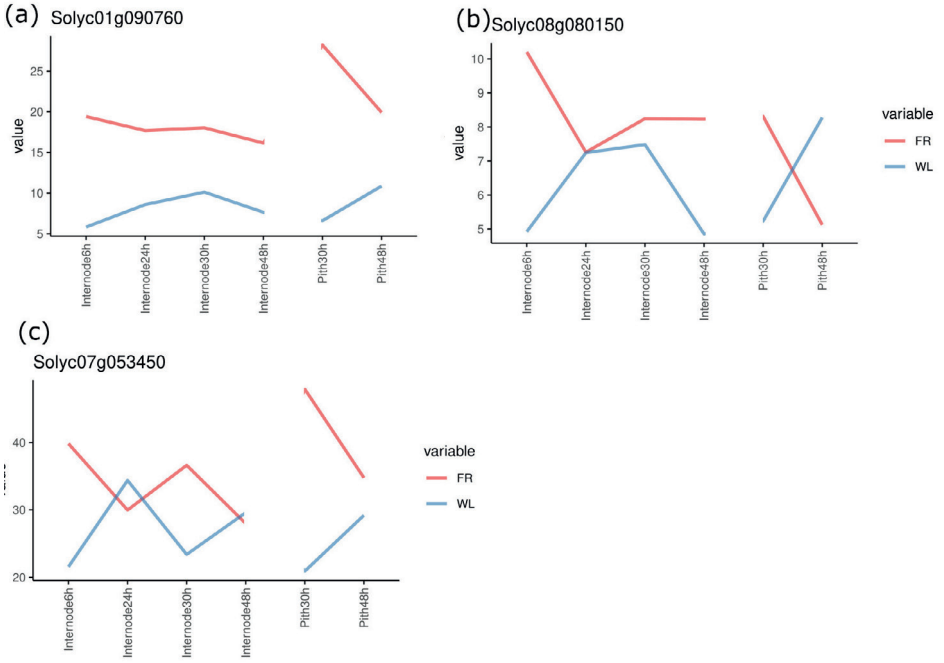

Figure 3.18. *Solyc08g080150*, *Solyc01g090760*, and *Solyc07g053450* expression pattern obtained from RNA-seq data. We used normalized expression of these three genes from RNA-seq data and plotted it with R 4.0 (R Development Core Team, 2010).

3.3 DISCUSSION

Progress has been made in the past decades to identify how the shoot elongation response is regulated during shade avoidance response (SAS) in Arabidopsis, especially at cellular level, i.e. how cell elongation is regulated. Petiole and hypocotyl elongation in Arabidopsis has been well-documented as a characteristic response to an increased presence of far-red (FR) light, with the involvement of auxin-mediated epidermal cell elongation having been substantiated (Bou-Torrent et al., 2014; Procko et al., 2016; Michaud et al., 2017). In the realm of Arabidopsis SAS research, significant attention has been given to deciphering the signals of shade-induced responses, which encompass auxin biosynthesis, transport, and sensitivity activation. These processes are orchestrating organ elongation, notably in petioles (Ma and Li, 2019). While these studies have enriched our understanding of plant responses to environmental cues, there remains a need to unravel the mechanisms governing internode cell elongation in stem-forming plant species, as this area holds the potential to unveil novel insights into plant adaptation and growth under varying light conditions. Here, we focus on the gene expression changes in stem elongation during SAS in tomato, which was described in phenotypic detail in the previous chapter.

3.3.1 Auxin could be the key regulator for elongation in tomato SAS

"Response to auxin" GO term was highly enriched in our GO analysis, largely due to many *SAURs* (*Small Auxin-Up-regulated RNAs*) upregulated in our data. The actual auxin pathway DEGs had changes of up to 38-fold. Auxin function in cell elongation and stem elongation has already been reported before (Kutschera and Niklas, 2007; Bou-Torrent et al., 2014), but here, we also found auxin response upregulated specifically in pith, linked to the pith cell elongation and division patterns that we reported in the Chapter 2. ATP and ADP activity and carbohydrate metabolism pathways were also enriched in FR-upregulated DEGs in pith (Figure 3.7), which might indicate auxin-induced the cell division and expansion activities are especially active in pith compared to the whole internode.

SAURs are a class of small, non-coding RNAs that are involved in the regulation of auxin signaling in plants. SAURs have been implicated in a wide range of physiological processes in plants, including growth, development, and stress responses (Ren and Gray, 2015; Stortenbeker and Bemer, 2019). In the context of SAS, SAURs have been shown to be upregulated in response to low R:FR ratio in Arabidopsis. Specifically, SAUR19 and SAUR20 have been identified as key regulators of hypocotyl elongation in Arabidopsis under low R:FR. SAURs are thought to act downstream of the phytochrome signaling pathway, and their upregulation is possibly driven by PIF-regulated auxin, which is also involved in SAS (Devlin et al., 2003; Vandenbussche et al., 2007; Franklin and Quail, 2010). *SAUR* genes, a prominent family of early auxin-response genes, have demonstrated their rapid upregulation by auxin in various plant species, including Arabidopsis, rice, and tomato, suggesting a conserved role in auxin responses (Ren and Gray, 2015). Specifically, many *SAUR*s in Arabidopsis exhibit swift induction in response to shade treatment, implicating their involvement in the shade avoidance response (Devlin et al., 2003; Kohnen et al., 2016a). Notably, overexpressing SAUR19 in the *pif4* mutant background effectively rescued impaired hypocotyl elongation at high temperatures, and SAUR36 overexpression also promoted hypocotyl elongation (Franklin et al., 2011; Stamm et al., 2013).

SAUR proteins play a crucial role in regulating cell elongation by affecting proton pumps and subsequently activating cell wall modifying enzymes. The mechanism underlying SAUR-mediated cell expansion involves the interaction of SAUR proteins with PP2C.D phosphatases, which leads to the activation of plasma membrane H^+-ATPases, thus promoting cell expansion. This process results in the acidification of the cell wall and the subsequent activation of cell wall modifying enzymes, which facilitate cell

elongation(Ma and Li, 2019; Stortenbeker and Bemer, 2019) Additionally, *SAUR* genes can be regulated by various factors, including auxin and other environmental cues, and their overexpression has been shown to induce growth, indicating their significant role in plant development. Furthermore, SAUR proteins are involved in the induction of growth via cell elongation, and their activity is not limited to the juvenile stage but extends to various tissues, indicating their widespread function in plant growth and development (Stortenbeker and Bemer, 2019). Therefore, SAUR proteins act as effectors of hormonal and environmental signals in plant growth, with their main function being the induction of cell elongation by repressing PP2C.D activity and promoting cell expansion (Ma and Li, 2019; Stortenbeker and Bemer, 2019).

Furthermore, *SAUR* gene expression is subject to regulation by various factors in different species. Studies in tomato, cotton, poplar, citrus, watermelon, maize, and Arabidopsis have unveiled specific expression patterns for different *SAUR* genes throughout plant development. Additionally, the expression of distinct sets of *SAUR* genes can be either positively or negatively regulated by multiple hormones, including auxin, cytokinin, gibberellic acid (GA), brassinosteroids, ethylene, ABA, and JA, as well as by varying light conditions, temperature, and stress factors in different plant species. In general, *SAUR* genes tend to be upregulated in response to growth-inducing factors like auxin and downregulated under stress conditions or in response to growth-inhibiting hormones such as ABA and JA. This dynamic regulation likely represents a plant's adaptive strategy to balance growth and defense mechanisms (Knauss et al., 2003; Franklin et al., 2011; Walcher and Nemhauser, 2012; Qiu et al., 2013; Stamm et al., 2013; Luo et al., 2018). Notably, the responsiveness of *SAUR* genes to environmental and hormonal cues primarily occurs in the tissues where they are already expressed, emphasizing their tissue-specific expression patterns (Hagen and Guilfoyle, 2002; Markakis et al., 2013; Ren and Gray, 2015; van Mourik et al., 2017). Overall, the upregulation of *SAURs* in response to shade conditions is believed to be an important component of SAS by promoting cell elongation, allowing plants to modulate their growth and development in response to changing light conditions.

3.3.2 Much of the variance of expression data is due to diurnal rhythm

FR effect on elongation of tomato first internode was seen at two days (Figure 3.1), considerably slower than the FR effect on elongation of petiole of Arabidopsis (Walter et al., 2007; Ciolfi et al., 2013; Morón-García et al., 2022). Therefore, based on our data

where stem elongation is distinguishable at two days, we selected earlier timepoints, including two different times of day for the diurnal rhythm to understand the response. When we analyzed the transcriptome data the major effect (Montavon et al., 1983) is coming from diurnal rhythm in the first few principle components (PC1, PC2, PC3) in PCA analysis and DE analysis (Figure S1, Figure 3.4c). Diurnal rhythm adaptation could have been important for tomato (Xiang et al., 2022). In Figures 3.10 and 3.11, we found that some clear diurnal rhythm responses when comparing morning vs afternoon transcriptomes. In the previous research into tomato diurnal rhythm, the elongation of stems declined during the day while the soluble sugars increased in the morning and decreased from afternoon till night (Went, 1944). During our observations, the expression of gene *Solyc08g082860* related to the sugar trehalose showed a reduction in levels during the afternoon, suggesting less protein from trehalose from damaging cellular structures and molecules caused by environmental stress (Lunn et al., 2014). Additionally, we observed an activation of sugar transfer processes, particularly involving the activity of methyltransferases, indicating an increase in sugar transfer activities during the afternoon period. These findings collectively indicate dynamic changes in sugar metabolism and transfer processes over the course of the day. Therefore, the response of tomato stem elongation to far-red light unveils dynamic changes in sugar metabolism influenced by diurnal rhythm.

In the context of WGCNA, we observed intriguing patterns across multiple gene modules (Figures 3.12-3.14, S3.3). One of the standout findings is within the green module, where FR response exhibits a diurnal rhythm in the internode. These genes are functionally associated with essential processes such as photosynthesis and protein translation. It's worth noting that the impact of FR on this module may be limited, as key regulators could have already reached their peak expression levels due to diurnal clock influences, darkolivegreen module associated with intracellular carbohydrate metabolism, shows a clearer diurnal pattern in WL but not that obvious in FR, even though the expression value is higher (Figure 3.19). The diverse responses of various gene modules shed light on the intricate regulatory mechanisms at play in plant adaptation to changing light environments and provide insights for further investigation.

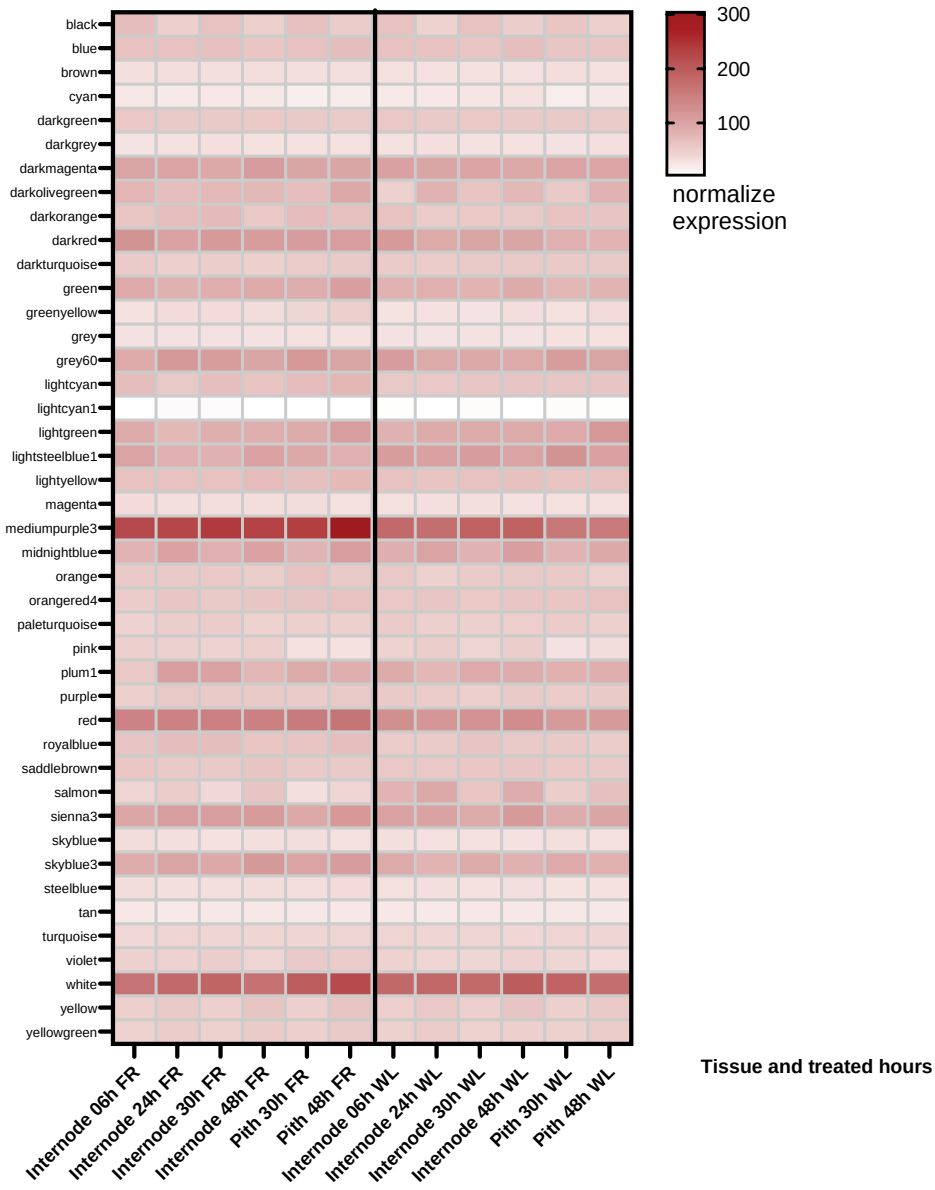

Figure 3.19. Average normalized expression values for each module, categorized by WGCNA, under conditions of WL and FR.

3.3.3 Stable photosynthesis expression showed in the internode and pith

We identified distinct modules representing clusters of nodes with shared attributes or connectivity patterns (Figure 3.12). Heatmaps revealed consistent FR-upregulation of genes in specific modules, including mediumpurplegrey3, enriched in GO terms relating to photosynthesis and protein synthesis. Conversely, salmon and lightsteelblue1 modules showed downregulation. Additionally, genes within the turquoise module, mainly downregulated over time, play pivotal roles in plant development and maintenance, particularly in ribosome, nucleosome, and photosystem I-related functions.

Stems possess a notable photosynthetic activity (Hetherington et al., 1998). The stems capture and fix carbon dioxide generated during respiration concurrent with photosynthesis, yet there is a lack of observable carbon exchange (Xu et al., 1997). Under high R:FR ratios, stems exhibit enhanced photosynthetic capacity compared to lower R:FR conditions (Hattrup et al., 2007). Our WGCNA modules, specifically the blue and green modules, align with these observations. These modules reveal stable expression patterns of photosynthesis-related genes over time, with a distinct downregulation in FR compared to WL conditions (Figure 3.12). Intriguingly, key regulators, primarily from the turquoise module and yellow modules (as seen in Figures 3.12-3.14), maintain little fold change between FR and WL. However, at certain timepoints, we observed the absence of GO terms associated with carbon dioxide or carbohydrate exchange which was enriched in the morning timepoint especially in pith (Figures 3.9-3.11). This discovery suggests that the plant's inherent homeostatic mechanisms governing photosynthesis may also support respiration processes, thereby stabilizing internal metabolism. This dynamic interplay between gene modules and metabolic processes underscores the plant's remarkable ability to maintain equilibrium in response to shifting environmental conditions.

3.3.4 Summary

In the face of low R:FR conditions, we observed a significant upregulation of auxin-responsive genes, particularly SAURs. The diurnal rhythm emerged as a key regulator, influencing various pathways such as hormone response, sugar metabolism, and respiration. A detailed examination of pith tissue-specific transcriptomes revealed substantial differences comparable to the whole internode, unveiling specific regulatory pathways. Notably, several transcription factors previously mentioned were identified in the differentially expressed genes, underscoring their role in the response to low R:FR. Subsequently, our focus shifted to hormones and these transcription factors in the subsequent chapters for a deeper exploration of their regulatory roles.

3.4 ACKNOWLEDGEMENTS

We express our gratitude to the Utrecht Sequencing Facility team (USEQ) for their expertise in performing sequencing, multiplexing, and mapping. Special thanks to Dr. Sara Buti, Dr. Cheyang Liao, and MSc Muthanna Biddanda Devaiah for their invaluable assistance with library preparation and troubleshooting. We also extend our appreciation to Dr. Leonardo Jo, Dr. Maria Angelica Sanclemente, and Dr. Andres Romanowski for their guidance in bioinformatics analysis.

3.5 MATERIALS AND METHODS

3.5.1 Plant materials and growth conditions

We germinated *Solanum lycopersicum* seeds (cv Moneymaker (obtained from Intratuin B.V) and M82 (obtained from Tomato Genetics Resource Center)) for one week in sealed plastic boxes padded with a paper towel soaked with tap water. After one week, similarly sized seedlings were transferred to a 7 cm square pot filled with sieved Primasta ® soil. One week after transfer, plants were randomly separated into two groups and put into far-red or white light treatment.

We grew the seedlings grown at 20°C, 70% humidity, 16/8 hour light/ dark cycle in white light conditions for 7 days before the start of the light treatments. For this experiment two treatments with different light conditions were used: white light (WL) and far-red (WL+FR). WL condition light intensity was 200 PAR (photosynthetically active radiation). WL+FR condition light intensity was 200 PAR white light supplemented with additional FR to reach R:FR (red-light: far-red light = 0.21).

3.5.2 Phenotype measurements

Stem and internode length were measured with digital caliper every day at 10:30am and 4:30pm.

3.5.3 Tissue harvest for RNA-seq

The first internode (between the cotyledons and first true leaf) was harvested. Each group of internodes were collected at 6, 24, 30, 48 hours after treatment start. In the end, 200+ samples were collected for two light treatments (WL and WL+FR), two cultivars, four timepoints and two tissues with at least 4 biological replicates per group. Samples were placed immediately into liquid nitrogen until mRNA isolation.

3.5.4 RNA-seq library preparation

3.5.4.1 RNA isolation and fragmentation

We prepared RNA-seq libraries according to the random-primer primed method published originally in (Townsley et al., 2015) with modifications from Kajala et al., 2021. Tissue samples were ground by hand and immediately incubated in 250 μL lysis buffer (LBB: 100 mM Tris-HCl, 1000 mM LiCl, 10 mM EDTA, 1% SD, 5 mM DTT, Antifoam A) supplemented with 5 μ l/ml β-mercaptoethanol before use. The samples were transferred to 2ml tubes and the tubes were beat 2 times for 1min at 30 Hz. The samples were incubated at room temperature for 10 min and spun down at 13,000 rpm for 10 min. One uL of 12.5 μM biotin-20nt-dT (Table 3.1) oligo was mixed into 200 μL of lysate in PCR tubes and incubated at room temperature for 10 min. Then, we added 20 μL Biolabs® streptavidin beads per reaction for incubation. The mRNA from samples binds the oligo through the polyA tail, and the biotin in the oligo binds the streptavidin on the beads. This allows pulling down only the mRNA and washing the rest of the material off. So, the samples were separated into magnetic bead-bound mRNA and supernatant by 96 well Magwell® magnetic separator. The bead pellets were washed with 200 μl washing buffer series: washing buffer A (WBA; 10 mM Tris-HCl, 150 mM LiCl, 1 mM EDTA, 0.1% SDS), washing buffer B (WBB; 10 mM Tris-HCl, 150 mM LiCl,1mM EDTA), and low salt buffer LSB (20 mM Tris-HCl,150 mM NaCl, 1 mM EDTA). The mRNA was eluted in 16 uL Tris-HCl with 80°C. These pulldown and washing steps were repeated a second time to remove non-specifically associating rRNA from the samples.

RNA fragmentation was carried out by preparing 10 μL mixtures of 1.5 μl 5X Thermo Scientific RT buffer, 0.5 μl Invitrogen ® random primers, 8 μl mRNA from the above elution. The mixtures were put into thermocycler for temperature-induced fragmentation and priming of 1st strand of cDNA (25°C 1 sec, 94°C 1.5 min, 4°C 5 min, 4°C hold).

3.5.4.2 cDNA synthesis

We prepared first strand master mixture as following: 1.5 μL 5X Thermo Scientific RT buffer, 1.5 μL 0.1M DTT, 1 μL H_2O, 0.5 μL 25mM dNTPs, 0.5 μL RevertAid H minus reverse transcriptase enzyme (Thermo Scientific). The mixture was added onto the samples and incubated in thermocycler: 25°C 10min, 42°C 50min, 50°C 10min, 70°C 10min, 4°C hold.

The second strand synthesis, end repair, and A-tailing were performed by adding a 5 μL mixture to the first strand, consisting of 1.5 μL H2O, 0.4 μL 25mM dNTPs, 1 μL

DNA polymerase I (Thermo Fisher), 0.1 μL RNaseH (NEB), 0.4 μL NEBNext® End Repair Module enzyme mix, 0.2 μL Taq, and 1.4 μL. This mixture was incubated in a thermocycler following these temperature and time settings: 16°C for 20 minutes, 20°C for 20 minutes, 72°C for 20 minutes, and held at 4°C.

Subsequently, the reaction mixture was left at room temperature for 5 minutes with a mix of Beckman® Ampure XP beads at 1.5 times the volume, followed by two washes with 200 μL of 80% ethanol each, until the beads were completely dry.

3.5.4.3 Adapter ligation

The dry beads were mixed with 3 ul of annealed 1 μM universal adapter primers (8μL of 100μM each primer was combined with 784 μL of H_2O and cooled through the program: 94°C 1min, (94°C 10sec) * 60 cycles -1°C /cycle, 20°C 1min, 4°C hold). Then, 7 μL ligase mixture (5 μL Enzymatics 2X Rapid T4 ligation buffer, 0.25 μL Biolabs® DNA ligase) was added for 15-min room temperature incubation.

We added 10 μL of 50 mM EDTA and 25 μL Ampure XP Bead Resuspension buffer (15% PEG 8000, 2.5M NaCl) to each sample, washed with 80% EtOH twice, and eluted the ligated DNA fragments with 20-22 μL 10mM Tris.

3.5.4.4 Enrichment, indexing and quantification

We used 10 μl of cDNA into enrichment mixed with 4 μL 5X Phusion HF (Thermo Fisher) buffer,2.6 μL H_2O, 1 μL 2 μM PE1 primer, 1 μl 8 μM each EnrichS1 + S2 primers (Table 3.1), 0.2 μl 25mM dNTPs, and 0.2 μl Phusion Polymerase (Thermo Fisher). Each sample used 1 μl of appropriate unique indexed enrichment oligo (Townsley et al., 2015). The mixture was heated in thermocycler with the following program: 98°C 30 sec, (98 °C 10 sec, 65 °C 30 sec, 72 °C 30 sec) *12 cycles, 72 °C 5 min, 10 °C hold.

We cleaned the enriched libraries according to Bailey-Serres lab protocol: 1.1 volume of well-resuspended Ampure beads are mixed well with the samples, followed by washing twice by 200 μl of 80% EtOH and resuspending in 10 μl 10mM Tris pH 8.0.

One μl of the samples were used for quality check by Bioanalyzer High Sensitivity DNA Analysis kit, and we selected cleaned library of 200-350 bps based on the peaks. Libraries were pooled together for sequencing with the same target concentration. A final clean-up was done with 0.8 volumes of Ampure beads and elution to the final target volume.

Table 3.1. Primer sequences adapted in library preparation.

Primer name	Sequence
PE1-lig	5'-CACTCTTTCCCTACACGACGCTCTTCCGATCT-3'
ILL-lig	5'-P-GATCGGAAGAGCACACGTCTGAACTCCAGTCAC-3'
EnrichS1	5'-AATGATACGGCGACCACCGA-3'
EnrichS2	5'-CAAGCAGAAGACGGCATACGA-3'
Biotin	5'-ACAGGACATTCGTCGCTTCCTTTTTTTTTTTTTTTTTT-3'

3.5.5 Sequencing and alignment

Barcoded libraries were sequenced on the High Output : 1 x 75 bp Illumina NextSeq500 at USEQ (Utrecht Sequencing Facility). The initial read quality assessment with FastQC, followed by sequence trimming using TrimGalore (https://github.com/FelixKrueger/TrimGalore/blob/master/Docs/Trim_Galore_User_Guide.md), rRNA removal via SortMeRNA, read mapping and read-group annotation utilizing STAR (Dobin et al., 2013), alignment quality control with RSeQC (Wang et al., 2012) and Preseq (https://smithlabresearch.org/software/preseq/), PCR duplicate detection employing Sambamba MarkDup (Tarasov et al., 2015) , and gene expression and biotype quantification through featureCounts (Liao et al., 2014). The sequences were mapped against ITAG4.1 annotation of tomato reference genome SL4.1 https://solgenomics.net/organism/Solanum_lycopersicum/genome.

3.5.6 Differential expression analysis

We adapted the DE analysis method from literature (Kajala et al., 2021). Libraries with at least 500,000 mapped raw exon counts were selected for further analysis. First, we wanted to identify the differentially expressed genes (DEGs) for various comparisons. Raw counts were firstly converted to count per million (CPM) using with edgeR package (Robinson et al., 2009). Genes with CPM > 0.5 in at least one sample for all 4 biological replicates were kept for the analysis. CPM values were quantile normalized with the voom function (Law et al., 2014). Principal component analysis (PCA) was conducted to distinguish the separation of samples by timepoint, treatment and cultivar with the ggplot2 package (Wickham, 2009) in R.4.1.3 (R Development Core Team, 2010). DEGs were detected with the limma R package (Ritchie et al., 2015). The data underwent a Log2 transformation, and a significance threshold of FDR-adjusted p-value (adj.P.Val) ≤ 0.15 was applied to identify differentially expressed genes. The adjusted P value list of DEGs were obtained for further analysis. Venn plots were generated by DEGs using imageGP website (Chen et al., 2022b).

3.5.7 Gene ontology enrichment analysis

Gene Ontology enrichment analyses were done with the GOseq R package (Young et al., 2010) with Kallisto output (TPM). Gene Ontology annotation (ITAG4.1) was obtained from Sol Genomics Network (solgenomics.net). A term was considered significantly enriched if it has a p value < 0.05 and a fold enrichment > 1. Fold enrichment was calculated as (genes annotated with a term in the query dataset / total genes in the dataset) / (genes annotated with a term in the background set / total expressed genes). The results were visualized using R's "pheatmap" function.

3.5.8 Co-expression network analysis

Co-expression network modules were generated using the WGCNA R package (version 1.68) (Horvath and Langfelder, 2009). To prepare the data, individual libraries for each treatment and tissue were first quantile normalized using RPKM and then log-transformed with log2(x+1) prior to analysis. 75% of the most variable genes were used for analysis The selection of a threshold value was guided by visualizing the scale-free topology model fit (R^2) across a range of soft thresholds, ultimately opting for a threshold of 7. Subsequently, an unsigned network was constructed using the "blockwiseModules" function, employing the bicor correlation measure and specifying specific parameters, including a maximum portion of outliers at 0.05, a mergeCutHeight of 0.35, and a minimum module size of 20To have a visual representation of gene expression in each module, we drew heat maps for each module with Graphpad Prism 9 (Figure S3.3). GO enrichment analysis was performed via GOseq R package and adjusted P value cut-off of 0.05 and q value cut-off of 0.05. The network was visualized using Cytoscape (version 3.9.1). To identify key genes within the network, we employed the CytoHubba plugin (Chin et al., 2014). We extracted the top 20 genes, and those genes that appeared in the top ranks across all four CytoHubba ranking methods, namely maximal clique centrality (MCC), edge percolated component (EPC), maximum neighborhood component (MNC), and node connect degree, were designated as hub genes.

3.5.9 Motif enrichment and TF identification

To predict motifs, we followed this procedure: Firstly, we acquired 500 bp promoters of the FR-responsive DEGs from the Phytozome database (Goodstein et al., 2012). Subsequently, we employed MEME Suite (McLeay & Bailey, 2010) with default settings to conduct motif prediction. Later, we conduct our result with Tomtom for comparison of one or more motifs with a database of established motifs (O'Malley et al., 2016).

For the identification of transcription factors (TFs), we sourced TF lists from the Plant Cistrome Database (O'Malley et al., 2016) and cross-referenced them with the ITAG 3.2 database to ensure accurate TF matching. Ortholog information for Arabidopsis was obtained from TAIR (Lamesch et al., 2012). We queried the TF multifasta file against the latest Ensemble 53 release (2022-07) of Arabidopsis peptides. The metadata encompasses Gene ID (derived from a blast match with Ensemble 53 release - 2022-07), Gene symbol, Description, and Curator summary (all sourced from TAIR Public data release 2021-06-30), as well as the Family of TF as categorized by PlantTFDB and AGRIS_AtTFDB.

3.6 SUPPLEMENTARY DATA

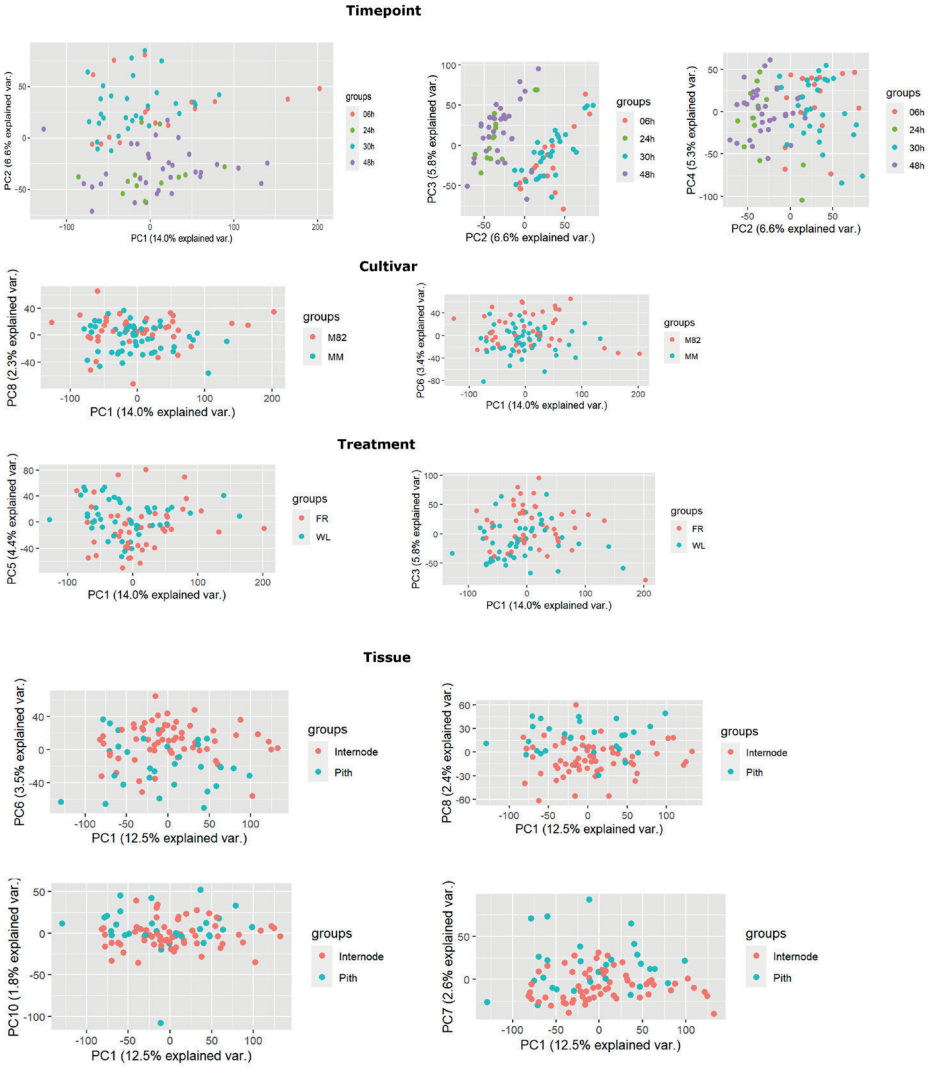

Figure S3.1. Principal component analysis of RNA-seq samples, colored by different experimental factors including treatment, cultivar, timepoint and tissue.

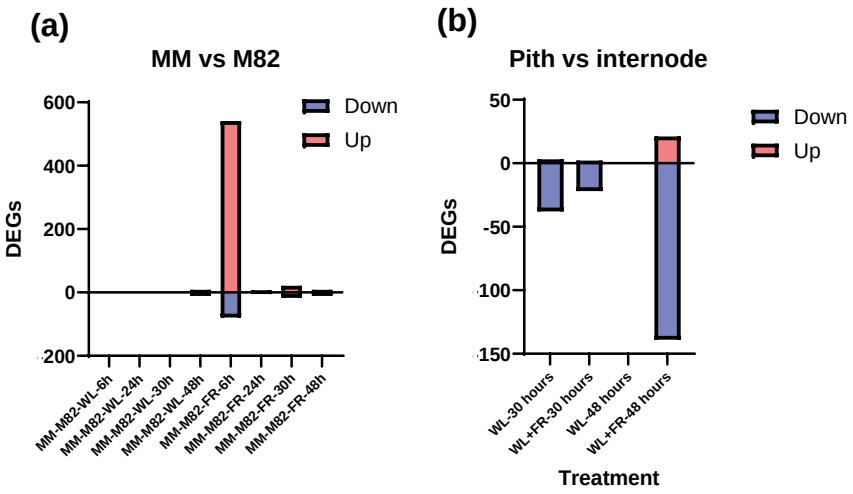

Figure S3.2. Differentially expressed genes (DEGs) between cultivars and tissues. Bar plot shows the number of DEGs in different comparisons. (a) First internode DEGs comparing Moneymaker vs M82 at each timepoint and treatment. (b) Tissue-specific DEG from comparison of first internode vs pith DEGs at each timepoint and treatment.

Table S3.1. Gene numbers belonging to each module from WGCNA analysis.

Color of modules	Count of genes
turquoise	2423
blue	1885
brown	1884
yellow	1779
grey	1740
green	1469
red	852
black	559
pink	433
magenta	407
purple	372
greenyellow	349
tan	201
cyan	183
salmon	183
midnightblue	175
lightcyan	171
grey60	166
lightgreen	162
lightyellow	161
darkred	125
royalblue	125
darkgreen	124
darkturquoise	122
darkgrey	119
orange	110
darkorange	105
white	101
skyblue	97
saddlebrown	90
steelblue	87
paleturquoise	72
violet	65
darkolivegreen	64
darkmagenta	47
sienna3	42
yellowgreen	41
skyblue3	35
plum1	34
orangered4	33
lightsteelblue1	26
mediumpurple3	26
lightcyan1	25
Grand Total	**17269**

Table S3.2. DEGs from DEG analysis which are transcriptome factor. Functional annotations were obtained from Plant Transcription Factor Database (Jin et al., 2015; Jin et al., 2017), Solgenomics network (Fernandez-Pozo et al., 2015) and literature (Yang et al., 2015; Padmanabhan et al., 2022). Homologs from Arabidopsis were identified by multi-blast using Arabidopsis protein sequences. Red color indicates pith specific regulators.

DEGs list	altName	nodeAttr	Function annotation from database	TAIR_ID	Short description_ (30-06-2021)	Curator_summary_(30-06-2021)
Solyc04g007000	AP2/B3 transcription factor family protein	pink	Ethylene-responsive transcription factor4	AT1G13260	related to ABI3/ VP1 1	Encodes an AP2/B3 domain transcription factor which is upregulated in response to low temperature. It contains a B3 DNA binding domain. It has diurnal regulation and may function as a negative growth regulator. The mRNA is cell-to-cell mobile.
Solyc07g005400	bHLH transcription factor 050	yellow	Regulation of cell size	AT2G24260	LJRHL1-like 1	Encodes a basic helix-loop-helix (bHLH) protein that regulates root hair and sperm cell development. One of the three Arabidopsis homologs of the Lotus japonicus ROOTHAIRLESS1 (LjRHL1) gene: At2g24260 (AtLRL1), At4g30980 (AtLRL2), and At5g58010 (AtLRL3).
Solyc08g080150	TCP transcription factor 20	grey	Regulation of cell size	AT2G43060	TCP family transcription factor	-
Solyc01g090760	GATA transcription factor	blue		AT2G45050	GATA transcription factor 2	Encodes a member of the GATA factor family of zinc finger transcription factors. A positive regulator of photomorphogenesis.
Solyc04g077780	LIM domain-containing protein	brown		AT1G10200	GATA type zinc finger transcription factor family protein	Encodes a member of the Arabidopsis LIM proteins: a family of actin bundlers with distinct expression patterns. WLIM1, WLIM2a, and WLIM2b are widely expressed, whereas PLIM2a, PLIM2b, and PLIM2c are predominantly expressed in pollen. Regulates actin cytoskeleton organization.
Solyc10g079070	bHLH transcription factor 065	darko-livegreen		AT3G57800	basic helix-loop-helix (bHLH) DNA-binding superfamily protein	Together with bHLH48 associates with phytochrome interacting factor 7 to regulate hypocotyl elongation.
Solyc07g053450	Basic-leucine zipper (BZIP) transcription factor family protein	turquoise	Leaf cell number and cell size	AT2G42380	Basic-leucine zipper (bZIP) transcription factor family protein	Encodes a member of the BZIP family of transcription factors. Forms heterodimers with the related protein AtbZIP61. Binds to G-boxes in vitro and is localized to the nucleus in onion epidermal cells.

DEGs list	altName	nodeAttr	Function annotation from database	TAIR_ID	Short description_ (30-06-2021)	Curator_summary_(30-06-2021)
Solyc05g009660	Transcription factor PERIANTHIA	black	Regulation of flower development	AT1G68640	bZIP transcription factor family protein	Encodes bZIP-transcription factor. Mutant plants have extra floral organs. PAN is essential for AG activation in early flowers of short-day-grown plants. Binds directly to 5'-AAGAAT-3'regulatory sequence in AG promoter.
Solyc05g048830	MYB transcription factor	grey		AT3G61250	myb domain protein 17	LATE MERISTEM IDENTITY2 (LMI2) is a target of the meristem identity regulator LEAFY (LFY). Has a role in the meristem identity transition from vegetative growth to flowering. Member of the R2R3 factor gene family.
Solyc06g049040	Basic-leucine zipper (BZIP) transcription factor family protein	grey		AT2G40620	Basic-leucine zipper (bZIP) transcription factor family protein	Basic leucine zipper transcription factor. Localizes from cytoplasm to the nucleus under heat stress.
Solyc07g043580	bHLH transcription factor 052	green	De-etiolation;red light signaling pathway;response to low fluence blue light stimulus by blue low-fluence system;regulation of auxin biosynthetic process;	AT2G43010	phytochrome interacting factor 4	Isolated as a semidominant mutation defective in red -light responses. Encodes a nuclear localized bHLH protein that interacts with active PhyB protein. Negatively regulates phyB mediated red light responses. Involved in shade avoidance response. Protein abundance is negatively regulated by PhyB.Involved in the regulation of response to nutrient levels. Controls the resistance to B. cinerea in a COI1- and EIN2-dependent manner.
Solyc01g109700	bHLH transcription factor 010	green	Response to blue light;positive regulation of flower development;	AT4G34530	cryptochrome-interacting basic-helix-loop-helix 1	Encodes a transcription factor CIB1 (cryptochrome-interacting basic-helix-loop-helix). CIB1 interacts with CRY2 (cryptochrome 2) in a blue light-specific manner in yeast and Arabidopsis cells, and it acts together with additional CIB1-related proteins to promote CRY2-dependent floral initiation. CIB1 positively regulates FT expression.

DEGs list	altName	nodeAttr	Function annotation from database	TAIR_ID	Short description_ (30-06-2021)	Curator_summary_(30-06-2021)
Solyc05g055940	Vacuolar protein sorting-associated protein (DUF946)	green		AT5G29000	Homeodomain-like superfamily protein	MYB-CC family member. PHL1 acts redundantly with PHR1 to regulate responses to Pi starvation.
Solyc06g083170	bHLH transcription factor 049	turquoise		AT3G07340	basic helix-loop-helix (bHLH) DNA-binding superfamily protein	-
Solyc09g014250	Transcription factor DIVARICATA	grey		AT2G38090	Duplicated homeodomain-like superfamily protein	-
Solyc02g076640		royalblue		AT4G18650	transcription factor-related	A maternally expressed imprinted gene in the endosperm. It’s expression is positively regulated by ROS1.
Solyc02g078130		turquoise	Regulation of transcription from RNA polymerase II promoter;RNA polymerase II transcription factor complex;defense response to fungus;	AT4G20970	basic helix-loop-helix (bHLH) DNA-binding superfamily protein	-
Solyc03g006910				AT4G25410	basic helix-loop-helix (bHLH) DNA-binding superfamily protein	-
Solyc04g005660				AT3G28857	basic helix-loop-helix (bHLH) DNA-binding family protein	Encodes a atypical member of the bHLH (basic helix-loop-helix) family transcriptional factors.

DEGs list	altName	nodeAttr	Function annotation from database	TAIR_ID	Short description_ (30-06-2021)	Curator_summary_(30-06-2021)
Solyc04g007430				AT1G09530	phytochrome interacting factor 3	Transcription factor interacting with photoreceptors phyA and phyB. Forms a ternary complex in vitro with G-box element of the promoters of LHY, CCA1. Acts as a negative regulator of phyB signalling. It degrades rapidly after irradiation of dark grown seedlings in a process controlled by phytochromes. Does not play a significant role in controlling light input and function of the diurnal clockwork. Binds to G- and E-boxes, but not to other ACEs. Binds to anthocyanin biosynthetic genes in a light- and HY5-independent fashion. PIF3 function as a transcriptional activator can be functionally and mechanistically separated from its role in repression of PhyB mediated processes.
Solyc06g062460		yellow		AT3G21330	basic helix-loop-helix (bHLH) DNA-binding superfamily protein	-
Solyc07g008010	R2R3MYB transcription factor 82	grey	Trichome differentiation	AT5G52600	myb domain protein 82	Encodes a nuclear-localized transcription activator that is a member of the R2R3 factor gene family. MYB82 and GL1 can form homodimers and heterodimers at R2R3-MYB domains. At least one of the two introns in MYB82 is essential to the protein?s trichome developmental function.
Solyc07g056360		turquoise		AT2G42870	phy rapidly regulated 1	Encodes PHYTOCHROME RAPIDLY REGULATED1 (PAR1), an atypical basic helix-loop-helix (bHLP) protein. Closely related to PAR2 (At3g58850). Up regulated after simulated shade perception. Acts in the nucleus to control plant development and as a negative regulator of shade avoidance response. Functions as transcriptional repressor of auxin-responsive genes SAUR15 (AT4G38850) and SAUR68 (AT1G29510).

DEGs list	altName	nodeAttr	Function annotation from database	TAIR_ID	Short description_ (30-06-2021)	Curator_summary_(30-06-2021)
Solyc09g065100	bHLH transcription factor 150	royalblue	Trichome differentiation; seed coat development; regulation of proanthocyanidin biosynthetic process	AT4G09820	basic helix-loop-helix (bHLH) DNA-binding superfamily protein	TT8 is a regulation factor that acts in a concerted action with TT1, PAP1 and TTG1 on the regulation of flavonoid pathways, namely proanthocyanidin and anthocyanin biosynthesis. Affects dihydroflavonol 4-reductase gene expression. It is thought that a ternary complex composed of TT2, TT8 and TTG1 is necessary for correct expression of BAN in seed endothelium. Also important for important for marginal trichome development. It binds the promoter of both AT3G26790 and AT1G28300.TT8 interacts with JAZ proteins to regulate anthocyanin accumulation. TT8 acts maternally to affect seed FA biosynthesis and inhibits seed FA accumulation by down-regulating a group of genes either critical to embryonic development or important in the FA biosynthesis pathway. TT8 represses the activities of LEAFY COTYLEDON1, LEAFY COTYLEDON2, and FUSCA3, the critical transcriptional factors important for seed development.
Solyc10g052470	Myb family transcription factor (Fragment)			AT4G39250	RAD-like 1	-
Solyc10g076820	Myb family transcription factor	black		AT2G38090	Duplicated homeodomain-like superfamily protein	-
Solyc10g084340				AT2G28550	related to AP2.7	AP2 family transcription factor that is involved in regulation of flowering and innate immunity. Interacts with CRY2 to regulate CO and FT. TOE1 binds to activation domain of CO and binds CORE sequences of the FT promoter.TOE1/TOE2 are also targets of MiR172b and function in regulation of innate immunity.
Solyc10g086250	R2R3MYB transcription factor 75	yellow		AT1G66370	myb domain protein 113	Encodes a member of the MYB family of transcription factors. Involved in regulation of anthocyanin biosynthesis. Affects the expression of enzymes involved in later steps of anthocyanin biosynthesis.

DEGs list	altName	nodeAttr	Function annotation from database	TAIR_ID	Short description_ (30-06-2021)	Curator_summary_(30-06-2021)
Solyc12g008800	MYB transcription factor	brown		AT5G56840	myb-like transcription factor family protein	-
Solyc12g010800	BZIP transcription factor family protein	turquoise	Leaf cell number and cell size	AT3G58120	Basic-leucine zipper (bZIP) transcription factor family protein	Encodes a member of the BZIP family of transcription factors. Forms heterodimers with the related protein AtbZIP34. Binds to G-boxes in vitro and is localized to the nucleus in onion epidermal cells.
Solyc12g049350	R2R3MYB transcription factor 11			AT2G47460	myb domain protein 12	MYB12 belongs to subgroup 7 of the R2R3-MYB family. It strongly activates the promoters of chalcone synthase (CHS), flavanone 3-hydroxylase (F3H), flavonol synthase (FLS) and - to a lesser extent - chalcone flavanone isomerase (CHI), but cannot activate the promoters of flavonoid-3'hydroxylase (F3'H) and dihydroflavonol 4-reductase (DF). The activation requires a functional MYB recognition element (MRE). Results from the myb12-1f allele indicate that an activation domain might be present in the C-terminus. Overexpression or knock-out plants do not show any obvious phenotype under greenhouse conditions. Young myb12-ko seedlings contain reduced amounts of flavonoids (quercetin and kaempferol), while seedlings as well as leaves of MYB12-OX plants displayed an increased flavonoid content. They did not show any significant difference in anthocyanin content. Expression of CHS and FLS shows a clear correlation to MYB12 expression levels. CHI and F3H show increased transcript levels in the MYB12-OX lines, but no differences in the knock-out. Even in the absence of functional MYB12, flavonol biosynthesis is not completely absent, suggesting functional redundancy. The redundant factors are MYB11 and MYB111 although MYB12 is primarily required for flavonol biosynthesis in roots. Mutations in MYB12 block both auxin and ethylene stimulation of flavonoid synthesis.

DEGs list	altName	nodeAttr	Function annotation from database	TAIR_ID	Short description_ (30-06-2021)	Curator_summary_(30-06-2021)
Solyc01g010910	MYB transcription factor		Lateral organ boundaries	AT2G03810	18S pre-ribosomal assembly protein gar2-like protein	
Solyc01g090460	HD-ZIP	green	INDUCTION: By transition from light to far-red light. {ECO:0000269| PubMed:8106086}	AT1G80810	One of 5 PO76/ PDS5 cohesion cofactor orthologs of Arabidopsis.	Involvement of the Cohesin Cofactor PDS5 (SPO76) During Meiosis and DNA Repair in Arabidopsis thaliana
Solyc01g091630	cutin deficient 2	greenyellow	regulation of transcription, DNA-templated;plant-type cell wall modification; cuticle development; anthocyanin accumulation in tissues in response to UV light; root hair cell differentiation	AT4G00730	AHDP, ANL2, ANTHOCYANIN-LESS 2, ARABIDOPSIS THALIANA HOMEODOMAIN PROTEIN	Encodes a homeodomain protein of the HD-GLABRA2 group. Involved in the accumulation of anthocyanin and in root development. Loss of function mutants have increased cell wall polysaccharide content.
Solyc01g102340	R2R3MYB transcription factor 61	lightyellow	DNA binding regulation of transcription	AT1G74440	MHL	Similar to MPH1, can complement mph1-1 salt sensitivity phenotype.
Solyc01g107190	LOB domain-containing protein 38	grey	Lateral organ boundaries	AT2G03810		18S pre-ribosomal assembly protein gar2-like protein,regulation of asymmetric cell division
Solyc02g077590	Homeobox-leucine zipper-like protein	greenyellow	regulation of transcription, DNA-dependent;response to blue light and absence of light	AT3G59010	PECTIN METHYL-ESTERASE 35, PECTIN METHYL-ESTERASE 61, PME35, PME61	Encodes PME35, a pectin methylesterase. PME35-mediated demethylesterification of the primary cell wall regulates the mechanical strength of the supporting tissue; involved in cell wall modification, pectin catabolic process

DEGs list	altName	nodeAttr	Function annotation from database	TAIR_ID	Short description_ (30-06-2021)	Curator_summary_(30-06-2021)
Solyc02g080260	Woolly	pink	binding to specific DNA	AT4G00730	ANTHOCYANIN-LESS 2	Encodes a homeodomain protein of the HD-GLABRA2 group. Involved in the accumulation of anthocyanin and in root development. Loss of function mutants have increased cell wall polysaccharide content.
Solyc02g081270	NAC domain-containing protein 53	brown	regulation of transcription	AT3G56900	ALADIN	Encodes ALADIN, a component of the nuclear pore complex.
Solyc02g086930	Homeobox-leucine zipper protein HAT5	yellow	sequence-specific DNA binding	AT2G44230	hypothetical protein	
Solyc02g087960	R2R3MYB transcription factor 94	darkorange	sequence-specific DNA binding transcription factor activity	AT1G76990	ACT domain repeat 3	
Solyc02g088190	MYB transcription factor	cyan	sequence-specific DNA binding transcription factor activity	AT1G74440	Similar to MPH1, can complement mph1-1 salt sensitivity phenotype	cellular response to hormone stimulus, cellular response to lipid, cellular response to oxygen-containing compound, response to osmotic stress, response to water, signal transduction
Solyc02g089420	Basic leucine zipper 43	brown	protein heterodimerization activity	AT5G52170	HOMEODOMAIN GLABROUS 7	Encodes a homeobox-leucine zipper family protein belonging to the HD-ZIP IV family.
Solyc02g090400	Myb family transcription factor	yellow	regulation of transcription, DNA-templated; specification of organ identity; negative regulation of gene expression;floral organ formation	AT5G24400	6-PHOSPHO-GLUCONO-LACTONASE 3, EMB2024, EMBRYO DEFECTIVE 2024, PGL3	Encodes a protein with 6-phosphoglucunolactonase activity that localizes to the chloroplasts and the peroxisome. However, mutant phenotypes observed in pgl3 mutant plants can be complemented with a chloroplast-targeted version of the protein. PGL3 likely functions in the oxidative branch of the pentose phosphate pathway. pgl3 mutant phenotypes suggest that it is important in pathogen defense and maintenance of cellular redox homeostasis.

DEGs list	altName	nodeAttr	Function annotation from database	TAIR_ID	Short description_ (30-06-2021)	Curator_summary_(30-06-2021)
Solyc03g007410	Basic helix-loop-helix (BHLH) DNA-binding superfamily protein	grey	stomatal complex development	AT5G07770	Actin-binding FH2 protein	
Solyc03g082430	Growth-regulating factor 5	greenyellow	regulation of transcription, DNA-template; response to red light; response to far red light; response to karrikin	AT2G45480	ATGRF9, GRF9, GROWTH-REGULATING FACTOR 9	Growth regulating factor encoding transcription activator. One of the nine members of a GRF gene family, containing nuclear targeting domain. Involved in leaf development.

HORMONE INTERPLAY IN THE REGULATION FAR-RED-RESPONSIVE STEM ELONGATION IN TOMATO

Linge Li, Ticho Helming, Jesse Wonder, Tjitske Zeekant, Wouter Kohlen,
Gijs van Asselt, Xiren Cao, Ronald Pierik and Kaisa Kajala

ABSTRACT

Understanding shade avoidance mechanisms is crucial for global tomato cultivation. This study explored hormone dynamics underlying neighbor detection responses, focusing on auxin (Indole-3-Acetic Acid (IAA)), gibberellins (GA), and brassinosteroids (BR).

While the origin of auxin during far-red (FR)-response remained elusive, auxin treatment on the internode and the first true leaf induced some elongation. IAA increased cell elongation and division but failed to recapitulate the far-red-induced internode elongation fully. Auxin inhibitors Peo-IAA and BBo had weak effects. Auxin combined with its polar transport inhibitor NPA had an unexpected effect. These results indicate auxin has a role in regulating stem elongation, but there is a need for other actors, potentially GA or BR, to achieve FR-like elongation.

Examining also GA and BR in tomato FR-response showed stem elongation in response to of GA and BR treatment comparable with FR treatment. While IAA-induced transcriptional changes resembled FR-responsive gene expression, GA and BR induced greater elongation, emphasizing their potency. GA or BR inhibition during FR treatment halted elongation, indicating their essential roles. Additionally, inhibition of GA or BR during FR treatment were rescued by BR+IAA or GA+IAA, respectively.

In conclusion, this study uncovers some of the hormonal interactions in regulating FR-induced stem elongation in tomato. IAA, GA, and BR play distinct roles. The findings shed light on dynamic hormone networks governing plant growth responses to light signals informing the plant of its neighbors. Further research into molecular mechanisms promises deeper insights into optimizing plant growth across environments.

4.1 INTRODUCTION

Plants exhibit remarkable plasticity in response to their environment, and light perception is a critical factor influencing growth, development, and reproductive success, ultimately affecting plant fitness. The availability and quality of light are influenced by neighboring plants, leading to changes in the light spectrum, particularly the red to far-red (R:FR) light ratio. This phenomenon, known as shade avoidance syndrome (SAS), triggers a series of morphological changes that enable plants to optimize light capture and photosynthesis (Casal, 2012). Photoreceptors, such as cryptochromes and phytochromes, detect these light signals and initiate complex hormone pathways, contributing to the SAS. In our investigation, we focus on the SAS triggered by low R:FR conditions.

4.1.1 Role of hormones in shade avoidance

Plants have developed intricate physiological reactions to shade, with various phytohormones playing a crucial role in the shade avoidance response. Among these, auxin, gibberellins (GAs), and brassinosteroids (BRs) have been identified as vital for controlling the elongation of hypocotyls induced by shading (Yang and Li, 2017). Auxin plays a pivotal role. Auxin is well known as a very important growth hormone in plant growth. The Dutch biologist Frits Went started the study of the secrets behind plant growth regulation by hormones in the 1920s. One of his early research topics was the influence of the plant tissues surrounding embryonic leaves on plant growth and development. Upon removal of these, plants were much shorter. When looking into the hormones involved, he confirmed the existence of auxin, a growth-promoting hormone (Went, 1928). Auxin is involved in a myriad of plant processes, including organ patterning, tropic responses, vascular development, and growth regulation (Davies, 2010). In *Arabidopsis thaliana*, a defective auxin biosynthesis *taa1* gene was shown to impair the SAS, highlighting the significance of auxin in this process (Tao et al., 2008). In Arabidopsis, an increased concentration of auxin was found to hypocotyl and petiole elongation (Kohnen et al., 2016a; van Gelderen et al., 2018; Küpers et al., 2018), as well as hyponasty (Pantazopoulou et al., 2017, PNAS).

Similarly, gibberellin (GA), initially discovered in rice plants with elongated seedlings due to fungal infection in an 1898 paper published by Shotaro Hori, also contributes to the shade avoidance response by promoting stem elongation through the degradation of DELLA proteins, which are growth repressors by inhibiting a set of growth-promoting transcription factors (Hedden and Sponsel, 2015). In earlier research, the treatment with IAA and GAs could stimulate stem elongation in pea (*Pisum sativum*) (Yang et al., 1996).

Brassinosteroids, another important plant hormone, is essential for normal plant growth (Li and Chory, 1999). Studies in Arabidopsis seedlings have demonstrated that brassinosteroid and auxin activity are required for shade avoidance initiated by reduced blue light (Keuskamp et al., 2012). Besides, it has been demonstrated that BRs play a role in plant growth and development by interacting with auxin and other phytohormones (Kim et al., 2006). Brassinazole (BZ) has been validated as a specific inhibitor of BR biosynthesis, a number of which have been shown to inhibit cytochrome P450s (Asami et al., 2000). Arabidopsis plants treated with BZ exhibit dwarf phenotypes reminiscent of BR biosynthesis mutants (Asami et al., 2000). It is noted that shade-induced stem elongation relies on BRs in Arabidopsis, as BR biosynthesis mutants and BZ-treated Arabidopsis plants fail to elongate in shade condition (Keuskamp et al., 2011)(Luccioni et al., 2002). However, numerous questions regarding how BRs and their interactions with other phytohormones modulate shade avoidance still remain to be answered.

Plant responses to shade involve also other hormones (Figure 4.1). Ethylene plays a role in stem elongation and petiole growth under low light in tobacco (Pierik et al., 2004). In leaves, auxin accumulation stimulates cytokinin oxidase, inhibiting leaf growth (Yang and Li, 2017). Shade-induced abscisic acid (ABA) inhibits branching, and ABA biosynthesis mutants exhibit increased branching under low R:FR (Finlayson et al., 2010; Su et al., 2011). Strigolactone (SL), known for controlling lateral shoot growth, influences branching suppression in shade. *max2* mutants, affected in SL signaling, show longer hypocotyls under various light conditions (Shen et al., 2012; González-Grandío et al., 2013). Karrikins, enhancing light sensitivity, could be key in mitigating shade-induced responses (Waters and Smith, 2013; Meng et al., 2017). Recent studies in Arabidopsis have provided an insight into the intricate interplay among all these hormones. However, many details remain unclear, and the regulation of SAS beyond Arabidopsis has still a lot to explore.

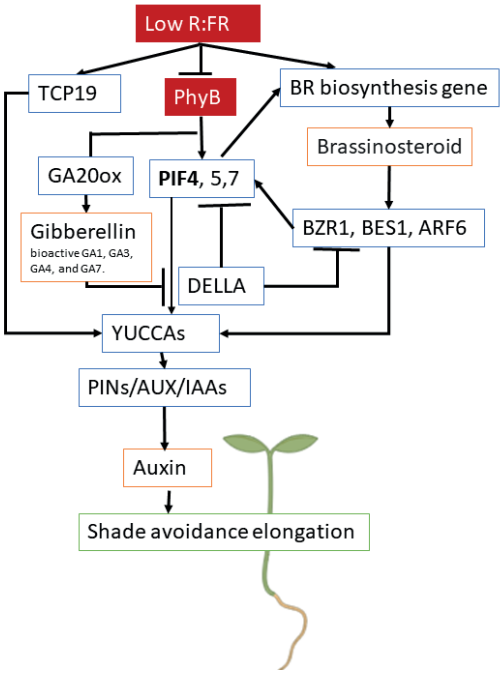

Figure 4.1 Arabidopsis SAS elongation regulated by auxin, gibberellin, and brassinosteroids. Regulation scheme adapted from literature (Yang and Li, 2017; Wang et al., 2020; Liu et al., 2021). Arabi dopsis picture is from Biorender.com.

4.1.2 Pharmacological tools for studying auxin, GA, and BR

In this chapter, we employed a pharmaceutical approach involving hormone and hormone transport, signaling, and biosynthesis inhibitors to unravel the impact on various hormone regulations in response to far-red treatment. This approach enables us to dissect the hormone interactions, providing valuable insights into the complex hormonal dynamics of SAS.

The effects of auxin can be simulated by exogenous treatments with various auxins, especially Indole-3-Acetic Acid (hereafter IAA), the most commonly occurring natural auxin. With the use of IAA, plants can be treated to cause auxin-induced growth and allows for further insight into the role of auxin in SAS. The effects of auxin can also be inhibited in different manners, in this chapter, we used three chemicals to reduce auxin biosynthesis, transport and signaling - Naphthylphthalamic acid (hereafter NPA), 4-biphenylboronic acid (BBo) and 2-(1H-Indol-3-yl)-4-oxo-4-phenyl-butyric acid)(PEO-IAA). NPA binds to the auxin transporters which makes it prevent active

directional auxin flow from cell to cell. These in turn prevent auxin-induced functions in plant tissues (Křeček et al., 2009; Abas et al., 2020). BBo is a chemical which inhibits auxin biosynthesis by targeting YUCCA (YUC). YUC-type flavin-containing monooxygenases (FMO) facilitate the oxidative decarboxylation of IPyA to generate IAA (Zhao et al., 2001; Zheng et al., 2013). BBo suppresses recombinant YUC activity *in vitro* and thus likely decreases endogenous IAA content (Kakei et al., 2015). PEO-IAA is an auxin antagonist that competitively binds the auxin receptor, TIR1/AFB proteins (TRANSPORT INHIBITOR RESPONSE 1/AUXIN SIGNALING F-BOX PROTEINS) (Šenkyřík et al., 2023).

To study gibberellins (GAs), we use gibberellic acid 3 (GA_3) as the exogeneous application, and we use paclobutrazol (PBZ) as an inhibitor of gibberellin signaling. PBZ hinders plant growth by inhibiting GA synthesis, as it blocks the oxidation of ent-kaurene to ent-kauronoic acid. This interference occurs through the inactivation of cytochrome P450-dependent oxygenase (Gallardo et al., 2002; Desta and Amare, 2021).

And finally, we studied brassinosteroids (BRs) which play a crucial role in normal plant growth and are essential for shade avoidance responses in Arabidopsis seedlings (Asami et al., 2000). To test the effects of BRs, we treated plants with brassinolide- the active BR form. To inhibit the brassinosteroid signalling, we investigated the effects of brassinazole (BZ), an inhibitor of brassinosteroids biosynthesis. By exploring the interactions and effects of these exogenous hormone treatments and inhibitors, we aim to deepen our understanding of the hormonal regulation underlying the shade avoidance response in tomato stems and shed light on the molecular mechanisms governing their growth and development in varying light conditions.

In this chapter, our primary focus was to study the roles of auxin, brassinosteroids and gibberellins in tomato stem elongation responses to light. We used a pharmacological approach and applied the chemicals described above. As these treatments were not previously published on tomato, we first optimized the chemical application methods, precise timings and frequencies of treatment, and chemical concentrations. Then, we sought to recapitulate the intricate FR response by applying one or multiple hormones or hormone inhibitors. Our aim was to construct a hormone network of SAS in tomato, and indeed, we found evidence for all three hormones in FR-responsive tomato stem elongation.

4.2 RESULTS

4.2.1 IAA and GA-related transcripts show a robust fold change response to FR, while BR-related genes exhibit a muted response

We wanted to explore how hormone-related genes were responding to FR in our tomato RNAseq data (described in detail in Chapter 3). Given the shortness of tomato gene lists for hormone responses in the current (ITAG4.1) tomato GO annotation, we used Arabidopsis Gene Ontology (GO) annotations (Table 4.1) from TAIR (The Arabidopsis Information Resource)(Lamesch et al., 2012) to identify the genes of interest. Then, we employed a multi-blast strategy against the tomato transcripts in the Solgenomics database (https://solgenomics.net/tools/blast/). This approach allowed us to identify putative tomato genes responsive to hormones in our RNA-seq dataset. This was also supplemented by tomato hormone literature (Li et al., 1994; Knauss et al., 2003; Wu et al., 2012; Stortenbeker and Bemer, 2019). We visualized the FR-responsiveness of these genes of interest in our transcriptome data (Figures 4.2, S4.1, S4.2).

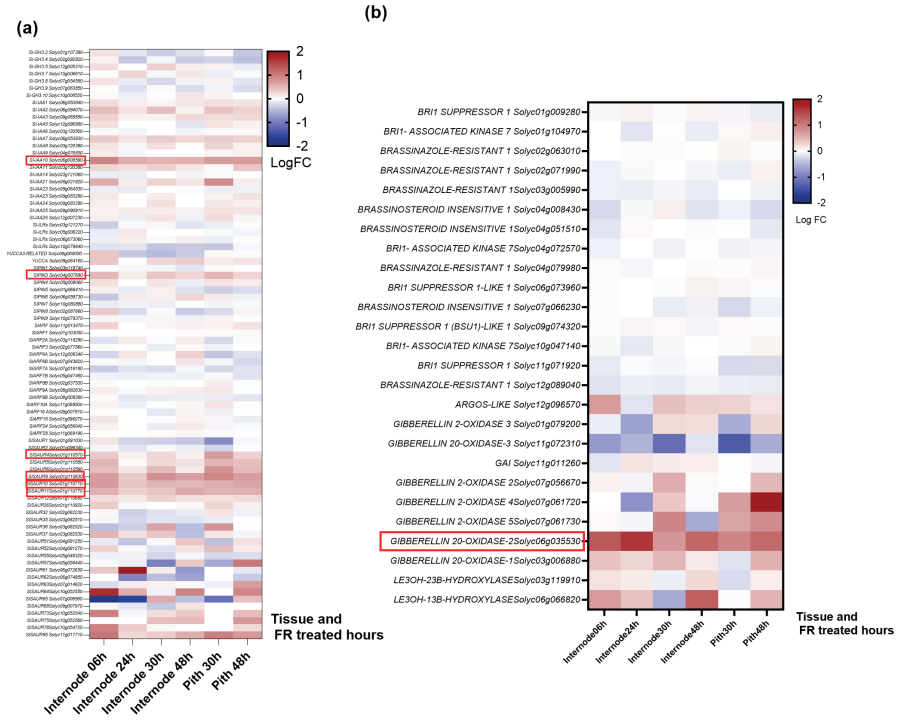

Figure 4.2. FR response of IAA, BR and GA-related genes in tomato. Heatmap generated from RNA-seq data illustrates the log fold change in gene expression associated with (a) IAA, (b) GA and BR. Upregulation is represented in red, while downregulation in blue. FR-responsive DEGs are boxed in red.

We found strong foldchange responses to FR in our auxin and GA gene lists, namely in *SAUR (small auxin up-regulated RNA)* genes and *GA oxidase* genes, while BR-related genes exhibited a more subdued response (Figure 4.2). *SAUR*s regulate growth by regulation of cell activity, and they are responsive to multiple hormones not limited to auxin (Stortenbeker and Bemer, 2019). GA oxidases catalyse the conversion of active GAs to inactive forms, thereby regulating the levels of bioactive GAs in plants. Gibberellin 2-oxidases (GA2oxs) regulate plant growth by inactivating endogenous bioactive GAs (Lo et al., 2018), while gibberellin 20-oxidase (GA20ox) is responsible for catalyzing consecutive oxidation steps in the late phase of the GA biosynthetic pathway. These observations highlight the sensitivity of these genes to FR conditions. The FR-induced gene expression changes suggest interplay between light signaling and hormone pathways, warranting further exploration into the specific mechanisms governing these responses.

4.2.2 Signal triggering internode 1 elongation might derive from leaf 1 or internode 1

Based on the findings from Chapter 2, we focused our investigation on internode 1, which corresponds to the internode between the cotyledons and the first true leaf. We wanted to dissect the hormone signalling pathway in more detail, but we wanted first to identify what was the location of FR light perception triggering the internode elongation. In previous research on *Datura ferox* and *Sinapis alba*, local FR applied only on a leaf can induce stem elongation response in the adjacent internode (Ballaré et al., 1990). Similarly, local FR treatment on tomato can induce a local response from the terminal leaflet (Courbier et al., 2020). First, we conducted a local FR experiment (Figure 4.3) to test which local FR treatments would induce internode 1 elongation. When we exposed internode 1, leaf 1, or the meristem to a localised R:FR=0.01 FR with a spot lamp, we observed elongation in the first internode, akin to the effect seen in the entire plant under FR light. This suggests the mobility of the signal from this localized FR treatment that was not always on the responding tissue.

Figure 4.3. Local FR treatment on each tissue as captured with infrared camera.

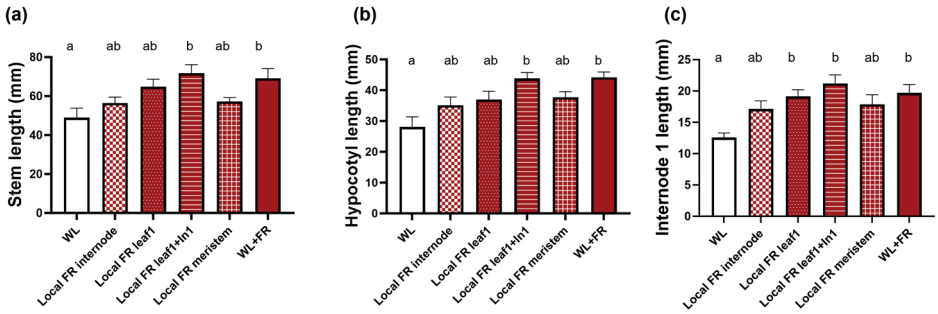

Figure 4.4. Stem elongation in response to different local FR applications. We treated 14-day-old tomatoes with local or global supplemental FR light. The data include measurements of (a) stem length, (b) hypocotyl length, and (c) internode 1 length. The data are presented as mean ± SEM, and different letters indicate significant differences between treatments based on ANOVA analysis with Tukey's post hoc test ($P<0.05$). There were 15 plants per local treatment, and the experiment was repeated three times.

4.2.3 IAA induces mild stem elongation when applied on first internode or first true leaf

Commencing our exploration of the effects of different hormones, we started with the IAA-responsive pathway, indicated by our RNAseq data (Chapter 3). IAA is known to play a role in SAS in other species, specifically by induction of IAA in leaves by FR, consequently influencing petiole and hypocotyl growth. IAA application in Arabidopsis SAS studies is commonly achieved through treatments applied to diverse leaf regions or introduced into the growth medium (Michaud et al., 2017; Pantazopoulou et al., 2017). However, considering the stem growth habit of tomato compared to Arabidopsis rosette habit, we wanted to explore and test different IAA application methods. Specifically, we investigated the use of a whole plant spray and a brushing method onto both internode 1 and leaf 1 (Figure 4.5). By carefully evaluating these application techniques, we aimed to determine the most effective approach to studying IAA's role in tomato SAS.

Initially, a whole-plant spray failed to elicit a significant internode 1 response at both 25 μM and 100 μM (Figure 4.5). However, when 100 μM IAA was applied through brushing on internode 1 and leaf 1, a mild elongation in both hypocotyl and internode was observed (Figure 4.5). This outcome serves as a promising indication of the efficacy of the brushing method.

We also wanted to test if we could mimic the local FR treatment (Figure 4.4) by local IAA applications. We applied 100 μM IAA separately to both leaf 1 and internode 1, each with three applications of brushing over a week-long treatment period (Figures 4.5 and S4.3). We observed that the internode 1 elongated in response to IAA treatment in WL with both internode and leaf treatments, and the response was similar in WL for both tissues but did not reach the level of FR-responsive elongation (Figure 4.5g). However, we did not find any significant IAA-induced changes in supplemental FR conditions for either treatment location (Figures 4.5g,h and S4.3).

We also quantified leaf growth, to assess negative effects that the IAA treatment might be causing. Application of IAA to leaf 1 or to Internode 1 led to a significant decrease in both leaf 1 and 2 areas (Figure 4.5i,j). We here considered some assumptions: first, auxins are known to promote apical dominance. When IAA is applied to the stem, it may enhance apical dominance, directing more resources towards the main stem and inhibiting lateral growth, including leaf expansion. Second, the application of IAA to the stem may disrupt the hormonal balance, leading to altered growth patterns in a complex network that regulates plant growth and development. Imbalances in these hormone levels can impact leaf development. Further investigation of this effect is needed, but it is not the focus in this chapter.

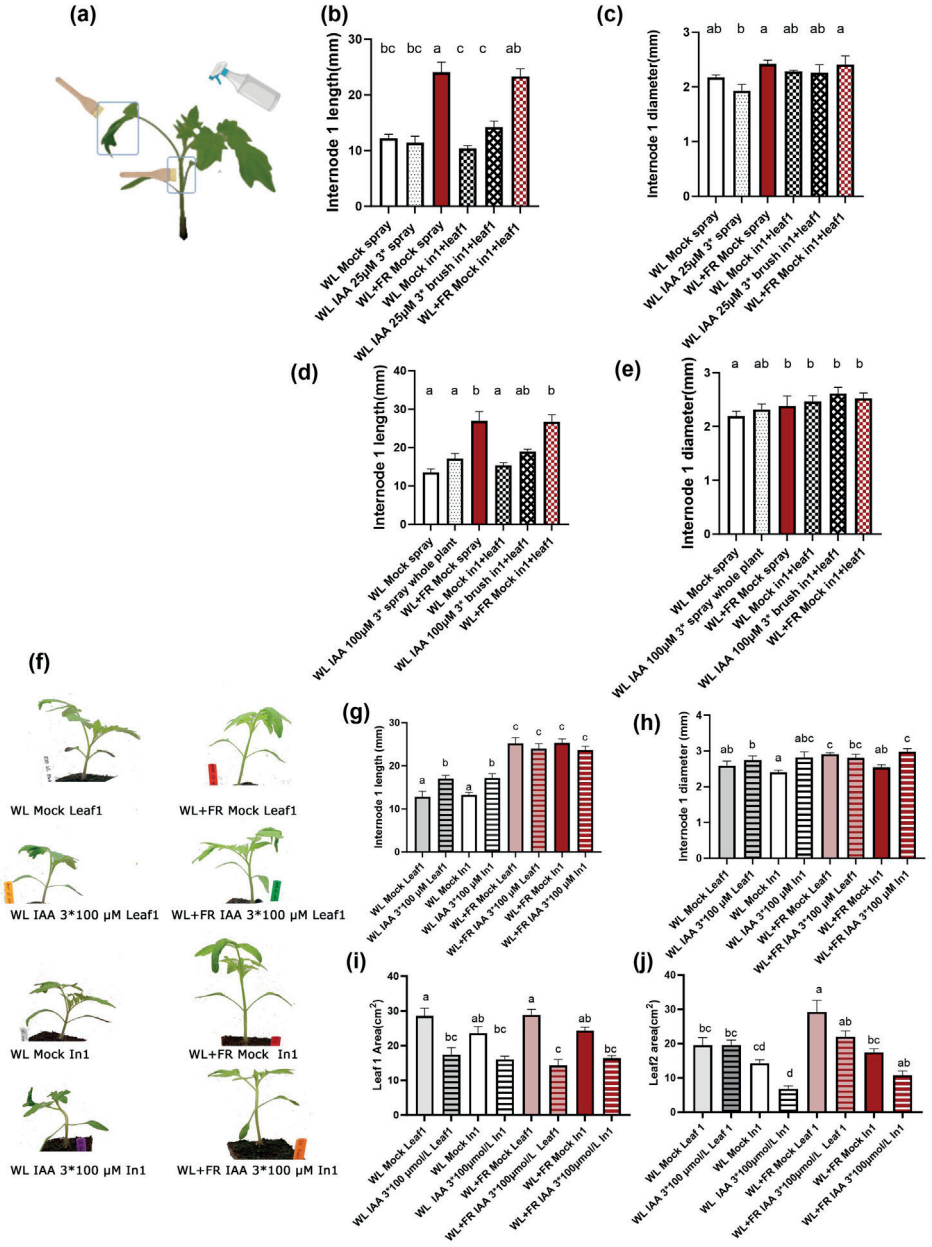

Figure 4.5. Stem responses to different IAA treatments. We treated 14 day-old tomatoes with 25 μM or 100 μM IAA by whole plant spray, or by brushing onto leaf 1 and internode 1. Spray and brush were applied 3 times over one week treatment period. The data includes measurements of (a) illustration of how internode+leaf brush or whole plant spray were carried out, (b) internode 1 length of 25 μM IAA treatment, (c) internode 1 diameter of 25 μM IAA treatment, (d) internode 1 length of 100 μM IAA treatment, (e) internode 1 diameter of 100 μM IAA treatment, (f) representative photos of the phenotypes for brushing IAA on internode or leaf 1, (g) internode 1

length to brushing 100 μM IAA on internode or leaf 1, (h) internode 1 diameter to brushing 100 μM IAA on internode or leaf 1, (i) first leaf area (oldest leaf) to brushing 100 μM IAA on internode or leaf 1, (j) second leaf area brushing 100 μM IAA on internode or leaf 1. The data are presented as mean ± SEM, and different letters indicate significant differences between treatments based on ANOVA analysis with Tukey's post hoc test (P<0.05). There were 6-9 biological replicates, and the experiment was repeated twice. Picture (a) was created with Biorender.

4.2.4 The elongation of internode 1 did not show IAA dose dependency

Next, we wanted to investigate if the IAA concentration we were applying was either too high or too low to induce the full FR-like internode 1 elongation. We applied a range of IAA concentrations through brushing on Internode 1 by three applications during one week (length of the FR treatment). We observed that the elongation of internode 1 did not change in response to the IAA concentration (Figure 4.6a). Surprisingly, at both 5 μM and 200 μM IAA, the elongation level of internode 1 remained virtually the same. This suggests that IAA-responsive internode 1 elongation is not dose-dependent on IAA concentration and that our lowest IAA treatment already induced the maximal response possible by IAA alone (Figure 4.6, S4.4).

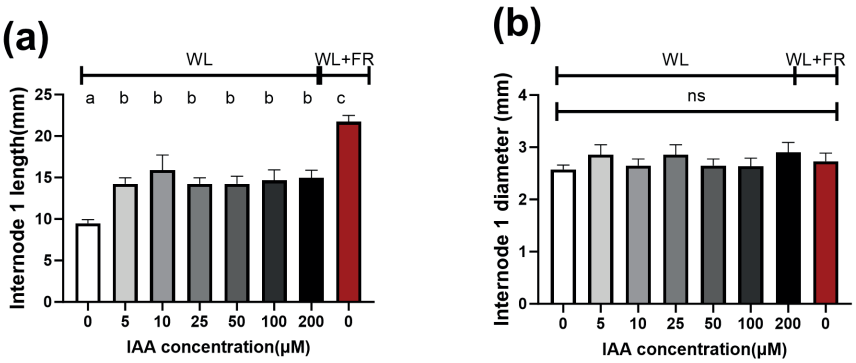

Figure 4.6. Internode responses to different IAA concentrations. We treated 14 day-old tomatoes with different concentration IAA by brushing onto internode 1. Brush were applied 3 times over one week treatment period. The data includes measurements of (a) Internode1 length. (b) Internode1 diameter. Data are presented as mean ± SEM, and different letters indicate significant differences between treatments based on ANOVA analysis with Tukey's post hoc test (P<0.05). There are 12 biological replicates, and the experiment was repeated twice.

We also quantified internode 1 cellular morphology in response to IAA treatments by microscopy to collect clues on how different cell types respond to IAA. In our microscopy analysis of IAA treatment on internode 1, we observed that all cell lengths

increased with an increase in IAA concentration to a similar level as FR (Figure 4.7). Our inability to synchronize the cell division rate in our analysis could potentially explain why IAA cannot induce internode elongation at a level similar to that observed under FR conditions. Moreover, we assessed periclinal pith cell divisions by counting cell layers and measuring pith radial thickness (Figure 4.7). It was evident that IAA promoted both cell elongation and cell division in internode 1. However, the overall phenotypic response to IAA was less pronounced compared to far-red light (FR) treatment, potentially due to missing hormone interactions and balance. Despite showing similar cellular responses to FR, the effects on overall plant phenotype were not as strong. In summary, IAA does influence cellular processes, including elongation and division in internode 1. However, the complex interplay of hormones and their balances might limit the full phenotypic expression of these cellular changes, resulting in a less prominent overall response compared to FR treatment (Figure 4.7).

4.2.5 NPA induced elongation and diameter decrease in tomato

In our quest to understand how plants respond to light, we next tested N-1-naphthylphthalamic acid (NPA), a polar auxin transport blocker, to disrupt signals from the leaf. We hypothesized that inhibiting auxin transport would disrupt the response to light. This approach aims to uncover the role of leaf-derived auxin in the complex interaction between light signals and plant growth. In our experiments, we tested various concentrations of NPA brushed on internode 1, namely 250 μM, 125 μM, and 50 μM (Figures 4.8-4.9). We applied the treatments one day prior to FR treatment and then phenotyped the plants after one week of exposure to FR light. We employed NPA in our initial test at a concentration of 250 μM, resulting in a significant impact on overall plant fitness. The stems exhibited substantial elongation, becoming thin to the point of fragility. Following this, we reduced the concentration. As we decreased the concentration to 125 μM, the plants required additional support to stand upright, while at 50 μM, the plants displayed a more robust growth (Figure 4.8). Therefore, we selected 125 μM and 50 μM as the concentrations for our subsequent experiments.

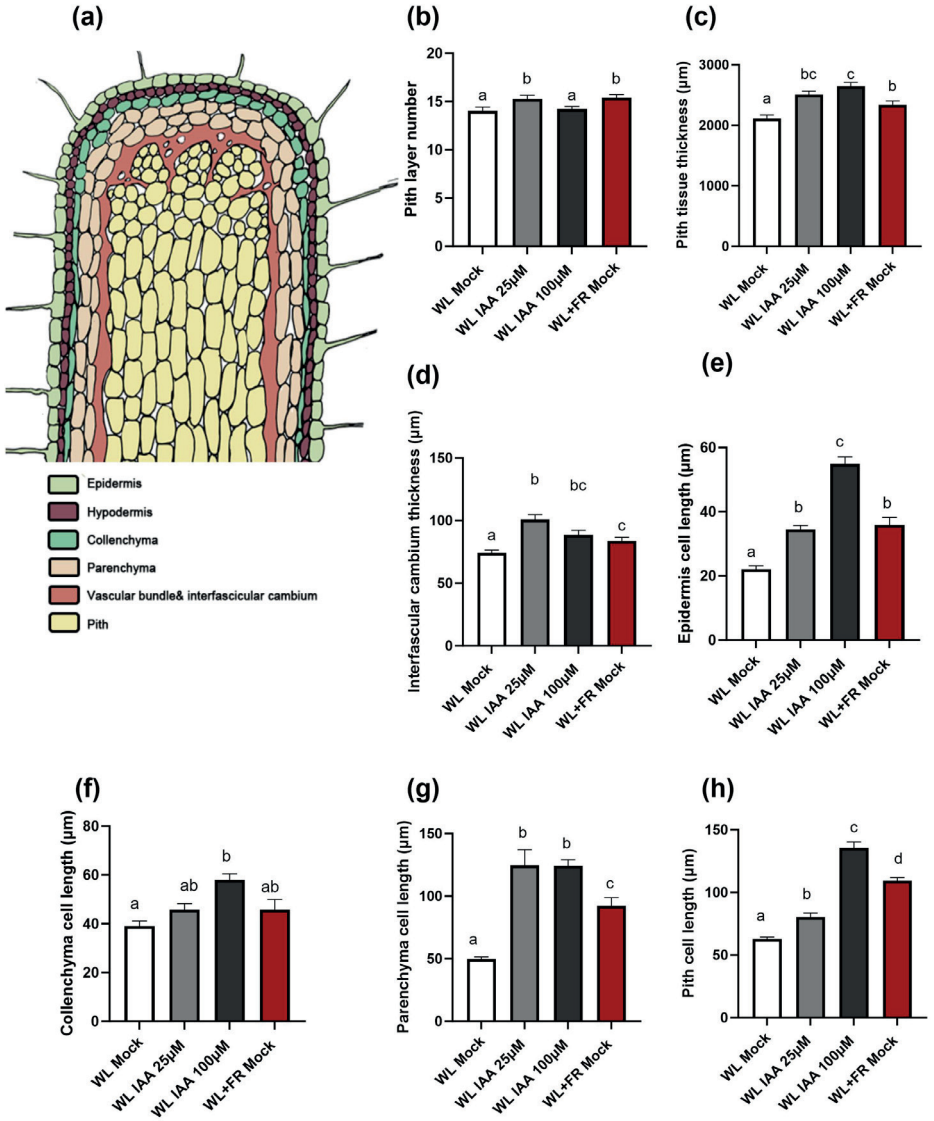

Figure 4.7. Cell type responses to different IAA concentrations. We treated 14-day-old tomatoes with different concentration IAA by brushing onto internode 1and analyzed the cell types response by microscopy. The data includes measurement of (a) cell types illustration of internode 1, (b) pith layer numbers, (c) pith thickness, (d) interfascicular cambium thickness, (e)epidermis cell length, (f) collenchyma cell length, (g) parenchyma cell length, and (h) pith cell length. Data are represented as mean ± SEM, and different letters indicate significant differences between treatments based on ANOVA analysis with Tukey's post hoc test ($P<0.05$). The sample size for each treatment was 60 and the experiment was repeated twice.

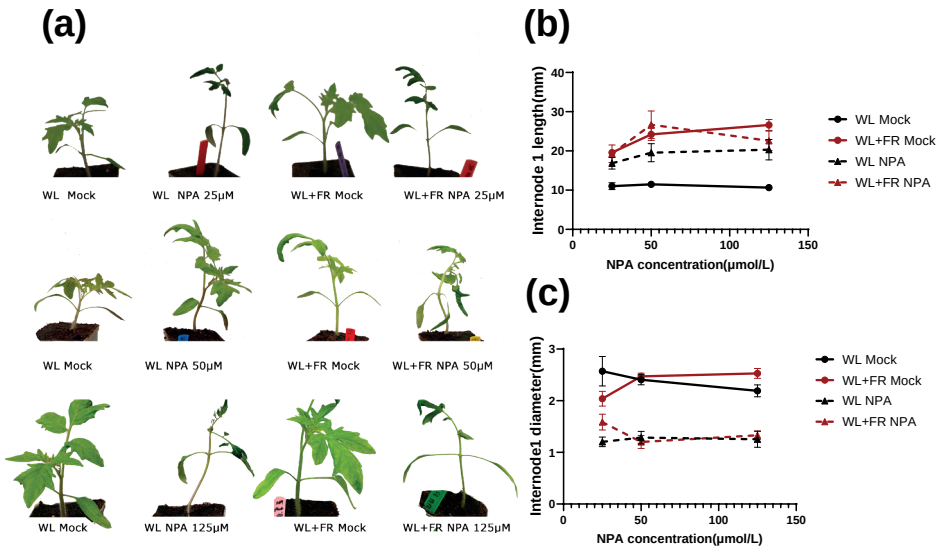

Figure 4.8. **Stem responses to different NPA concentrations**. We treated the first internode of 13 dag tomatoes with 25, 50, 125 µM NPA (or mock) in WL conditions one day prior to the start of the one-week FR treatment. (a) Representative images of NPA phenotypes, (b) internode 1 length, (c) internode 1 diameter. Data are presented as mean ± SEM, and different letters indicate significant differences between treatments based on ANOVA analysis with Tukey's post hoc test ($P<0.05$). There are 12 biological replicates, and the experiment was repeated twice.

Regardless of the NPA concentration used (50 µM and 125 µM), NPA consistently induced significant stem elongation in the hypocotyl and internode 1 (Figures 4.8, S4.5). However, we observed different responses to FR light depending on the NPA concentration. With 50 µM NPA, the stems elongated during white light (WL) treatment and this elongation was further enhanced with FR light response. Conversely, with 125 µM NPA, internode 1 elongation occurred but was reduced when exposed to FR light.

Regarding stem diameter, we had noticed that hypocotyl diameter increased with FR treatment (Chapter 2). NPA consistently leads to a substantial reduction in diameter , possibly explaining why 125 µM NPA caused a significant decrease caused plants fragility (Figure 4.8(a), S4.6).

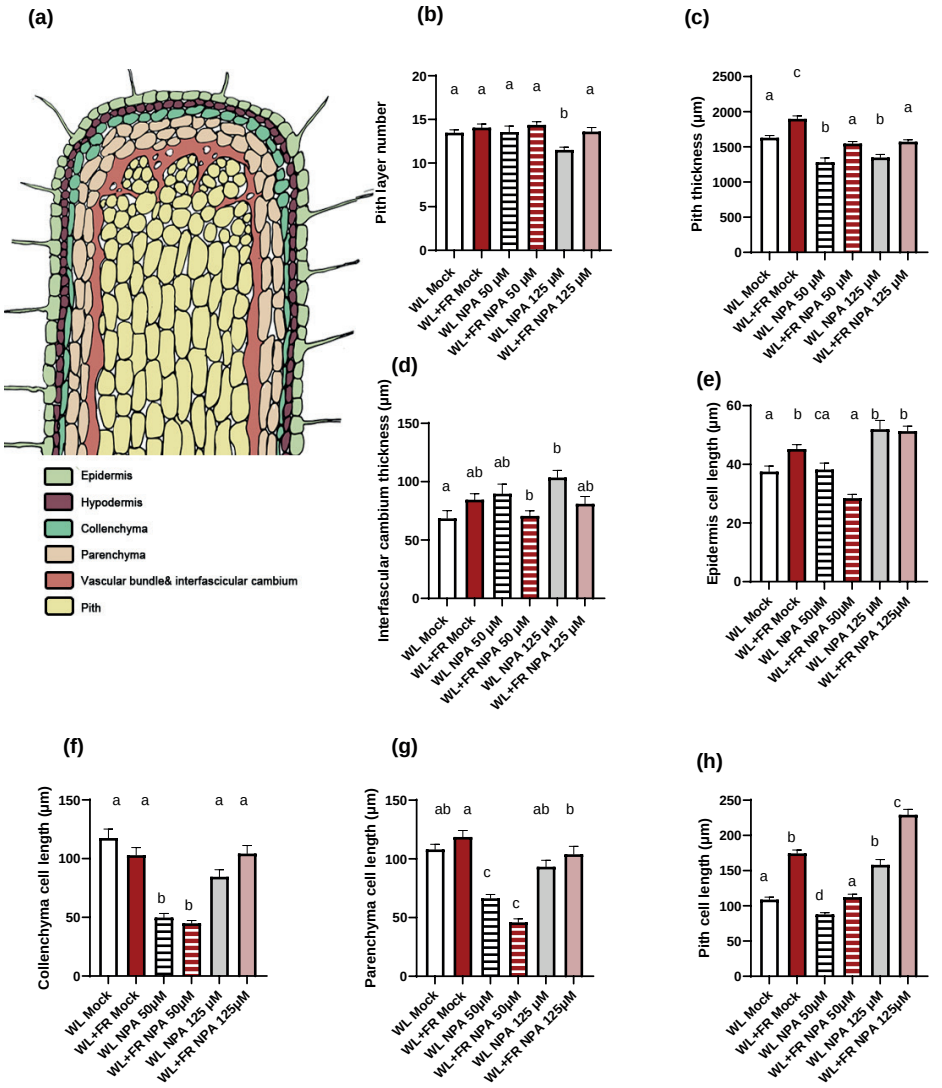

Figure 4.9. Cell type responses to different NPA concentrations. We treated 14 day-old tomatoes with different concentration NPA by brushing onto internode 1 and analyzed the cell type responses by microscopy. Data includes measurement of (a) cell types illustration of internode 1, (b) pith layer numbers, (c) pith thickness, (d) interfascicular cambium thickness, (e) epidermis cell length, (f) collenchyma cell length, (g) parenchyma cell length, and (h) pith cell length. Data are represented as mean ± SEM, and different letters indicate significant differences between treatments based on ANOVA analysis with Tukey's post hoc test ($P<0.05$). The sample size for each treatment was n=60, and the experiment was repeated twice.

We also investigated the effects of NPA treatment on the cellular morphology in the stem. The application of 50 μM of NPA resulted in a decrease in cell length in all cell types under both WL and WL+FR treatments (Figure 4.9). Conversely, at a higher concentration of 125 μM of NPA, we observed a slight increase in cell lengths. Furthermore, the thickness of the pith decreased in response to NPA application at both concentrations, regardless of the light treatment (Figure 4.9). Interestingly, at 125 μM of NPA, there was a significant decrease in the number of pith cells. This finding suggests that NPA or its effects on auxin localization may inhibit cell division.

Overall, the effects of NPA were not what we had hypothesised. Instead of blocking the FR-responsive elongation, we observed strong internode 1 elongation even at WL. We considered alternative explanations, and one was that the NPA treatment in the internode would cause IAA to pool in the internode. In other words, instead of NPA inhibiting IAA from entering, NPA would lock it in. To try an alternative approach to circumvent the possible side effects of our NPA treatment, we tried also other IAA inhibitors.

4.2.6 Auxin antagonist PEO-IAA and biosynthesis inhibitor BBo did not affect stem elongation

Next, we tested the effect from an application with PEO-IAA, an auxin antagonist (Hayashi et al., 2008). PEO-IAA interacts with TIR1/AFB (TRANSPORT INHIBITOR RESPONSE 1/AUXIN SIGNALING F-BOX) proteins similarly to -alkyl-IAA, and leads to an anti-auxin effect on auxin-responsive gene expression, cell division, and elongation pathways (Šenkyřík et al., 2023). In this experiment, we tested different concentrations of PEO-IAA applied to the first internodes of tomato plants in either WL or WL+FR conditions on one day before FR treatment (Figure 4.10). Above, we showed that IAA application triggered a mild stem elongation response. Unexpectedly, no significant differences were observed in stem elongation with any concentration of PEO-IAA. These outcomes suggest that PEO-IAA does not influence stem elongation in tomato, and this could be attributed to unsuccessful penetration. Alternatively, it may be indicative of a limited responsiveness of tomato plants to PEO-IAA.

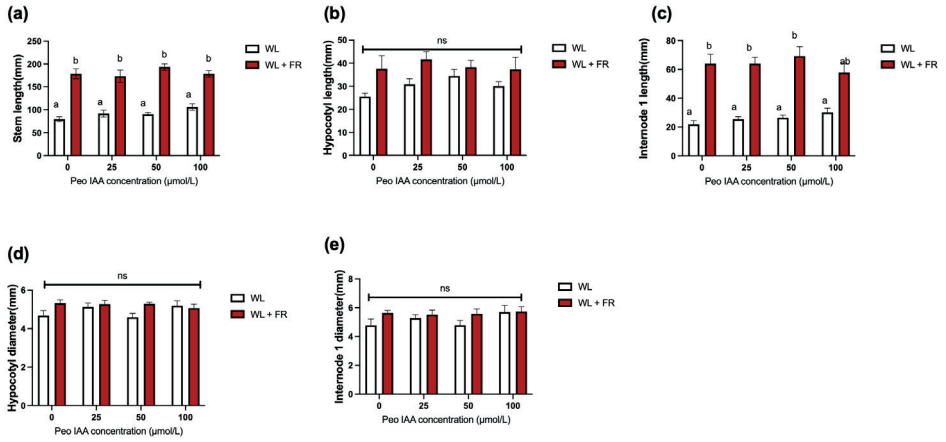

Figure 4.10. Stem response to different PEO-IAA concentrations. We treated the first internode of 13 dag tomatoes with different concentration PEO-IAA (or mock) in WL conditions one day prior to the start of the one week FR treatment. The data includes measurements of (a) Stem length, (b) Hypocotyl length, (c) First internode length (d) Hypocotyl diameter. (e) First internode diameter. Data are presented as mean ± SEM, and different letters indicate significant differences between treatments based on ANOVA analysis with Tukey's post hoc test ($P<0.05$). There are 12 biological replicates, and the experiment was repeated twice.

Finally, we wanted to test an inhibitor of auxin biosynthesis, 4-biphenylboronic acid (BBo). BBo is a chemical that targets YUCCA, the last step in IAA biosynthesis pathway. Bbo suppressed recombinant YUC activity in vitro and decreased endogenous IAA content (Kakei et al., 2015). We firstly used a brushing method as application: we applied Bbo on the internode 1 by brushing one day in advance of FR treatment. BBo had no significant inhibitor effects (Figure S4.7). Due to the mobility of chemicals and intake time consideration, we applied BBo (and later in this chapter PBZ and BZ) also through soil penetration (Figure 4.11). To ensure proper soil penetration, we applied the inhibitors 2 days before the FR treatment by withholding water 4 days in advance and then adding 40ml of each inhibitor solution to the individual pots. However, the BBo treatment did not have any effect when applied through this method either.

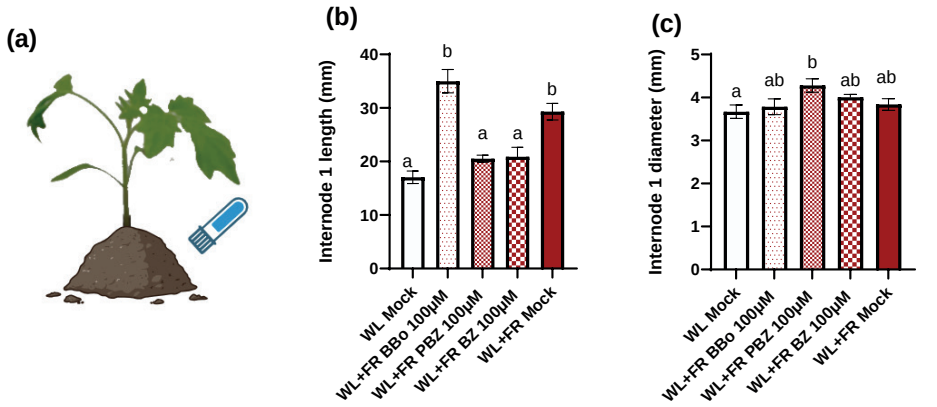

Figure 4.11. Stem response to 100 µM BBo, PBZ, BZ. We drained the soil 4 days before FR treatment, and applied BBo, PBZ and BZ directly to the soil 2 days before FR treatment in FR conditions. Data include measurements of (a) illustration of how to apply the soil penetration, (b) Internode 1 length, (c) Internode 1 diameter. Data are presented as mean ± SEM, and different letters indicate significant differences between treatments based on ANOVA analysis with Tukey's post hoc test ($P<0.05$). There are 12 biological replicates, and the experiment was repeated twice.

4.2.7 Auxin concentration in the internode is not affected by FR treatment

Considering the induction of auxin response in the transcriptome and the effect of exogenous IAA, we were curious whether the IAA concentration changes in response to FR enrichment. To investigate this, we employed liquid chromatography-tandem mass spectrometry to quantify the IAA concentration in internode 1 in response to 1-hour, 2-hour, and 6-hour whole-plant FR treatments. Additionally, we assessed the potential circadian influence by subjecting samples to a 1-hour FR treatment in both the morning and afternoon (Figure 4.12). However, we did not uncover definitive evidence of IAA concentration increasing in response to FR in bulk tissue of internode 1, indicating that either IAA is not regulated, or that we missed subtle changes in concentration and/or distribution of IAA.

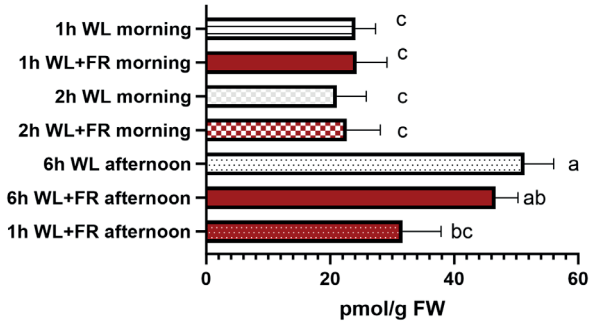

Figure 4.12. IAA concentration in internode 1 in response to 1-hour, 2-hour, and 6-hour FR treatments. We also assessed the circadian influence through 1-hour far-red treatment initiated in morning and afternoon.

4.2.8 A high concentration of GA can completely recapitulate the elongation induced by FR.

Given that the application of auxin did not yield as strong an elongation response as we observed in supplemental FR-treated plants, we proceeded to investigate the impacts of other hormones. GA-related gene expression was affected in FR-enriched stems (Figure 4.2), and also GA is known to play a role in FR-responsive elongation in Arabidopsis (Djakovic-Petrovic et al., 2007; Kohnen et al., 2016b). So, we next investigated the role of gibberellin (Figure 4.13) and the combined influence of gibberellin and auxin (Figure 4.14).

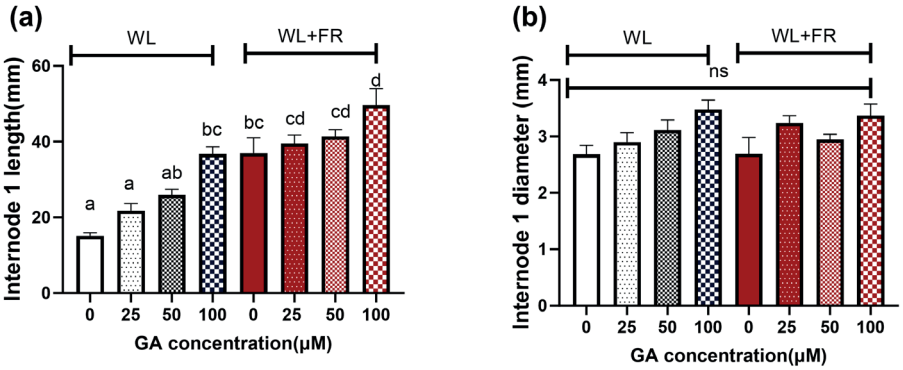

Figure 4.13. Stem response to different GA_3 concentrations. We brushed the first internode of 14 -day-old tomatoes with different concentration GA (or mock) in WL or FR conditions over one week FR treatment. Brush were applied 3 times over one-week treatment period. The data includes measurements of (a) First internode length (b) First internode diameter. Data are presented as mean ± SEM, and different letters indicate significant differences between treatments based on ANOVA analysis with Tukey's post hoc test ($P<0.05$). There are 12 biological replicates, and the experiment was repeated twice.

Notably, when we tested different concentrations of bioactive gibberellin 3 (GA_3), we observed a dose-dependent trend in the elongation of the first internode (Figures 4.13, S4.7). This experiment was performed by brushing GA_3 three times (on days 1, 3 and 5 of the light treatment) onto the first internode of tomatoes placed in either WL or WL+FR, and the parameters were measured at 7 days. We found that tomato plants growing in WL responded to a rising GA_3 concentration. Namely, the stem length and the first internode length were gradually getting bigger. At 100 μM GA_3, the internode 1 elongation reached the level of FR-induced elongation. In supplemental FR, no significant differences were found in stem- and first internode length except for 100 μM GA_3. In addition, no significant differences were found in hypocotyl length, hypocotyl diameter and first internode diameter in both the WL and FR light treatment. Therefore, we conclude that GA_3 causes an significant elongation response only with 100 μM in FR and WL.

4.2.9 Adding IAA to the GA treatment had minimal effect on elongation

We wanted to test if the GA effect was additive with the previously observed mild effect from IAA, and if these effects could also be additive with FR-induced elongation. Hence, we treated plants with both GA and IAA, either 50 or 100 μM of each. All the plants grown under white light (WL) and treated with 100 μM GA_3, or with 50 or 100 μM GA_3+IAA had longer internode 1 lengths compared to the control group (Figure 4.14). Furthermore, the first internode of plants treated with 50 or 100 μM GA_3 and IAA displayed a significantly larger diameter in comparison to the control group. However, the treatment with 100 μM GA_3 alone did not lead to a notable difference in the diameter of the first internode. Conversely, no noteworthy disparities were observed in the stem and first internode lengths between plants treated with 100 μM GA_3 and those treated with 50 or 100 μM GA_3 and IAA. Likewise, there were no significant variations detected in hypocotyl length and diameter. These outcomes collectively indicate that the addition of IAA, when compared to the exclusive GA_3 treatment, does not induce any supplementary response (Figure 4.14). However, the 100 μM GA_3 and IAA treatment induced an additive internode elongation effect on top of the FR effect.

Treating with GA alone also affected cellular morphology (Figure 4.15). GA alone resulted in a reduction in the number of pith cell layers, suggesting an inhibition of cell division by GA. However, this effect was overcome when GA was combined with IAA. Remarkably, under FR conditions, the combination of GA and IAA not only overcame the cell division inhibition but also induced even more cell division (Figure

4.15b). Furthermore, an increase in pith cell thickness and number was observed with the application of GA, and this effect was enhanced in the presence of GA+IAA. These findings indicate cell enlargement and elongation across all cell types when assessing their lengths (Figure 4.15c, e, f, g, h). The collective evidence highlights that the combined action of GA and IAA not only overcomes the inhibitory effect on cell division but also promotes cell elongation.

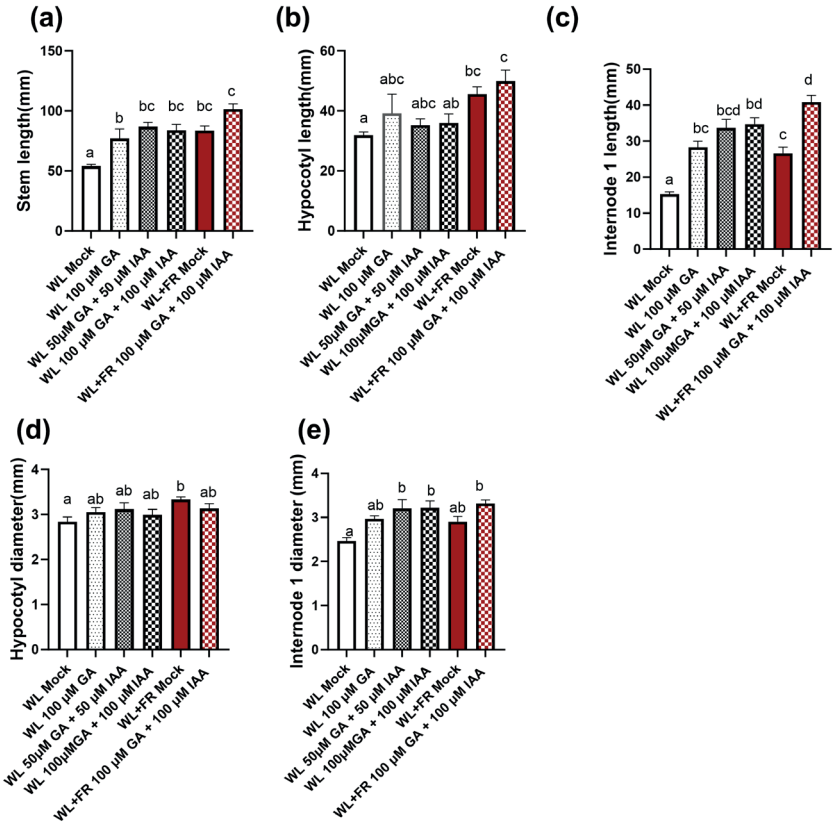

Figure 4.14. Stem response to different concentration GA_3 combined with IAA. We brushed the first internode of 14 day-old tomatoes with different concentration GA_3 and IAA (or mock) in WL or FR conditions over one week FR treatment. Brushing was applied 3 times over one-week treatment period. Data includes measurements of (a) Stem length, (b) Hypocotyl length, (c) Internode 1 length, (d) Hypocotyl diameter, (e)Internode 1diameter. Data are presented as mean ± SEM, and different letters indicate significant differences between treatments based on ANOVA analysis with Tukey's post hoc test ($P<0.05$). There are 12 biological replicates, and the experiment was repeated twice.

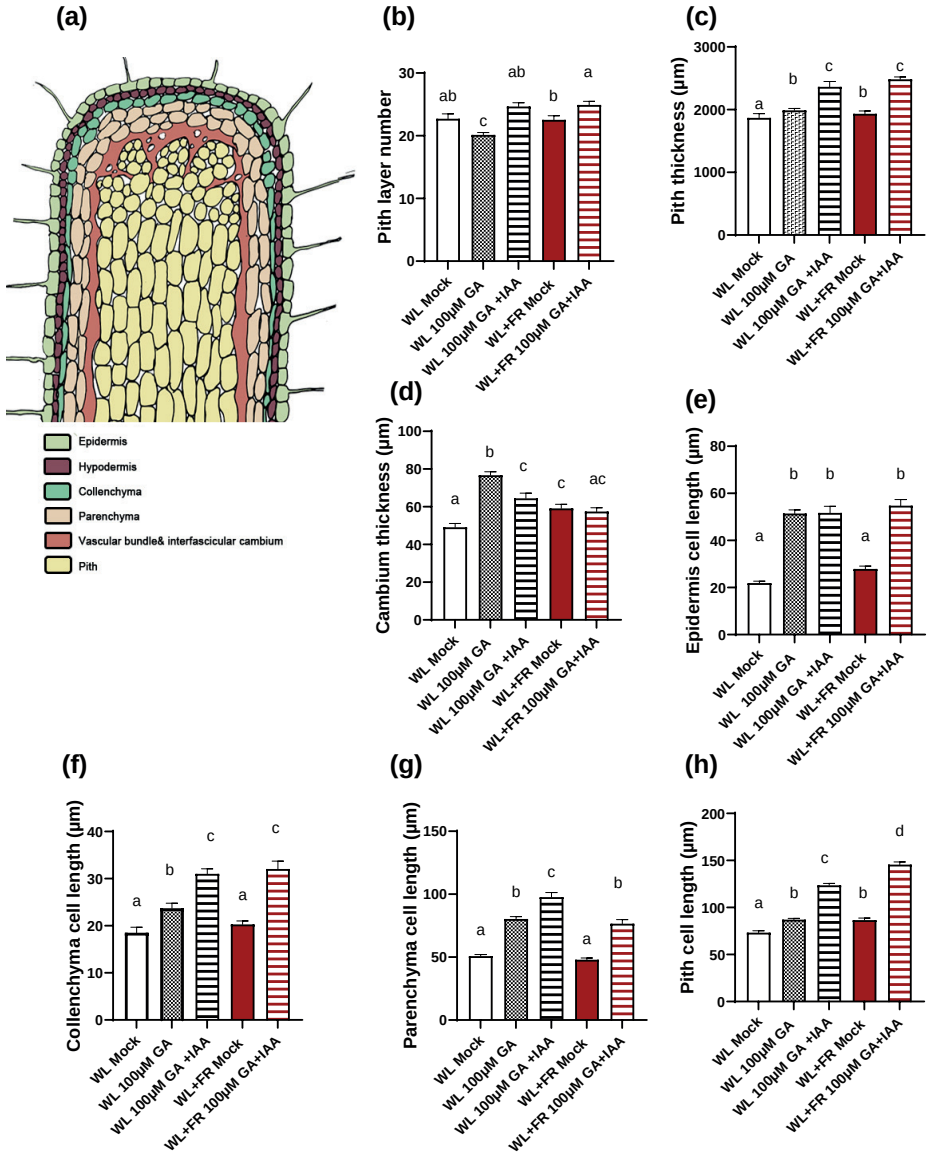

Figure 4.15. Cell type responses to different GA+IAA treatments. We treated 14 day-old tomatoes with different concentration GA+IAA by brushing onto internode 1and analyzed the cell types response by microscopy. Data includes measurement of (a) cell type illustration of internode 1, (b) pith layer numbers, (c) pith thickness, (d) interfascicular cambium thickness, (e)epidermis cell length, (f) collenchyma cell length, (g) parenchyma cell length, and (h) pith cell length. Data are represented as mean ± SEM, and different letters indicate significant differences between treatments based on ANOVA analysis with Tukey's post hoc test ($P<0.05$). The sample size for each treatment was n=80 and the experiment were repeated twice.

4.2.10 Inhibiting GA signalling abolished FR-responsive stem elongation

After showing that GA application can mimic supplemental FR-induced elongation, we wanted to see if GA was necessary for the FR-responsive stem elongation. In this experiment, we used paclobutrazol (PBZ), a known antagonist of gibberellin, acting by inhibiting gibberellin biosynthesis (Kamoutsis et al., 1999). After trial of different application methods, namely brushing (Figure S4.9) and soil penetration (Figure 4.11), we established a working protocol. With the soil penetration treatment, we observed that blocking GA synthesis in supplemental FR led to WL-like internodes, thus indicating that GA is required for the FR-responsive stem elongation (Figure 4.14).

4.2.11 Exogenous brassinosteroid treatment induced elongation comparable to FR

Although the RNAseq data showed only mild effects on the expression of brassinosteroid-related genes, Auxin and brassinosteroids (BR) are interconnected in numerous growth processes, with cell elongation serving as the driving force behind hypocotyl elongation for both (Keuskamp et al., 2010b; Keuskamp et al., 2012). BR are known to play a crucial role in normal plant growth and are essential for shade avoidance responses in Arabidopsis seedlings (Asami et al., 2000).

First, we tested effects of different concentrations of BR in WL (Figure 4.16). In this experiment, we utilized brassinolide as a representative of BR. The treatment commenced with brushing the internode of 14-day-old seedlings. With a high concentration of BR, the elongation observed in the BR-treated internode reached a level comparable to that induced by supplemental FR (Figure 4.16). BR also triggered cell elongation in correspondence with the changes in concentration (Figure 4.17).

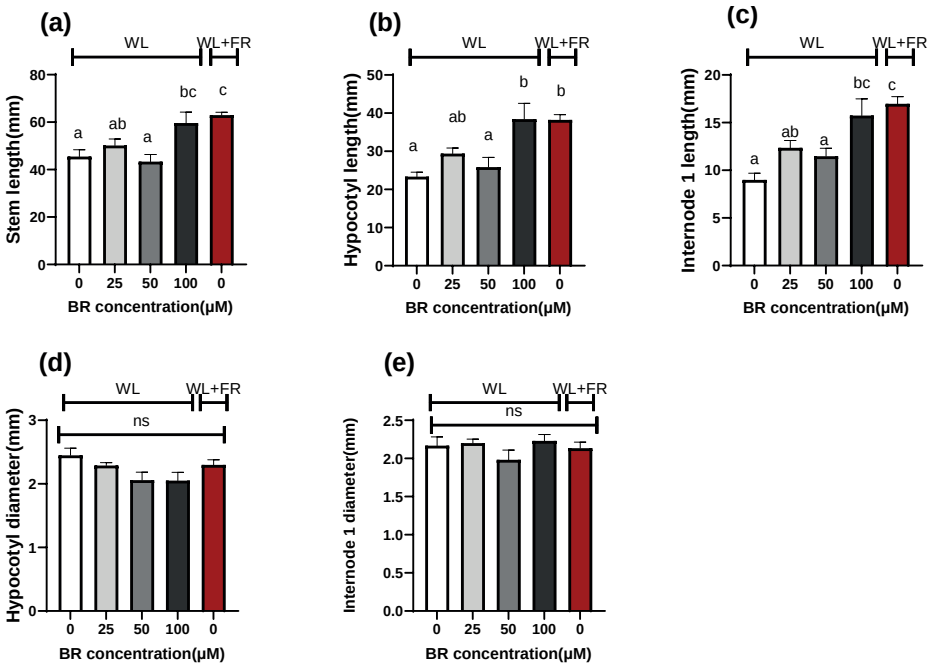

Figure 4.16. Stem responses to different concentration BR. We brushed the first internode of 14 day-old tomatoes with different concentration BR (or mock) in WL or FR conditions over one-week treatment. Brushing was applied 3 times over one week treatment period. Data includes measurements of (a) Stem length, (b) Hypocotyl length, (c) Internode 1 length, (d) Hypocotyl diameter, (e) Internode 1 diameter. Data are presented as mean ± SEM, and different letters indicate significant differences between treatments based on ANOVA analysis with Tukey's post hoc test ($P<0.05$). There are 12 biological replicates, and the experiment was repeated twice.

We followed this up by testing the combined effects of GA and BR at a concentration of 100 μM (Figure 4.18). We observed that BR alone was able to induce internode elongation similar to the supplemental FR treatment. We found that GA resulted in significantly greater elongation than supplemental FR unlike in our previous experiment (Figure 4.14). The combination of GA and BR did not show a further increase in elongation compared to GA alone. Additionally, we investigated the effects of GA and BR on stem diameter. Both GA and BR were found to induce an increase in diameter, with GA inducing a greater increase compared to BR when tested individually. To summarize, GA induces greater internode elongation than FR or BR, and the combined effects of BR and GA are not additive.

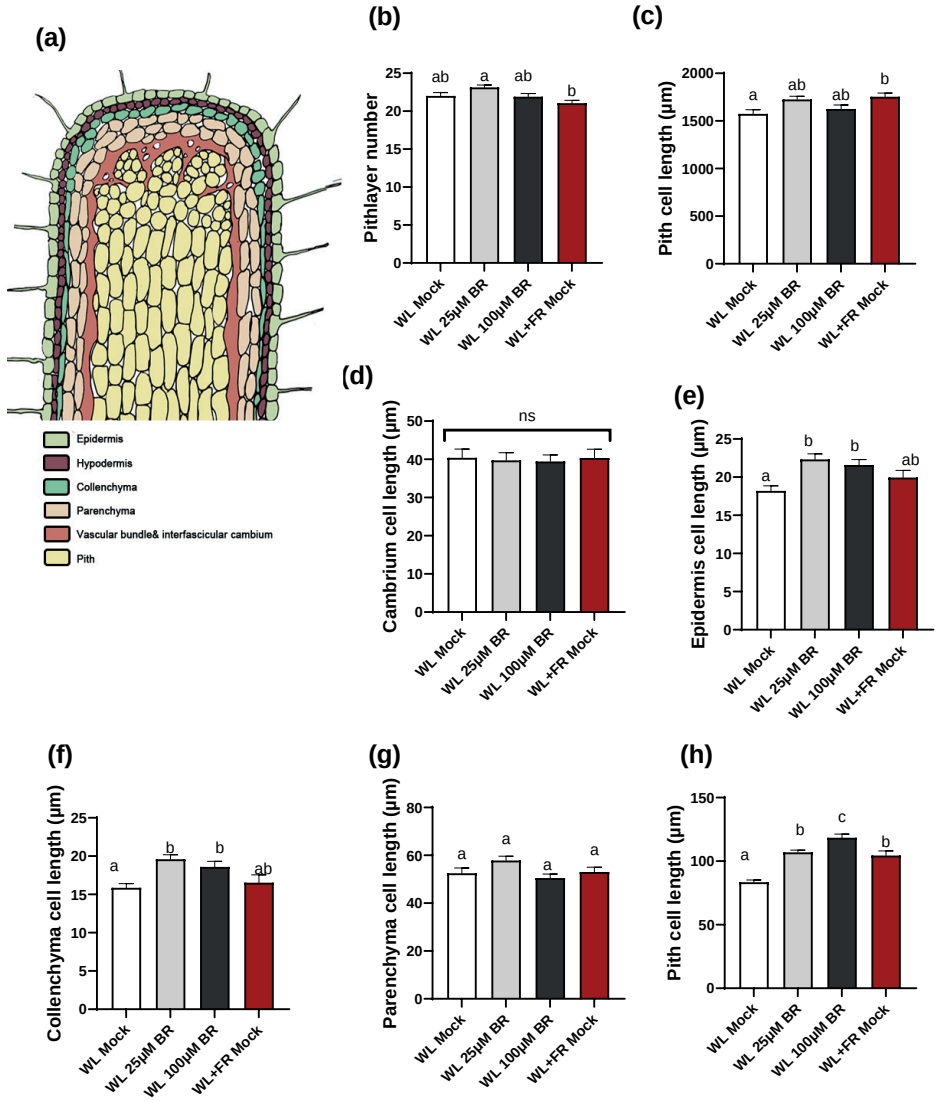

Figure 4.17. Cell type responses to different BR concentrations. We treated 14 day-old tomatoes with different concentration BR by brushing onto internode 1 and analyzed the cell types response by microscopy. Data includes measurement of (a) cell types illustration of internode 1, (b) pith layer numbers, (c) pith thickness, (d) interfascicular cambium thickness, (e)epidermis cell length, (f)collenchyma cell length, (g) parenchyma cell length, and (h) pith cell length. Data are represented as mean ± SEM, and different letters indicate significant differences between treatments based on ANOVA analysis with Tukey's post hoc test ($P<0.05$). The sample size for each treatment was n=80 and the experiment was repeated twice.

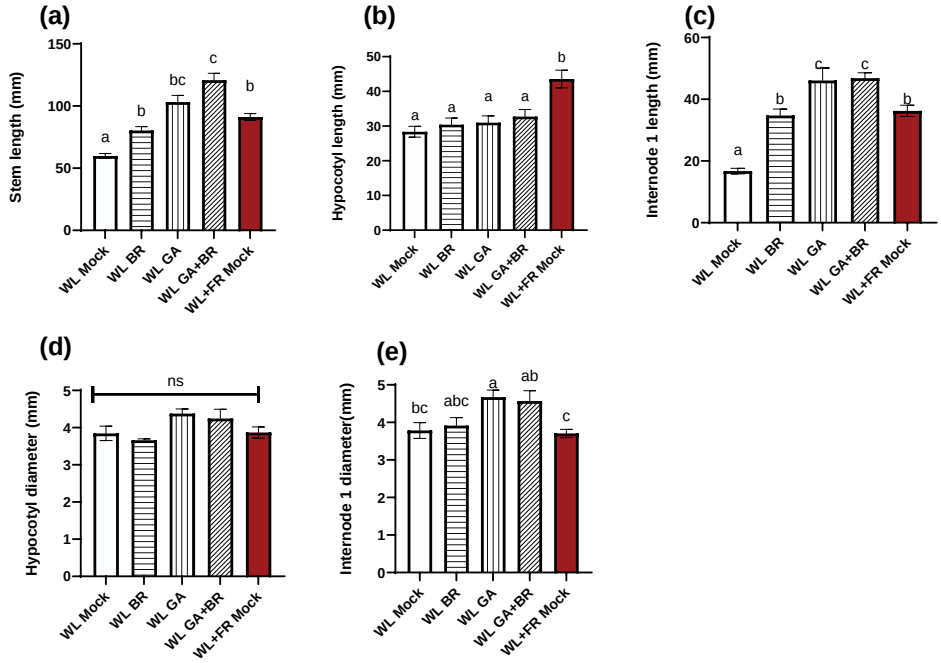

Figure 4.18. Stem response to 100 µM BR, GA or BR+GA. We brushed the first internode of 14 -day-old tomatoes with different concentration BR (or mock) in WL or FR conditions over one-week light treatment. Brushing was applied 3 times over one-week treatment period. Data includes measurements of (a) Stem length, (b) Hypocotyl length, (c) Internode 1 length, (d) Hypocotyl diameter, (e) Internode 1diameter. Data are presented as mean ± SEM, and different letters indicate significant differences between treatments based on ANOVA analysis with Tukey's post hoc test ($P<0.05$). There are 12 biological replicates, and the experiment was repeated twice.

4.2.12 Inhibiting BR signaling abolished FR-responsive stem elongation

Since brassinolide boosted stem elongation in white light, we verified if inhibition of brassinosteroids would impair supplemental FR-induced elongation. We investigated this using Brassinazole, (BZ), a triazole derivative that serves as an inhibitor of brassinosteroid biosynthesis by cytochrome P450s (Asami et al., 2000).We tested the two application methods, brushing on the internode and soil penetration. We found that the BZ application by brushing was not fully effective (Figure S4.10), while with the soil penetration method BZ completely inhibited FR-responsive stem elongation (Figure 4.11, S4.11)

4.2.13 Interplay of IAA, GA and BR

Given the significant elongation response observed with the application of GA, BR and IAA individually, we wanted to evaluate the effects of the combined treatment of GA+IAA+BR on plant growth (Figure 4.19). Specifically, internode 1 was brushed three times over a week with either 50 or 100 μM of the treatment. The results showed that the combined treatment induced similar elongation levels on internode 1 compared to the FR treatment. This is an interesting contrast to the GA only and GA+BR combined treatments (Figure 4.18), where internode elongation exceeded that of FR-induction. This possibly indicates hormones have addictive effect, since auxin potentially has a restricting role in the elongation and GA with high concentration in our experiment was able to induce elongation. Additionally, a noticeable and significant elongation was observed in the hypocotyl, which could potentially be attributed to the effect of BR because this phenomenon was not observed with IAA or GA treatment alone. Combined treatment involving GA, IAA, and BR significantly promotes cell elongation, surpassing the elongation induced by FR treatment alone (Figure 4.20).

In our endeavour to comprehensively explore the effects of GA, IAA, and BR, we sought to investigate whether the suppression of supplemental FR-induced elongation by applying PBZ or BZ could be rescued by the other two hormones. Building upon insights from our previous results and assumptions, we formulated a hypothesis to determine if the combination of two hormones could rescue the blockage caused by the absence of one hormone. We had previously shown that GA treatment in WL leads to internode elongation greater than FR (Figure 4.15), and that inhibiting BR signaling by BZ abolishes the FR-induced internode elongation (Figure 4.11). We investigated if GA with IAA would overcome the BZ-induced inhibition, and also vice versa. We conducted an experiment using the soil penetration method. Four days before supplemental FR, we stopped watering and added 40 ml of the inhibitors, PBZ or BZ, to the soil two days prior to the experiment. During the experiment, we applied either IAA+BR with PBZ, or IAA+GA with BZ under supplemental FR light conditions (Figure 4.21). Here, we observed that GA+IAA treatment in supplemental FR, while inhibiting BR with BZ, led to internode elongation even stronger than supplemental FR alone. This indicates that GA+IAA treatment can rescue the internode elongation in BR inhibition, suggesting that brassinosteroid is not needed for these two hormones to promote elongation. Conversely, BR+IAA treatment in supplemental FR combined GA inhibition via PBZ led to internode elongation similar to the effect of supplemental FR. This indicates that BR-induced internode elongation is not dependent on GA availability, or that BR+IAA treatment can rescue the internode elongation during GA inhibition.

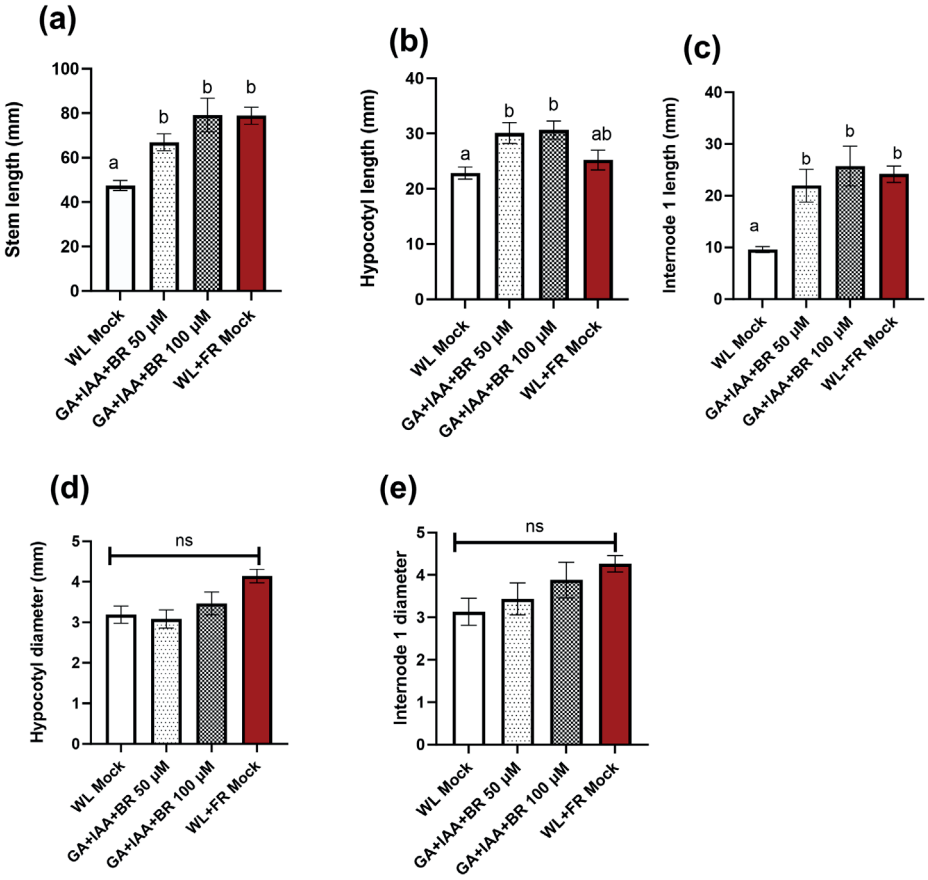

Figure 4.19. Stem responses to 50, 100 µM GA+IAA+BR. We brushed the first internode of 14 -day-old tomatoes with different concentration combine hormones (or mock) in WL or FR conditions over one week FR treatment. Brushing was applied 3 times over one-week treatment period. The data includes measurements of (a) Stem length. (b). Hypocotyl length. (c) First internode length. (d) Hypocotyl diameter. (e) First internode diameter. Data are presented as mean ± SEM, and different letters indicate significant differences between treatments based on ANOVA analysis with Tukey's post hoc test ($P<0.05$). There are 6 biological replicates and the experiment was repeated twice.

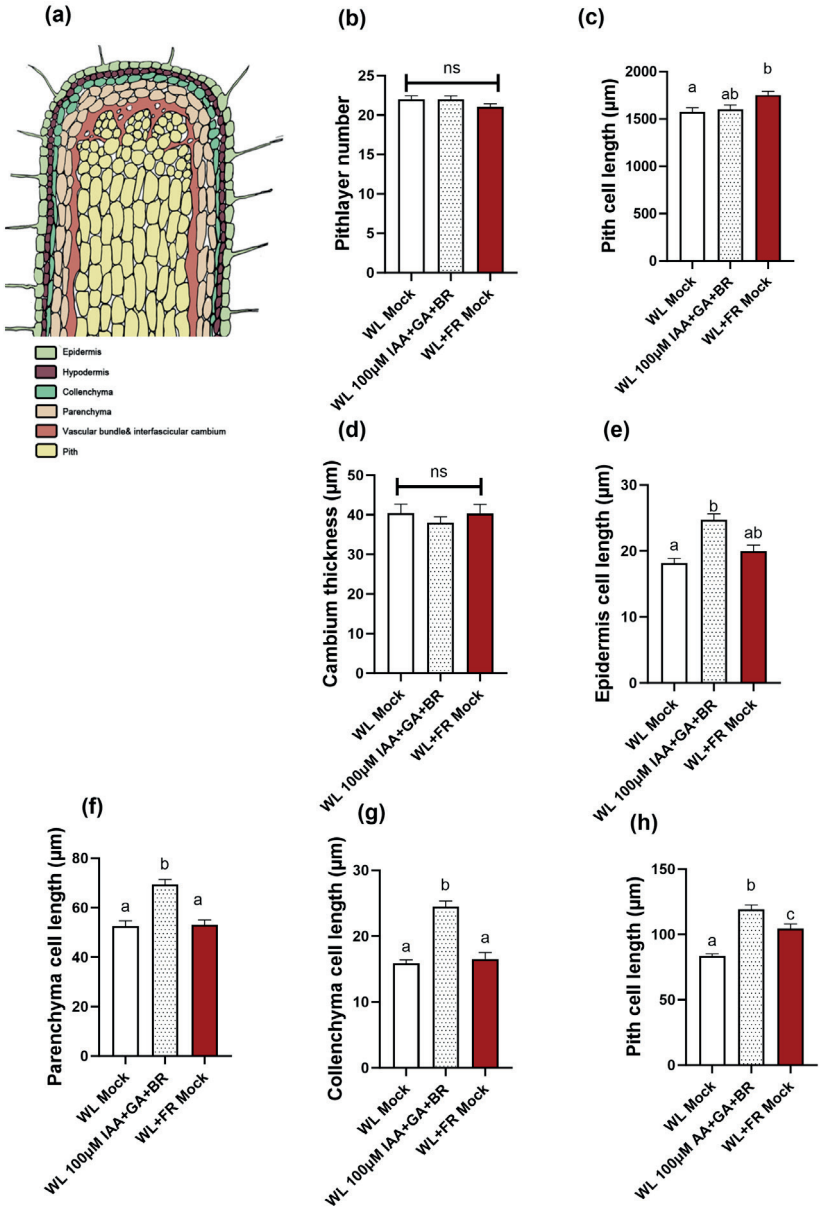

Figure 4.20. Cell type responses to 100 µM GA+IAA+BR. We treated 14 day-old tomatoes with 100 µM GA+IAA+BR by brushing onto internode 1 and analyzed the cell types response by microscopy. Data includes measurement of (a) cell types illustration of internode 1, (b) pith layer numbers, (c) pith thickness, (d) interfascicular cambium thickness, (e)epidermis cell length, (f)collenchyma cell length, (g) parenchyma cell length, and (h) pith cell length. Data areData are represented as mean ± SEM, and different letters indicate significant differences between treatments based on ANOVA analysis with Tukey's post hoc test ($P<0.05$). The sample size for each treatment was n=80 and the experiment was repeated twice.

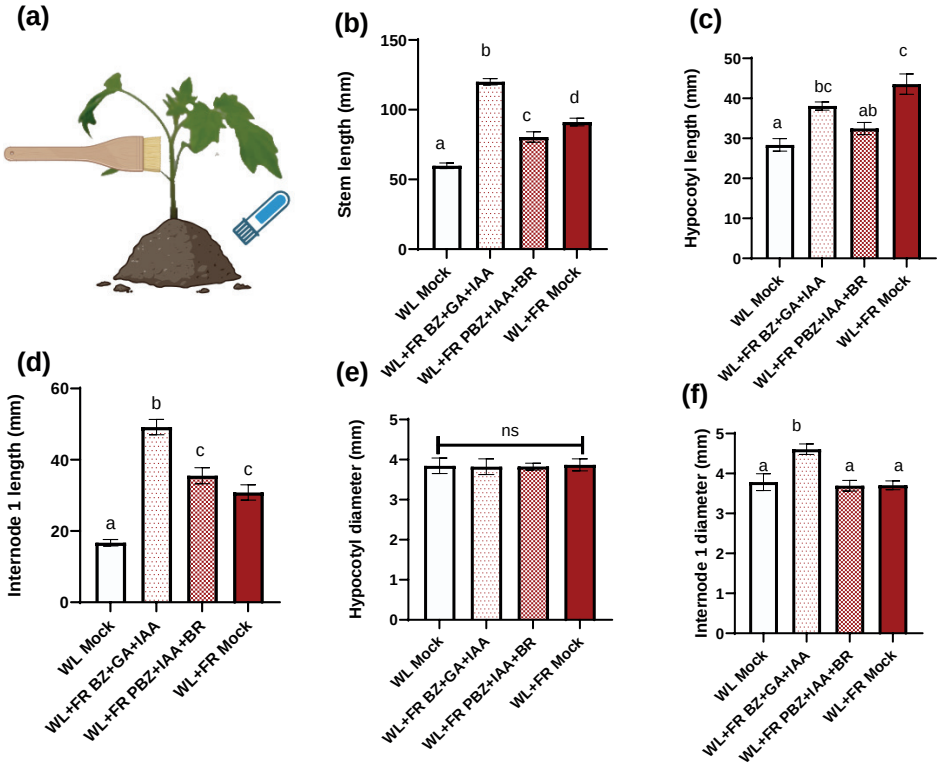

Figure 4.21. Stem responses to 100 µM PBZ and BZ with the other two hormones. We drained the soil 4 days before FR treatment, and applied BBo, PBZ and BZ directly to the soil 2 days before FR treatment in FR conditions. We brushed the first internode of 14 day-old tomatoes with different concentration BR(or mock) in WL or FR conditions over one week FR treatment. Brushing was applied 3 times over one week treatment period. (a)Illustration of how to apply the soil penetration and hormone. The data includes measurements of (b) Stem length, (c) Hypocotyl length, (d) Internode 1 length, (e) Hypocotyl diameter, (f) Internode 1 diameter. The data are presented as mean ± SEM, and different letters indicate significant differences between treatments based on ANOVA analysis with Tukey's post hoc test ($P<0.05$).There are 8 biological replicates. Picture was created by Biorender.

In conclusion, our experiments testing the interplay of BR, IAA and GA demonstrated that the both BR and GA are necessary for the FR-induced internode elongation, but either one of them can be rescued by the other one (combined with IAA in our experiments). We also saw that the effects of GA and BR might be additive, so it indicates both of them play a role in the FR-induced internode elongation. The role of IAA and how it interacts with BR and GA remains elusive, and might be complicated by internal concentrations or spatial patterns that cannot be emulated though exogenous IAA or inhibitor applications.

4.2.14 Comparative analysis of gene expression patterns in timepoints and tissues

Finally, we wanted to verify how the different hormones induced gene expression in the internode, and if these changes resembled the supplemental FR-induced changes. Building on previous results from Chapter 3, we had observed that pith tissue responded differently to FR enrichment compared to the whole internode 1. In order to further characterize these differences and investigate earlier timepoints, we first analyzed FR-responsive gene expression changes with qRT-PCR in both pith tissue and the first internode tissue at 1, 2, and 6 hours after applying supplementary far-red light.

For the first qRT-PCR analysis, we selected transcription factors and hormone-related and hormone-responsive genes that were identified as DEGs in the transcriptome data at the six hour timepoint. We found distinct FR-responses in the two tissues (Figure 4.22). Overall, we observed the clearest changes in gene expression at the two hour timepoint. As certain transcription factors showed only mild effects, they were excluded from subsequent experiments.

4.2.15 The effect of different hormones on gene expression patterns

After confirming the FR-induced differences between the two tissues and discovering that the largest changes were observed at two hours of WL+FR treatment, we decided to sample the hormone qPCR experiment at this time point. In the hormone experiment, we harvested the plant material after two hours of treatment with WL, GA, IAA, GA+IAA, BR, BR+GA+IAA, and WL+FR, and performed a second gene expression study on the entire internode 1, as well as the pith tissues of this internode (Figures 4.22, 4.23). We found that GA induced expression of most of the studied genes in the internode. Research has shown that *ELONGATED HYPOCOTYL5* (*HY5*) is a shade marker gene that is dependent on Phytochrome A, which gets upregulated in low R/FR (Ciolfi et al., 2013). Here, we also found an upregulation of *HY5* in both tissues of FR-enriched plants. GA and IAA treated plants also show upregulation of *HY5* but only in the whole internode tissue. Interestingly, the combined GA+IAA treatment shows downregulation of *HY5*. Furthermore, we found that *INDOLE-3-ACETIC ACID INDUCIBLE 19* (*IAA19*), *IAA22*, *PIN-FORMED 3* (*PIN3*) and *SMALL AUXIN UPREGULATED RNA* (*SAUR*) were upregulated in supplemental FR light and a similar pattern was found for the GA treated plants. In contrast, this pattern was not found in the IAA or GA + IAA treated plants. *IAA19* and *IAA22* are auxin responsive genes, There is an overall up-regulation of

IAA19 expression in low R:FR, and other studies have published gene expression work for IAA19 in low R:FR in Arabidopsis, also being confirmed by GUS expression (Pierik et al., 2009; Keuskamp et al., 2010a; de Wit et al., 2016). PIN3 is a protein that regulates auxin transport and has been found to relocate in response to shade, inducing an increase in auxin concentration in Arabidopsis hypocotyls (Keuskamp et al., 2010b). Previous studies have demonstrated that shade promotes *SAUR* expression in Arabidopsis, suggesting that *SAUR*s play a role in SAS (Ren and Gray, 2015). *GA20ox2* expression patterns are more complex. We found no expression change in *GA20ox1* in both the FR and GA treatments, while the IAA and GA+ IAA-treatment show downregulation of *GA20ox1*.

These results also further reinforce that pith cells respond differently to entire internode to FR treatment or to hormones. Pith exhibits distinct responsiveness to FR depending on the hormone treatment, as well as in comparison to supplemental FR alone. In supplemental FR, *HY5*, *SAUR*, *PIN3*, *PIN9*, *IAA22*, *YUC9*, and *GA20 ox* show higher expression in pith compared to the entire internode, suggesting an augmented IAA signaling and GA influence. However, for *HY5*, only GA and IAA induce upregulation, with pith showing a less pronounced response compared to the entire internode. The responsiveness of pith varies more widely in other treatments, further emphasizing complexity in the hormone network.

To analyse the expression pattern similarities between treatments and to identify which hormone(s) were most similar to FR treatment, we performed Pearson correlation analysis (Figure 4.24). The regression fit parameters indicated that IAA exhibited the most similar pattern compared to FR among these genes, followed by GA and GA+IAA. The fact that IAA treatment led to a gene expression pattern most similar to far-red light (Figure 4.24) suggests that auxin plays a significant role in mediating the elongation response.

From the correlations it was also apparent that the BR treatment induced a very strong expression pattern different to the other hormones and FR. Also, this strong effect of BR overcame the effects of the two other hormones, as the BR treatment pattern correlated highly with that of BR+GA+IAA treatment. Our qPCR data also suggests an opposing expression shift for many transcription factors in BR-treated plants compared to far-red treatment (Figures 4.23, 4.24). Overall, the qPCR results indicate that while BR is necessary for the FR-induced internode elongation in tomato, it is not able to induce the FR-like gene expression patterns, while IAA and GA are able to induce some of these changes. However, before overinterpreting this data, we need to keep in mind that a large portion of the qPCR targets are auxin responsive genes.

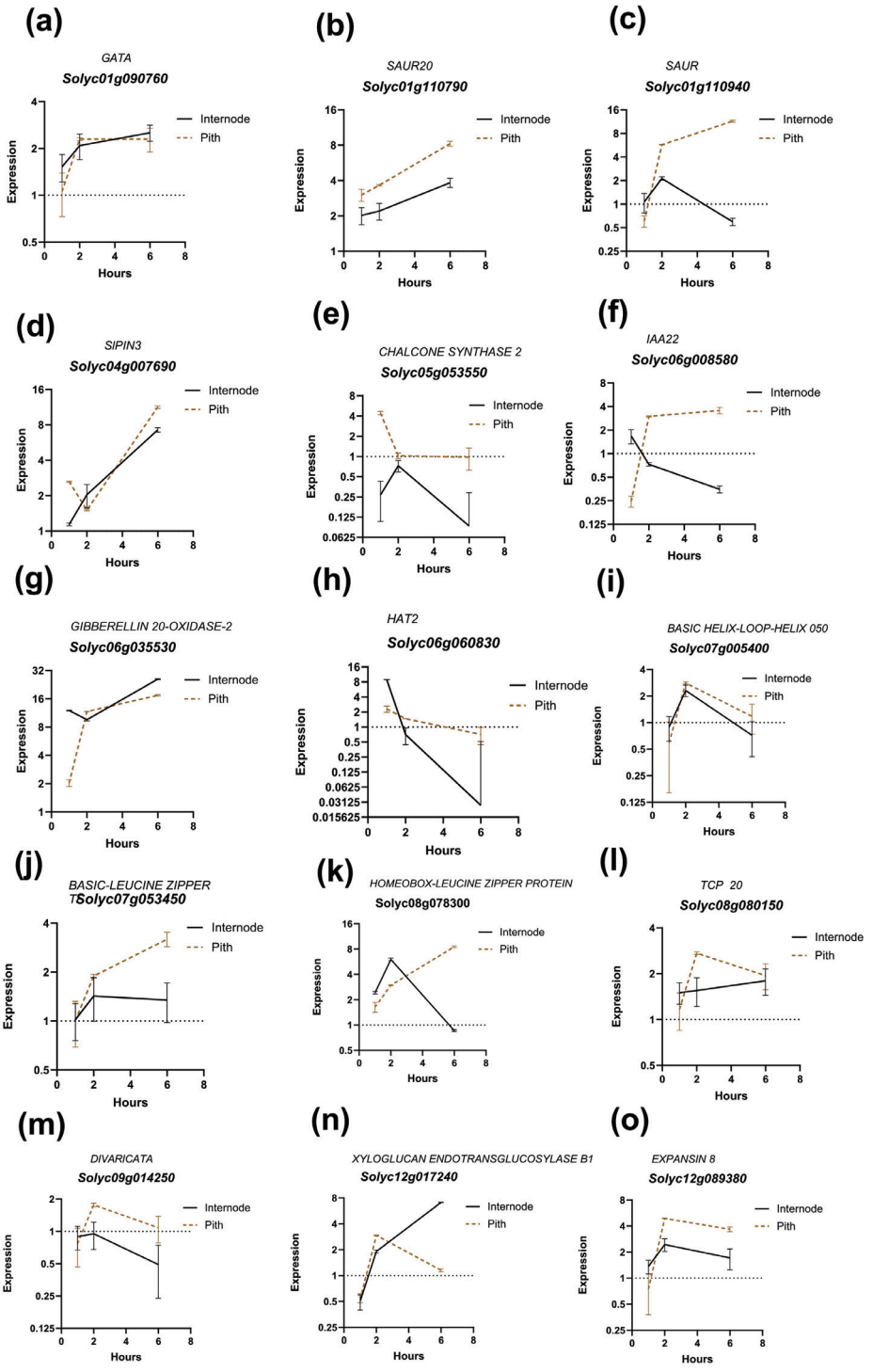
(a)
GATA
Solyc01g090760
(b)
SAUR20
Solyc01g110790
(c)
SAUR
Solyc01g110940
(d)
SlPIN3
Solyc04g007690
(e)
CHALCONE SYNTHASE 2
Solyc05g053550
(f)
IAA22
Solyc06g008580
(g)
GIBBERELLIN 20-OXIDASE-2
Solyc06g035530
(h)
HAT2
Solyc06g060830
(i)
BASIC HELIX-LOOP-HELIX 050
Solyc07g005400
(j)
BASIC-LEUCINE ZIPPER T
Solyc07g053450
(k)
HOMEOBOX-LEUCINE ZIPPER PROTEIN
Solyc08g078300
(l)
TCP 20
Solyc08g080150
(m)
DIVARICATA
Solyc09g014250
(n)
XYLOGLUCAN ENDOTRANSGLUCOSYLASE B1
Solyc12g017240
(o)
EXPANSIN 8
Solyc12g089380
Internode
Pith
Expression
Hours

► **Figure 4.22. Gene expression in response to FR for selected TFs and hormone-related and -responsive genes.** We analysed gene expression using qPCR to examine the effects of FR treatment on internode and pith tissues at three different time points: 1 hour, 2 hours, and 6 hours. The expression levels were obtained by comparing the response to WL and WL+FR conditions. The following genes were investigated: (a) *GATA*, (b) *AUXIN-RESPONSIVE PROTEIN SAUR20*, (c) *AUXIN-RESPONSIVE PROTEIN SAUR*, (d) *SIPIN3*, (e) *CHALCONE SYNTHASE 2*, (f) *AUXIN-REGULATED IAA22*, (g) *GIBBERELLIN 20-OXIDASE-2*, (h) HOMEOBOX-LEUCINE ZIPPER PROTEIN *HAT2*, (i) *bHLH050*, (j) *BASIC-LEUCINE ZIPPER (BZIP)* TF, (k) HOMEOBOX-LEUCINE ZIPPER PROTEIN, (l) *TCP20*, (m) *DIVARICATA*, (n) *XYLOGLUCAN ENDO-TRANSGLYCOSYLASE B1*, (o) *EXPANSIN 8*. The experiment included 4 biological replicates, each consisting of 8-12 plants. Additionally, 3 technical replicates were performed to ensure the accuracy of the measurements.

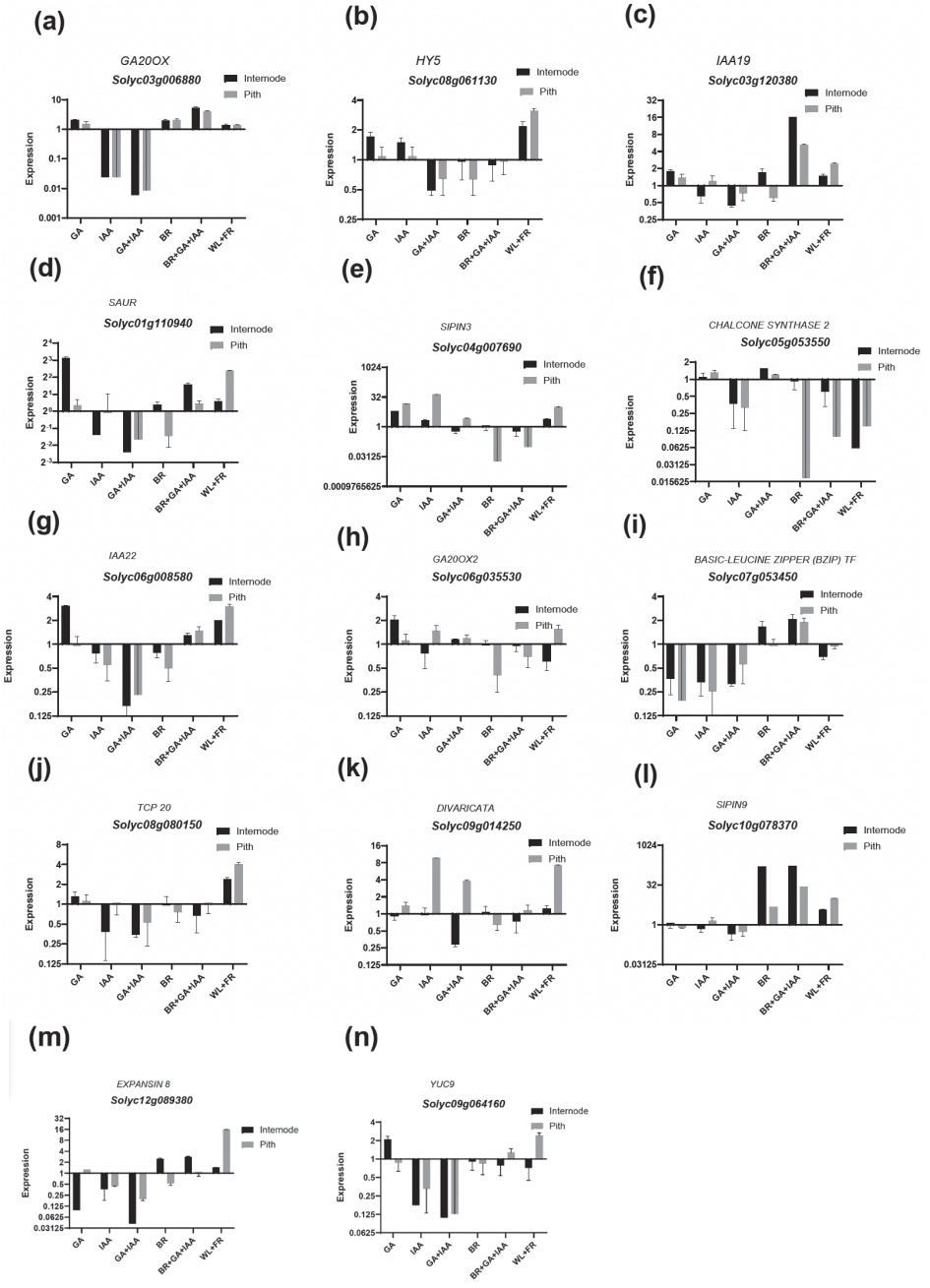
(a)
GA20OX
Solyc03g006880
Internode
Pith
Expression
GA
IAA
GA+IAA
BR
BR+GA+IAA
WL+FR
(b)
HY5
Solyc08g061130
(c)
IAA19
Solyc03g120380
(d)
SAUR
Solyc01g110940
(e)
SIPIN3
Solyc04g007690
(f)
CHALCONE SYNTHASE 2
Solyc05g053550
(g)
IAA22
Solyc06g008580
(h)
GA20OX2
Solyc06g035530
(i)
BASIC-LEUCINE ZIPPER (BZIP) TF
Solyc07g053450
(j)
TCP 20
Solyc08g080150
(k)
DIVARICATA
Solyc09g014250
(l)
SIPIN9
Solyc10g078370
(m)
EXPANSIN 8
Solyc12g089380
(n)
YUC9
Solyc09g064160

► **Figure 4.23. Gene expression in response to hormones for select TFs and hormone-related and -responsive genes.** We profiled gene expression using qPCR of hormone treatment with 100 µM GA, IAA, BR or GA+IAA, BR+GA+IAA or FR light after 2 hours to investigate expression in internode and pith tissues. The following genes were examined: a) *GA20ox*, b) *HY5*, c) *IAA19*, d) *SAUR*, e) *SIPIN3*, f) *CHALCONE SYNTHASE 2*, g) *IAA22*, h) *GIBBERELLIN 20-OXIDASE-2*, i) *BASIC-LEUCINE ZIPPER (BZIP) TF*, j) *TCP* transcription factor 20, k)*DIVARICATA*, l) *SIPIN9*, m) *EXPANSIN 8*, n) *YUC9*. To ensure reliability, the experiment included 4 biological replicates, each consisting of 8-12 plants. Moreover, 3 technical replicates were performed to validate the accuracy of the measurements.

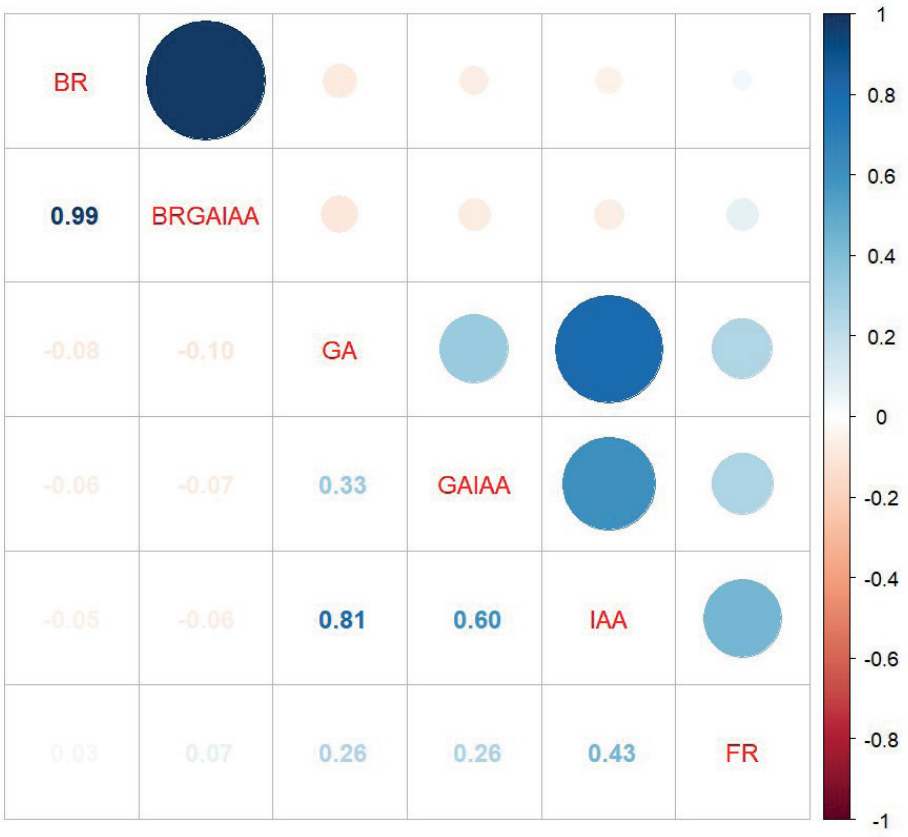

Figure 4.24. Correlations of hormone- and FR-induced gene expression changes in comparison to WL control. Pearson's correlation matrix between FR and each individual hormone or GA+IAA, BR+GA+IAA with gene expression date from Figure 4.23. Significant differences at $p<0.05$ among relatedness treatments after post hoc multiple comparison are shown separately for each treatment on the left and representation of the fitness with dot colored in blue for positive correlation, red for negative correlation.

4.3 DISCUSSION

In this chapter, we have provided insights into the hormone dynamics governing shade avoidance syndrome (SAS) in tomato. Our investigation shed light on the role of the hormones, auxins (IAA), gibberellins (GA), and brassinosteroids (BR), in mediating internode 1 elongation responses under changing light conditions. Our findings contribute to a deeper understanding of the regulatory mechanisms that plants employ to optimize growth in response to reduced red-to-far-red (R:FR) ratio.

4.3.1 The FR-responsive transcriptome included IAA and GA-responsive genes

We initiated our analysis using the multi-blast method to identify IAA, GA, and BR-related genes that were absent in the tomato (ITAG4.1) GO annotation, and then visualized the FR-responsive log foldchanges in a heatmap (Figure 4.2). We observed IAA-responsive *SAURs* displaying notable up- and downregulation, hinting at functional redundancy between *SAUR* genes. Other IAA-related genes had very mild changes except for few genes such as *IAA10* (Figure 4.2, red boxes). *SAURs* have been shown to respond not only to auxin, but also GA and BR (Luo et al., 2018; Stortenbeker and Bemer, 2019). GA-related genes, particularly *GA oxidases*, showed a pattern of FR-response. The fold change in their expression hinted at an underlying GA function in SAS. In the gene responses to the hormone and light treatments (Figures 4.22-4.23), we observed a surprisingly similar expression pattern between FR-, IAA- and GA-treated plants. The inducive expression patterns of GA and IAA exhibit a strong positive correlation, with IAA showing the highest correlation with FR responsiveness, followed by GA+IAA and GA alone. This suggests that the influence of GA inducive expression cannot be reversed by IAA. On the other hand, BR functions independently by inducing negative regulation, and combining it with GA and IAA does not reverse this effect. Due to the limitation of the number of genes that could be included in our analysis, these interpetations need to be taken cautiously.

In contrast, BR-treated plants displayed a unique expression pattern not resembling any other of our treatments (Figure 4.24). This divergence might be for the same reason as the fact that BR-related pathways did not exhibit significant up- or downregulation in our FR RNA-seq data (Figure 4.2b). Consequently, the gene expression patterns caused by BR treatment would be also different from FR treatment. Overall, this would indicate that the BR pathway would be either distinct from, or only a small part of the FR response in the tomato internode.

4.3.2 IAA can induce partial elongation response

Building on previous knowledge of SAS regulation with hormones and supported by the GO enrichment of RNA sequencing data (Chapter 3) and the behaviour of auxin-related genes (Figure 4.2a), we hypotheses that IAA has a major function in SAS. We, therefore, first continued with examining the effect of IAA on internode elongation. Although the primary source of auxin production is understood to be in young leaves and meristems, the exact origin and distribution of auxin during the shade avoidance response remains elusive (Chandler, 2009). The hypothesis that the first and second true leaves and the meristem are prime candidates due to their elevated position in the plant was supported by our results, as IAA treatment on the first true leaf and first internode both caused similar increases in hypocotyl and first internode length (Figure 4.5, S4.3). In local internode IAA treatment, all tested concentrations induced the same elongation response (Figure 4.6), leaving the optimal application concentration uncertain. At the microscopic level, IAA treatment resulted in increased cell elongation but did not significantly result in a high level of total elongation of the internode to recapitulate FR (Figure 4.7). However, we observed no change in the overall IAA concentration of first internode or first true leaf at 1h, 2h and 6h treatments with supplemental FR (Figure 4.12). Notably, the inhibitors PEO-IAA and BBo also did not significant affects supplemental FR-induced elongation (Figure 4.10, 4.11, S4.7), which indicates either that the application was not effective (did not penetrate to the necessary tissues, or did not target the pathway in tomato), or that IAA regulated pathway are regulated by the feedback loop of other hormones in the tomato FR-induced internode elongation. Overall, we were not able to find a clear indication that IAA level is increased in FR response building upon current experiment.

Interestingly, the auxin transport inhibitor NPA decreased the stem diameter in comparison to the mock treatment (Figure 4.8). Disturbance of IAA transport made plants tend to bend over due to fragility (Figure 4.8a). The results imply that auxin plays a role in regulating stem growth to ensure proper support. The NPA effect is likely causing an auxin imbalance in the first internode. Above this region, higher NPA concentrations hindered development and caused leaf curling, accompanied by a surge in hypocotyl length (Figure 4.8 S4.6). However, due to the complexity of IAA transport, we cannot further infer the distribution dynamic of IAA concentration.

Collectively, these findings indicate that auxin alone does not replicate the plant growth observed during the shade avoidance response. Hence, we followed up by investigating if the FR-induced internode elongation could be explained by hormone balance between

IAA and other hormones, including gibberellins (GA) and brassinosteroids (BR), which are also implicated in SAS (Yang et al., 1996; Djakovic-Petrovic et al., 2007; Keuskamp et al., 2012; Colebrook et al., 2014).

4.3.3 GA and BR induce full elongation, while their inhibitors fully block FR-induced elongation-are they more important than IAA?

Therefore, we examined the roles of gibberellins and brassinosteroids, also jointly with auxin in far-red light-induced shade avoidance response in *Solanum lycopersicum.* GA, BR and GA+BR treated plants in white light exhibited comparable internode elongation responses as tomato plants in supplemental far-red (Figures 4.13, 4.16, 4.17). Internode elongation appeared responsive to GA concentration changes (Figure 4.13). Interestingly, combining GA with IAA did not significantly impact hypocotyl or first internode length/ diameter (Figure 4.14). Experiments with GA and BR treatments demonstrated that these hormones have a more pronounced effect on internode elongation compared to IAA. This observation raises some possibilities. One potential explanation for the observed effects is that GA and BR may activate distinct downstream pathways or engage with pivotal regulators, fostering increased cell expansion and elongation, possibly linked to their divergent impacts on cell wall extensibility or the modulation of cell division processes. But this function is not be influenced by IAA Understanding the molecular mechanisms underlying the distinct elongation responses to GA, BR, and IAA would provide valuable insights into the nuanced roles each hormone plays in plant growth and development.

Inhibition of GA and BR biosynthesis, paclobutrazol (PBZ) and brassinazole (BRZ) respectively, led to shortened first internodes in FR-enriched plants (Figure 4.11). The inhibition of GA in the presence of far-red light resulted in the cessation of elongation, emphasizing the crucial role of GA in promoting stem growth during shade avoidance. Both IAA+BR or IAA+GA can overcome the depletion of GA or BR with inhibitor suggest a potential interactions between IAA,BR and GA. We were not able to carry on an experiment with PBZ or BZ complemented with only IAA/BR/GA compared to IAA+BR, IAA+GA, which might help us to confirm if there is a functional redundancy in the absence of IAA. This highlights the potential compensatory role of GA and IAA in overcoming the effects of BR deficiency, further emphasizing the intricate balance between these hormones. In conclusion, our findings highlight the essential role of both GA and BR in FR-induced elongation. Interestingly, the ability of either GA or BR to overcome the inhibition of the

other emphasizes a level of functional interchangeability between these hormones in FR. This mutual compensation indicates the collaborative nature of IAA, GA and BR signaling pathways in regulating plant elongation under FR conditions.

4.3.4 Summary

In conclusion, these findings underscore the complexity of hormonal interactions in regulating stem elongation during the shade avoidance response. While IAA contributes significantly to the gene expression pattern resembling far-red light treatment, GA and BR also play pivotal roles in modulating elongation. The intricate interplay between these hormones suggests a dynamic and finely tuned regulatory network that orchestrates plant growth in response to changing light conditions. These studies collectively highlight the complexity of hormone interactions, particularly auxin, gibberellins, and brassinosteroids, in various aspects of plant growth, including shade avoidance responses. This study's findings provide insights specific to tomato plants and their shade avoidance response. Further investigation guided by these fundamental works could lead to a comprehensive understanding of hormonal regulation for agriculture, exploration of hormones/inhibitors/combination that can be applied to specific traits (elongation of stem).

4.4 MATERIAL AND METHODS

4.4.1 Multiblast analysis

We sourced Arabidopsis Gene Ontology annotations from TAIR, extracted a list of genes annotated as responsive to GA, IAA, and BR, and conducted a multi-blast on Solgenomics to annotate these genes with corresponding names from TAIR. Gene list are put as supplement: https://docs.google.com/spreadsheets/d/12oYbPxeVWsOKH36vFiQIC37vfTyk9ezhI52F8LwkKcE/edit?usp=sharing

Table 4.1. GO term used for Arabidopsis hormone responsive gene multiblast in Solgenomic.net.

GO term	annotation
GO:0009733	response to auxin
GO:0009739	response to gibberellin
GO:0009735	response to cytokinin
GO:1902347	response to strigolactone
GO:0009741	response to brassinosteroid
GO:0009723	response to ethylene
GO:0009751	response to salicylic acid
GO:0009753	response to jasmonic acid

4.4.2 Plant material and growth conditions

In this study, we used *Solanum lycopersicum* cv Moneymaker obtained from Intratuin B.V. Growing conditions are identical to those listed in Chapter 2 of this thesis.

4.4.3 Phenotyping measurements

On the seventh day of far-red or hormone treatments at 10:30, using a digital caliper, measurements were taken for the stem length, first internode length, hypocotyl length, first internode diameter, and hypocotyl diameter. Each experiment consisted of at least 12 biological replicates, and every experiment was repeated a minimum of two times.

The hormone and hormone inhibitor treatments commenced when the seedlings reached sufficient size, approximately 14 days after germination.

For the plants subjected to a white light (WL) + FR treatment, they were transferred to a red to far-red light ratio (R/FR) of 0.2 on the first day of the treatment. All measurements were taken on the seventh day after treatment to assess the effects of the hormone and light treatments on the specified plant parameters.

4.4.4 Pharmacological treatments

In this chapter, multiple chemicals were utilized to explore the influence of plant hormones and their inhibitors on tomato growth and development under varying light conditions (Table 4.2). The plant hormones examined were mentioned in Table 4.2 (Kamoutsis et al., 1999; Asami et al., 2000; Hayashi et al., 2008; Mashiguchi et al., 2011; Kakei et al., 2015)

To investigate the effects of chemical treatment, 14-day old tomato plants were subjected working concentrations brushed by paint brush on the first true leaf or locally on the internode 1. For the hormone treatments, hormones were applied on day 1, 3, and 5 of the treatment, on of each plant's entire first internode. As for the hormone inhibitors, they were either applied one day before the treatment's initiation on the internode, or to the soil with a 40 ml working solution two days before the far-red (FR) treatment. For 100 μM IAA and100, 200 μM BBo, homogeneous spray of whole plants was also tested.

Subsequently, cross and longitudinal sections were collected from the middle of the first internode and preserved in 70% ethanol for subsequent microscopy.

Table 4.2. Chemicals information used in this chapter.

	Molecular weight	CAS	Stock solution	Working solution
GA_3	346.4	77-06-5	0.2 M	25, 50, 100 µM
IAA	175.2	87-51-4	0.1 M	5, 10, 25, 50, 100 µM
Brassinolide	480.7	72962-43-7	0.1 M	25, 50, 100 µM
Naphthylphthalamic acid (NPA)	291.3	132-66-1	0.1 M	25, 50, 125, 250 µM
4-Biphenylboronic acid (BBo)	198.0	5122-94-1	0.1 M	100, 200 µM
PEO IAA	293.3	6266-66-6	0.1 M	25, 50,100 µM
Paclobutrazol	293.8	76738-62-0	0.5 M	25, 50,100 µM
Brassinazole	327.8	280129-83-1	0.5 M	25, 50,100 µM

4.4.5 Microscopy

Handmade sections were obtained from the middle of internode, then they were stained with Safrinin O (0.01% w/v) for 5 minutes and put back into 70% ethanol and imaged using a Leica M205 fluorescence microscope. The collected images were measured using ImageJ (Schindelin et al., 2012) . The cell length data were obtained from longitudinal sections, cell layer number/thickness data were obtained from cross sections. We measure cross section for at least three angles for these features.

4.4.6 Extraction and Quantification of IAA through Liquid Chromatography-Tandem Mass Spectrometry

To extract IAA from leaf and internode, approximately 20 mg of snap-frozen leaf material was used per sample. The tissue was finely powdered at -80°C by manual grinding. The powdered samples were subjected to extraction using 1 mL of cold methanol containing [phenyl 13C6]-IAA (at a concentration of 0.1 nmol/mL) as an internal standard, following a previously established protocol. After extraction, the samples were filtered using a 0.45 mm Minisart SRP4 filter and analyzed on the same day. The IAA content was assessed using a Waters Xevo TQs tandem quadrupole mass spectrometer, as detailed in previous descriptions from literature (Küpers et al., 2023).

4.4.7 RNA extraction and cDNA synthesis

In the first qPCR experiment plants were either placed in WL or in R/FR=0.2. In the second qPCR treatment plants were either treated with GA, IAA, or GA + IAA, BR, IAA+GA+BR and placed in WL or treated with a mock and placed in either WL or R/FR = 0.2. We used four biological replicates, consisting of 8-12 plants, for one biological replicate,

minimum three internodes were put in tube.. For qPCR we had three technical replicates. In the first experiment tomato plants were harvested after FR treatment after 1 hours, 2 hours and 6 hours. In the second experiment, the plant material was harvested 2 hours after pharmacological treatment. Samples were snap frozen by liquid nitrogen and stored at -80 degrees Celsius. Total RNA was extracted by the RNeasy kit (Qiagen) according to manufacturer's instructions. RNA was quantified with nanodrop (Thermo Fisher Scientific). The reverse transcription was done using random hexamer primers with RevertAid H Minus (Thermo Fisher Scientific™) according to manufacturer's instructions.

4.4.8 Quantitative RT-PCR

The CFX opus 384, Bio-rad CFX Maestro was used to perform quantitative reverse transcription PCR. Primers used are listed in Table 4.3. We used SYBRgreen super mix dye (Thermo Fisher Scientific™). Relative transcript abundance was calculated using the comparative $2^{-\Delta\Delta Ct}$ method using *ACTIN2* as the reference gene.

4.4.9 Statistical analysis

Data was analyzed by R v4.3 using an Anova followed by a Tukey test and Pearson correlation analysis. The illustration of the data was made by GraphPad (Version 9.5.1 (528), January 24, 2023).

Table 4.3. Primer list of qPCR in this chapter.

Primer name	Target	Sequence
0150-L	Solyc08g080150	GTCGTGCTCCAGTATCCTCA
0150-R	Solyc08g080150	CGATCCAATTTTAGGCCCCG
0760-L	Solyc01g090760	CAAATCAGGCCGGCTAGTTC
0760-R	Solyc01g090760	TCAGCAGACCCGAAAGTGAT
0790-L	Solyc01g110790	AATTTGGCTTCGCTCATCCA
0790-R	Solyc01g110790	AGCTGACTGTACATGGTCCT
0830-L	Solyc06g060830	ACTCCTCGTCTCCATGTTCC
0830-R	Solyc06g060830	AGAAGATCTGGGGTTGAGCC
0940-L	Solyc01g110940	TCTCGGCAGGGAATTGTGAT
0940-R	Solyc01g110940	GGCTATCCGTGTTCCTCGTA
3450-L	Solyc07g053450	GAGGAGCAGCAACAACAACT
3450-R	Solyc07g053450	CTCACCCTTGACCTTTGTGC
3550-L	Solyc05g053550	TAGTGGTGGTTGAAGTGCCA
3550-R	Solyc05g053550	ACCAGCAAAGCAACCTTGTT
4250-L	Solyc07g053450	CGTATGGACTCGAGCATGGA
4250-R	Solyc07g053450	GTTGTTTTCGCTCGTGGTCT
5400-L	Solyc07g005400	AGGAAATGTTGGGAGGGGAG
5400-R	Solyc07g005400	TAGGAGAAGTTGAGCCACCG
5530-L	Solyc06g035530	ATCATGGAACTCTTGGGCGA
5530-R	Solyc06g035530	TTTGGACTGATAGAGCGCCA
7240-L	Solyc12g017240	TAGTGACAGTGCCAGCAGAA
7240-R	Solyc12g017240	CTTTGGTGATCAGCGAGCTC
7690-L	Solyc04g007690	CCCCAAATCCGGAAATTGCT
7690-R	Solyc04g007690	TAAAATCCGTGCCACCGAAC
8300-L	Solyc08g078300	CCTAGGCCTCAATCCCAGTC
8300-R	Solyc08g078300	TCGCCGAACAGTACGATTTC
8370-L	Solyc10g078370	CAGCCCTGACCAATGTTCTG
8370-R	Solyc10g078370	TGGACCATTCAAGGGATCCC
8580-L	Solyc06g008580	TCGAACCCACAAAATCTGCC
8580-R	Solyc06g008580	GTTCAAGCATCCCATTGGTGT
9380-L	Solyc12g089380	CCCTCCACGTCCACATTTTG
9380-R	Solyc12g089380	ATCCTGCCCCTCCTACATTG
GA20ox2-L	Solyc03g006880	TTTGTGGACGATGAATGGCG
GA20ox2-R	Solyc03g006880	TAGGCCATGTGAAATCGGGA
HY5 -L	Solyc08g061130	GATCAGAAGAGTGCCGGAGA
HY5-R	Solyc08g061130	CCCTTGCTTGTTGTGCTGAT
IAA19-L	Solyc03g120380	AGTGATCGAAACAGCAGCAG
IAA19-R	Solyc03g120380	AAAACGGTGCTCCATCCATG
YUC9-L	Solyc09g064160	GTTTGGTGGGGAAGTGGTTC
YUC9-R	Solyc09g064160	CTTGGCAAAACATGAACCGC
SlACT2-L	Solyc11g005330	TGTGCTCAGTGGTGGTTCAA
SlACT2-R	Solyc11g005330	CCGGTGGAGCAACAACCTTA

4.5 SUPPLEMENTARY DATA

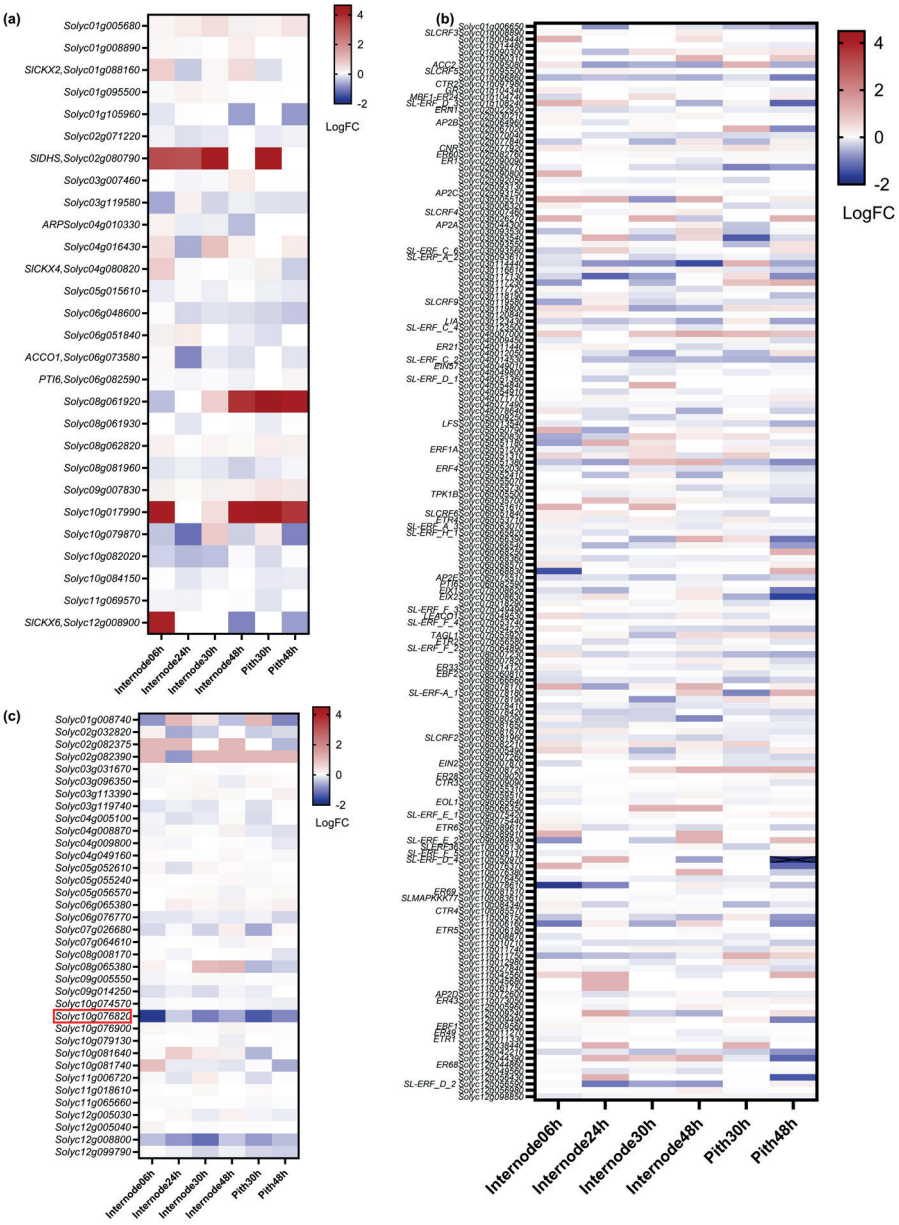

Figure S4.1. FR response of cytokinin, ethylene and strigolactone-related genes in tomato. Heatmap generated from RNA-seq data illustrates the log fold change in gene expression associated with (a) Cytokinin, (b) Ethylene, (c) Strigolactone. Upregulation is represented in red, while downregulation is depicted in blue. FR-responsive DEGs are boxed in red.

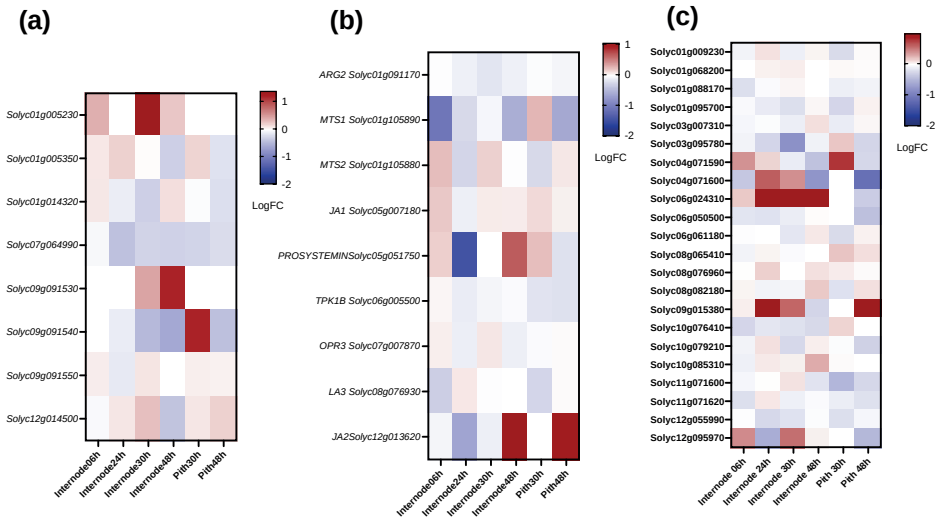

Figure S4.2. FR response of SA, JA and ABA-related genes in tomato. Heatmap generated from RNA-seq data illustrates the log fold change in gene expression associated with (a) salicylic acid (SA), and (b) jasmonic acid (JA), (c)ABA. Upregulation is represented in red, while downregulation is depicted in blue.

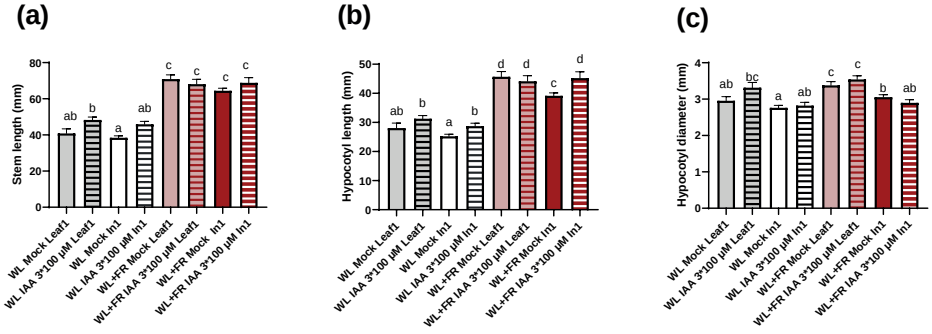

Figure S4.3. Stem responses to 100 µM IAA brushing treatments applied either on leaf 1 or internode 1. We treated 14 day-old tomatoes with 100 µM IAA by brushing onto leaf 1 and internode 1. Brushing was applied 3 times over one-week treatment period. The data include measurements of (a) stem length, (b) hypocotyl length, (c) hypocotyl diameter. The data are presented as mean ± SEM, and different letters indicate significant differences between treatments based on ANOVA analysis with Tukey's post hoc test ($P<0.05$). There were 12 biological replicates, and the experiment was repeated twice.

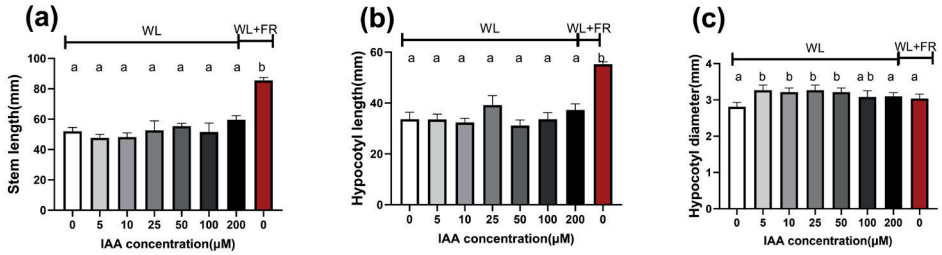

Figure S4.4. Stem responses to different IAA concentration by brushing treatments applied on internode 1. We treated 14 day-old tomatoes with different concentration of IAA by brushing onto internode 1. Brushing was applied 3 times over one week treatment period. The data include measurements of (a) stem length, (b) hypocotyl length, (c) hypocotyl diameter. The data are presented as mean ± SEM, and different letters indicate significant differences between treatments based on ANOVA analysis with Tukey's post hoc test ($P<0.05$). There were 12 biological replicates, and the experiment was repeated twice.

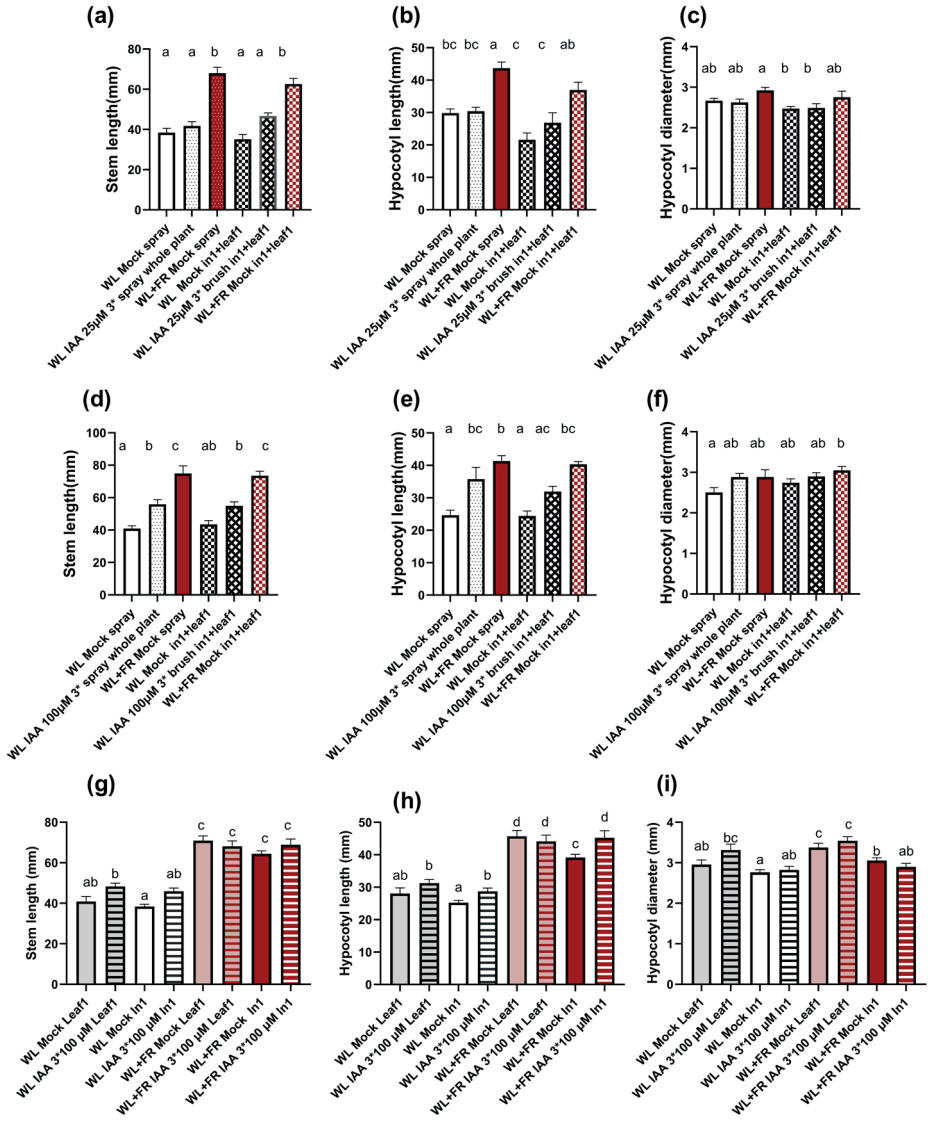

Figure S4.5. Stem responses to different IAA treatments. We treated 14 day-old tomatoes with 25 μM or 100 μM IAA by whole plant spray, or by brushing onto leaf 1 and internode 1. Spray and brush were applied 3 times over one week treatment period. The data includes measurements of (a) stem length of 25 μM IAA treatment, (b) hypocotyl length of 25 μM IAA treatment, (c) hypocotyl diameter of 25 μM IAA treatment, (d) stem length of 100 μM IAA treatment, © hypocotyl length of 100 μM IAA treatment , (f) hypocotyl diameter of 100 μM IAA treatment, (g) stem length of brushing 100 μM IAA on internode or leaf 1, (h) hypocotyl length of brushing 100 μM IAA on internode or leaf 1, (i) hypocotyl diameter of brushing 100 μM IAA on internode or leaf 1,. The data are presented as mean ± SEM, and different letters indicate significant differences between treatments based on ANOVA analysis with Tukey's post hoc test ($P<0.05$). There were 6-9 biological replicates, and the experiment was repeated twice. Picture (a) was created with Biorender.

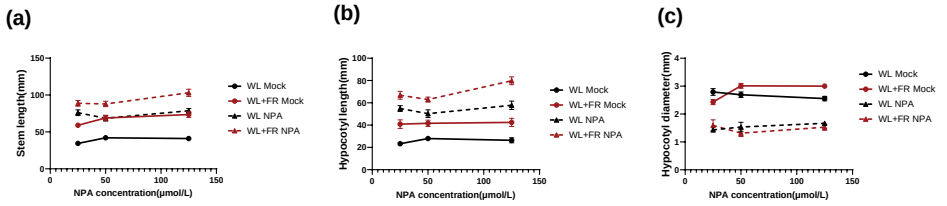

Figure S4.6. Stem response to different NPA concentrations. We treated the first internode of 13 dag tomatoes with 25, 50, 125 µM NPA (or mock) in WL conditions one day prior to the start of the one week FR treatment. The data include measurements of (a)stem length, (b) hypocotyl length, (c) hypocotyl diameter. Data are presented as mean ± SEM, and different letters indicate significant differences between treatments based on ANOVA analysis with Tukey's post hoc test ($P<0.05$). There are 12 biological replicates, and the experiment was repeated twice.

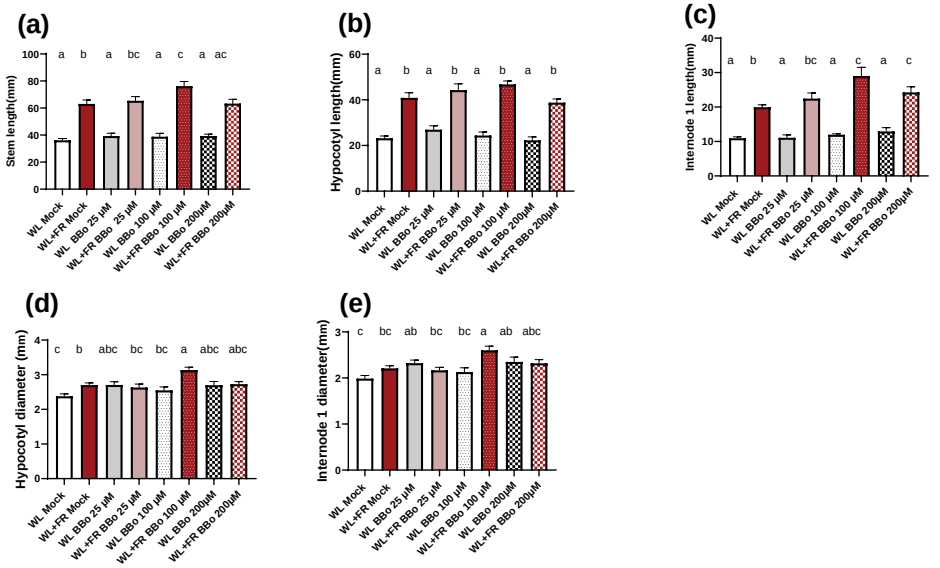

Figure S4.7. Stem response to different BBo concentrations by spray. We treated the first internode of 13 dag tomatoes with BBo (or mock) in WL conditions one day prior to the start of the one-week FR treatment. The data include measurements of The data includes measurements of (a) Stem length (b). Hypocotyl length (c) First internode length (d) Hypocotyl diamete©(e) First internode diameter. Data are presented as mean ± SEM, and different letters indicate significant differences between treatments based on ANOVA analysis with'Tukey's post hoc test ($P<0.05$). There are 12 biological replicates, and the experiment was repeated twice.

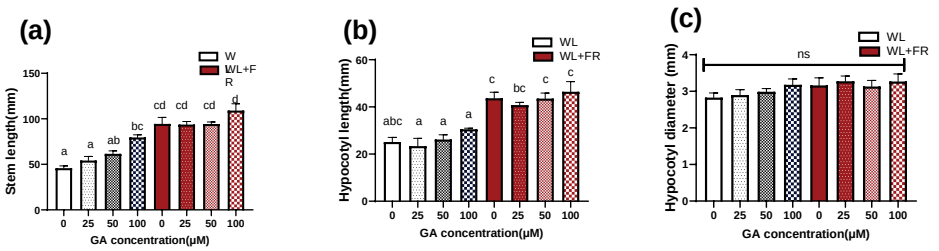

Figure S4.8. Stem response to different GA concentrations. We brushed the first internode of 14 day-old tomatoes with different concentration GA (or mock) in WL or FR conditions over one-week FR treatment. Brushing was applied 3 times over one week treatment period. The data include measurements of (a)Stem length, (b) Hypocotyl length, (c) Hypocotyl diameter. (Data are presented as mean ± SEM, and different letters indicate significant differences between treatments based on ANOVA analysis with Tukey's post hoc test (P<0.05). There are 12 biological replicates, and the experiment was repeated twice.

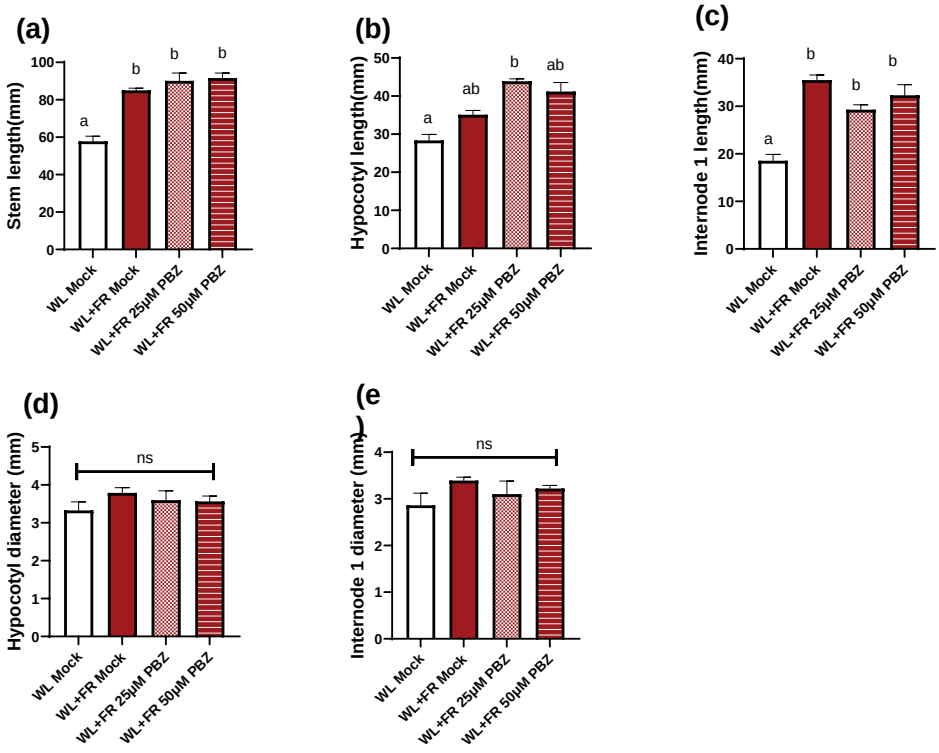

Figure S4.9. Stem response to different concentration PBZ. We brushed the first internode of 13 dag tomatoes with different concentration PBZ (or mock) in FR conditions one day in advance of one week FR treatment. Brushing was applied 3 times over one week treatment period. The data include measurements of (a) Stem length, (b) Hypocotyl length, (c) Hypocotyl diameter, (d) Hypocotyl diameter, (e) Internode 1 diameter. Data are presented as mean ± SEM, and different letters indicate significant differences between treatments based on ANOVA analysis with Tukey's post hoc test (P<0.05). There are 6 biological replicates.

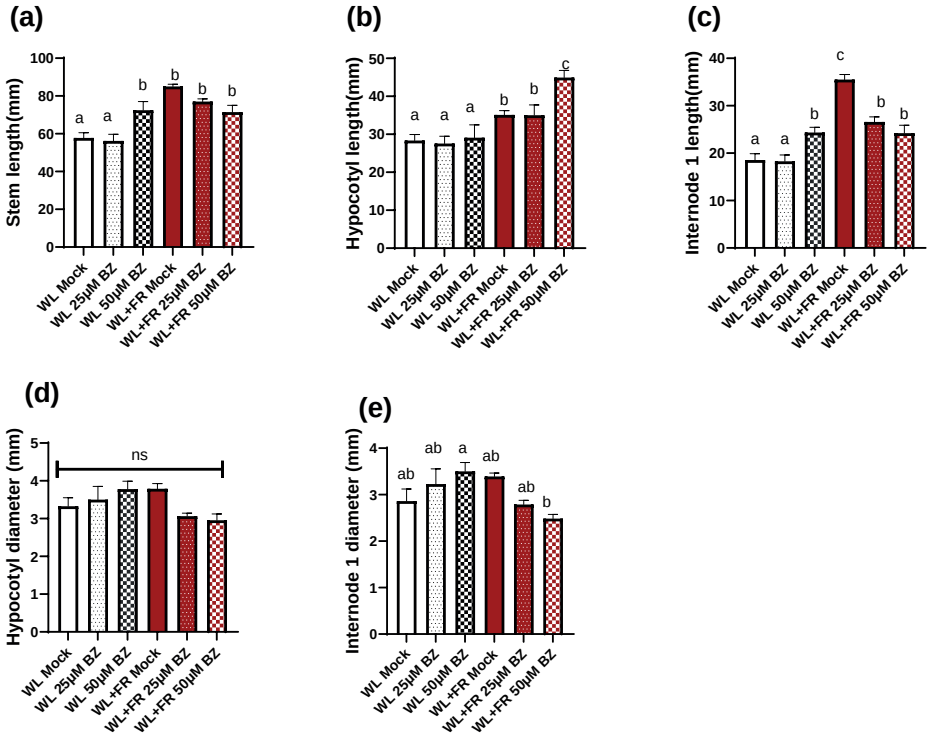

Figure S4.10. Stem response to different concentration BZ. We brushed the first internode of 13 dag tomatoes with different concentration BZ (or mock) in FR conditions one day in advance of one week FR treatment. Brushing was applied 3 times over one week treatment period. The data include measurements of (a) Stem length, (b) Hypocotyl length, (c) Hypocotyl diameter, (d) Hypocotyl diameter, (e) Internode 1 diameter. Data are presented as mean ± SEM, and different letters indicate significant differences between treatments based on ANOVA analysis with Tukey's post hoc test ($P<0.05$). There are 6 biological replicates.

.

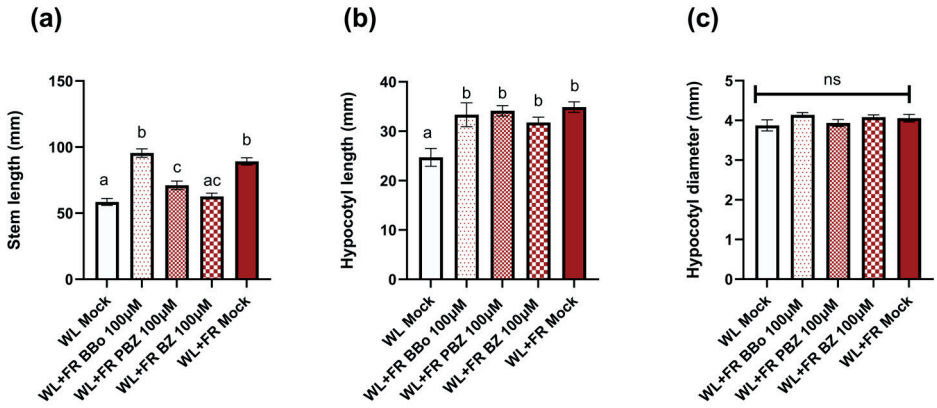

Figure S4.11. Stem response to 100 µM BBo, PBZ, BZ. We drained the soil three days before FR treatment, and applied BBo, PBZ and BZ directly to the soil one day before FR treatment in FR conditions. The data include measurements of (a) Stem length, (b) Hypocotyl length, (c)Hypocotyl diameter. The data are presented as mean ± SEM, and different letters indicate significant differences between treatments based on ANOVA analysis with Tukey's post hoc test ($P<0.05$). There are 12 biological replicates, and the experiment was repeated twice.

EXPLORING CONSERVATION OF CELLULAR-LEVEL TRAITS IN SHADE AVOIDANCE SYNDROME AMONG SPECIES

Linge Li, Annemieke Nieuwhof, Cornalijn Hazelebach, Lotte van der Krabben,
Ronald Pierik and Kaisa Kajala

ABSTRACT

This chapter explores the diversity of internode elongation responses to supplemental far-red light, delving into pith cell elongation, and the regulatory roles of specific GATA, TCP, and bZIP transcription factors (TFs). First, we extended our phenotypic investigation from tomato to eight dicots and found that they are diverse in responsiveness to treatment with supplemental far-red (FR) light. We also revealed quantifiable pith elongation happening in species with strong response to the FR signal. We followed up with the expression of three candidate transcription factor genes that had FR-responsive pattern in pith and/or internode in tomato. We identified the homologs for the genes encoding these transcription factors from each of the species, quantified their FR-responsive expression in internodes and piths, and found that the expression patterns were conserved within Solanaceae. In our study into pith in shade avoidance in these species, we saw the gene expression patterns that differed from the whole internode, indicating that the pith responses are distinct, likely cell-type-specific. Looking ahead, the pursuit of insights into transcriptional regulation, evolutionary conservation, and molecular mechanisms governing FR responses across dicots remains an interesting line to follow. Our work has started to shed light on the functional divergence and conservation of the factors that respond during shade avoidance.

5.1 INTRODUCTION

Shade avoidance syndrome is a prevalent response observed in various species such as tomato, as described at length in Chapters 2 to 4. Shade tolerance levels differ among species, but the full extent of diversification remains unclear. In this Chapter. we expanded our work to include a broader spectrum of dicotyledonous species and investigate the conservation of transcription factor responsiveness to far-red (FR), unveiling some underlying conserved mechanisms of the shade avoidance syndrome response.

Plants display shade avoidance responses that help them reach the light at high planting density, upon light-mediated detection of neighbors. Plants have evolved mechanisms to sense changes in light quality and adjust their growth strategy accordingly. Phytochromes serve as key indicators by measuring the ratio of red to far-red light, allowing plants to detect whether they are, or soon will be, in the shade of neighboring plants (Green-Tracewicz et al., 2011; Pierik and De Wit, 2014; Ranade et al., 2019). In response to FR enrichment, plants adopt various common and well-studied growth strategies, termed shade avoidance syndrome (SAS). This response involves a suite of morphological changes, including the elongation of petioles and stems, alterations in flowering time, and a reduction in chlorophyll content (Green-Tracewicz et al., 2011; Pierik and De Wit, 2014; Ranade et al., 2019). The SAS represents a strategy of considerable adaptive significance in plants, particularly in dense natural communities, where increased shoot elongation can enhance relative fitness (Schmitt, 1997). However, it can also result in reduced crop productivity as plants invest their resources to growth in non-harvestable parts of the plant at the cost of the harvestable parts.

In the preceding chapters, we delved into the cellular (Chapter 2) and transcriptomic changes (Chapter 3) occurring in the stem, with a focus on the transcription factors (TFs) associated with these changes. In this chapter, we will compare the FR-responses of different dicotyledonous species and look into the conservation of the FR-responsiveness of the transcription factors that we identified from tomato RNAseq data in Chapter 3. To provide a better framework to consider shade avoidance in an evolutionary context, we will first provide an overview of relevant background, starting with the ecological aspects of playing into shade avoidance and its adaptive value in different environments.

5.1.1 Shade avoidance, shade tolerance and their evolution

Exploring the dynamic strategies of plant species in different ecosystems reveals contrasting approaches to competing for light. Pioneer species and shade-tolerant species

showcase distinct lifestyles and evolutionary insight into shade responses. They are case studies with varied responses into how plants adapt and compete within diverse environmental contexts. Pioneer plant species are adapted to colonize harsh, sterile and sun-exposed environments and grow quickly to take advantage of available resources before larger competitors arrive (Miyazawa et al., 2014; Sottosanti, 2023). However, as the environment changes and the intermediate species grow taller, the shade they cast can deprive the pioneer species of adequate sunlight (Sottosanti, 2023). In response to this shade, the species composition undergoes a transition from pioneers to a mixed ecosystem with dominant plants favoring high light and understory species thriving in the shade of the forest canopy (Hagen et al., 2015; Avalos and Avalos, 2019). For these shade-tolerant species, it is not beneficial to produce shade avoidance responses in deeply shaded habitats, such as forest understory, as they would suffer reduced performance without any benefit to be gained. In contrast, shade-tolerant species have a slower growth rate and a more restricted capacity to respond to sudden environmental changes (Coverdale and Agrawal, 2021). Shade-tolerant species tend to have larger seeds, high wood density, high leaf specific mass, low photosynthetic rates, and slow growth (Taiz et al., 2010; Coverdale and Agrawal, 2021). Shade tolerance appears to involve efficient light harvesting at constant low irradiance and efficient harvesting of sunflecks (Henry and Aarssen, 1997).

Shade avoidance responses have possibly evolved with shade, as early as the Devonian period, and are possibly more ancient than shade tolerance in plants (Casal, 2012). In contrast, the evolution of shade tolerance is associated with attenuation of shade avoidance and reduced phenotypic plasticity in certain plant species such as milkweeds and *Geranium robertianum* (Gommers et al., 2017; Coverdale and Agrawal, 2021). Therefore, is evidence that in these lineages, shade avoidance responses predate the evolution of shade tolerance in plants.

5.1.2 Stem evolution and diversity

The evolution of terrestrial life ushered in a period of intense competition for sunlight among plants, where the ability to grow taller and reach the canopy ahead of competitors conferred a distinct advantage. However, as plants increased in height and expanded along their primary axis, they encountered new challenges. These challenges included the need for innovative structural support for aerial organs and an efficient mechanism to transport water and nutrients to greater heights, beyond the limitations of capillary forces (Hetherington et al., 1998; Parra et al., 2010).

To address these challenges, certain seed plants evolved an additional stem cell population known as the vascular cambium. This remarkable adaptation gave rise to a hollow cylinder within the plant's stems, facilitating radial growth of primary axes (Venning, 1949). This phenomenon, termed secondary growth, independently evolved multiple times in seed plants, suggesting that factors governing primary growth were repurposed to coordinate secondary growth (Melzer et al., 2008). Mechanical strength was not solely achieved through stem thickening via vascular cambium activity; it also involved specialized cell types with thickened cell walls found within the two tissues—the phloem and xylem—that the vascular cambium generates (Etchells et al., 2012). This growth flexibility serves as a crucial survival strategy in diverse stressful conditions.

The detailed study and reporting of pith cell elongation (Chapter 2) in the context of the SAS is relatively unexplored territory. Pith, a tissue located in the center of dicotyledonous stems and composed of undifferentiated parenchyma cells (Zabel and Morrell, 2020). While pith is found in dicots, monocots also have pith, which extends in the center of monocot roots, composed of parenchyma (Roodt et al., 2019). The diversity of pith in vascular plants can provide insights into their evolution. Medullary bundles, which are vascular units in the pith, have evolved multiple times in vascular plants (da Cunha Neto et al., 2020). The development of the primary vascular system within Nyctaginaceae has been studied, and it was found that medullary bundles diversified within the family (da Cunha Neto et al., 2020). In the Early Devonian euphyllophyte *Leptocentroxyla*, a protoxylem pathway to the evolution of pith has been hypothesized (Tomescu and Mcqueen, 2022). The delayed and shortened protoxylem differentiation hypothesis explains the evolution of pith by delaying the onset of differentiation and lengthening cell growth duration in a central protoxylem strand, and shortening the interval of differentiation of those tracheids, leading to the evolution of pith (Tomescu and Mcqueen, 2022). Here, we are able to limit our investigation of pith inside of dicots, where diversity of pith patterns was also observed. By exploring the relationship between SAS and pith elongation, we hope to query the conservation of pith elongation within dicots' adaptation strategies.

5.1.3 Target dicot species for studying evolution of FR-responses in the stem

In this chapter, our aim is to see how conserved the internode FR-responses are within dicots with stem growth habit. We subjected seven plant species from four families (Figure 5.1) —*Pisum sativum* (Pea) and *Glycine max* (Soybean) from Fabaceae,

Brassica nigra (Black mustard) from Brassicaceae, and *S. lycopersicum* Moneymaker (Tomato), *Capsicum annuum* (Pepper), and *Solanum melongena* (eggplant) from the Solanaceae family, and *Ocimum basilicum* (Basil) from Lamiaceae family—to either white light (WL) or white light with supplemental far-red (WL+FR) conditions for one or two weeks, assessing the presence of the shade avoidance response. We found some conservation in the pith responses, but not across all dicots, and family-specific conservation of transcription factor response in SAS. This research can help us develop a further understanding of morphological and molecular regulation in SAS and how it has evolved across dicots.

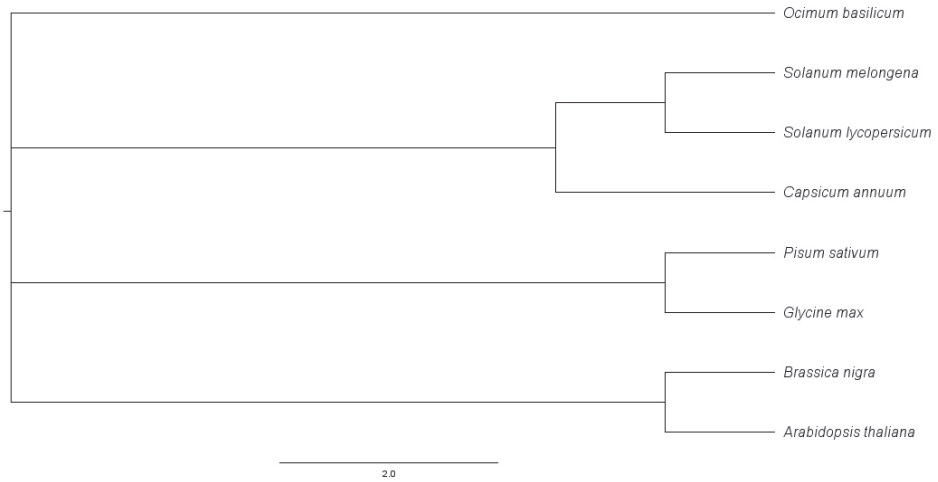

Figure 5.1 Species included in this study. This taxonomy common tree was generated by https://www.ncbi.nlm.nih.gov/Taxonomy/CommonTree/wwwcmt.cgi.

We also wanted to explore if our hypotheses could be addressed in the model species *Arabidopsis thaliana* Col-0 that has rosette growth habit instead. Arabidopsis has long served as a model system for exploring the shade avoidance response (SAS), so we explored the responses of the Arabidopsis inflorescence stem, which exhibits secondary growth and pith development. Using Arabidopsis for addressing questions related to SAS is advantageous due to the availability of mutants and the ease of conducting transgenics in this model plant. However, regrettably we found that the inflorescence stem proved to be suboptimal for this purpose.

In this chapter, we also delved into the conservation of transcription factor (TFs) gene expression within the context of SAS across multiple plant species. For the analysis of

conservation of FR-responsiveness, we used an interspecies analysis with the homologs of three FR-responsive TFs we discovered in tomato in Chapter 3. First, *Solyc01g090760* encodes a GATA TF, belonging to the zinc finger DNA binding protein family. A GATA homolog in humans is vital for development and cell differentiation (Gao et al., 2015; Lu et al., 2021; Hou et al., 2022). Second, *Solyc08g080150*, or *SlTCP20*, encoding for a TCP transcription factor, exhibits diverse functions in leaf development, flower symmetry regulation, shoot branching, and senescence (Cubas et al., 1999; Parapunova et al., 2014). Third, *Solyc07g053450*, encodes a bZIP transcription factor which plays a pivotal role in various biological processes, particularly abiotic stress responses (Liu et al., 2023a). We carried out an homology analysis and qPCR analysis to see if the FR-induced expression in internodes was conserved. The investigation strived to illuminate the connection between TFs, SAS, and the development of essential plant structures, providing insights into how various plant species acclimate and thrive in response to shifting light condition.

5.2 RESULTS

5.2.1 Arabidopsis inflorescence stem elongates in response to lower R:FR ratio in long day conditions

Arabidopsis thaliana accession Col-0 is widely used to study petiole elongation and leaf hyponasty in SAS (Kohnen et al., 2016b; Müller-Moulé et al., 2016; Michaud et al., 2017; Pantazopoulou et al., 2017). However, there is limited information on the elongation of inflorescence stem, that undergoes major secondary growth, in response to environmental cues such as FR enrichment. We wanted to test if the tomato stem FR responses were conserved in Arabidopsis and if we could use the wide Arabidopsis genetic resources for dissecting our tomato radial growth and pith findings. In tomato supplemental FR treatment, a long day condition of 16 hours of daylight and 8 hours of darkness with 200 PAR is typically used. In Arabidopsis experiments in our group, a lower light level ranging from 120 PAR to 150 PAR before flowering is used, and plants are usually subjected to short day conditions. Therefore, we needed to test if specific conditions, if any, were suitable for inducing stem elongation FR-response in Arabidopsis. We conducted a FR treatment with bolted inflorescence stems measuring 0.5-1.5 cm.

We first tested the effect of day length: long day (LD, 16h light, 8h dark) or short day (SD, 8h light, 16h dark). We started with R:FR (“WL+FR”) of 0.2 in SD with 150 PAR, same R:FR ratio as we tested tomato. Inflorescence stem elongation response was

observed in the WL+FR, although the response was mild (Figure 5.2a). Next, later we subjected Arabidopsis to LD with 150 PAR with same R:FR=0.2, and the result was stronger (Figure 5.2a).

We then continued with test LD and SD with R:FR=0.11 to see if lower R:FR ratio would increase the response (Figure 5.2b). In LD, the response was significant already at 5 days with 150 PAR, accompanied by a significant increase in inflorescence stem diameter (Figure 5.2b, c).

Then we tested the effect of light intensity and if it could induce a stronger or a more robust response (Figures 5.2d, e). With higher light intensity of 200 PAR and R:FR 0.20 in LD, we observed FR-induced elongation also at 5 days, with the diameter first narrowing before the radial growth was observed (Figure 5.2d, e). All in all, we concluded that the robustness of the FR-induced elongation in the Arabidopsis inflorescence stem was highly dependent on light level and the day length, and observable only in a brief window of time.

5.2.2 Infloresence stem elongation in SAS is not associated to pith elongation in Col-0

We investigated the cellular morphology, including the pith cell elongation response in Arabidopsis inflorescence stems in response to low R:FR. Previous literature (Franklin, 2008) had reported consistent elongation of inlorescence stem structures in such conditions. Inspired by the phenomenon that we observed in Chapter 2 in tomato cultivars Moneymaker and M82, where pith cells exhibited elongation, we applied a similar sectioning method to assess pith cell response in Arabidopsis Col-0. We used 200 PAR in LD with R:FR=0.11 for further work.

The pith cell sizes appear heterogeneous already by eye (Figure 5.3a), so we quantified them from different locations within the pith cylinder. We measured the length of pith cells in the outermost two layers and the middle layers, comparing different light treatments in Col-0 (Figure 5.3). Surprisingly, pith cell length in either location did not exhibit significant elongation in the WL+FR treatment. However, we observed a significant increase in pith thickness in WL+FR, and radial diameter, suggesting some level of cell expansion in the radial dimension. So, the pith cell response in Col-0 was not consistent with our expectations but the radial growth aligned with tomato data.

Given that the radial growth phenotype was observed, we wanted to test what would happen to the FR-responsive influorescence stem elongation in radial growth mutants

(*pxy*, *pxy pxl1 pxl2 er erl*, all in the Col-0 background))(Etchells et al., 2013). However, our exploration of mutants with impaired secondary growth in Arabidopsis was difficult in achieving alignment during bolting. These mutants exhibited minimal germination and struggled to thrive, leading to a vulnerable system that ultimately rendered the pursuit of this trait in Arabidopsis impractical. Thus, we still include Arabidopsis for gene expression analysis later in this chapter, but we did not pursue further genetics directions in Arabidopsis.

5.2.3 Pith elongation is a conserved behavior in shade avoiding species

In chapter 2 we observed the responses to FR light in tomato, a species within the Solanaceae family. We wanted to explore if these responses were conserved across species, and we tested other dicots with stem growth habit, starting with other species from the Solanaceae family; *Capsicum annuum* (commonly known as bell pepper, Figure 5.4) and *Solanum melongena* (eggplant, Figure 5.5). As we had been testing if Arabidopsis could be used as a stem-response model, we also wanted to test a species with stem growth habit from the Brassicaceae family, so we tested *Brassica nigra* (Figure 5.6). We also tested species from the Fabaceae (legume) family, *Glycine max* (soybean, Figure 5.7) to expand our understanding in dicot crops. For this set of species, we identified a strong elongation response specifically in internode 1 when these plants were exposed to supplemental far-red light (Figures 5.4-5.7). Furthermore, another common characteristic that emerged across these species was the elongation of pith cells in all species, except for the Arabidopsis inflorescence. These findings collectively establish tomato, bell pepper, eggplant, *B. nigra*, and soybean as notable examples of FR-responsive species in our diversity panel.

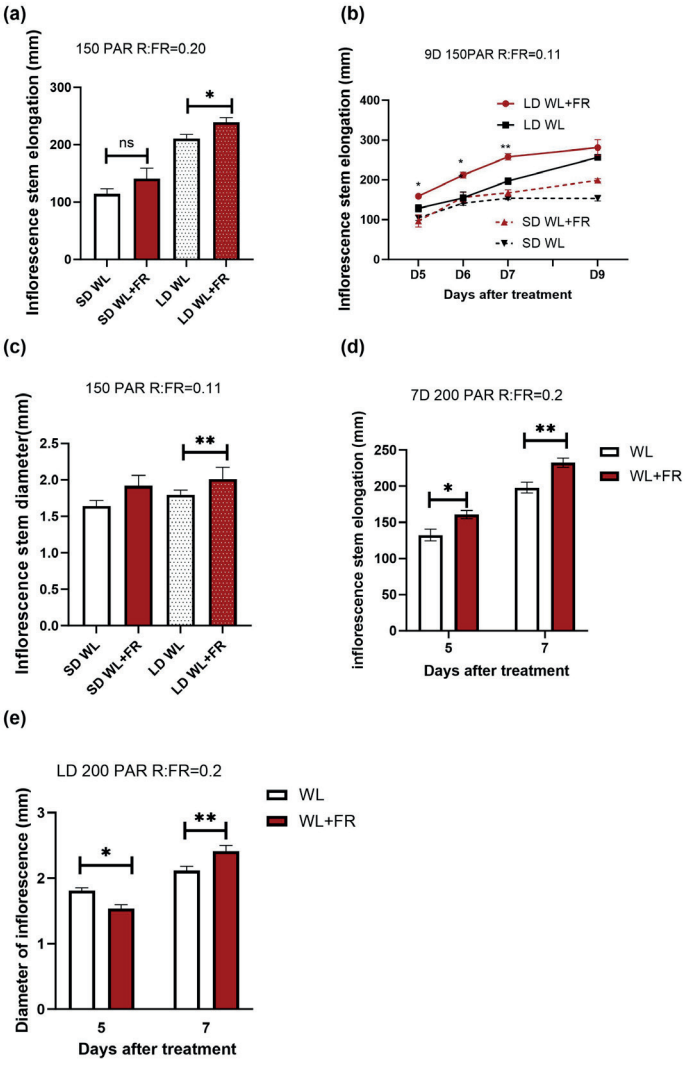

Figure 5.2. Col-0 inflorescence elongation in response to FR-enrichment in different light settings. (a) Effect of day length on Col-0 inflorescence stem elongation over 9 days of WL+FR treatment in both Short Day (SD: 8h day light, 16h dark) and Long Day (LD: 16h day light, 8h dark) conditions at 150 PAR with an R:FR ratio of 0.2. The study included 2 independent replicates with a sample size of n=12. (b) Col-0 inflorescence stem diameter after 9 days of WL+FR treatment in SD and LD conditions at 150 PAR with an R:FR ratio of 0.11. The study comprised 30 biological replicates and was repeated three times. (c) Col-0 inflorescence diameter after 7 days of WL+FR treatment in LD or SD at 150 PAR, R:FR=0.11. (d) Effect of R/FR ratios on Col-0 inflorescence stem elongation after 7 days of WL+FR treatment in LD at 200 PAR. The study included 20 replicates with 2 repeats. (e) Col-0 inflorescence stem elongation after 7 days of WL+FR treatment in LD at 200 PAR, R:FR=0.2. The study for (d,e) comprised 12 biological replicates and was repeated twice. Significance between WL and WL+FR is denoted by asterisks (* $p \leq 0.05$, ** $p \leq 0.01$). Error bars represent ± SE.

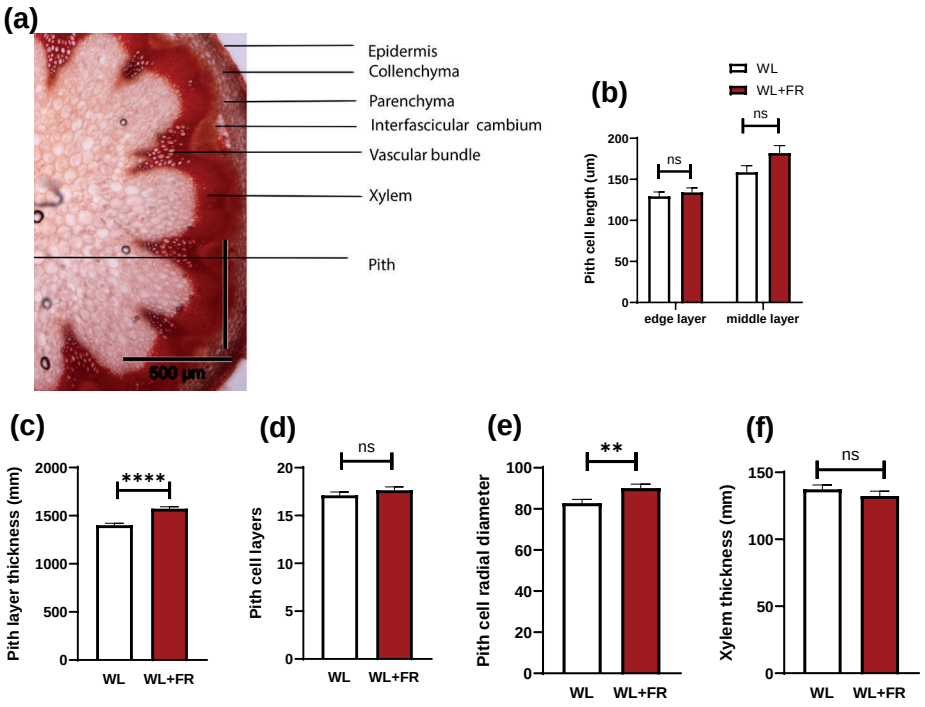

Figure 5.3. Pith and xylem responses to FR treatment in Arabidopsis inflorescence stems. Microscopy analysis results comparing different cell types in 4-week-old Col-0 under LD conditions with 200 PAR R:FR=0.20, specifically focusing on the effects of one week of WL versus WL+FR. (a) Presents a representative picture illustrating various cell types in Col-0, obtained from a cross-section. The study investigated the following aspects: (b) length of pith cells from longitudinal sections, (c) thickness of the pith layer from cross sections, (d) count of pith cell layers from cross sections, (e) pith cell radial diameter from cross section, and (f) thickness of the cambium layer from cross sections. Asterisks in the figure indicate the significance of differences between WL and WL+FR treatments, with the following significance levels: * $p \leq 0.05$; ** $p \leq 0.01$; *** $p \leq 0.001$. Error bars represent the standard error (SE), and the sample size for each measurement is n=40.

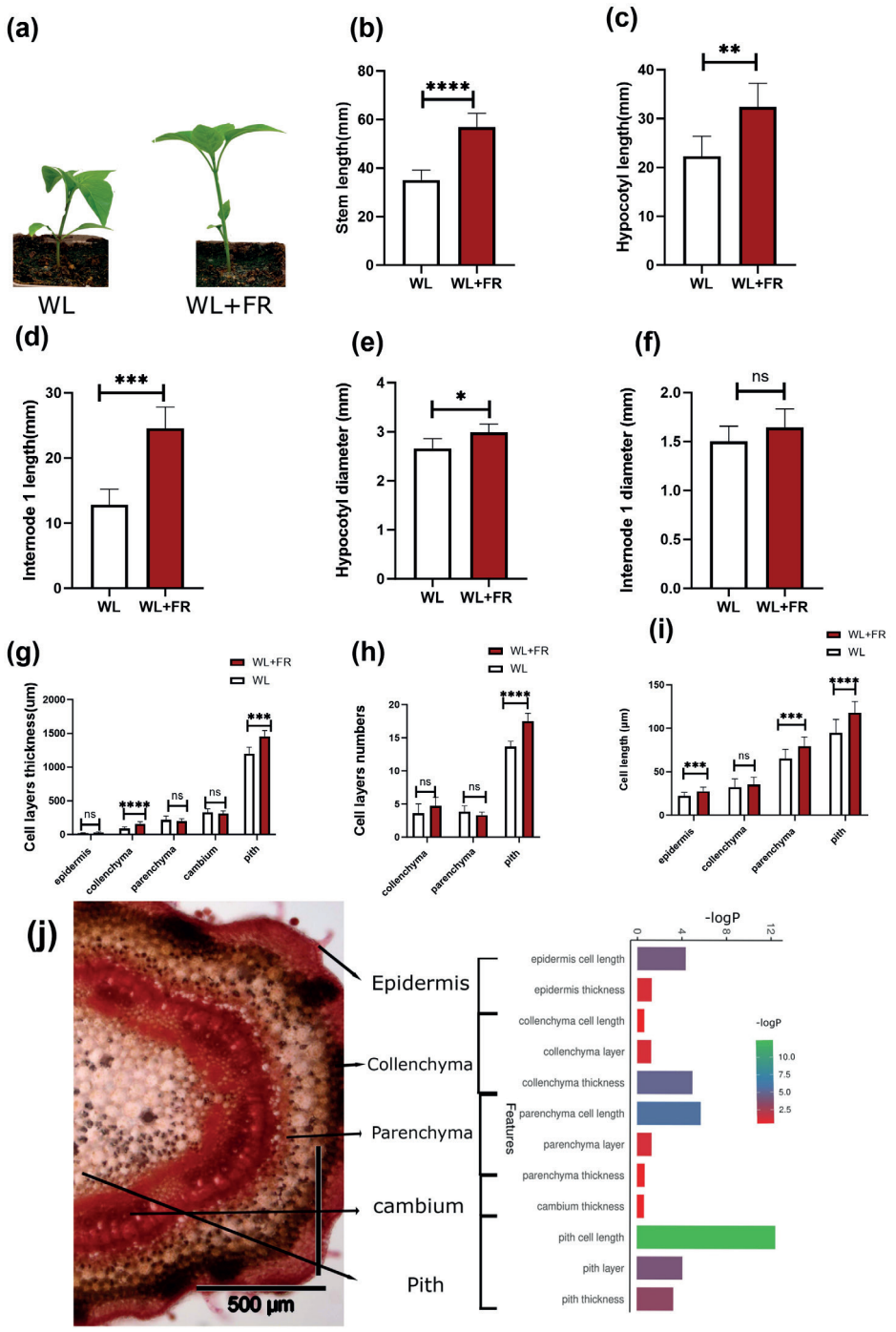
(a)
WL
WL+FR
(b)
Stem length(mm)
****
WL
WL+FR
(c)
Hypocotyl length(mm)
**
WL
WL+FR
(d)
Internode 1 length(mm)
***
WL
WL+FR
(e)
Hypocotyl diameter (mm)
*
WL
WL+FR
(f)
Internode 1 diameter (mm)
ns
WL
WL+FR
(g)
Cell layers thickness(um)
WL+FR
WL
epidermis
collenchyma
parenchyma
cambium
pith
(h)
Cell layers numbers
WL+FR
WL
collenchyma
parenchyma
pith
(i)
Cell length (μm)
WL+FR
WL
epidermis
collenchyma
parenchyma
pith
(j)
500 μm
Epidermis
Collenchyma
Parenchyma
cambium
Pith
-logP
epidermis cell length
epidermis thickness
collenchyma cell length
collenchyma layer
collenchyma thickness
parenchyma cell length
parenchyma layer
parenchyma thickness
cambium thickness
pith cell length
pith layer
pith thickness
Features
-logP

► **Figure 5.4. Bell pepper (*Capsicum annuum*) stem elongation in response to FR.** *C. annuum* seedlings were subjected to one week of WL+FR treatment versus WL treatment. (a) Phenotype of pepper in WL and WL+FR. The phenotyping data include measurements of (b) stem length, (c) hypocotyl length, (d) internode 1 length, (e) hypocotyl diameter, and (f) internode1 diameter. The data are presented as mean ± SEM, and different letters indicate significant differences between treatments based on ANOVA analysis with Tukey's post hoc test ($P<0.05$). There are 12 biological replicates, and the experiment was repeated twice. The following microscopy analysis results aspects are examined: (g) cell layers thickness from cross sections, (h) number of cell layers from cross section, and (i) cell length from longitudinal section. Asterisks in the figure indicate the significance of differences between WL and WL+FR treatments, with the following significance levels: * $p\leq0.05$; ** $p\leq0.01$; *** $p\leq0.001$. Error bars represent the standard error (SE), and the sample size for each measurement is n=40. (j) Negative logarithm of p values for cell type feature comparison of WL vs WL+FR measurement in pepper.

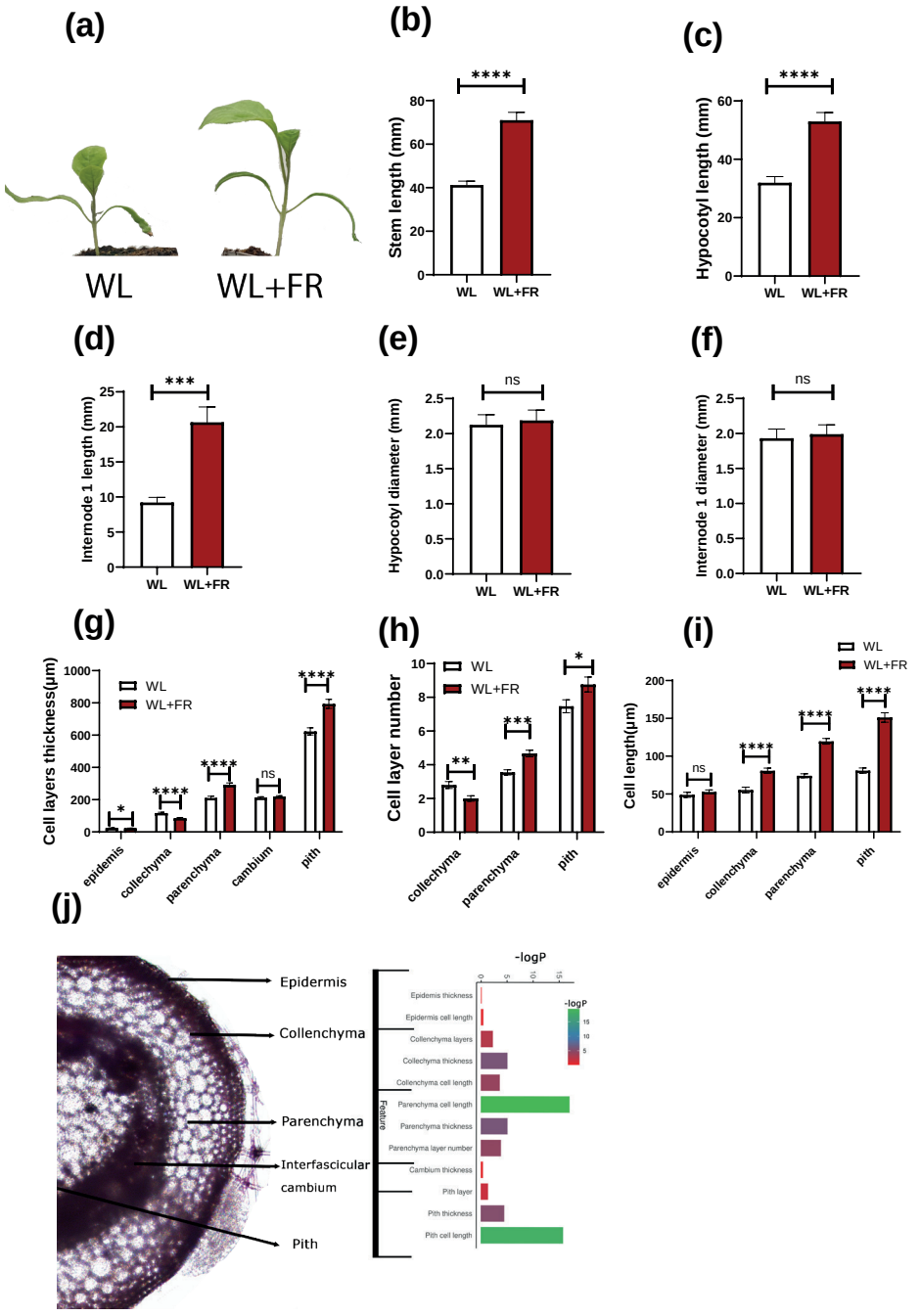
(a)
WL
WL+FR
(b)
Stem length (mm)
****
WL
WL+FR
(c)
Hypocotyl length (mm)
****
WL
WL+FR
(d)
Internode 1 length (mm)
***
WL
WL+FR
(e)
Hypocotyl diameter (mm)
ns
WL
WL+FR
(f)
Internode 1 diameter (mm)
ns
WL
WL+FR
(g)
Cell layers thickness(μm)
WL
WL+FR
epidemis
collechyma
parenchyma
cambium
pith
(h)
Cell layer number
WL
WL+FR
collechyma
parenchyma
pith
(i)
Cell length(μm)
WL
WL+FR
epidermis
collechyma
parenchyma
pith
(j)
Epidermis
Collenchyma
Parenchyma
Interfascicular cambium
Pith
-logP
Epidemis thickness
Epidermis cell length
Collenchyma layers
Collechyma thickness
Collenchyma cell length
Parenchyma cell length
Parenchyma thickness
Parenchyma layer number
Cambium thickness
Pith layer
Pith thickness
Pith cell length
Features

► **Figure 5.5. Eggplant (*Solanum melongena*) stem elongation in response to FR.** *S. melogena* seedlings were subjected to one week of WL+FR treatment versus WL treatment. (a) phenotype of eggplant in FR or WL. The phenotyping data include measurements of (b) stem length, (c) hypocotyl length, (d) Internode1 length, (e) hypocotyl diameter, and (f) internode1 diameter. The data are presented as mean ± SEM, and different letters indicate significant differences between treatments based on ANOVA analysis with Tukey's post hoc test ($P<0.05$). There are 12 biological replicates, and the experiment was repeated twice. The following microscopy analysis results aspects are examined: (g) cell layers thickness from cross sections, (h) number of cell layers from cross section, and (i) cell length from longitudinal section. Asterisks in the figure indicate the significance of differences between WL and WL+FR treatments, with the following significance levels: * $p\leq0.05$; ** $p\leq0.01$; *** $p\leq0.001$. Error bars represent the standard error (SE), and the sample size for each measurement is n=40. (j) Negative logarithm of p values for cell type feature comparison of WL vs WL+FR measurement in eggplant.

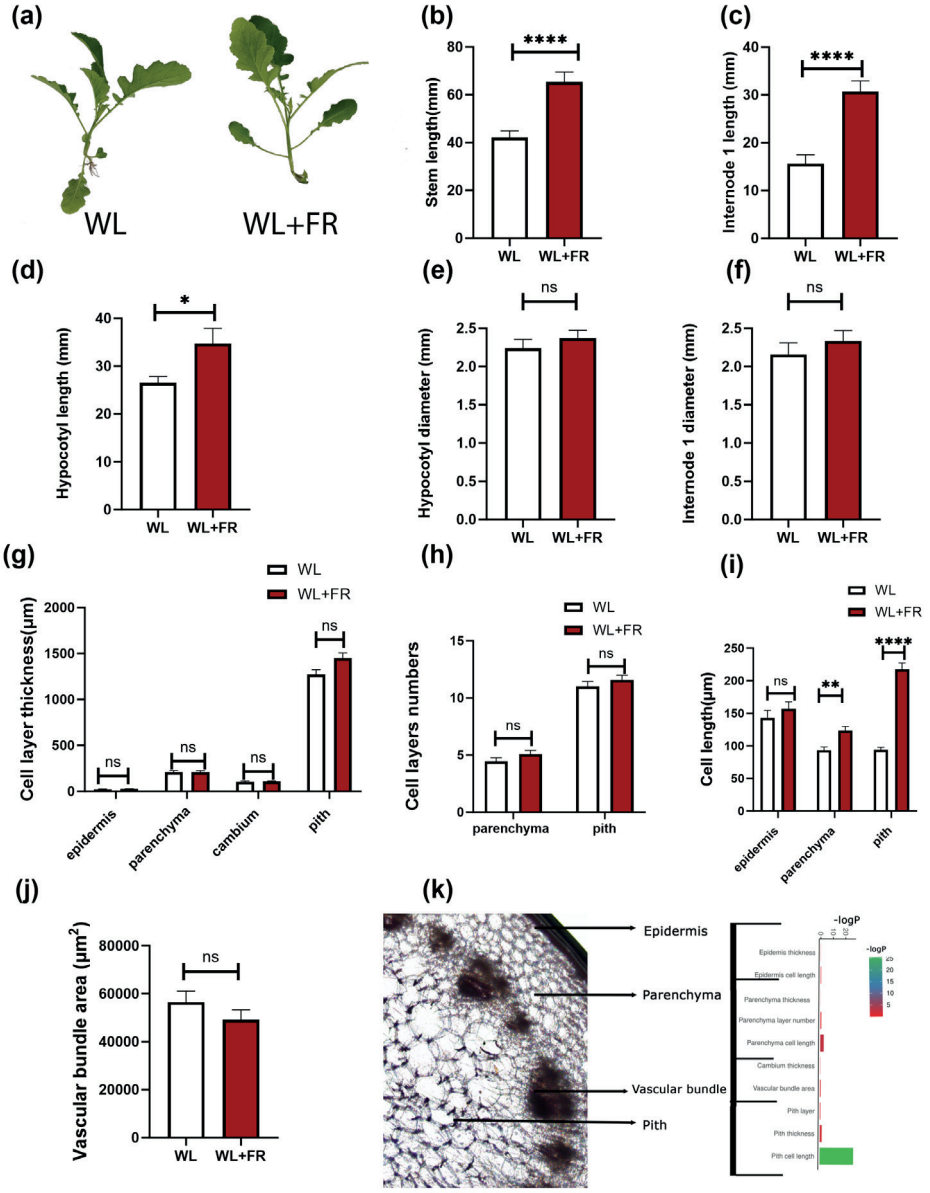
(a)
WL
WL+FR
(b)
Stem length(mm)
****
WL
WL+FR
(c)
Internode 1 length (mm)
****
WL
WL+FR
(d)
Hypocotyl length (mm)
*
WL
WL+FR
(e)
Hypocotyl diameter (mm)
ns
WL
WL+FR
(f)
Internode 1 diameter (mm)
ns
WL
WL+FR
(g)
Cell layer thickness(μm)
WL
WL+FR
ns
epidermis
parenchyma
cambium
pith
(h)
Cell layers numbers
WL
WL+FR
ns
parenchyma
pith
(i)
Cell length(μm)
WL
WL+FR
ns
**
****
epidermis
parenchyma
pith
(j)
Vascular bundle area (μm²)
ns
WL
WL+FR
(k)
Epidermis
Parenchyma
Vascular bundle
Pith
-logP
Epidermis thickness
Epidermis cell length
Parenchyma thickness
Parenchyma layer number
Parenchyma cell length
Cambium thickness
Vascular bundle area
Pith layer
Pith thickness
Pith cell length

► **Figure 5.6. Black mustard (*Brassica nigra*) stem elongation in response to FR.** *B. nigra* seedlings were subjected to one week of WL+FR treatment versus WL treatment. (a) Phenotype of *B. nigra* in FR or WL. The phenotyping data include measurements of (b) stem length, (c) hypocotyl length, (d) internode1 length, (e) hypocotyl diameter, and (f) internode1 diameter. The data are presented as mean ± SEM, and different letters indicate significant differences between treatments based on ANOVA analysis with Tukey's post hoc test ($P<0.05$). There are 12 biological replicates, and the experiment was repeated twice. The following microscopy analysis results aspects are examined:(g) cell layers thickness from cross sections, (h) number of cell layers from cross section, (i) cell length from longitudinal sections, and (j) vasculature bundle area from cross section. Asterisks in the figure indicate the significance of differences between WL and WL+FR treatments, with the following significance levels: * $p\leq0.05$; ** $p\leq0.01$; *** $p\leq0.001$. Error bars represent the standard error (SE), and the sample size for each measurement is n=40.Microscoping data of *P. sativum* after one week of treatment. (k) Negative logarithm of p values for cell type feature comparison of WL vs WL+FR measurement in basil.

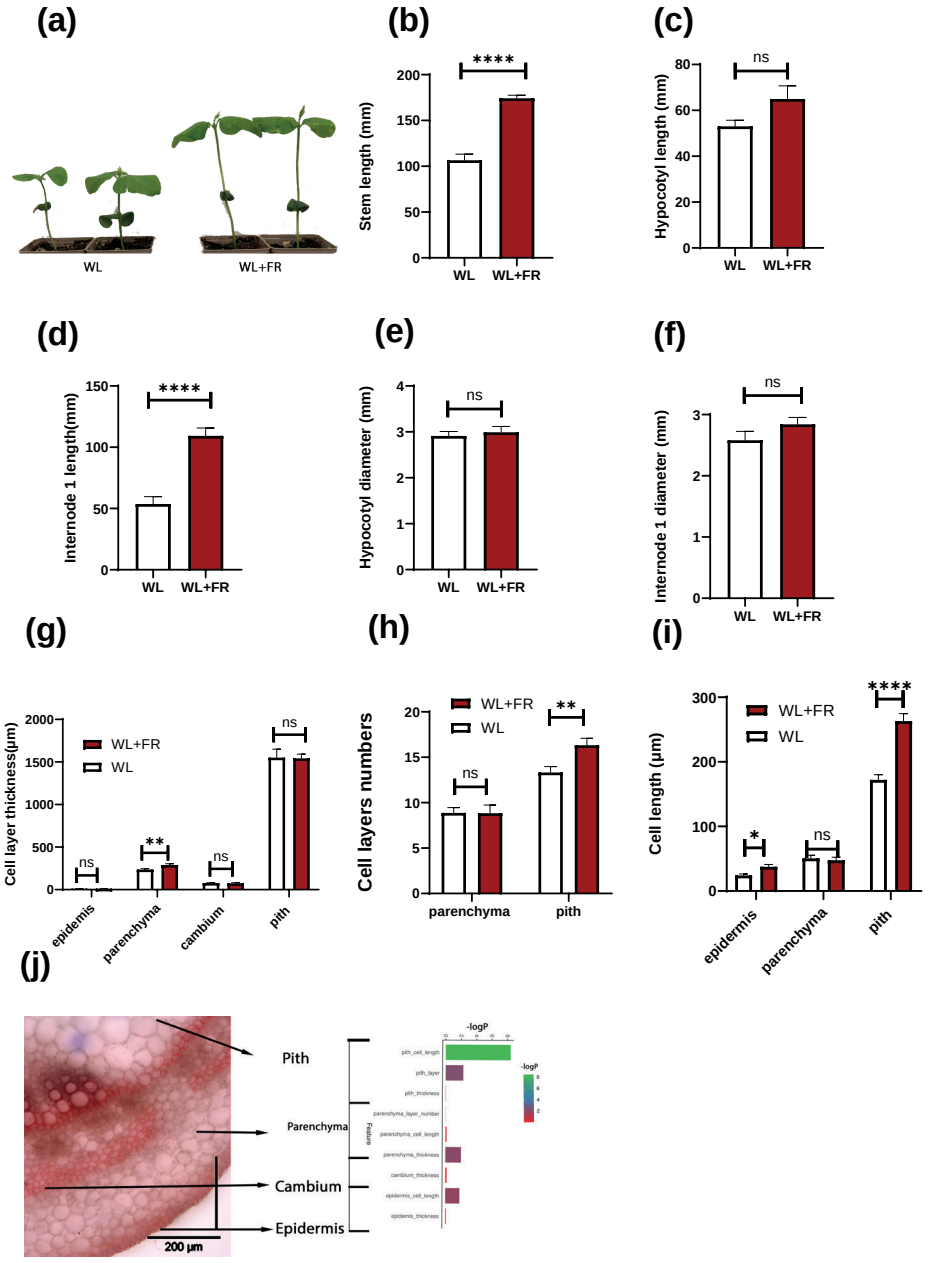
(a)
WL
WL+FR
(b)
Stem length (mm)
****
WL
WL+FR
(c)
Hypocotyl length (mm)
ns
WL
WL+FR
(d)
Internode 1 length(mm)
****
WL
WL+FR
(e)
Hypocotyl diameter (mm)
ns
WL
WL+FR
(f)
Internode 1 diameter (mm)
ns
WL
WL+FR
(g)
Cell layer thickness(μm)
WL+FR
WL
ns
**
ns
ns
epidemis
parenchyma
cambium
pith
(h)
Cell layers numbers
WL+FR
WL
ns
**
parenchyma
pith
(i)
Cell length (μm)
WL+FR
WL
*
ns
****
epidermis
parenchyma
pith
(j)
Pith
Parenchyma
Cambium
Epidermis
200 μm
-logP

► **Figure 5.7. Soybean (*Glycine max*) stem elongation in response to FR.** *G. max* seedlings were subjected to one week of WL+FR treatment versus WL treatment. (a)Phenotype of soybean in FR or WL. The phenotyping data include measurements of (b) stem length, (c) hypocotyl length, (d) internode1 length, (e) hypocotyl diameter, and (f) internode1 diameter. The data are presented as mean ± SEM, and different letters indicate significant differences between treatments based on ANOVA analysis with Tukey's post hoc test ($P<0.05$). There are 12 biological replicates, and the experiment was repeated twice. The following microscopy analysis results aspects are examined:(g) cell layers thickness from cross sections, (h) number of cell layers from cross section, (i) cell length from longitudinal sections, and (j) vasculature bundle area from cross section. Asterisks in the figure indicate the significance of differences between WL and WL+FR treatments, with the following significance levels: * $p\leq0.05$; ** $p\leq0.01$; *** $p\leq0.001$. Error bars represent the standard error (SE), and the sample size for each measurement is n=40. (k) Negative logarithm of p values for cell type feature comparison of WL vs WL+FR measurement in soybean.

5.2.4 Minimal FR responsiveness in basil and pea

We also tested the FR-responsiveness of species that did not have such clear FR responses. Firstly, *O. basilicum* (basil) from Lamiaceae (mint family) exhibited a mild internode elongation response to FR light, though this response did not manifest at the cellular level (Figure 5.8). When treated with WL+FR, basil plants displayed differences only after two weeks of FR treatment; no noticeable elongation occurred after one week. Notably, there were also no disparities in the diameter of the first internode (Figure 5.8). Regarding basil's cellular characteristics, pith cell elongation in response to FR light was not observed either.

Secondly, another legume, pea (*Pisum sativum*) showed no significant differences in stem length or diameter between the two treatments (Figure 5.9). Diameter measurements were taken from at least three locations along the stem's length and the average was calculated. Pea stem cross-sections revealed a tetrarch symmetry leading to an X-shaped pith, necessitating specific measurement directions (Figure 5.9). Pith measurements focused on the pith area, predominantly composed of cells stained with dense red color, inside of the X-shaped area between vascular bundles (Figure 5.9h). We found no differences between treatments for the measured cell types (Figure 5.9 i,k,l,m).

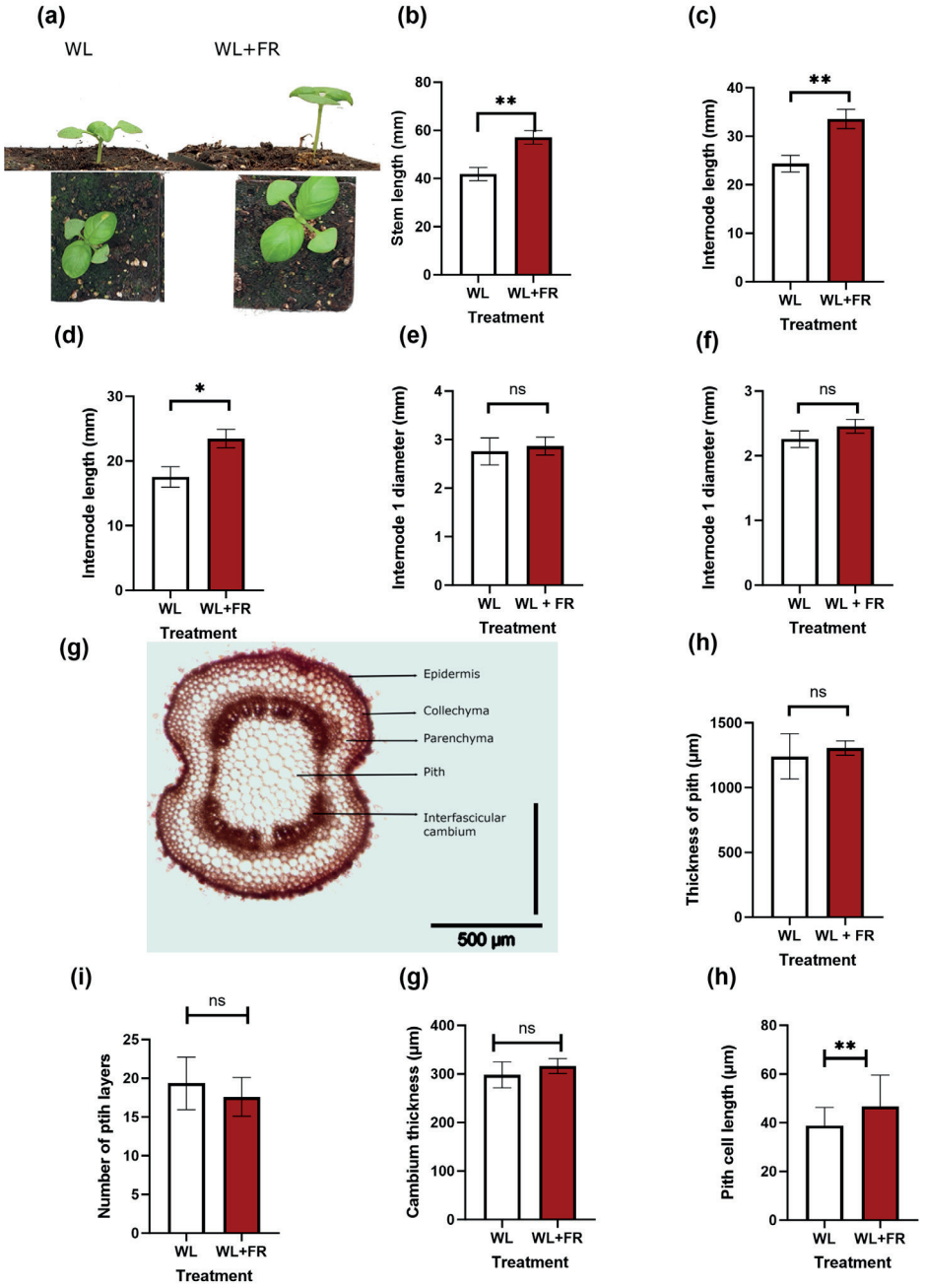
(a)
WL
WL+FR
(b)
Stem length (mm)
**
WL
WL+FR
Treatment
(c)
Internode length (mm)
**
WL
WL+FR
Treatment
(d)
Internode length (mm)
*
WL
WL+FR
Treatment
(e)
Internode 1 diameter (mm)
ns
WL
WL + FR
Treatment
(f)
Internode 1 diameter (mm)
ns
WL
WL + FR
Treatment
(g)
Epidermis
Collechyma
Parenchyma
Pith
Interfascicular cambium
500 µm
(h)
Thickness of pith (µm)
ns
WL
WL + FR
Treatment
(i)
Number of ptih layers
ns
WL
WL+FR
Treatment
(g)
Cambium thickness (µm)
ns
WL
WL+FR
Treatment
(h)
Pith cell length (µm)
**
WL
WL+FR
Treatment

► **Figure 5.8. Basil (*O.basilicum*) stem elongation is slow in response to FR.** *O. basilicum* seedlings were subjected to two weeks of WL+FR treatment versus WL treatment. (a) Phenotype of *O.basilicum* in FR or WL. The phenotyping data include measurements of (b) stem length, (c) hypocotyl length, (d) internode1 length (e) hypocotyl diameter, and (f) internode1 diameter. The data are presented as mean ± SEM, and different letters indicate significant differences between treatments based on ANOVA analysis with Tukey's post hoc test ($P<0.05$). There are 18 biological replicates, and the experiment was repeated twice. The following microscopy analysis results aspects are examined: (g) pith thickness from cross sections, (h) number of cell layers from cross section, (i) cell length from longitudinal sections, and (j) vasculature bundle area from cross section. Asterisks in the figure indicate the significance of differences between WL and WL+FR treatments, with the following significance levels: * $p\leq0.05$; ** $p\leq0.01$; *** $p\leq0.001$. Error bars represent the standard error (SE), and the sample size for each measurement is n=40.

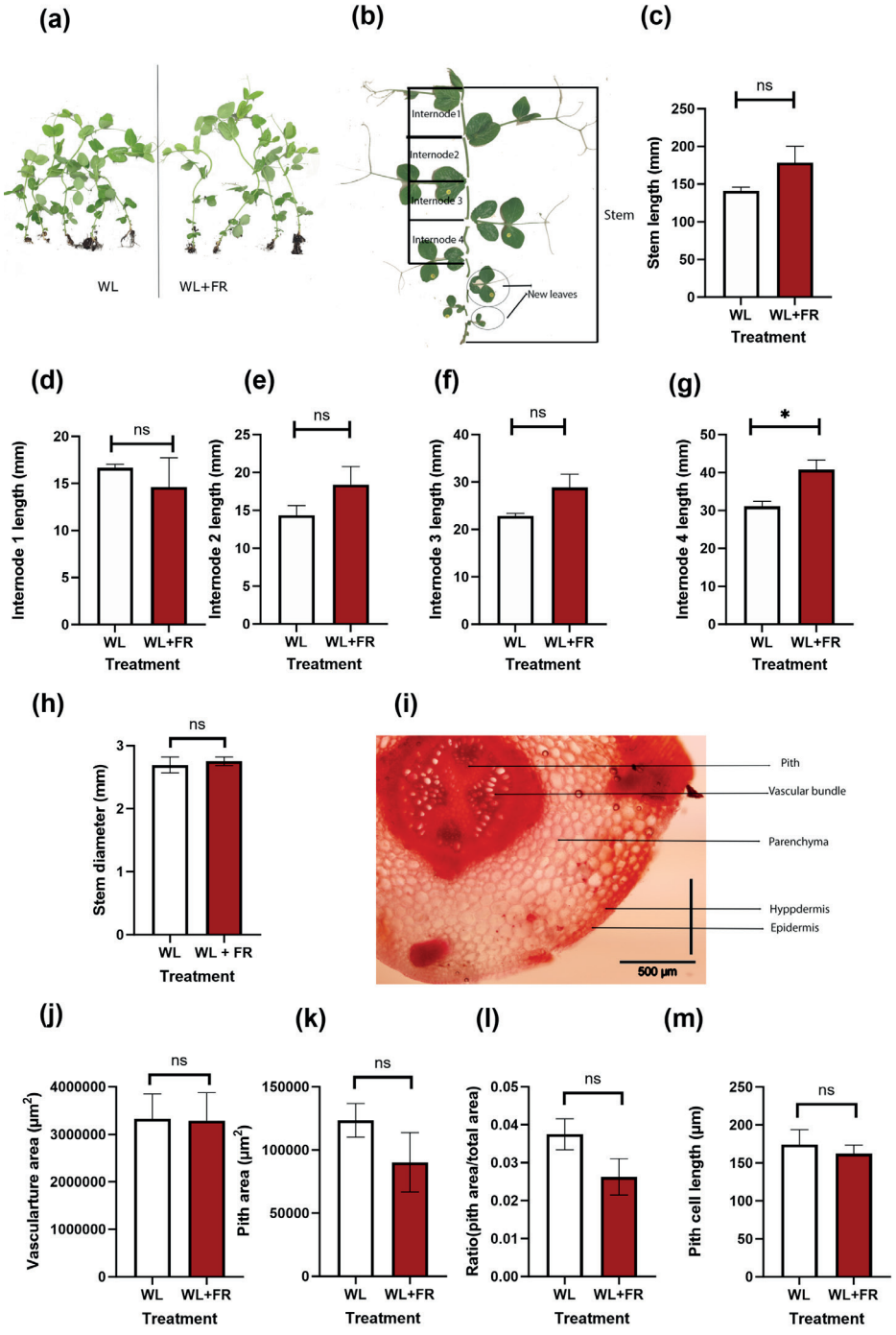
(a)
WL
WL+FR
(b)
Internode1
Internode2
Internode 3
Internode 4
Stem
New leaves
(c)
ns
Stem length (mm)
WL
WL+FR
Treatment
(d)
ns
Internode 1 length (mm)
(e)
ns
Internode 2 length (mm)
(f)
ns
Internode 3 length (mm)
(g)
*
Internode 4 length (mm)
(h)
ns
Stem diameter (mm)
WL + FR
(i)
Pith
Vascular bundle
Parenchyma
Hyppdermis
Epidermis
500 µm
(j)
ns
Vascularture area (µm²)
(k)
ns
Pith area (µm²)
(l)
ns
Ratio(pith area/total area)
(m)
ns
Pith cell length (µm)

► **Figure 5.9. Pea (*P. sativum*) has mild stem elongation in response to FR.** *P. sativum* seedlings were subjected to one week of WL+FR treatment versus WL treatment. (a) A comparison of pea growth phenotypes between WL and WL+FR conditions after 7 days of treatment. (b) Illustration of *P. sativum* growth after one week of treatment. This figure provides insights into each internode and leaf, revealing stem bending and a tendency for plants in both treatments to tip over. Phenotyping data for *P. sativum* is presented as follows (c) stem length, (d) internode 1 length, (e) internode 2 length, (f) internode 3 length, (g) internode 4 length, and (h) stem diameter. The data is expressed as mean values ± SEM, with different letters indicating significant differences between treatments based on ANOVA analysis with Tukey's post hoc test ($P<0.05$). There are 6 biological replicates. The following microscopy analysis results aspects are examined: (i) microscopy example of each cell type from cross section in pea, (j) vasculature area from cross sections, (k) pith total area from cross sections, (l) ratio of pith area/total area from cross section, and (m) pith cell length from longitudinal sections. Asterisks in the figure indicate the significance of differences between WL and WL+FR treatments, with the following significance levels: * $p\leq0.05$; ** $p\leq0.01$; *** $p\leq0.001$. Error bars represent the standard error (SE), and the sample size for each measurement is n=40.

5.2.5 FR-responsive tomato TFs have family-specific and tissue-specific expression patterns

To investigate the molecular events underlying the internode and pith elongation responses, we delved into the behavior of the transcription factor (TF) encoding genes that we identified as our TFs of interest in Chapter 3, *Solyc08g080150*, *Solyc01g090760*, *Solyc07g053450*, across various species. In Chapter 3, we identified these three genes not only as DEGs (Table S3.5) upregulated in response to FR in the entire internode 1, but they also exhibited a significant upregulation in the pith after 30 hours of FR treatment (see Figure 3.18). We wanted to test if the FR-responsive gene expression, especially in pith, was conserved in our species panel. This approach aims to uncover the broader similarities and differences in TF expression patterns among dicot relatives.

For this section, we selected species from our previous experiments (Figures 5.2-5.9) based on genome sequence availability. Hence, we worked with tomato, Arabidopsis, pepper, eggplant, black mustard, soybean, and pea to construct an expression analysis of TF homologs.

First, we needed to identify homologs of the three TFs in each species to conduct an interspecies qPCR analysis. We conducted ortholog searches using default BLAST searches on various websites (details in methods) (Fernandez-Pozo et al., 2015; The Arabidopsis Information Resource, 2015; Chen et al., 2022a). For the other two Solanaceae species, pepper and eggplant, the top result was a single hit for each of the three genes (with one exception). In the case of Arabidopsis, we considered not only the BLAST result but also literature annotations to identify a homolog with a potentially conserved function. For pea, soybean, and black mustard, we selected genes based on the highest similarity results (85% and up), and we found the chosen genes closely resembled each

other. We visualized the relationships of these homologs based on sequence similarities by generating maximum likelihood phylogenies (Figures 5.10-5.12). The phylogenies of the three TFs tend to align with the relationships between the plant species (Figure 5.1). The phylogenies also reflect the recent gene or even whole genome duplication events with occurrences of two closely related paralogs, for example in pea for each gene.

For the qPCR quantification of gene expression, we collected whole internode and pith samples simultaneously at 6 h and 24 h time points for WL and WL+FR for all species except pea, where we harvested only the whole internode due to the challenging pith morphology (as depicted in Figure 5.9i). For the orthologs of *Solyc07g053450* and *Solyc08g080150*, we observed a uniform FR-upregulation in both internode and pith in each member of the Solanaceae family (Figures 5.10, 5.12, S5.1, S5.3). Notably, for *Solyc01g090760*, we identified two bell pepper homologs (Figure 5.11). The homolog with lower sequence similarity had stronger correlation in expression patterns with tomato, while the other ortholog, we observed a non-FR-responsive expression pattern (Figure 5.11, S5.2). This indicates that even with high sequence similarity, homologs can have diverged function, especially if another homolog has retained its role.

Then, outside of the Solanaceae family, we looked at two Brassicaceae species, Arabidopsis and *Brassica nigra*, and two legumes, pea and soybean. In these families, we found a prevalent downregulation of TF homologs in most instances (Figures 5.10-5.12).

In pea we had observed limited stem growth under FR and different stem morphology that made it difficult to get pith data, and there we observed that the expression of three TF homologs consistently decreased. We identified multiple best homologs in pea, and none of them exhibited the expected FR-responsive function. This would indicate that during evolution these TFs potentially gained their FR-responsive behavior within the Solanaceae lineage, or lost it in the lineage leading to pea despite the expansion of the TF family.

In the FR-responsive soybean, while there is not such a clear downregulation in FR, there is also no clear homolog that would match the tomato patterns. For the two soybean homologs of *Solyc08g080150* we observed a strong FR-induction specifically in pith at 6h (Figure 5.12), so potentially the role of these two homologs is retained to some extent in soybean.

So, we found that the FR-responsive expression patterns for these genes resembles each other in Solanaceae, and it is distinct from Brassicaceae and Fabaceae. Even though some Brassicaceae and Fabaceae species exhibit similar elongation responses to Solanaceae, the TF expression pattern is not conserved.

To also benefit from existing Arabidopsis gene expression data, we examined the expression patterns of homologs *AT5G51910*, *AT2G45050*, *AT2G45680*, and *AT2G42380* in Arabidopsis using the eFP browser (Winter et al., 2007)(Figures S5.4-5.8). The homolog of *Solyc08g080150* in Arabidopsis, *AT5G51910*, reveals heightened expression in inflorescence and seed, hinting at a role in later developmental stages. *AT2G45680* shows high expression in leaves and second internode of inflorescence stem. Then, the homolog of *Solyc01g090760* in Arabidopsis, *AT2G45050*, displays its peak expression in petals, while the homolog of *Solyc07g053450*, *AT2G42380*, shows strong expression in mature pollen. Together, these distinct expression patterns suggest specific involvement of each homolog in later stages of Arabidopsis development. Additionally, *AT2G45050*, *AT2G45680*, and *AT2G42380* were also reported to be upregulated in FR response in Arabidopsis leaf tip (Küpers et al., 2023), these three genes were found in differentially expressed in hypocotyl after FR seedling treatment (Kohnen et al., 2016b), indicating that they have FR-responsive regulation in other parts of Arabidopsis than what we profiled.

This lack of conservation of FR-responsive expression patterns between the Solanaceae and Brassicaceae/Fabaceae families sparks intriguing questions about the underlying genetics and evolution of the FR-response. This disparity prompts the hypothesis that the observed transcription factor behaviors—upregulation in Solanaceae and downregulation in Brassicaceae/Fabaceae—may signify a family-specific FR-induced function for these TFs. An alternative hypothesis would be these transcription factors are not functionally related to shade avoidance it is very specific upregulated in our qPCR and RNA-seq results due to tissue/timepoint limitations. This finding opens avenues for deeper investigation into the unique regulators in shade avoidance syndrome in Solanaceae family compared to other diverse families.

When TF expression is not conserved across different species, it indicates that the regulatory mechanisms inducing these TFs may have diverged during evolution, resulting in differences in gene expression patterns. Studies have shown that the conservation of TF binding events is associated with the conservation of gene expression at the individual gene level (Hemberg and Kreiman, 2011). However, it is important to note that the conservation of TF binding events and gene expression can vary across different species and tissues (Diehl and Boyle, 2018). Therefore, the lack of conservation in TF expression across species suggests that the regulatory control of gene expression by these TFs has evolved differently, potentially leading to species-specific or tissue-specific gene expression patterns.

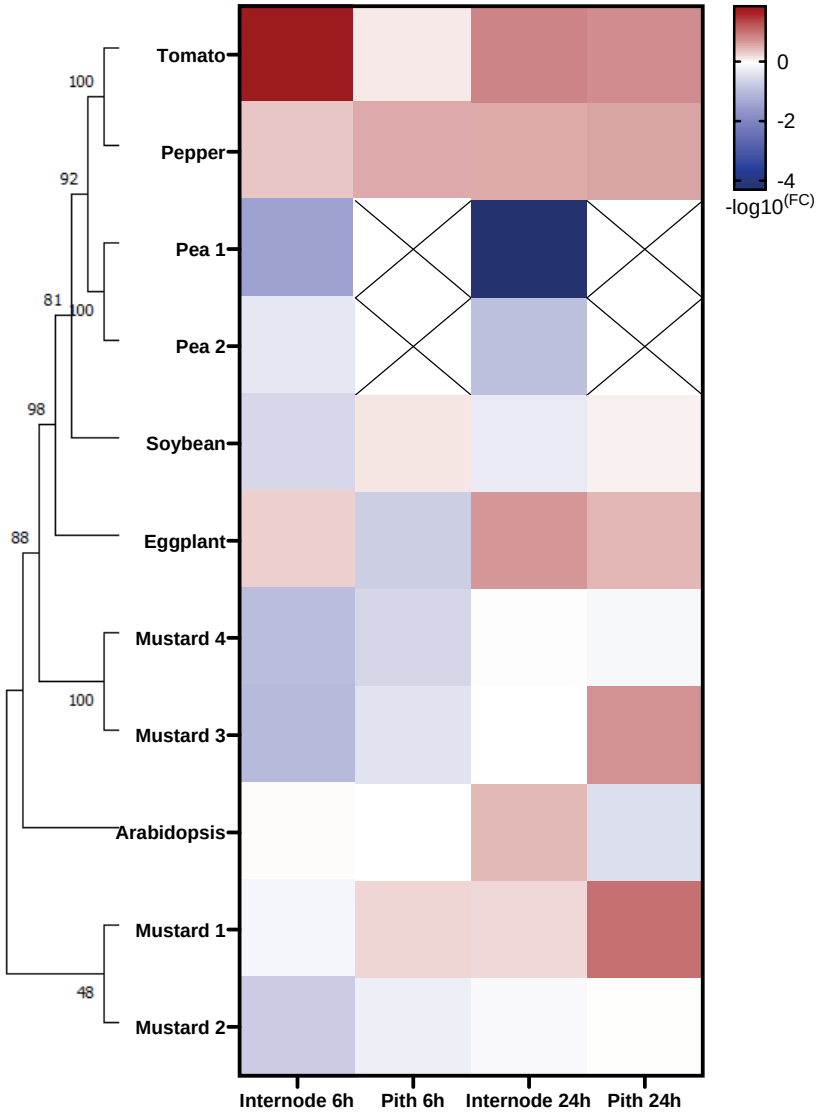

Figure 5.10. Phylogeny and FR-responsive gene expression of *Solyc07g053450* homologs. Genes are Tomato: *Solyc07g053450*, Pepper: *CA00g71840:1-921*, Eggplant: *SMEL4.1_07g019740.1.01*, Arabidopsis: *AT2G42380*, Mustard1: *BniB06g001480.2N.1*, Mustard 2: *BniB08g027470.2N.1*, Mustard3: *BniB08g072820.2N.1*, Mustard4: *BniB06g055220.2N.1*, Soybean: *Gm06:49537899..49539195*, Pea1: *XM_051027770.1*, Pea2: *XM_051045459.1*. On the left: phylogenetic relationship by maximum likelihood, constructed by software Mega X, using a Tamura Nei model generating the ML tree. Bootstrap analysis (1000 replicates) enhances reliability, with values above each branch reflecting robust bootstrap support. On the right: expression heatmap demonstrating log fold change from qPCR for WL+FR vs. WL expression in internode or pith at 6h and 24h FR treatment. Red signifies upregulation in WL+FR, blue denotes downregulation, while a baseline of white is established when logFC=0.

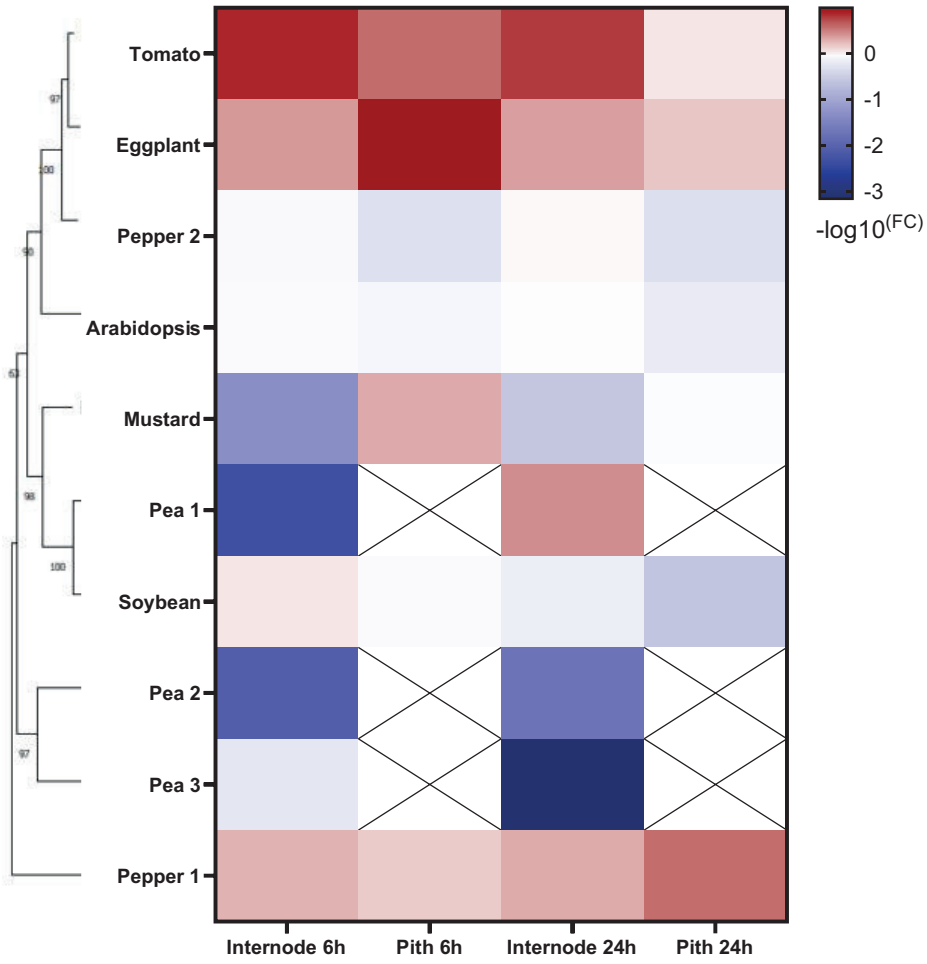

Figure 5.11. Phylogeny and gene expression patterns of *Solyc01g090760* homologs. Genes are: Tomato: *Solyc01g090760*, Pepper1: *chr3:267174801-267176100* (*CA00g71840:1-921*), Pepper2*: chr8:35902201-35904000*, Eggplant: *chr8:35902201-35904000*, Arabidopsis: *AT2G45050*, Mustard: *BniB07g039570.2N.1*, Soybean: *GlysoPI483463.06G078800.1*, Pea1: *XM_051027377*, Pea2: *XM_051030552.1*, Pea3: *XM_051038772.1*. On the left: phylogenetic relationship by maximum likelihood, constructed by software Mega X, using a Tamura Nei model generating the ML tree. Bootstrap analysis (1000 replicates) enhances reliability, with values above each branch reflecting robust bootstrap support. On the right: expression heatmap demonstrating log fold change from qPCR for WL+FR vs. WL expression in internode or pith at 6h and 24h FR treatment. Red signifies upregulation in WL+FR, blue denotes downregulation, while a baseline of white is established when logFC=0.

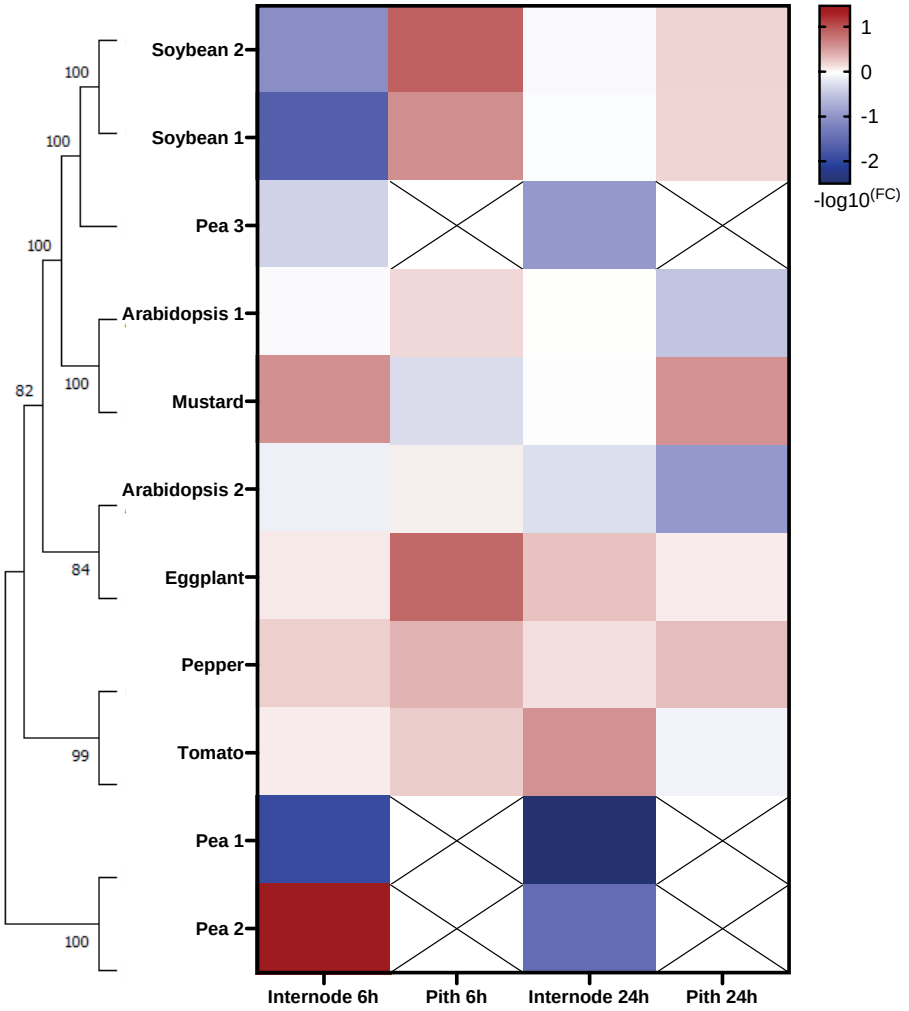

Figure 5.12. Phylogeny and gene expression patterns of *Solyc08g080150* homologs. Genes are Tomato: *Solyc08g080150*, Pepper: *TCP19*, Eggplant: *chr8:85852001-85853900*, Arabidopsis1: *AT2G45680*, Arabidopsis2: *AT5G51910*, Mustard: *BniB08g029800.2N.1*, Soybean1: *Glyma.07G080300.1*, Soybean2: *Glyma07g08710.2*, Pea1: *XM_051030490.1*, Pea2: *XM_051030491.1*. On the left: phylogenetic relationship by maximum likelihood, constructed by software Mega X, using a Tamura Nei model generating the ML tree. Bootstrap analysis (1000 replicates) enhances reliability, with values above each branch reflecting robust bootstrap support. On the right: expression heatmap demonstrating log fold change from qPCR for WL+FR vs. WL expression in internode or pith at 6h and 24h FR treatment. Red signifies upregulation in WL+FR, blue denotes downregulation, while a baseline of white is established when logFC=0.

5.2.6 The similarity among TFs is linked to similarity in their expression

The exploration of conservation of TF gene expression patterns in Solanaceae not only highlights distinctive traits in these transcription factors but also prompts questions about their functions and evolutionary dynamics compared to counterparts in other plants. Investigating if the function of these TFs is conserved between the dicot families opens avenues to uncover nuanced aspects of TF evolution and gene regulation.

To grasp conservation of TF molecular structure, we employed mVISTA to identify conserved sequences in lengthy alignments (Frazer et al., 2004). We used Muscle (Edgar, 2004) to align the transcription factor (TF) homologs. The resulting alignments are visually represented by mVista (Mayor et al., 2000) in Figures 5.13-15, with a red color to denote regions of conservation compared to the tomato gene. Unsurprisingly, the tomato genes are mostly conserved in other Solanaceae, but interestingly, the conservation is quite restricted outside the family.

The similarity in TF sequences among tomato, eggplant, and pepper extends beyond the Solanaceae family (Figures 5.13-5.15). In pepper, there are two homologs of *Solyc01g090760*: pepper1 homolog has very low conservation (~76% of 169bp, Figure 5.14), but its expression pattern is similar to the tomato homolog (Figure 5.11), while pepper2 homolog has high similarity (86% of 703 bp) and non-conserved response to FR. This could be a showcase of functional divergence and co-option of homologs.

This insight into the conservation patterns of TFs within S. lycopersicum not only sheds light on the unique characteristics of these particular transcription factors but also raises questions about their functional roles and evolutionary dynamics in comparison to their counterparts in other plant species: Has the evolutionary path in Solanaceae driven both the FR-responsive expression and the SAS function of these TFs? Further exploration of these patterns would have potential to unravel nuanced aspects of TF evolution and gene regulation.

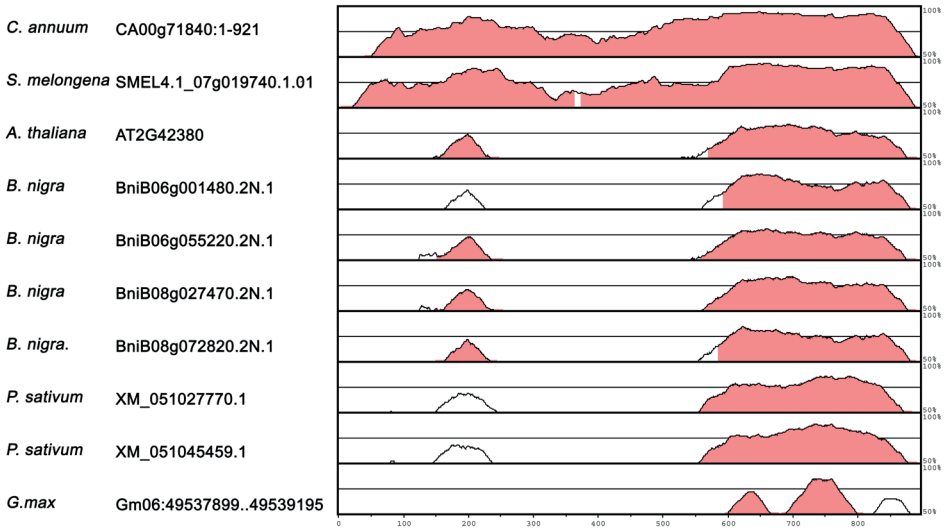

Figure 5.13. Conservation patterns of homologs of *Solyc07g053450*. The alignment shows regions of conservation highlighted in red, illustrating >50% identity, white indicates <50% identity.

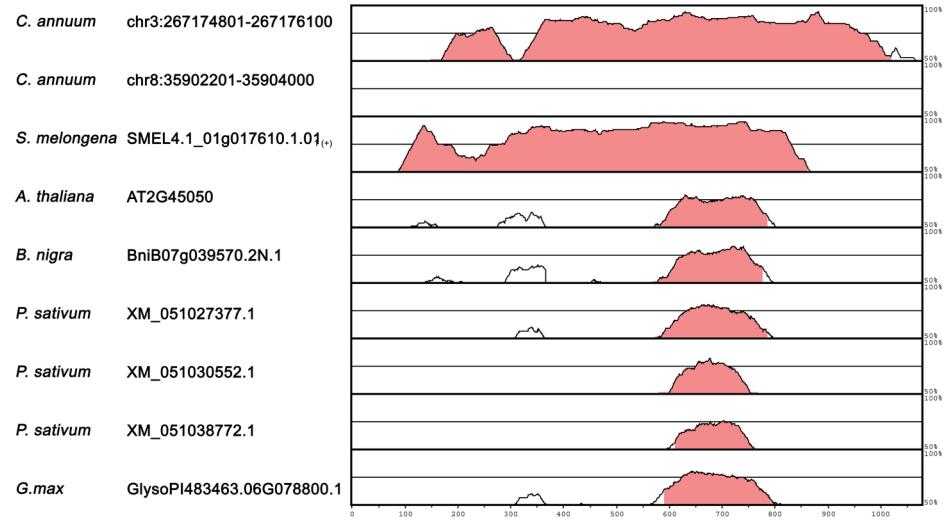

Figure 5.14. Conservation patterns of homologs of *Solyc01g090760*. The alignment shows regions of conservation highlighted in red, illustrating >50% identity, white indicates <50% identity.

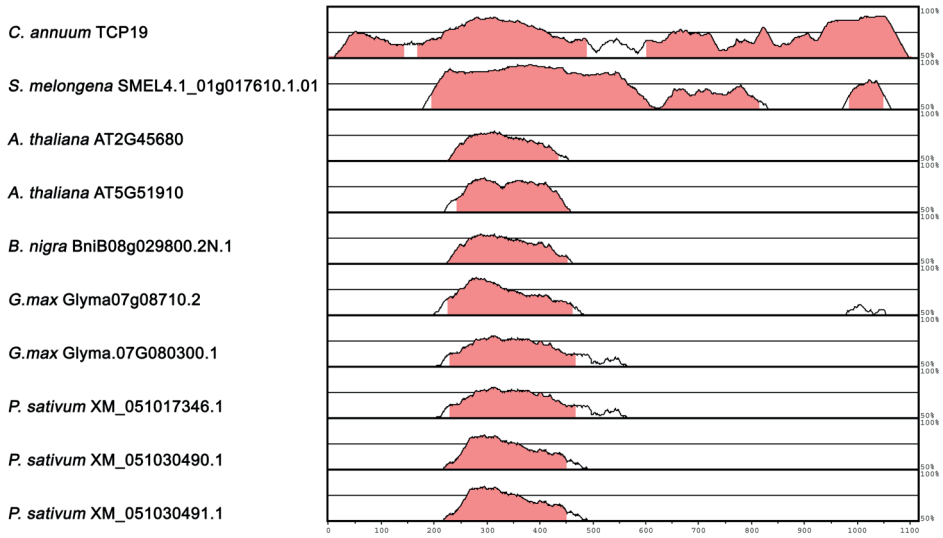

Figure 5.15. Conservation patterns of homologs of *Solyc08g080150*. The alignment shows regions of conservation highlighted in red, illustrating >50% identity, white indicates <50% identity.

5.3 DISCUSSION

5.3.1 Shade avoidance elongation is most likely conserved but with exceptions

In the preceding chapters, we explored the mechanism of stem elongation and the associated radial growth in tomato, which prompted us to try and transfer this question to be studied in Arabidopsis (Figures 5.2, 5.3). The rationale behind this transfer was rooted in the rich genetic resources already established in Arabidopsis, presenting an ideal foundation for further investigation. However, our experimentation revealed that the FR-responsive stem elongation in Arabidopsis was not experimentally robust, highlighted by the lack of the response under short-day conditions. Under long-day conditions and relatively low photosynthetically active radiation (150 PAR), we employed a very low red to far-red light ratio (R:FR) of 0.11 to elicit a response. When we tested a higher R:FR ratio of 0.25 in this setting, the elongation response vanished. Inflorescence stem elongation in response to FR in long day was observed also at 200 PAR. Integrating both sets of conditions, we hypothesize that the actual amount of far-red light and its duration of exposure play pivotal roles in inducing inflorescence stem elongation.

In Arabidopsis, the radial expansion of the stem is influenced by various factors, including light quality, genetic interactions between receptor kinases, and the activity of multiple transcription factor genes (Génard et al., 2001; Greb, 2019; Spaninks et al., 2023). The stem

diameter appears to be unresponsive or even reduced in FR in our set up, leading to a fragile long stem (Figure 5.2 c), which is a common problem in SAS that plants become very vulnerable to lodging. Meanwhile, Arabidopsis also shows limitations in secondary growth (Turnerag1 and Somervilleb, 1997; Oh et al., 2003; Paul-Victor and Rowe, 2011). This could be a plausible explanation for the weak FR-response of stem elongation in Arabidopsis.

After investigating Arabidopsis, we then sought to unravel whether the FR-induced stem elongation and associated cellular changes would be conserved in other dicot species with stem growth habit. Overall, we sampled *S. lycopersicum*, *C. annuum*, *P. sativum*, *G.max*, *S. melongena*, *B. nigra*, and *O. basilicum.* Most of the species we looked at were responsive to FR in their internode elongation (Figures 5.4-5.9). In contrast, we also found that *P. sativum* and *O. basilicum* were only mildly or not responsive to FR, and neither showed secondary growth despite the development of lateral meristem (Ko et al., 2004; Skubisz et al., 2007).

Is there a relationship between radial growth, elongation growth and pith cell expansion and elongation? We still don't have a clear answer. Herbaceous (non-woody) plants mostly undergo primary growth, with very little secondary growth, However, some nonwoody plants, such as potato tubers, carrot taproot, and sweet potato tuberous root, do undergo remarkable secondary growth (Hardwick and Elliott, 2016; Groover, 2023). Therefore, the occurrence of secondary growth in plants varies depending on the species, and it is not a universal feature of all plants. Recent studies have explored the genetic space of radial plant growth in *Arabidopsis thaliana* (Greb, 2019), but the question remains of how conserved it is among dicot species.

Pith cell elongation is one of the clearest responses we found in our shade avoiding species whose stems elongated. While specific information regarding the conservation of pith cell elongation in Arabidopsis and other plants is not readily available, it is known that the expansion of stem tissues, including pith cells, is influenced by various factors such as hormonal signaling and genetic regulation (Nagata et al., 2004; Ye et al., 2021).

5.3.2 The responsiveness of the three TFs to FR is unique to the Solanaceae family

In addition to investigating the conservation of plant architectural and cellular traits in response to FR, we also wanted to see if some of the TFs we found as novel FR-responsive genes that are regulated in the tomato internode (Chapter 3) were conserved across FR-responsive dicots. Understanding the extent of the conservation of these TFs' expression patterns can shed light on evolution of the regulatory networks of stem elongation and potentially help us understand the cell activities in SAS.

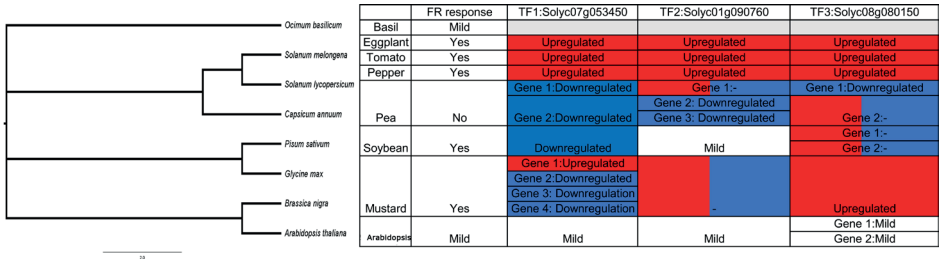

	FR response	TF1:Solyc07g053450	TF2:Solyc01g090760	TF3:Solyc08g080150
Basil	Mild			
Eggplant	Yes	Upregulated	Upregulated	Upregulated
Tomato	Yes	Upregulated	Upregulated	Upregulated
Pepper	Yes	Upregulated	Upregulated	Upregulated
Pea	No	Gene 1:Downregulated Gene 2:Downregulated	Gene 1:- Gene 2: Downregulated Gene 3: Downregulated	Gene 1:Downregulated Gene 2:-
Soybean	Yes	Downregulated	Mild	Gene 1:- Gene 2:-
Mustard	Yes	Gene 1:Upregulated Gene 2:Downregulated Gene 3: Downregulation Gene 4: Downregulation	-	Upregulated
Arabidopsis	Mild	Mild	Mild	Gene 1:Mild Gene 2:Mild

Figure 5.16. Summary of gene expression in response to FR.

Discovering the FR-responsiveness of these transcription factors exclusive to Solanaceae is interesting. This finding not only highlights a distinctive regulation within this family but also implies that their elongation mechanisms or other downstream processes likely diverge from those observed in other plant families. Our findings revealed a consistent expression pattern within the family and a clear downregulation observed in Fabaceae species, underscoring that the opposite behaviour of the TF homologs was conserved within legumes (Fig 5.10-12, 5.16). We found that the regulatory network governing elongation or other SAS-induced processes appears to vary between dicots.

Additionally, the observation that auxin does not play as clear a role in tomato shade avoidance as it does in Arabidopsis (Chapter 4) suggests a fundamental difference in the wiring of shade avoidance responses between tomato and Arabidopsis. This nuanced understanding opens up exciting avenues for exploring the unique dynamics of plant growth and regulatory pathways within the Solanaceae family.

So why is Solanaceae special? With the limitation of our species selections, we could not find a clear pattern, so expanding our method to more species and families to construct a detailed evolutionary picture might help to answer this question.

5.3.3 Summary

In conclusion, our species diversity approach has underscored the diverse responsiveness to supplemental FR light with respect to internode elongation, expression of transcription factor genes and cellular dynamics between a panel of dicotyledonous plant species. We are paving the way for future inquiries into SAS regulation in different species with the potential to understand how these responses became wired at the molecular level through the course of evolution.

5.4 ACKNOWLEDGEMENTS

We want to express our gratitude to Dr. Peter Etchells to provide Arabidopsis lines for testing, and guidance in stem structure identification.

5.5 MATERIALS AND METHODS

5.5.1 Germination

We initiated the germination for *S. lycopersicum* seeds cv Moneymaker, *Capsicum annuum*, *Solanum melongena*, *Ocimum basilicum* (obtained from Intratuin B.V), *Pisum sativum* Cameor (obtained from Dr. Judith Burstin lab) and *Glycine max* (cv green shell) (obtained from https://www.dehobbytuinder.nl/) by placing them in sealed plastic containers lined with paper towels soaked in tap water for one week. After this germination period, seedlings of uniform size were transplanted into 7 cm square pots filled with sieved Primasta® soil. Approximately one week following the transfer, we randomly allocated the plants into two distinct groups and subjected them to either white light (WL) or supplemental far-red light (WL+FR) treatments.

Arabidopsis thaliana seeds of the Colombia-0 (Col-0) accession, as well as *Brassica nigra* seeds provided by Dr. Chrysoula K. Pantazopoulou, were used in this study. These seeds were sown directly into soil, underwent a stratification period of 3 days in darkness at 4°C, and were subsequently transferred to controlled growth rooms. These growth rooms had the conditions: LD: 16 hours of light, 8 hours of darkness, SD: 8 hours of light, 11 hours of darkness a photosynthetically active radiation (PAR) of 150 $\mu mol \cdot m^{-2} \cdot s^{-1}$, an R/FR ratio of 2.0, a temperature of 20°C, and a relative humidity of 70%. Following a 7-day growth period, the seedlings were transplanted into 70 mL pots containing Primasta® soil. At the age of approximately 2 months, these plants were employed in inflorescence stem elongation experiments, commencing when the inflorescence reached approximately 0.5 cm to 2 cm in length. All experimental procedures were initiated at 10:30 AM.

5.5.2 Light conditions

The seedlings were cultivated at a temperature of 20°C, maintaining a humidity level of 70%, under a 16-hour light/8-hour dark cycle. The experiment incorporated two different light conditions: white light (WL) and far-red (WL+FR). In the WL conditions, the light intensity measured 200 PAR (photosynthetically active radiation). In contrast, the WL+FR conditions involved a light intensity of 200 PAR in white light supplemented with additional far-red light to achieve a specific red-light to far-red light ratio (R:FR) of 0.20.

5.5.3 Phenotyping

To conduct plant phenotyping, a digital caliper was employed to measure specific plant attributes, which varied depending on the plant species. For the phenotyping of *O. basilicum*, *P. sativum*, *S. lycopersicum* Moneymaker, *Capsicum annuum*, *Solanum melongena* and *Brassica nigra* each sample had 8 replicates and experiments were repeated twice. Arabidopsis measurement was conducted with 12 replicates and three times replication.

5.5.4 Microscope analysis

To stain the samples, we utilized a 0.1% (w/v) safranin solution, exposing the internode samples to it for two minutes. Subsequently, the samples underwent rinsing with 70% ethanol until the ethanol became clear. The samples were then returned to a 70% ethanol solution for storage.

For microscope analysis, we employed the Leica 700 Microscope in conjunction with analyzeD software to capture images. Subsequently, ImageJ was utilized to measure specific components as outlined for each species in Table 1. The images were captured at a 10X magnification. Regarding data analysis and graph generation, we employed GraphPad Prism 9. Additionally, statistical analysis, including the Student t-test, was conducted using Microsoft Excel.

5.5.5 RNA Extraction and cDNA Synthesis

In the initial qPCR experiment, plants were subjected to two conditions: exposure to white light (WL) or a low R/FR ratio of 0.2 (WL+FR). The plants were harvested for whole internode or pith after 6h or 24h light treatment. Each experimental condition was replicated four times, with each replicate consisting of 8 to 12 plants. Technical replicates for qPCR were performed three times. For each biological replicate, three internodes were placed in a tube, snap-frozen using liquid nitrogen, and stored at -80 degrees Celsius. Total RNA was extracted using the RNeasy kit (Qiagen), and the RNA concentration was determined using a nanodrop spectrophotometer (Thermo Fisher Scientific). Reverse transcription was carried out using random hexamer primers with RevertAid H Minus reverse transcriptase. To facilitate comparison, the Log_2FC (Logarithm of Fold Change) was employed.

5.5.6 Quantitative RT-PCR

Real-time PCR was conducted using the Bio-rad CFX opus 384 system with the Bio-rad CFX Maestro software. Primers listed in Table 1 were employed along with SYBRgreen

super mix dye (Thermo Fisher Scientific). Relative transcript abundance was determined using the comparative $2^{\Delta\Delta Ct}$ method, with *ACTIN2* serving as the reference gene. Statistical analysis of the qPCR data was performed using R, involving an ANOVA followed by a Tukey post hoc test. Data visualization was accomplished using GraphPad software (Version 9.5.1, released on January 24, 2023).

5.5.7 Homolog analysis

We conducted an homolog search involving several plant species from distinct families and utilized the default BLAST search various websites: for cDNA sequences of Arabidopsis, we sourced them from TAIR (The Arabidopsis Information Resource, 2015), while soybean *Pisum sativum* and *Glycine max* sequences were obtained from Phytozome (Goodstein et al., 2012). Additionally, we accessed Solanaceae sequences from Solgenemics (Solgenomics.net) (Mueller et al., 2005) with ITAG4.0 for *Solanum lycopersicum*, *Capsicum annuum* UCD 10X genome chromosome v1.0 for *Capsicum annuum*, eggplant V4 for *Solanum melongena*. Orthologs for *Brassica nigra* were obtained from http://brassicadb.cn/#/BLAST/ as part of our comprehensive ortholog search methodology. We keep the highest score of similarity over 70%, only similarity difference less than 10% would lead to keeping multiple homologs

5.5.8 Alignment, sub-sampling, and phylogenetic analyses

Homologs of all transcription factors (TFs) were aligned using Muscle v3.8.31 (Edgar, 2004). Subsequently, the phylogeny were generated using the Maximum likelihood constructed by software Mega X (Kumar et al., 2016), with a Tamura Nei model generating the ML tree. Bootstrap analysis utilized 1000 rapid bootstraps. The consensus tree method was then applied to select the genes for each species. Resulting output file was subsequently employed to construct a consensus tree using a majority rule consensus, ensuring that only nodes with bootstrap support values exceeding 50 were incorporated. The outcomes of the ML analysis were visualized and adjusted using Figtree v1.4.3 (Rambaut, 2012).

5.5.9 Conservation analysis

We carried out conservation analysis with mVista (Mayor et al., 2000; Frazer et al., 2004), alignment was carried out by LAGAN (Brudno et al., 2003), and conservation area was denoted with red color.

Table 5.1. Primer sequences used in multispecies qPCR.

Oligo Name	Seq (5' - 3')	Target gene	Species
Bnigra-3450ref-L1	CTCCCTCAAGCAACGAATCG	BniB06g001480.2N.1	*Brassica nigra*
Bnigra-3450ref-R1	ATGTCAACGGCCGAATTAGC	BniB06g001480.2N.1	*Brassica nigra*
Bnigra-3450ref-L2	GACTGCTTCTCAACGTCGAC	BniB06g055220.2N.1	*Brassica nigra*
Bnigra-3450ref-R2	CTGCTCTTTCTCAACGGACG	BniB06g055220.2N.1	*Brassica nigra*
Bnigra-3450ref-L3	GAGTCGCGTTCTTGGATCAC	BniB08g027470.2N.1	*Brassica nigra*
Bnigra-3450ref-R3	ACTCCCGTCTCTGGTGAATG	BniB08g027470.2N.1	*Brassica nigra*
Bnigra-3450ref-L4	GACGACGAGCAGTTCATGTC	BniB08g072820.2N.1	*Brassica nigra*
Bnigra-3450ref-R4	GACGGTGGCTGTTCTTTGTT	BniB08g072820.2N.1	*Brassica nigra*
Bnigra-0150ref-L1	CTCATCAACGGCGTCAGAAG	BniB08g029800.2N.1	*Brassica nigra*
Bnigra-0150ref-R1	CTTCAACCTTGGTGTGACGG	BniB08g029800.2N.1	*Brassica nigra*
Bnigra-0760ref-L1	CTCCAGCCTCTTCCTGTCTC	BniB07g039570.2N.1	*Brassica nigra*
Bnigra-0760ref-R1	ACGCCCTGATTTGTACCTCA	BniB07g039570.2N.2	*Brassica nigra*
Brassinactin-L	AGCAACTGGGATGACATGGA	BniB05g027120.2N.1	*Brassica nigra*
Brassinactin-R	TCACCAGAGTCGAGCACAAT	BniB05g027120.2N.1	*Brassica nigra*
TCP19-0150ref-L	CGCGCTGAAAATTCCTACGA	XM_016712397.2	*Capsicum annuum*
TCP19-0150ref-R	CAGTATCTGCTGTTGTCGCC	XM_016712397.2	*Capsicum annuum*
Cannuum-0760ref-L1	TGTCTTCCAACGCTGAGCTA	chr8:35902201-35904000	*Capsicum annuum*
Cannuum-0760ref-R1	CCCCTCCCCAATTGGTAGTT	chr8:35902201-35904000	*Capsicum annuum*
Cannuum-0760ref-L2	TTCCTCGACGGTGCTTTACT	chr3:267174801-267176100	*Capsicum annuum*
Cannuum-0760ref-R2	AGCTCTCCACTTGTCTTCCC	chr3:267174801-267176100	*Capsicum annuum*
Cannuum-3450ref-L	ACCGAAACAATCACCACTGC	CA00g71840:1-921	*Capsicum annuum*
Cannuum-3450ref-R	TCGGCATTCTTCGACCATTG	CA00g71840:1-921	*Capsicum annuum*
Capsiumactin-L	ACACCCTGTTCTCCTAACGG	CA03g11540	*Capsicum annuum*
Capsiumactin-R	TCACACCATCACCAGAGTCC	CA03g11540	*Capsicum annuum*
AT5G51910-q-L	GGCAACGCGATACAAGTGAT	AT5G51910	Col-0
AT5G51910-q-R	AATTGAAAGACCCGAGCAGC	AT5G51910	Col-0

Oligo Name	Seq (5' - 3')	Target gene	Species
AT2G45680-q-L	CTTCCTCCGGTTTAGCTCCA	AT2G45680	Col-0
AT2G45680-q-R	CAAGAAGAAAGCTCCGACCG	AT2G45680	Col-0
AT2G45050-L	CGGAAAGTGATGGAGCTTCG	AT2G45050.1	Col-0
AT2G45050-R	GTTACCCAAAACCCAACCCC	AT2G45050.1	Col-0
AT2G42380-L	TGCAAGATGGAGCCAGAAGA	AT2G42380	Col-0
AT2G42380-R	TAACACTGACACTTCCGCCT	AT2G42380	Col-0
UBQ10_F	GGCCTTGTATAATCCCTGATGAATAAG		Col-0
UBQ10_R	AAAGAGATAACAGGAACGGAAACATAGT		Col-0
Soy0150ref-L1	TGTCTCTTCCCTGGTCACAC	Glyma.07G080300.1	*Glycine max*
Soy0150ref-R1	ACTCAATGCTTGGAAGACGC	Glyma.07G080300.1	*Glycine max*
Soy0150ref-L2	CAACCACTTCACCTTCCGAC	Glyma07g08710.2	*Glycine max*
Soy0150ref-R2	TCGTTGCTGCGTTTTGGTTA	Glyma07g08710.2	*Glycine max*
Soyactin-L	AGGTGATGAAGCCCAGTCAA	Gm04:51853938..51855330	*Glycine max*
Soyactin-R	ACATGGCAGGCACATTGAAG	Gm04:51853938..51855330	*Glycine max*
Soy3450ref-L	TCTGCGCAAAGATCAAGAGTG	Gm06:49537899..49539195	*Glycine max*
Soy3450ref-R	CGGCCTTCATTGGTCAACAT	Gm06:49537899..49539195	*Glycine max*
Soy0760ref-L	AATTTGCCCTCCTCCTCCTC	GlysoPI483463.06G078800.1	*Glycine max*
Soy0760ref-R	GACACTTGCGGGTTGAACAT	GlysoPI483463.06G078800.1	*Glycine max*
Pea0150ref-L	TTCCAAGCCCAAACTCAAGC	XM_051017346.1	*Pisum sativum*
Pea0150ref-R	GGCGGAAATAATGGCAGGTT	XM_051017346.1	*Pisum sativum*
Pea0150ref2-L	GACCCTCTCTTCCAGACGAC	XM_051030491.1	*Pisum sativum*
Pea0150ref2-R	GAGCTCTTCTTTCATCGCCG	XM_051030491.1	*Pisum sativum*
Pea0150ref3-L	CGGCGATGAAAGAAGAGCTC	XM_051030490.1	*Pisum sativum*
Pea0150ref3-R	GATTTGTGACCAAGCTCCCG	XM_051030490.1	*Pisum sativum*
Pea3450ref-L	GCCAACCTCCTTTTCAACCA	XM_051027770.1	*Pisum sativum*
Pea3450ref-R	TTTTCACCATCTTTCCCGCG	XM_051027770.1	*Pisum sativum*
Pea3450ref2-L	ATTCCCTCTGGCTCCTTCAC	XM_051045459.1	*Pisum sativum*
Pea3450ref2-R	GGCCAAGGTTGTGTCATGTT	XM_051045459.1	*Pisum sativum*
Pea3450ref3-L	AAGTGGTGGTGATGGAGAGG	XM_051026994.1	*Pisum sativum*
Pea3450ref3-R	CAACCGCTTCATCCTTAGGC	XM_051026994.1	*Pisum sativum*
Pea0760ref-L	CGACAGCAGCAGGGATTTAC	XM_051030552.1	*Pisum sativum*
Pea0760ref-R	AGGCAGCTTTGGTTTCTTGG	XM_051030552.1	*Pisum sativum*

Oligo Name	Seq (5’ - 3’)	Target gene	Species
Pea0760ref2-L	CACCGCCGTTTAAACTTCCA	XM_051038772.1	*Pisum sativum*
Pea0760ref2-R	GCCGCACAAATCAAACGATG	XM_051038772.1	*Pisum sativum*
Pea0760ref3-L	CACCCTCCTCAAGTGTCTGT	XM_051027377.1	*Pisum sativum*
Pea0760ref3-R	GGTGTTTTATCAGTGGCGCA	XM_051027377.1	*Pisum sativum*
Peaactin-L	CGGGTATCCATGAGACGACA	X90378.1	*Pisum sativum*
Peaactin-R	CCTCTCTGGTGGTGCTACAA	X90378.1	*Pisum sativum*
Eggplant0150ref-L	TGTCACCGGAGCAAATTGTG	8:85852001-85853900	*S. melongena*
Eggplant0150ref-R	CTGTTCGGTGGTTGCTTGAA	8:85852001-85853900	*S. melongena*
Eggplant0760ref-L	AACACTCTGCAATGCCTGTG	1:18346701-18348500	*S. melongena*
Eggplant0760ref-R	GATGGCGGCATTTGTTGTTG	1:18346701-18348500	*S. melongena*
Eggplant3450ref-L	GGGCGCTGAATTCGAGAAAT	07g019740.1.01	*S. melongena*
Eggplant3450ref-R	GCTGCTCCGTAGACACATTG	07g019740.1.01	*S. melongena*
Eggplant-ubi-L	TCCTATCTCTGCCCTGACCT	4:327201-328500	*S. melongena*
Eggplant-ubi-R	CCTGGCAAGCAACACATACA	4:327201-328500	*S. melongena*

5.6 SUPPLEMENTARY DATA

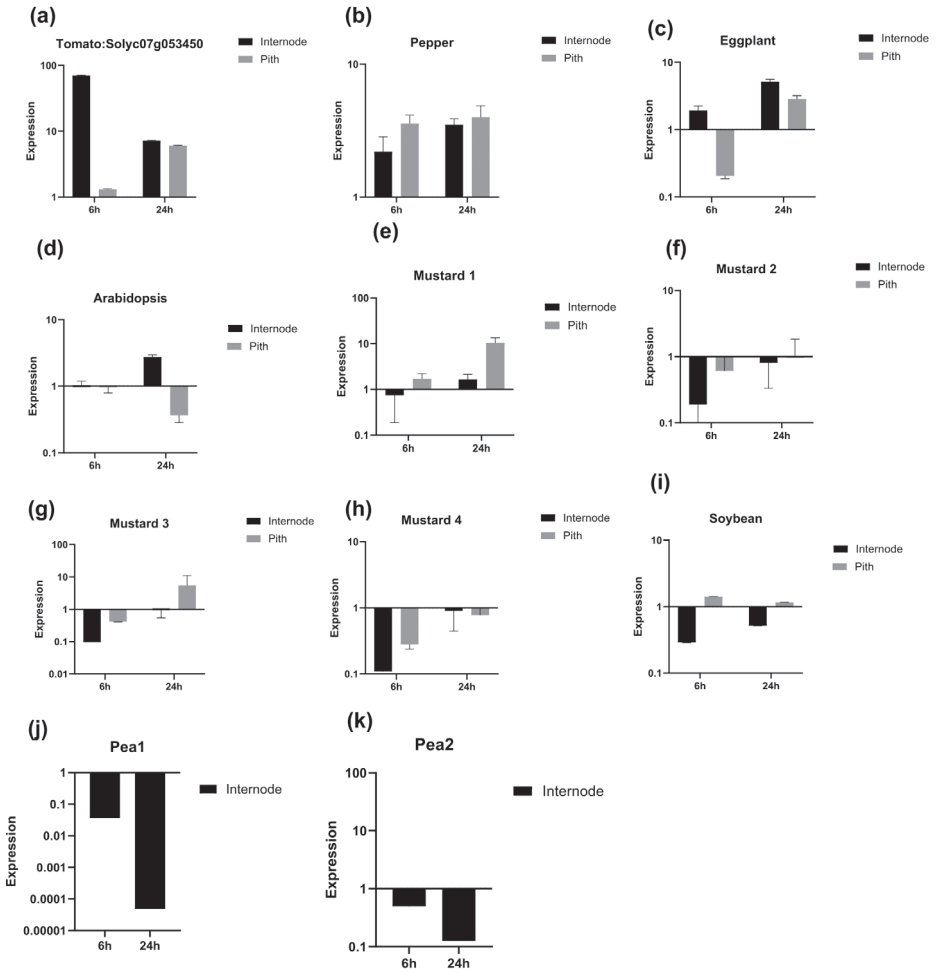

Figure S5.1. *Solyc07g053450* transcript abundance in response to FR treatment. Analysis was conducted using qPCR to examine the transcript abundance in internode 1 and its pith at two different time points: 6 hours, and 24 hours on top homologs in multiple species. The expression levels were obtained by comparing the response to WL and WL+FR conditions. The following genes were investigated: (a) Tomato: *Solyc07g053450*, (b) Pepper: *CA00g71840:1-921*, (c) Eggplant: *SMEL4.1_07g019740.1.01*, (d) Arabidopsis: *AT2G42380*, (e) Mustard1: *BniB06g001480.2N.1*, (f) Mustard2: *BniB08g027470.2N.1*, (g) Mustard3: *BniB08g072820.2N.1*, (h) Mustard4: *BniB06g055220.2N.1*, (i) Soybean: *Gm06:49537899..49539195*, (j) Pea1: *XM_051027770.1*, (k) Pea2: *XM_051045459.1*. The experiment included 4 biological replicates, each consisting of 8-12 plants. Additionally, 4 technical replicates were performed to ensure the accuracy of the measurements.

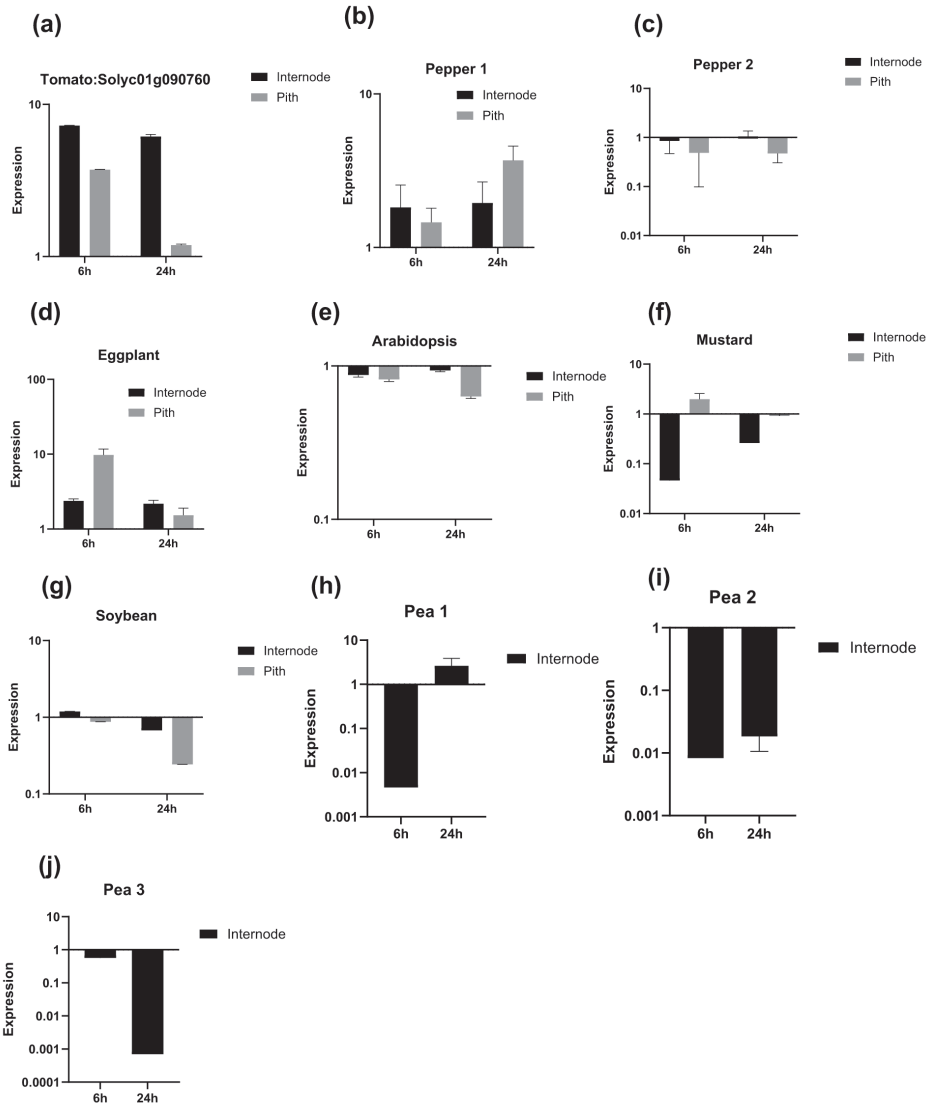

Figure S5.2. *Solyc01g090760* transcript abundance in response to FR treatment. Analysis was conducted using qPCR to examine the transcript abundance in internode 1 and its pith at two different time points: 6 hours, and 24 hours on top homologs in multiple species. The expression levels were obtained by comparing the response to WL and WL+FR conditions. The following genes were investigated: (a) Tomato: *Solyc01g090760*, (b) Pepper1: *chr3:267174801-267176100* (*CA00g71840:1-921*), (c) Pepper2*: chr8:35902201-35904000*, (d) Eggplant: *chr8:35902201-35904000*, (e) Arabidopsis: *AT2G45050*, (e) Mustard: *BniB07g039570.2N.1*, (f) Soybean: *GlysoPI483463.06G078800.1*, (g) Pea1: *XM_051027377*, (h) Pea2: *XM_051030552.1*, (i) Pea3: *XM_051038772.1*. The experiment included 4 biological replicates, each consisting of 8-12 plants. Additionally, 4 technical replicates were performed to ensure the accuracy of the measurements.

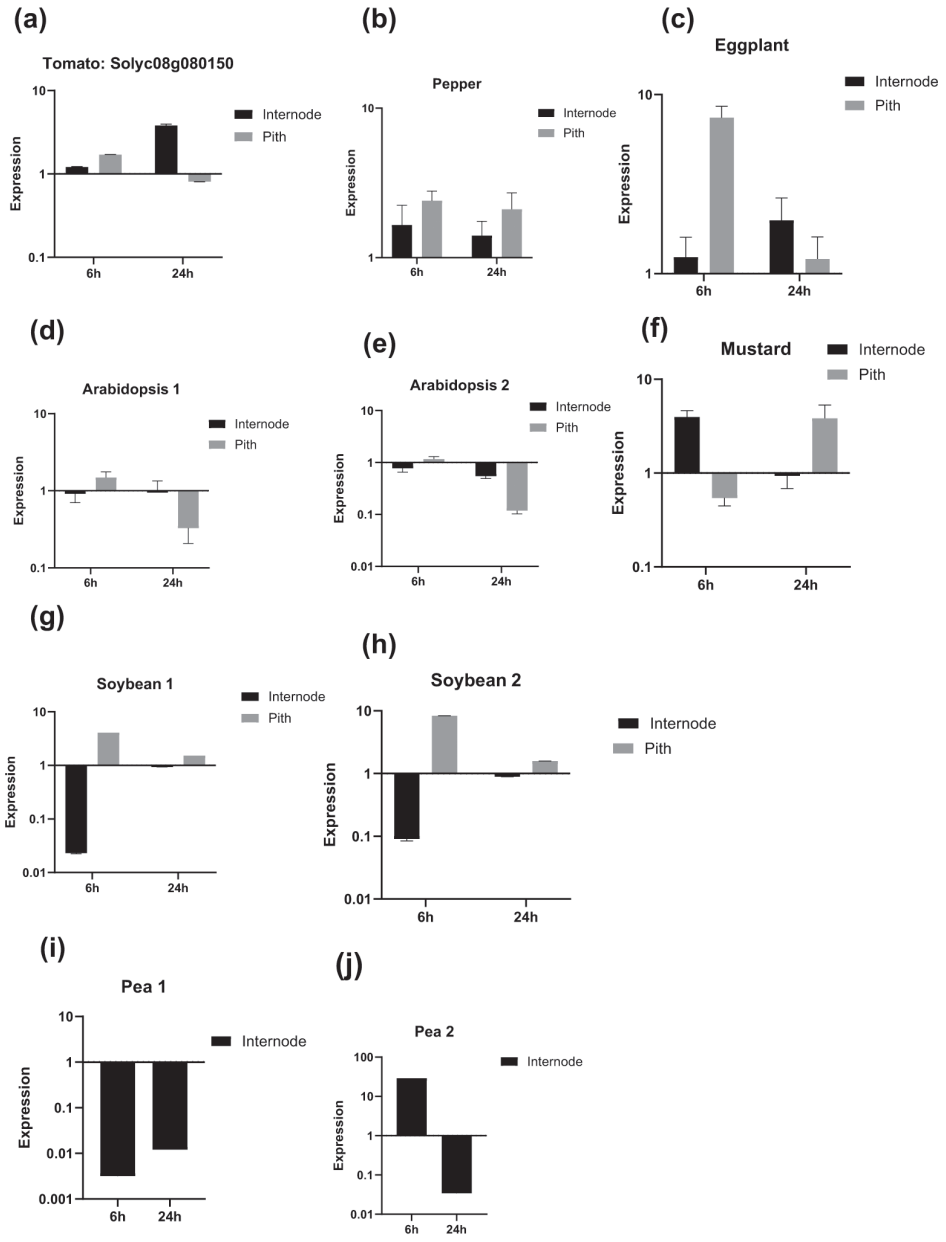
(a)
Tomato: Solyc08g080150
Expression
10
1
0.1
6h
24h
Internode
Pith
(b)
Pepper
Expression
10
1
6h
24h
Internode
Pith
(c)
Eggplant
Expression
10
1
6h
24h
Internode
Pith
(d)
Arabidopsis 1
Expression
10
1
0.1
6h
24h
Internode
Pith
(e)
Arabidopsis 2
Expression
10
1
0.1
0.01
6h
24h
Internode
Pith
(f)
Mustard
Expression
10
1
0.1
6h
24h
Internode
Pith
(g)
Soybean 1
Expression
10
1
0.1
0.01
6h
24h
Internode
Pith
(h)
Soybean 2
Expression
10
1
0.1
0.01
6h
24h
Internode
Pith
(i)
Pea 1
Expression
10
1
0.1
0.01
0.001
6h
24h
Internode
(j)
Pea 2
Expression
100
10
1
0.1
0.01
6h
24h
Internode

► **Figure S5.3. *Solyc08g080150* transcript abundance in response to FR treatment.** Analysis was conducted using qPCR to examine the transcript abundance in internode 1 and its pith at two different time points: 6 hours, and 24 hours on top homologs in multiple species. The expression levels were obtained by comparing the response to WL and WL+FR conditions. The following genes were investigated: (a) Tomato: *Solyc08g080150*, (b) Pepper: *TCP19*, (c) Eggplant: *chr8:85852001-85853900*, (d) Arabidopsis1: *AT2G45680*, (e) Arabidopsis2: *AT5G51910*, (f) Mustard: *BniB08g029800.2N.1*, (g) Soybean1: *Glyma.07G080300.1*, (h) Soybean2: *Glyma07g08710.2*, (i) Pea1: *XM_051030490.1*, (j) Pea2: *XM_051030491.1*. The experiment included 4 biological replicates, each consisting of 8-12 plants. Additionally, 4 technical replicates were performed to ensure the accuracy of the measurements.

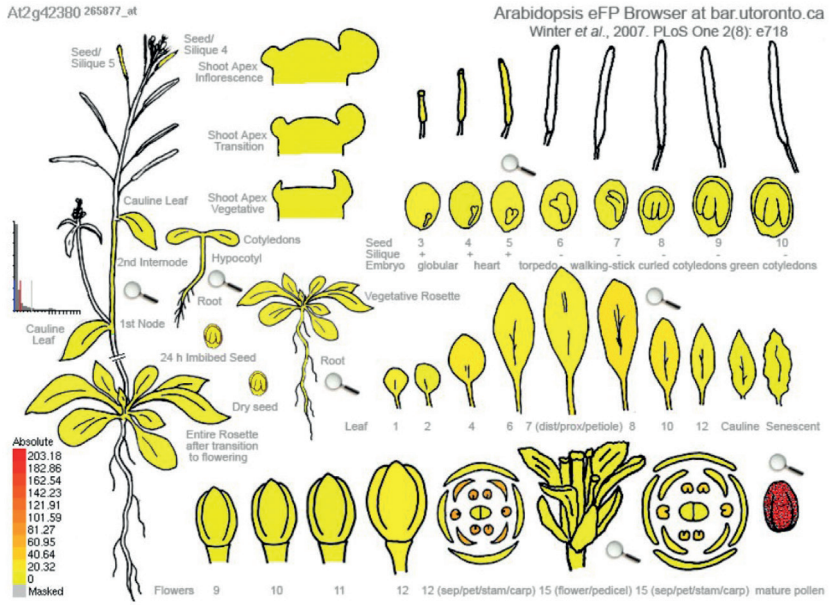

Figure S5.4. Expression pattern of *AT2G42380* in Arabidopsis development (Nakabayashi et al., 2005; Schmid et al., 2005)**.**

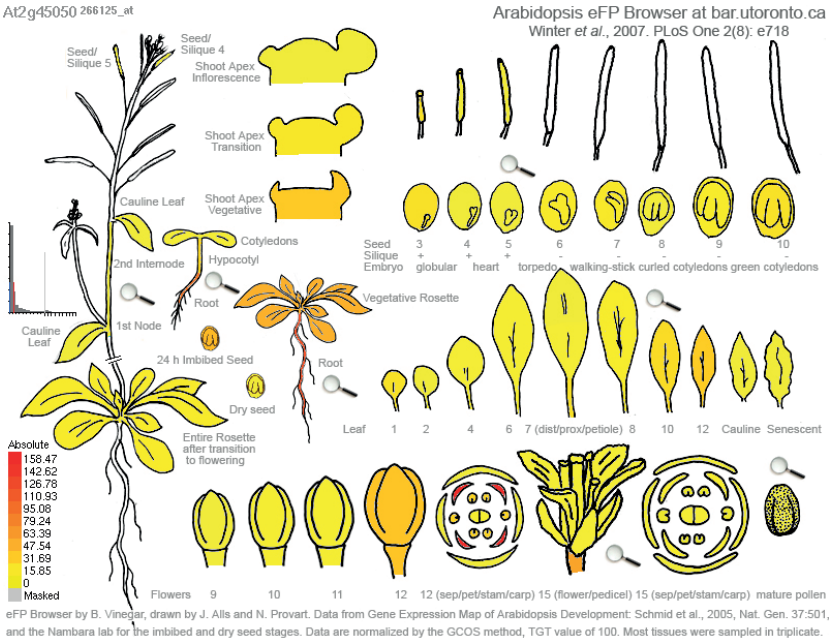

Figure S5.5. Expression pattern of *AT2G45050* in Arabidopsis development (Nakabayashi et al., 2005; Schmid et al., 2005)**.**

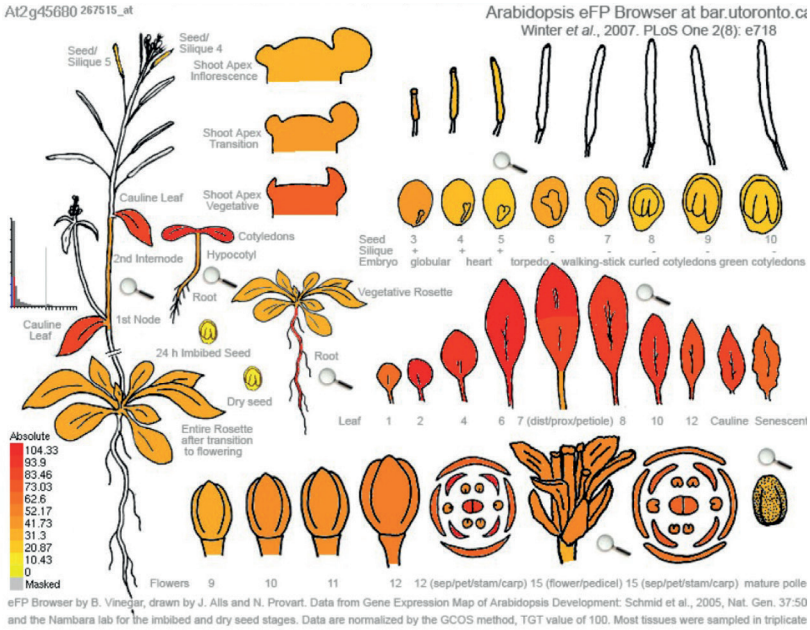

Figure S5.6. Expression pattern of *AT2G45680* in Arabidopsis development (Nakabayashi et al., 2005; Schmid et al., 2005)**.**

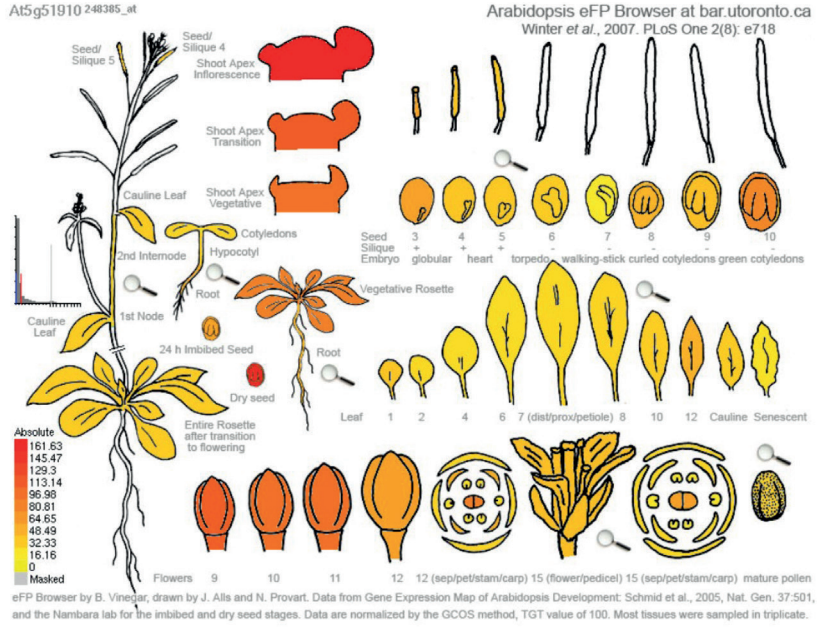

Figure S5.7. Expression pattern of *AT5G51910* in Arabidopsis development (Nakabayashi et al., 2005; Schmid et al., 2005)**.**

GENERAL DISCUSSION

This thesis explores the interplay between plants and their environment, with a specific focus on shade avoidance syndrome (SAS). This behavior in plants is triggered by the detection of a shift in the red (R) to far-red (FR) light ratio, typically indicating competition and impending shading by neighboring plants.

Plants are sessile organisms; they are unable to walk away from an unfavorable situation. Because of their inability to move, they have evolved to acclimate to changes in their environment. Plants convert sunlight into energy that can be used by cellular processes, and it is the main source of energy for the plant. So, light is an environmental factor that influences a plant's function to a great extent. Light availability and composition can alter a plant's phenotype and photosynthetic capabilities (Kami et al., 2010). A changing light environment can be detected directly via light intensity, or by far-red or blue light enrichment depending on environmental circumstances and the plant species (Navrátil et al., 2007), and a widely researched of these is the supplemental far-red (FR) response. The FR response is initiated when plants grow with an increased abundance of FR light about red light, which happens when a plant grows near or underneath a canopy of leaves, creating a change in light composition (Navrátil et al., 2007). Overviews of this response are widely available as it has been researched extensively (Bongers et al., 2014; Courbier and Pierik, 2019; Wang et al., 2020) and will therefore only be touched upon briefly in this thesis.

This thesis expands the knowledge of SAS into the crop species tomato, as understanding shade avoidance mechanisms outside of model species is important to see if findings are translatable to support global food production, in this case, tomato cultivation. In **Chapter 2** we characterized the phenotypic changes in juvenile tomatoes in response to FR supplementation. We identified the 1st internode as a region that responded strongly by both elongation and radial growth. We then zoomed into its cellular morphology to discover strong changes in the pith parameters. We wanted to identify molecular processes underlying this phenotypic plasticity, so in **Chapter 3** we carried out RNAseq profiling of internode 1 and its pith in response to FR treatment. We discovered gene expression changes that could be auxin-induced, so in **Chapter 4**, we delved into the hormone dynamics governing neighbor detection responses. While we started with a focus on auxin (IAA), we also explored the roles of gibberellins (GA), and brassinosteroids (BR). While auxin exhibited a role in stem elongation, its full impact required the involvement of other actors, potentially GA or BR, to achieve far-red (FR)-like elongation. GA and BR treatments in tomato FR-response induced comparable stem elongation, emphasizing their potency, and both also turned out to be necessary for FR-

induced elongation. Then, finally in **Chapter 5**, we expanded our research from tomato to other dicots and explored the diversity of internode elongation in the shade avoidance response and the putative regulatory roles of specific GATA, TCP, and bZIP transcription factors identified in Chapter 3. The multi-species study unveiled diverse responsiveness to supplemental FR light across dicots, with quantifiable pith elongation observed in the species strongly responsive to the FR signal. The conservation of expression patterns of candidate TFs within Solanaceae suggests functional significance in this family. Distinct pith responses, indicated by cell-type-specific gene expression patterns of these TFs in some dicots (e.g. *Solyc08g080150* homologs in Soybean, Figure 5.13), also indicate that pith responses are regulated differently to the rest of the internode, and that pith plays a specific role in SAS. Overall, this thesis offers novel insights into transcriptional regulation, evolutionary conservation, and molecular mechanisms shaping FR responses across dicots.

Building on this, the thesis delves into the transcriptional regulation, evolutionary conservation, and molecular mechanisms governing FR responses across dicots. While the primary focus is on SAS in the physiological response of tomato crops, the evolutionary content enriches the scope of this study. In this general discussion chapter, I will bring together a number of topics that have emerged in the experimental chapters. Firstly, I will discuss the role of pith cells for stems, and what our findings in Chapters 2, 3 and 5 suggest as the relevance of pith in SAS. Then, I will discuss the role of different hormones in tomato SAS (Chapter 4), and how these might play integrate into the expression patterns of *SMALL AUXIN UPREGULATED RNAs* (*SAUR)*s we observed in Chapter 3. Finally, I will discuss TF evolution (Chapters 3 and 5) and conclude with general evolutionary hypothesis.

6.1 PITH IN SAS

6.1.1 What is pith?

The pith is the central, often spongy, tissue found in the stems of vascular plants. It consists of large, loosely packed parenchyma cells, and its primary function is to store and transport nutrients throughout the plant. The pith is encircled by a ring of xylem, which is in turn encircled by a ring of cambium, and then a ring of phloem. In some plants, the pith may play a role in providing structural support to the stem (Venning, 1949; Esau, 1953; Hardwick and Elliott, 2016). The pith can vary in size, shape, and composition among different plant species, and often it faces programmed cell death, leaving a hollow internal cylinder. The pith's cellular structure, specifically the arrangement and

characteristics of its cells, contributes to its functions in nutrient storage, transport, and support within the plant, but the molecular mechanisms underlying these pith functions remain largely uncharacterized.

Recent research has unveiled new roles for pith. Firstly, the intercalation of the xylem with the pith to separate xylem strands from each other decreases the risk of cavitation (Bouda et al., 2022), making complex pith patterns an evolutionary advantage in arid environments. Secondly, pith drives primary thickening growth (the diameter and strength of the stem structure) and culm size in bamboo underground shoots (Wei et al., 2017). The spiral growth of bamboo internodes, a manifestation of shoot wall cell expansion, exerts anisopleural force on the internal pith tissue, ultimately leading to the asymmetrical formation of the pith, this is an example of the unique growth niche of pith (Guo et al., 2019; Long et al., 2023). In this thesis, we saw radial pith divisions in FR-treated tomato stems, hand in hand with radial thickening of the elongating internode (Figures 2.6, 2.16), potentially linking pith with radial growth also in tomato.

The pathway of pith growth remains elusive, raising questions about its origin. It is commonly assumed that pith cells originate from the rib meristem, located at the top of the shoot and in close proximity to the shoot apical meristem (SAM). In this thesis, local treatment of SAM with far-red light induced a similar elongation effect as the overall far-red treatment (Figure 3.2). This observation suggests that the rib meristem, particularly in the early stages of growth, could serve as a trigger for pith generation.

In Chapter 2, we found that pith elongated and thickened radially in response to FR in tomato stems, and in Chapter 3 we generated pith-specific transcriptome data. When comparing the transcriptomes of pith and the whole internode in our data, we saw pith-specific pattern of multiple transcription factor (Sasidharan et al., 2010)(Table S.3.5 red color) encoding genes and *EXPANSINs*. This same observation can be made from Arabidopsis pith transcriptome (Shi et al., 2020). This suggests a noteworthy pattern that does not effectively prove pith function but does has an evolutionary significance of pith-related processes conserved across species.

An early study on testing the presence of cAMP in plants actually utilized excised tobacco pith tissue on auxin-containing media (Lundeen et al., 1973). In this setup, auxin induced both cell enlargement and DNA replication phases of the cell cycle, along with cytokinesis (Lundeen et al., 1973). Similarly, our Gene Ontology (GO) analysis (Figure 3.7) revealed a substantial upregulation in DNA replication and cell activities upon FR treatment in pith, offering molecular support to the cell divisions and elongation observed in Figure 2.16.

As the tissue ages in some plants, the pith in the middle of the stem may dry out and disintegrate, resulting in a hollow stem (Abercrombie et al., 1968; Kutschera and Köhiler, 1992; Brown et al., 1995b). The formation of the pith cavity, intricately linked to programmed cell death and governed by diverse physiological and molecular processes, is caused by stress conditions (Guo et al., 2019; Wang et al., 2022). Pith cavities in plant stems, such as those found in bamboo, are not unexpected, as they can form due to various factors, including disease, aging, and environmental conditions (Wei et al., 2017). Wheat stems typically exhibit solidity in the nodal region, with the formation of an internodal cavity occurring as pith cells undergo programmed cell death during internode elongation. The genes influencing stem pith thickness are likely associated with pith cell death and cell wall composition. For instance, modulating pith thickness can be achieved by either activating or inhibiting programmed cell death (which is also observed in sorghum) (Fujimoto et al., 2018) or altering cell wall composition, leading to increased stem cell wall thickness and lignin content (Kong et al., 2013; Liu et al., 2023b) (Kong et al., 2013).The significance of the pith and its programmed cell death extends beyond monocots, as evidenced by the presence of pith cavities also in dicots. In Figure 6.1, we observed a dicot *Vicia faba* forming a pith cavity early in the development of the third internode, while the older internodes remained filled with pith. This could offer a dicot model to study the role of pith cavity in phenotypic plasticity of the stem.

6.1.2 Pith cell elongation, a key contributor to stem elongation in multiple species within SAS

We observed a range of pith responses exhibited by different plant species when it comes to shade avoidance. We first noticed a pronounced pith cell elongation and radial divisions in FR in *S. lycopersicum* cultivars Moneymaker and M82 (Chapter 2). In the 8 species we selected (Chapter 5), most of them demonstrated typical stem elongation and similar to tomato, pith cell elongation in response to reduced R:FR. In SAS, the persistent correlation between pith elongation and stem elongation underscores its conservation across the panel. While radial growth of pith was observed in several species, its significance varied, leading us to hypothesize that pith activities during rapid growth primarily emphasize longitudinal direction.

The presence or absence of pith in plant stems is influenced by various factors related to the plant's growth habit, evolution, and ecological niche. One key reason for its presence in herbaceous plants, such as the species in our panel, is its role in nutrient storage and transport. Herbaceous plants often require the capacity to store nutrients and water for

rapid growth and seasonal fluctuations. On the other hand, (semi-)woody plants invest heavily in the development of secondary tissues, such as wood and bark, to support their height and withstand environmental stressors. Consequently, (semi-)woody plants often have reduced or absent pith, as their primary structural support comes from the surrounding tissues (Esau, 1965). The linkage of pith elongation and radial division with SAS is still unknown, but from our current data, we did observe that pith cell elongation is conserved in shade-responsive species' stem elongation, thus suggesting a potential connection between pith cell behavior and shade adaptation strategies in these plants.

Unlike the woody layers responsible for structural support, pith cells may have lower lignin content and they exhibit larger, rounder shapes (Gunning and Steer, 1996). Their differentiation and development from meristematic cells during growth set them apart, as they become specialized for nutrient and water storage, whereas other cell layers differentiate into cells dedicated to transport and structural support. Furthermore, in woody plants, secondary growth primarily occurs in the vascular cambium and cork cambium, distinct from the pith region, which generally does not directly contribute to secondary growth processes (Venning, 1949; Lovell et al., 1971). We hypothesize that their elongation in SAS is facilitated by relatively thinner cell walls and lower lignin content, allowing them to expand and store larger volumes of materials (Esau, 1953). Given the inherent capacity of pith cells for elongation, they are poised to play a role as key drivers in the elongation of differentiated vascular tissues.

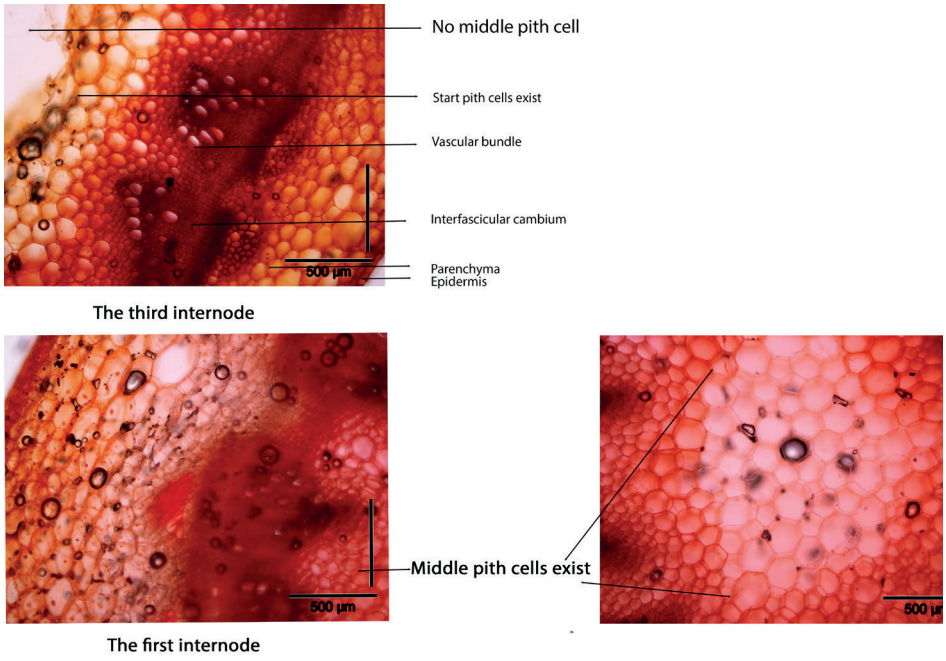

Figure 6.1. *Vicia faba* stem morphology shows a developmental trajectory of pith cells across internodes. The older internodes (first and second) are filled with live pith, while the third internode onwards we observed a pith cavity forming through middle pith programmed cell death.

6.1.3 The relationship between SAS and secondary growth is not resolved yet

In chapter 2, we observed a consistent promotion of cambium thickness in tomato during far-red (FR) analysis. The vascular cambium serves various functions, with a possible role in facilitating secondary growth. Secondary growth is a vital process in the growth and development of many plants, especially woody species. It involves the production of secondary tissues, such as wood and bark, in plant stems and roots. These secondary thickened tissues provide structural support, increase the girth of the plant, and allow it to grow taller and more robust over time. The two key meristematic tissues responsible for secondary growth are the vascular cambium and cork cambium. The vascular cambium generates a secondary xylem (wood) towards the inside of the stem and secondary phloem towards the outside, contributing to the plant's water transport and nutrient distribution. The cork cambium produces cork cells that form the protective outer bark layer. Secondary growth is critical for plants to attain sufficient height, access resources, and adapt to changing environmental conditions.

Shade avoidance is a well-documented plant response to low light conditions, where plants adjust their growth patterns to compete for sunlight. In shade conditions, plants often exhibit traits like elongated stems and increased apical dominance, focusing on reaching light sources. While shade avoidance primarily affects primary growth (the lengthening of stems and roots), our data in *S. lycopersicum* in Chapter 2 showed it can also influence secondary growth – either directly, or indirectly by altering the allocation of resources. However, the extent to which shade avoidance directly impacts secondary growth can vary among plant species. In Chapter 5 we observed diameter increase also in Arabidopsis inflorescence stems in response to FR, but no radial growth in response to FR for any other species in our panel. While there is evidence that shade avoidance can influence resource allocation and growth patterns, more research is needed to understand the precise mechanisms and consequences of this relationship on secondary growth across different plant species and environments.

6.2 HORMONAL REGULATION OF TOMATO SAS IN A BROADER CONTEXT

6.2.1 Interplay of hormone signals in Arabidopsis SAS

The perception and signaling of low R:FR in Arabidopsis involve complex interactions between photoreceptors, hormones, and transcription factors. In response to low R:FR, auxin concentrations increase rapidly, but this increase is often transient and lost on the second day of treatment (Bou-Torrent et al., 2014; de Wit et al., 2015; Pucciariello et al., 2018). A subsequent increase in auxin sensitivity is required to maintain auxin signaling for a longer duration in low R:FR. Arabidopsis senses low red:far red (R:FR) light conditions in the leaf lamina, which triggers PIF-regulated gene expression and auxin biosynthesis. The auxin signal then travels to the petiole/hypocotyl, where brassinosteroids (BRs) are involved in the elongation responses (Leivar and Monte, 2014; Galvão et al., 2019; Zhang et al., 2020). Additionally, other hormones may further stimulate growth beyond the first day, such as the increased synthesis of gibberellic acid (GA) through enhanced *GA20-OXIDASE* (Hisamatsu et al., 2005; Bou-Torrent et al., 2014; Gommers et al., 2017). Increasing GA concentrations promote the degradation of growth-repressive DELLA proteins, which are nuclear-localized repressors that inhibit the activity of many transcription factors, including the BR-responsive growth promoter BZR1 (BRASSINAZOLE-RESISTANT 1) and BES1 (BRI1-EMS-SUPPRESSOR 1), but also *ARF*s (*AUXIN RESPONSE FACTOR*) and PIFs. These transcription factors, together with their DELLA repressor, constitute the BZR-ARF-PIF/DELLA (BAP/D) module (Oh et al., 2014). BZR1, *ARF6*, and PIF4 stimulate cell growth through the

induction of many shared target genes and reinforce each other's activity at those targets (Oh et al., 2012; Oh et al., 2014). The interactions between these transcription factors explain why PIFs and BZR stimulate auxin sensitivity. However, each member of the BAP module also has its specific targets, indicating a complex growth-promoting network of interacting transcription factors stimulated by auxin, gibberellin, and brassinosteroid signaling, while being repressed by active phy and cry photoreceptors (Fu and Harberd, 2003; Ishida et al., 2010; Holalu and Finlayson, 2017; Galvão et al., 2019). This interplay is important to keep in mind as a reference when interpreting the tomato data in the following sections.

6.2.2 *SAUR*s are responsive during FR-triggered elongation of internode 1 and pith

In Chapter 3, focused on RNA-seq analysis of cell elongation, the most enriched pathway emerged as the auxin response Gene Ontology (GO) category, specifically comprising *SMALL AUXIN UP RNA (SAUR)*s. This finding underscores the significance of *SAUR*s in SAS. Auxin regulates hypocotyl growth in Arabidopsis (Gray et al., 1998; Zhao et al., 2001), and many *SAURs* are highly expressed in elongating hypocotyls (Franklin et al., 2011; Chae et al., 2012; Chalivendra et al., 2013; Stamm et al., 2013), and it has long been hypothesized that *SAUR*s may be involved in auxin-regulated cell expansion (Stortenbeker and Bemer, 2019). Experimental results supporting a positive role for SAURs in cell expansion were obtained from several recent studies in Arabidopsis. Overexpression of *SAUR36*, *SAUR41*, or stabilized fusion proteins of *SAUR19* or *SAUR63* promotes hypocotyl elongation by enhancing cell expansion. Conversely, seedlings expressing artificial microRNAs targeting *SAUR19* or *SAUR63* exhibit slightly shorter hypocotyls with smaller epidermal cells, indicating a positive regulatory role for these SAURs in cell expansion (Knauss et al., 2003; Park et al., 2007; Narsai et al., 2011; Qiu et al., 2013).

SAURs are key elements of the auxin growth mechanism to facilitate cell expansion that was established for more than 50 years (Spartz et al., 2014). Originating in the 1970s, the acid growth theory was initially introduced to elucidate auxin-mediated cell expansion (Rayle and Cleland, 1970; Rayle and Cleland, 1992; Hager, 2003). The auxin-mediated cell elongation response to various signals depends on the enhanced expression of *SAUR19-24* (Ishida et al., 2010). This response involves the stimulation of H^+-ATPase proton pumps, leading to rapid apoplast acidification and acid growth. In shade-exposed Arabidopsis petioles, apoplast acidification happens within minutes.

According to this theory, auxin induces proton release in susceptible cells, lowering apoplastic pH, increasing membrane potential, and activating cell wall-loosening proteins like EXPANSINs (Sasidharan et al., 2008; Sasidharan et al., 2010; Arsuffi and Braybrook, 2018), also upregulated in our data (Figure 4.22-23).

Intriguingly, certain *SAUR*s have been suggested to exert a negative regulatory influence on cell expansion. For example, transgenic seedlings overexpressing *SAUR32* exhibit reduced hypocotyl elongation in conditions of darkness or red light exposure (Park et al., 2007). Conversely, a potential negative regulatory role of *SAUR36* in inhibiting leaf growth is hinted by *saur36* T-DNA loss-of-function plants displaying larger leaves with expanded epidermal cells (Hou et al., 2013). However, *SAUR36* overexpression results in seedlings displaying an extended hypocotyl phenotype (Stamm et al., 2013). This indicates that *SAUR*s can have both promoting or inhibiting effects on cell expansion, and this might be also indicated in our data from RNAseq (Figure 4.2a). This interplay among *SAUR*s, with their potential dual roles, adds layers of complexity to our understanding of their functions. These nuanced regulatory mechanisms underscore the need for comprehensive investigations to unravel the diverse roles played by *SAUR* family members in tomato SAS.

Roig-Villanova et al., 2007 proposed a connection between *SAUR*s and SAS in Arabidopsis. The atypical bHLH proteins, *PHYTOCHROME RAPIDLY REGULATED1* (*PAR1*) and *PAR2*, lacking a basic domain for DNA-binding, are upregulated by shade, inhibiting SAS. PAR1 interacts with PIF4 to suppress its DNA-binding activity, resulting in the inhibition of *SAUR15* and *SAUR67*, potential direct targets of PIF4; this interaction, coupled with the transient induction of *SAUR15* and *SAUR67* by shade, suggests a feedback mechanism through PAR1 and PAR2 to mitigate shade-induced *SAUR* expression (Oh et al., 2014). Hornitschek et al., 2012 also supported the role of *SAUR*s in shade-stimulated elongation growth, identifying *SAUR19* subfamily genes and additional *SAUR* genes as potential direct targets of *PIF5*. The rapid induction of specific *SAUR* genes in elongating hypocotyls under far-red enrichment indicates their involvement in cell elongation, contributing to the increased growth observed in shade avoidance. In Chapter 3, we showcase the shade avoidance syndrome induction of *SAUR* in the stem of *S. lycopersicum*. Despite limited annotation in *S. lycopersicum*, in the expression analysis of IAA-related genes (Fig 4.2a), we performed ortholog search for *SAUR*s, and revealed a significant upregulation of many *SAUR*s.

6.2.3 *SAUR* regulation is not limited only to auxin

SAUR genes, in addition to being influenced by auxin, are regulated by brassinosteroids (BR) and gibberellins (GA), suggesting their involvement in diverse hormone-mediated aspects of plant growth (Ren and Gray, 2015). BR, a growth-promoting hormone, shares extensive crosstalk with auxin, converging at the transcriptional level to regulate common target genes, including various *SAUR* genes (Fàbregas and Caño-Delgado, 2014; Wang et al., 2014). BES1 and BZR1 transcription factors in the BR signaling pathway have been identified as potential regulators of *SAUR* gene expression. Chromatin immunoprecipitation studies confirm the binding of BZR1 and BES1 to *SAUR* promoters, implicating *SAUR*s as downstream effectors in BR-mediated expansion growth (He et al., 2005; Yin et al., 2005; Gory Vert et al., 2011). Similarly, GA, another growth-promoting hormone, impacts *SAUR* gene expression, with DELLAs, central regulators in the GA pathway, influencing *SAUR* promoters (Claeys et al., 2014; Xu et al., 2014). GA-induced degradation of DELLAs leads to enhanced *ARF*, PIF, and BZR1/BES1 transcription factor binding to *SAUR* promoters. Notably, *SAUR36* is upregulated by RGA-LIKE2 (RGL2), a major DELLA protein in seed germination regulation, with further research needed to elucidate its specific role in other processes (Feng et al., 2008; De Lucas et al., 2008; Bai et al., 2012).

The interaction between BR and auxin signaling is complex and involves overlapping gene activation, synergistic effects, and interdependent interactions. Microarray analyses have shown that BR and auxin activate similar sets of genes, and genetic and physiological studies have demonstrated their collaboration in various developmental processes, including hypocotyl elongation and vascular bundle patterning (Ibañes et al., 2009; Depuydt and Hardtke, 2011; Nemhauser and Torii, 2016). Several molecular mechanisms have been proposed to mediate BR-auxin interactions. BZR1, a key regulator in the BR pathway, controls genes involved in auxin synthesis, transport, and signaling (Sun et al., 2010). Auxin, in turn, activates BR biosynthetic genes and increases BR levels. The protein BIN2 phosphorylates an auxin-response factor (*ARF2*), and both BZR2 and *ARF5* bind to the same promoter involved in BR and auxin responses (Vert et al., 2008; Walcher and Nemhauser, 2012). Additionally, the actin cytoskeleton, regulated by both BR and auxin, plays a role in integrating their responses and feedback regulating auxin transport and BR signaling (Lanza et al., 2012). However, further evaluation is needed to fully understand the physiological implications of these mechanisms in BR-auxin interactions.

In chapter 3, we found *SAUR* upregulation and in chapter 4, we explored the role of hormones, specifically auxin (IAA), gibberellins (GA), and brassinosteroids (BR), in regulating stem elongation during SAS in tomato plants. In our RNAseq analysis,

SAUR upregulation was the main component of the auxin response Gene Ontology (GO) category enrichment, and we also assumed *SAUR* upregulation reflected IAA signaling. However, our findings revealed that while IAA alone had a limited effect on stem elongation and we observed no IAA change in the stem in response to FR. GA and BR, on the other hand, had a more pronounced impact on stem elongation compared to IAA. It might be that *SAUR* upregulation was not a reflection of IAA, but instead either GA or BR signaling. These findings highlight the restrictions of GO annotations and the complications coming from the multifaceted regulatory networks, in this case, of *SAUR* regulation by IAA, BR and GA pathways.

6.2.4 Limitations of GO annotation in tomato

To investigate the limitations of the GO analysis in tomato, we carried out a comparative analysis, to identify ratios of genes belonging to different categories in the well-annotated Arabidopsis and our model tomato (Table 6.1). With a focus on Brassinosteroid (BR), Gibberellic Acid (GA), auxin and far-red GO categories, it is clear that tomato annotations are severely lacking. Arabidopsis currently has annotations for 63 BR genes and 23 GA genes, while *S. lycopersicum* lacked BR annotations and had 5 GA annotations. The ratios highlighted the absence of BR annotations in tomato (0) and minimal GA annotations in both species. Poor GO annotation in *S. lycopersicum* will be a key limitation to our GO enrichment in Chapter 3, which we then overcame by plotting the FR-responsive behavior of tomato homologs of known hormone-related and -responsive genes (Figure 4.2, S4.1, S4.2). Also, should *SAURs* be only annotated as response to auxin? Since Auxin and BR signaling pathways are hugely overlapped, we assume the annotation might need to expand. Based on our experimental results from Chapter 4, we now assume that *SAUR* upregulation is not only from IAA signaling, but can be an outcome of GA, BR and IAA crosstalk in response to FR.

Table 6.1. Annotation ratio (GO category : total number of genes) in Arabiodopsis and *S. lycopersicum* for GO categories of interest.

	Arabidopsis (TAIR10 genome)	***S. lycopersicum* (ITAG4.0,)**
Total number of genes	25500	34075
Brassinosteroid	63	0
GA	23	5
Auxin	124	115
Far-red light	7	0
Ratio of BR annotation	0.25%	0.00%
Ratio of GA annotation	0.09%	0.01%
Ratio of Auxin annotation	0.49%	0.34%
Ratio of far-red light annotation	0.03%	0.00%

To overcome the limitations of the GO enrichment and to gain insight into the hormonal signatures in the transcriptome data, we curated lists of hormone responsive and related genes, identified their tomato homologs, and visualized these as heatmaps (Figures 4.2). Specifically in the case of GA and BR that are missing from tomato GO, we identified several genes, which show more pronounced FR effects on gene regulation in GA genes compared to BR-related genes, with up to a 4-fold change. BR-related genes show no significant change. Notably, GA oxidase genes, crucial in GA biosynthesis, are significantly upregulated. In other words, IAA and GA-related genes exhibit a remarkably similar expression pattern, with numerous genes showing high upregulation and downregulation, indicating that that IAA and GA play roles in the FR response in the stem, while BR response is not evident.

When we consider these results in the light of the hormone treatments, a new nuance emerges. GA and BR are necessary and sufficient for the internode elongation (Figures 4.13,14,16), while the role of IAA remains unsolved. Looking at the hormone treatment qPCR data (Figure 4.22-4.23), the story is complicated even further. IAA and GA give more similar responses, resembling that of FR-response, while BR application also leads to a substantial gene expression alteration, however with opposing effects to IAA and GA. Note that BR effects are clear in genes that are not annotated as BR-related, indicating that looking at proposed BR-related genes to infer BR function (e.g. GO enrichment, Figure 4.2b BR-heatmap) is not very effective.

In conclusion, the gene expression responses of IAA and GA demonstrate an increase in response to FR, whereas BR exhibit no alteration. Regarding the recapitulation of FR effects with exogenous hormone treatments, IAA has a minor impact, while GA and BR fully recapitulate the effect. From our inhibitor work, we saw that blocking GA and BR also blocks the FR response, indicating them being necessary for the FR-induced elongation. These effects are different from Arabidopsis SAS where auxin plays a core role, being the mobile signal, necessary and sufficient, to induce the petiole and hypocotyl elongation responses. It is likely that the relative hormonal regulation balances in SAS has diverged between tomato and Arabidopsis, and this will complicate translation of Arabidopsis SAS findings to crop applications.

Table 6.2. Summary of IAA, GA, and BR results in our FR experiments (Chapter 4).

	IAA	GA	BR
Signaling	↑	↑	=
concentration	=		
Sufficiency to recapitulate FR	little	full	full
Necessity		yes	yes

6.3 DIVERSITY OF SAS AND FR-RESPONSIVE TFS

Discovering transcription factors (TFs) important for shade avoidance is crucial for unraveling the intricate regulatory networks in plant responses to varying light conditions. These TFs, previously unknown for SAS could play a vital role as key regulators, influencing adaptive strategies in shade-exposed plants. Moreover, comprehending tissue-specific expression patterns is essential since different plant tissues may exhibit distinct responses to light conditions. The identification and characterization of these TFs with tissue-specific expression brings precision to our understanding of the molecular dynamics underlying the complex phenomenon of shade avoidance.

In our study on the conservation and evolution of FR-induced transcription factor genes in tomato, identified in Chapter 3 and followed up in Chapter 5, we focused on *Solyc01g090760* (GATA TF), *Solyc08g080150* (TCP TF), and *Solyc07g053450* (bZIP TF). The conservation of the FR-induced patterns of these TFs within Solanaceae provides insights into their potential roles during SAS. We observed divergence of Solanaceae FR-responsive expression patterns of these TFs from Fabaceae and Brassicaceae. This adds another layer of support to FR-responsive Solanaceae regulatory networks having diverged from e.g. Arabidopsis, and again indicates that translation of results from model organisms to non-closely-related crop species could be challenging and would require more focus on diversifying research strategies towards different plant families.

Notably, our findings in Chapter 5 also reveal expression in pith, sometimes exclusively, in response to supplemental FR. This finding might be consistent with a role of pith in stem elongation, but overall, our data are limited by the lack of a direct link between pith function and shade avoidance elongation. We have observed that internode elongation goes together with pith elongation in all of the species we looked at, and that typically transcriptionally inactive pith shows upregulation of these TFs in Solanaceae (summarized in Table 6.2). However, we were unable to establish stronger support for the connection between pith function and shade avoidance.

A promising avenue for subsequent research involves extending the investigation to additional species. Firstly, expanding to the sister families of Solanaceae, and continuing outwards until the FR-responsive behaviour of the three TFs is lost. However, it would be very helpful to also establish the functionality of these three genes in shade avoidance, by for example making knockout lines and testing their FR-responsiveness. Alternatively, we could explore plants with different pith morphologies, or preferably a species lacking pith in its internodes. An example of different pith structure is the legume *Vicia faba* (Figure 6.1). This species exhibits a distinctive developmental pattern where pith development in different internodes progresses through different developmental stages, namely undergoing programmed cell death in the younger internodes. It would be also interesting to see if we can identify if FR-responsive pith elongation and internode elongation are uncoupled in any dicot species.

Table 6.3 Summary of the evolutionary analysis of multiple species in SAS. Y means Yes, N means No, Up means upregulation.

Species	***S. lycopersicum***	***C. annuum***	***S. melongena***	***B. nigra***	***A. thaliana***	***P. sativum***	***G. max***
Elongation in FR	Y	Y	Y	Y	Y	N (slow)	Y
Pith elongation	Y	Y	Y	Y	N	N	Y
TF expression in FR	Up	Up	Up				
TF conservation	(reference point)	High	High				

6.4 CONCLUSION

In summary, this thesis has delved into diverse facets of shade avoidance in non-model dicots. We covered the phenotypic changes including cellular morphology, tissue-specific transcriptome changes, hormonal regulation of internode elongation and *SAUR*s in tomato. Then, we studied the conservation of FR-responsive behaviour of transcription factors and the pith elongation in dicots. Our examination highlighted unique growth patterns, underscoring the significance of such nuances in various plant species. It appears that tomato hormonal and TF regulatory networks in SAS have diverged from those of Arabidopsis. Looking forward, the pursuit of a deeper comprehension of transcriptional regulation, evolutionary conservation, and molecular mechanisms governing growth responses remain key foci in SAS research.

APPENDIX

REFERENCES

GENERAL SUMMARY

GENERAL SUMMARY (DUTCH)

GENERAL SUMMARY (CHINESE)

ABOUT THE AUTHOR

ACKNOWLEDGEMENTS

EPS EDUCATION STATEMENT

LIST OF PUBLICATIONS

REFERENCES

Abas L, Kolb M, Stadlmann J, Janacek DP, Lukic K, Schwechheimer C, Sazanov LA, Mach L, Friml J, Hammes UZ (2020) Naphthylphthalamic acid associates with and inhibits PIN auxin transporters. Proceedings of the National Academy of Sciences of the United States of America **118**: e2020857118

Abercrombie M (Michael), Brachet J (Jean), King TJ (1968) Advances in morphogenesis. Volume 7. Elsevier Science

Agusti J, Herold S, Schwarz M, Sanchez P, Ljung K, Dun EA, Brewer PB, Beveridge CA, Sieberer T, Sehr EM, et al (2011) Strigolactone signaling is required for auxin-dependent stimulation of secondary growth in plants. Proceedings of the National Academy of Sciences of the United States of America **108**: 20242–20247

Aichinger E, Kornet N, Friedrich T, Laux T (2012) Plant stem cell niches. Annual Review of Plant Biology **63**: 615–636

Anastasiou E, Kenz S, Gerstung M, MacLean D, Timmer J, Fleck C, Lenhard M (2007) Control of Plant Organ Size by KLUH/CYP78A5-Dependent Intercellular Signaling. Developmental Cell **13**: 843–856

Ariom TO, Dimon E, Nambeye E, Diouf NS, Adelusi OO, Boudalia S (2022) Climate-Smart Agriculture in African Countries: A Review of Strategies and Impacts on Smallholder Farmers. Sustainability (Switzerland) **14**: 11370

Arsuffi G, Braybrook SA (2018) Acid growth: An ongoing trip. Journal of Experimental Botany **69**: 137–146

Asami T, Min YK, Nagata N, Yamagishi K, Takatsuto S, Fujioka S, Murofushi N, Yamaguchi I, Yoshida S (2000) Characterization of brassinazole, a triazole-type brassinosteroid biosynthesis inhibitor. Plant Physiology **123**: 93–99

Avalos G, Avalos G (2019) Shade tolerance within the context of the successional process in tropical rain forests. Revista de Biología Tropical **67**: 53–77

Bai MY, Shang JX, Oh E, Fan M, Bai Y, Zentella R, Sun TP, Wang ZY (2012) Brassinosteroid, gibberellin and phytochrome impinge on a common transcription module in Arabidopsis. Nature cell biology **14**: 810–817

Ballaré CL, Pierik R (2017) The shade-avoidance syndrome: Multiple signals and ecological consequences. Plant Cell and Environment **40**: 2530–2543

Barone A, Chiusano ML, Ercolano MR, Giuliano G, Grandillo S, Frusciante L (2008) Structural and functional genomics of tomato. International Journal of Plant Genomics. doi: 10.1155/2008/820274

Bashir K, Todaka D, Rasheed S, Matsui A, Ahmad Z, Sako K, Utsumi Y, Vu AT, Tanaka M, Takahashi S, et al (2022) Ethanol-Mediated Novel Survival Strategy against Drought Stress in Plants. Plant & cell physiology **63**: 1181–1192

Baster P, Robert S, Kleine-Vehn J, Vanneste S, Kania U, Grunewald W, De Rybel B, Beeckman T, Friml J (2013) SCF(TIR1/AFB)-auxin signalling regulates PIN vacuolar trafficking and auxin fluxes during root gravitropism. The EMBO journal **32**: 260–274

Beall FD, Yeung EC, Pharis RP (1996) Far-red light stimulates internode elongation, cell division, cell elongation, and gibberellin levels in bean. Canadian Journal of Botany **74**: 743–752

Bernhardt C, Lee MM, Gonzalez A, Zhang F, Lloyd A, Schiefelbein J (2003) The bHLH genes GLABRA3 (GL3) and ENHANCER OF GLABRA3 (EGL3) specify epidermal cell fate in the Arabidopsis root. Development **130**: 6431–6439

Bhalerao RP, Eklöf J, Ljung K, Marchant A, Bennett M, Sandberg G (2002) Shoot-derived auxin is essential for early lateral root emergence in Arabidopsis seedlings. The Plant journal : for cell and molecular biology **29**: 325–332

Bischoff M, Hermann G, Rentsch S, Strehlow D (2001) First Steps in the Phytochrome Phototransformation: A Comparative Femtosecond Study on the Forward (Pr f Pfr) and Back Reaction (Pfr f Pr) †. doi: 10.1021/bi0011734

Bispo TM, Vieira EA (2022) Assimilatory deficit and energy regulation in young Handroanthus chrysotrichus plants under flooding stress. Journal of Plant Research **135**: 323–336

Bolger A, Scossa F, Bolger ME, Lanz C, Maumus F, Tohge T, Quesneville H, Alseekh S, Sørensen I, Lichtenstein G, et al (2014) The genome of the stress-tolerant wild tomato species Solanum pennellii. Nature Genetics **46**: 1034–1038

Bongers FJ, Evers JB, Anten NPR, Pierik R (2014) From shade avoidance responses to plant performance at vegetation level: using virtual plant modelling as a tool. New Phytologist **204**: 268–272

Botterweg-Paredes E, Blaakmeer A, Hong SY, Sun B, Mineri L, Kruusvee V, Xie Y, Straub D, Ménard D, Pesquet E, et al (2020) Light affects tissue patterning of the hypocotyl in the shade-avoidance response. PLoS Genetics **16**: e1008678

Bou-Torrent J, Galstyan A, Gallemí M, Cifuentes-Esquivel N, Molina-Contreras MJ, Salla-Martret M, Jikumaru Y, Yamaguchi S, Kamiya Y, Martínez-García JF (2014) Plant proximity perception dynamically modulates hormone levels and sensitivity in Arabidopsis. Journal of Experimental Botany **65**: 2937–2947

Bouda M, Huggett BA, Prats KA, Wason JW, Wilson JP, Brodersen CR (2022) Hydraulic failure as a primary driver of xylem network evolution in early vascular plants. Science (New York, NY) **378**: 642–646

Bravo A, York T, Pumplin N, Mueller LA, Harrison MJ (2016) Genes conserved for arbuscular mycorrhizal symbiosis identified through phylogenomics. doi: 10.1038/NPLANTS.2015.208

Briggs WR, Christie JM (2002) Phototropins 1 and 2: versatile plant blue-light receptors. Trends in Plant Science **7**: 204–210

Brooks C, Nekrasov V, Lippman ZB, Eck J Van (2014) Scientific Correspondence Efficient Gene Editing in Tomato in the First Generation Using the Clustered Regularly Interspaced Short Palindromic Repeats/CRISPR-Associated9 System 1. doi: 10.1104/pp.114.247577

Brown CL, Sommer HE, Pienaar L V. (1995a) The predominant role of the pith in the growth and development of internodes in Liquidambar styraciflua (Hamamelidaceae). I. Histological basis of compressive and tensile stresses in developing primary tissues. American Journal of Botany **82**: 769–776

Brown CL, Sommer HE, Pienaar L V. (1995b) The predominant role of the pith in the growth and development of internodes in Liquidambar styraciflua (Hamamelidaceae). II. Pattern of tissue stress and response of different tissues to specific surgical procedures. American Journal of Botany **82**: 777–781

Brudno M, Do CB, Cooper GM, Kim MF, Davydov E, Green ED, Sidow A, Batzoglou S (2003) LAGAN and Multi-LAGAN: efficient tools for large-scale multiple alignment of genomic DNA. Genome research **13**: 721–731

Bush SM, G, Carriedo L, Fulop D, Ichihashi Y, N.Maloof J, Carriedo L, Daniel F, Ichihashi Y, Covington M, Kumar R, et al (2015) Auxin signaling is a common factor underlying natural variation in tomato shade avoidance. bioRxiv **119**: 9

Buti S (2008) A gas-and-brake mechanism of bHLH proteins modulates shade avoidance in Arabidopsis.

Cagnola JI, Ploschuk E, Benech-Arnold T, Finlayson SA, Casal JJ (2012) Stem Transcriptome Reveals Mechanisms to Reduce the Energetic Cost of Shade-Avoidance Responses in Tomato. Plant Physiology **160**: 1110–1119

Casal JJ (2013) Photoreceptor Signaling Networks in Plant Responses to Shade. Annual Review of Plant Biology **64**: 403–427

Casal JJ (2012) Shade Avoidance. The Arabidopsis Book **10**: e0157

Casal JJ, Smith H (1988) The loci of perception for phytochrome control of internode growth in light-grown mustard: Promotion by low phytochrome photoequilibria in the internode is enhanced by blue light perceived by the leaves. Planta **176**: 277–282

Cerling TE, Harris JM, Macfadden BJ, Leakey MG, Quadek J, Eisenmann V, Ehleringer# JR (1997) Global vegetation change through the Miocene/Pliocene boundary. NATURE 389:

Chae K, Isaacs CG, Reeves PH, Maloney GS, Muday GK, Nagpal P, Reed JW (2012) Arabidopsis SMALL AUXIN UP RNA63 promotes hypocotyl and stamen filament elongation. The Plant journal : for cell and molecular biology **71**: 684–697

Chalivendra SC, Lopez-Casado G, Kumar A, Kassenbrock AR, Royer S, Tovar-Mèndez A, Covey PA, Dempsey LA, Randle AM, Stack SM, et al (2013) Developmental onset of reproductive barriers and associated proteome changes in stigma/styles of Solanum pennellii. Journal of Experimental Botany **64**: 265–279

Chandler JW (2009) Local auxin production: a small contribution to a big field. BioEssays **31**: 60–70

Chandler JW, Werr W (2015) Cytokinin-auxin crosstalk in cell type specification. Trends in Plant Science **20**: 291–300

Chen H, Wang T, He X, Cai X, Lin R, Liang J, Wu J, King G, Wang X (2022a) BRAD V3.0: an upgraded Brassicaceae database. Nucleic Acids Research **50**: D1432–D1441

Chen T, Liu Y, Huang L (2022b) ImageGP: An easy-to-use data visualization web server for scientific researchers. iMeta. doi: 10.1002/IMT2.5

Child R, Smith H (1987) Phytochrome action in light-grown mustard: kinetics, fluence-rate compensation and ecological significance. Planta **172**: 219–229

Chin CH, Chen SH, Wu HH, Ho CW, Ko MT, Lin CY (2014) cytoHubba: identifying hub objects and sub-networks from complex interactome. BMC Systems Biology **8**: S11

Chitwood DH, Headland LR, Filiault DL, Kumar R, Jiménez-Gómez JM, Schrager A V., Park DS, Peng J, Sinha NR, Maloof JN (2012) Native Environment Modulates Leaf Size and Response to Simulated Foliar Shade across Wild Tomato Species. PLOS ONE **7**: e29570

Chitwood DH, Kumar R, Ranjan A, Pelletier JM, Townsley B, Ichihashi Y, Martinez CC, Zumstein K, Harada JJ, Maloof JN, et al (2015) Light-induced indeterminacy alters shade avoiding tomato leaf morphology. Plant Physiology **169**: pp.01229.2015

Ciolfi A, Sessa G, Sassi M, Possenti M, Salvucci S, Carabelli M, Morelli G, Ruberti I (2013) Dynamics of the Shade-Avoidance Response in Arabidopsis. Plant Physiology. doi: 10.1104/PP.113.221549

Claeys H, De Bodt S, Inzé D (2014) Gibberellins and DELLAs: Central nodes in growth regulatory networks. Trends in Plant Science **19**: 231–239

Colebrook EH, Thomas SG, Phillips AL, Hedden P, Davies SA, Dow JAT, Lukowiak K (2014) The role of gibberellin signalling in plant responses to abiotic stress. Journal of Experimental Biology **217**: 67–75

Courbier S, Grevink S, Sluijs E, Bonhomme P-OO, Kajala K, Wees SCM Van, Pierik R, Van Wees SCM, Pierik R (2020) Far-red light promotes Botrytis cinerea disease development in tomato leaves via jasmonate-dependent modulation of soluble sugars. Plant, Cell & Environment **43**: 2769–2781

Courbier S, Pierik R (2019) Canopy Light Quality Modulates Stress Responses in Plants. iScience **22**: 441–452

Courbier S, Snoek BL, Kajala K, Li L, Van Wees SCMM, Pierik R (2021) Mechanisms of far-red light-mediated dampening of defense against Botrytis cinerea in tomato leaves. Plant Physiology **187**: 1250–1266

Coverdale TC, Agrawal AA (2021) Evolution of shade tolerance is associated with attenuation of shade avoidance and reduced phenotypic plasticity in North American milkweeds. American Journal of Botany **108**: 1705–1715

Covington MF, Harmer SL (2007) The Circadian Clock Regulates Auxin Signaling and Responses in Arabidopsis. PLoS Biology **5**: 1773–1784

Cubas P, Lauter N, Doebley J, Coen E (1999) The TCP domain: A motif found in proteins regulating plant growth and development. Plant Journal **18**: 215–222

da Cunha Neto IL, Pace MR, Douglas NA, Nee MH, de Sá CFC, Moore MJ, Angyalossy V (2020) Diversity, distribution, development, and evolution of medullary bundles in Nyctaginaceae. **107**: 707–725

Dang DT (2022) Molecular Approaches to Protein Dimerization: Opportunities for Supramolecular Chemistry. Frontiers in Chemistry **10**: 1–12

Davies PJ (2010) Plant hormones: Biosynthesis, signal transduction, action! Plant Hormones: Biosynthesis, Signal Transduction, Action! doi: 10.1007/978-1-4020-2686-7

Depuydt S, Hardtke CS (2011) Hormone signalling crosstalk in plant growth regulation. Current biology : CB. doi: 10.1016/J.CUB.2011.03.013

Desta B, Amare G (2021) Paclobutrazol as a plant growth regulator. Chemical and Biological Technologies in Agriculture **8**: 1

Devlin PF, Halliday KJ, Harberd NP, Whitelam GC (1996) The rosette habit of Arabidopsis thaliana is dependent upon phytochrome action: novel phytochromes control internode elongation and flowering time. The Plant Journal **10**: 1127–1134

Devlin PF, Robson PRHH, Patel SR, Goosey L, Sharrock RA, Whitelam GC (1999) Phytochrome D acts in the shade-avoidance syndrome in Arabidopsis by controlling elongation growth and flowering time. Plant physiology **119**: 909–15

Devlin PF, Yanovsky MJ, Kay SA (2003) A Genomic Analysis of the Shade Avoidance Response in Arabidopsis. Plant Physiology **133**: 1617–1629

Diehl AG, Boyle AP (2018) Conserved and species-specific transcription factor co-binding patterns drive divergent gene regulation in human and mouse. Nucleic Acids Research **46**: 1878–1894

Dillon A (2022) WPTC Forecasts 6.1% Reduction from Initial Production Intentions. https://www.morningstarco.com/2022-season-global-tomato-crop-update/

Djakovic-Petrovic T, Wit M De, Voesenek LACJ, Pierik R (2007) DELLA protein function in growth responses to canopy signals. Plant Journal **51**: 117–126

Dobin A, Davis CA, Schlesinger F, Drenkow J, Zaleski C, Jha S, Batut P, Chaisson M, Gingeras TR (2013) STAR: Ultrafast universal RNA-seq aligner. Bioinformatics **29**: 15–21

Domenici V, Ancora D, Cifelli M, Serani A, Veracini CA, Zandomeneghi M (2014) Extraction of pigment information from near-UV vis absorption spectra of extra virgin olive oils. Journal of Agricultural and Food Chemistry **62**: 9317–9325

Dun EA, De Saint Germain A, Rameau C, Beveridge CA (2013) Dynamics of strigolactone function and shoot branching responses in Pisum sativum. Molecular plant **6**: 128–140

Edgar RC (2004) MUSCLE: A multiple sequence alignment method with reduced time and space complexity. BMC Bioinformatics **5**: 113

EMBL-EBI QuickGO::Term GO:0009143. https://www.ebi.ac.uk/QuickGO/term/GO:0009143

Ergen Akçin Ö, Sabri Özyurt M, Şenel G (2011) PETIOLE ANATOMY OF SOME LAMIACEAE TAXA.

Esau K (1953) Plant anatomy.

Etchells JP, Provost CM, Mishr L, Turner SR (2013) WOX4 and WOX14 act downstream of the PXY receptor kinase to regulate plant vascular proliferation independently of any role in vascular organisation. Development (Cambridge) **140**: 2224–2234

Etchells JP, Provost CM, Turner SR (2012) Plant Vascular Cell Division Is Maintained by an Interaction between PXY and Ethylene Signalling. PLoS Genetics **8**: e1002997

Etchells JP, Turner SR (2010) The PXY-CLE41 receptor ligand pair defines a multifunctional pathway that controls the rate and orientation of vascular cell division. Development **137**: 767–774

Evert RF, Esau K (2006) Esau's Plant Anatomy: Meristems, Cells, and Tissues of the Plant Body: Their ... - Ray F. Evert. ESAU'S PLANT ANATOMY Canada: John Wiley & Sons 103–1125

Expósito-Rodríguez M, Borges AA, Borges-Pérez A, Pérez JA (2011) Gene structure and spatiotemporal expression profile of tomato genes encoding YUCCA-like flavin monooxygenases: The ToFZY gene family. Plant Physiology and Biochemistry **49**: 782–791

Fàbregas N, Caño-Delgado AI (2014) Turning on the microscope turret: a new view for the study of brassinosteroid signaling in plant development. Physiologia plantarum **151**: 172–183

Feller A, MacHemer K, Braun EL, Grotewold E (2011) Evolutionary and comparative analysis of MYB and bHLH plant transcription factors. Plant Journal **66**: 94–116

Feng S, Martinez C, Gusmaroli G, Wang Y, Zhou J, Wang F, Chen L, Yu L, Iglesias-Pedraz JM, Kircher S, et al (2008) Coordinated regulation of Arabidopsis thaliana development by light and gibberellins. Nature **451**: 475

Fernandez-Pozo N, Menda N, Edwards JD, Saha S, Tecle IY, Strickler SR, Bombarely A, Fisher-York T, Pujar A, Foerster H, et al (2015) The Sol Genomics Network (SGN)--from genotype to phenotype to breeding. Nucleic acids research **43**: D1036–D1041

Finlayson SA, Krishnareddy SR, Kebrom TH, Casal JJ (2010) Phytochrome Regulation of Branching in Arabidopsis. Plant Physiology **152**: 1914–1927

Finnegan EJ, Kovac KA (2000) Plant DNA methyltransferases. Plant Gene Silencing. Springer, Dordrecht, pp 69–81

Franklin KA (2008) Shade avoidance. Tansley review **179**: 930–944

Franklin KA (2020) PRR proteins of the circadian clock call time on shade avoidance. Proceedings of the National Academy of Sciences of the United States of America **117**: 5095–5096

Franklin KA, Lee SH, Patel D, Kumar SV, Spartz AK, Gu C, Ye S, Yu P, Breen G, Cohen JD, et al (2011) Phytochrome-Interacting Factor 4 (PIF4) regulates auxin biosynthesis at high temperature. Proceedings of the National Academy of Sciences of the United States of America **108**: 20231–20235

Franklin KA, Quail PH (2010) Phytochrome functions in Arabidopsis development. Journal of Experimental Botany **61**: 11–24

Fraser DP, Panter PE, Sharma A, Sharma B, Dodd AN, Franklin KA (2021) Phytochrome A elevates plant circadian-clock components to suppress shade avoidance in deep-canopy shade. Proceedings of the National Academy of Sciences of the United States of America. doi: 10.1073/pnas.2108176118

Frazer KA, Pachter L, Poliakov A, Rubin EM, Dubchak I (2004) VISTA: computational tools for comparative genomics. Nucleic acids research. doi: 10.1093/NAR/GKH458

Friml J, Benková E, Blilou I, Wisniewska J, Hamann T, Ljung K, Woody S, Sandberg G, Scheres B, Jürgens G, et al (2002) AtPIN4 Mediates Sink-Driven Auxin Gradients and Root Patterning in Arabidopsis. Cell **108**: 661–673

Fry SC (2004) Primary cell wall metabolism: Tracking the careers of wall polymers in living plant cells. New Phytologist **161**: 641–675

Fu X, Harberd NP (2003) Auxin promotes Arabidopsis root growth by modulating gibberellin response. Article in Nature **421**: 740–743

Fujimoto M, Sazuka T, Oda Y, Kawahigashi H, Wu J, Takanashi H, Ohnishi T, Yoneda J ichi, Ishimori M, Kajiya-Kanegae H, et al (2018) Transcriptional switch for programmed cell death in pith parenchyma of sorghum stems. Proceedings of the National Academy of Sciences of the United States of America **115**: E8783–E8792

Gallardo K, Job C, Groot SPC, Puype M, Demol H, Vandekerckhove J, Job D (2002) Proteomics of Arabidopsis Seed Germination. A Comparative Study of Wild-Type and Gibberellin-Deficient Seeds. Plant Physiology **129**: 823–837

Gallego-Giraldo L, Shadle G, Shen H, Barros-Rios J, Fresquet Corrales S, Wang H, Dixon RA (2016) Combining enhanced biomass density with reduced lignin level for improved forage quality. Plant Biotechnology Journal **14**: 895–904

Galvan-Ampudia CS, Julkowska MM, Darwish E, Gandullo J, Korver RA, Brunoud G, Haring MA, Munnik T, Vernoux T, Testerink C (2013) Halotropism is a response of plant roots to avoid a saline environment. Current Biology **23**: 2044–2050

Galvão VC, Fiorucci AS, Trevisan M, Franco-Zorilla JM, Goyal A, Schmid-Siegert E, Solano R, Fankhauser C (2019) PIF transcription factors link a neighbor threat cue to accelerated reproduction in Arabidopsis. **10**: 1–10

Gao J, Chen YH, Peterson LAC (2015) GATA family transcriptional factors: Emerging suspects in hematologic disorders. Experimental Hematology and Oncology **4**: 1–7

van Gelderen K, Kang C, Paalman R, Keuskamp D, Hayes S, Pierik R (2018) Far-Red Light Detection in the Shoot Regulates Lateral Root Development through the HY5 Transcription Factor. The Plant Cell **30**: 101–116

Van Gelderen K, Kang C, Pierik R (2018) Light Signaling, Root Development, and Plasticity. Plant Physiology **176**: 1049

Génard M, Fishman S, Vercambre G, Huguet JG, Bussi C, Besset J, Habib R (2001) A Biophysical Analysis of Stem and Root Diameter Variations in Woody Plants. Plant Physiology **126**: 188

Ghosh S, Nelson JF, Cobb GMC, Etchells JP, De Lucas M (2022) Light regulates xylem cell differentiation via PIF in Arabidopsis ll Light regulates xylem cell differentiation via PIF in Arabidopsis. doi: 10.1016/j.celrep.2022.111075

Gilbert IR, Jarvis PG, Smith H (2001) Proximity signal and shade avoidance differences between early and late successional trees. Nature **411**: 3–6

Gill RA, Ahmar S, Ali B, Saleem MH, Khan MU, Zhou W, Liu S (2021) The role of membrane transporters in plant growth and development, and abiotic stress tolerance. International Journal of Molecular Sciences **22**: 22

Glenn E The Physics Hypertextbook. Physics, https://physics.info/

Gommers CMM, Keuskamp DH, Buti S, van Veen H, Koevoets IT, Reinen E, Voesenek LACJ, Pierik R (2017) Molecular profiles of contrasting shade response strategies in wild plants: Differential control of immunity and shoot elongation. Plant Cell **29**: 331–344

Gong P, Zhang J, Li H, Yang C, Zhang C, Zhang X, Khurram Z, Zhang Y, Wang T, Fei Z, et al (2010) Transcriptional profiles of drought-responsive genes in modulating transcription signal transduction, and biochemical pathways in tomato. Journal of Experimental Botany **61**: 3563–3575

González-Grandío E, Poza-Carrión C, Sorzano COS, Cubas P (2013) BRANCHED1 Promotes Axillary Bud Dormancy in Response to Shade in Arabidopsis. The Plant Cell **25**: 834–850

Goodstein DM, Shu S, Howson R, Neupane R, Hayes RD, Fazo J, Mitros T, Dirks W, Hellsten U, Putnam N, et al (2012) Phytozome: a comparative platform for green plant genomics. Nucleic Acids Research **40**: D1178-86

Gory Vert G, Chory J, Vert G, Chory J, Gory Vert G, Chory J, Vert G, Chory J, Gory Vert G, Chory J (2011) Crosstalk in Cellular Signaling: Background Noise or the Real Thing? Developmental Cell **21**: 985

Gray WM, Östin A, Sandberg G, Romano CP, Estelle M, Ostin A, Sandberg G, Romano CP, Estelle M, Parry G, et al (1998) High temperature promotes auxin-mediated hypocotyl elongation in Arabidopsis. Proceedings of the National Academy of Sciences of the United States of America **95**: 7197–7202

Greb T (2019) Genetic space of radial plant growth. Nature Plants 2019 5:10 **5**: 1032–1032

Green-Tracewicz E, Page ER, Swanton CJ (2011) Shade Avoidance in Soybean Reduces Branching and Increases Plant-to-Plant Variability in Biomass and Yield Per Plant. Weed Science **59**: 43–49

Grennan AK (2007) The role of trehalose biosynthesis in plants. Plant Physiology **144**: 3–5

Greulach VA, Haesloop JG (1958) The Influence of Gibberellic Acid on Cell Acid on Cell Division and Cell Elongation in Phaseolus vulgaris. American Journal of Botany **45**: 566

Groover A (2023) The vascular cambium revisited. IAWA Journal 1–8

Gundel PE, Pierik R, Mommer L, Ballaré CL (2014) Competing neighbors: Light perception and root function. Oecologia **176**: 1–10

Gunning BES, Steer MW (1996) Plant cell biology : structure and function.

Guo L, Sun X, Li Z, Wang Y, Fei Z, Jiao C, Feng J, Cui D, Feng X, Ding Y, et al (2019) Morphological dissection and cellular and transcriptome characterizations of bamboo pith cavity formation reveal a pivotal role of genes related to programmed cell death. Plant Biotechnology Journal **17**: 982–997

Gupta S, Van Eck J (2016) Modification of plant regeneration medium decreases the time for recovery of Solanum lycopersicum cultivar M82 stable transgenic lines. Plant Cell, Tissue and Organ Culture **127**: 417–423

Hagen G, Guilfoyle T (2002) Auxin-responsive gene expression: Genes, promoters and regulatory factors. Plant Molecular Biology **49**: 373–385

Hagen G, Guilfoyle T, Weinig C, Fujinami R, Paul Ghogue J, Imaichi R, Miyashima S, Roszak P, Sevilem I, Toyokura K, et al (2015) Plasticity versus canalization: Population differences in the timing of shade-avoidance responses. Frontiers in Plant Science **54**: 1–11

Hager A (2003) Role of the plasma membrane H+-ATPase in auxin-induced elongation growth: historical and new aspects. Journal of plant research **116**: 483–505

Hardwick K, Elliott S (2016) Second Growth: The Promise of Tropical Rain Forest Regeneration in the Age of Deforestation. Restoration Ecology **24**: 137–137

Hattrup E, Neilson KA, Breci L, Haynes PA (2007) Proteomic analysis of shade-avoidance response in tomato leaves. Journal of Agricultural and Food Chemistry **55**: 8310–8318

Hayashi KI, Tan X, Zheng N, Hatate T, Kimura Y, Kepinski S, Nozaki H (2008) Small-molecule agonists and antagonists of F-box protein-substrate interactions in auxin perception and signaling. Proceedings of the National Academy of Sciences of the United States of America **105**: 5632–5637

He JX, Gendron JM, Sun Y, Gampala SSL, Gendron N, Sun CQ, Wang ZY (2005) BZR1 is a transcriptional repressor with dual roles in brassinosteroid homeostasis and growth responses. Science (New York, NY) **307**: 1634–1638

Hedden P, Sponsel V (2015) A Century of Gibberellin Research. Journal of plant growth regulation **34**: 740–760

Helariutta Y (2007) Cell signalling during vascular morphogenesis. Biochemical Society transactions **35**: 152–5

Hemberg M, Kreiman G (2011) Conservation of transcription factor binding events predicts gene expression across species. Nucleic Acids Research **39**: 7092

Henry HAL, Aarssen LW (1997) On the Relationship between Shade Tolerance and Shade Avoidance Strategies in Woodland Plants. Oikos **80**: 575

Hetherington SE, Smillie RM, Davies WJ (1998) Photosynthetic activities of vegetative and fruiting tissues of tomato. Journal of Experimental Botany **49**: 1173–1181

Hewitt N (1998) Seed size and shade-tolerance: A comparative analysis of North American temperate trees. Oecologia **114**: 432–440

Hirakawa Y, Kondo Y, Fukuda H (2010) TDIF peptide signaling regulates vascular stem cell proliferation via the WOX4 homeobox gene in Arabidopsis. Plant Cell **22**: 2618–2629

Hisamatsu T, King RW, Helliwell CA, Koshioka M (2005) The involvement of gibberellin 20-oxidase genes in phytochrome-regulated petiole elongation of Arabidopsis. Plant Physiology **138**: 1106–1116

Holalu S V., Finlayson SA (2017) The ratio of red light to far red light alters Arabidopsis axillary bud growth and abscisic acid signalling before stem auxin changes. Journal of Experimental Botany 68:

Hornitschek P, Kohnen M V., Lorrain S, Rougemont J, Ljung K, López-Vidriero I, Franco-Zorrilla JM, Solano R, Trevisan M, Pradervand S, et al (2012) Phytochrome interacting factors 4 and 5 control seedling growth in changing light conditions by directly controlling auxin signaling. Plant Journal **71**: 699–711

Horváth BM, Magyar Z, Zhang Y, Hamburger AW, Bakó L, Visser RGF, Bachem CWB, Bögre L (2006) EBP1 regulates organ size through cell growth and proliferation in plants. EMBO Journal **25**: 4909–4920

Horvath S, Langfelder P (2009) Tutorial for the WGCNA package for R : III . Using simulated data to evaluate different module detection methods and gene screening approaches 1 . Simulation of expression and trait data. Simulation 1–3

Hou K, Wu W, Gan SS (2013) SAUR36, a SMALL AUXIN UP RNA gene, is involved in the promotion of leaf senescence in arabidopsis. Plant Physiology **161**: 1002–1009

Hou Q, Zhao W, Lu L, Wang L, Zhang T, Hu B, Yan T, Qi Y, Zhang F, Chao N, et al (2022) Overexpression of HLH4 Inhibits Cell Elongation and Anthocyanin Biosynthesis in Arabidopsis thaliana. Cell 1–18

Hu Y, Xie Q, Chua NH (2003) The Arabidopsis auxin-inducible gene ARGOS controls lateral organ size. Plant Cell **15**: 1951–1961

Huber H, De Brouwer J, De Caluwe H, Wijschedé J, Anten NPR (2008) Shade induced changes in biomechanical petiole properties in the stoloniferous herb Trifolium repens. Evolutionary Ecology **22**: 399–416

Ibañes M, Fàbregas N, Chory J, Caño-Delgadob AI (2009) Brassinosteroid signaling and auxin transport are required to establish the periodic pattern of Arabidopsis shoot vascular bundles. Proceedings of the National Academy of Sciences of the United States of America **106**: 13630–13635

Iglesias MJ, Sellaro R, Zurbriggen MD, Casal JJ (2018) Multiple links between shade avoidance and auxin networks. Journal of Experimental Botany **69**: 213–228

Ikeda H, Shibuya T, Nishiyama M, Nakata Y, Kanayama Y (2017) Physiological mechanisms accounting for the lower incidence of blossom-end rot in tomato introgression line IL8-3 fruit. Horticulture Journal **86**: 327–333

Dello Ioio R, Linhares FS, Sabatini S (2008) Emerging role of cytokinin as a regulator of cellular differentiation. Current Opinion in Plant Biology **11**: 23–27

Ishida T, Adachi S, Yoshimura M, Shimizu K, Umeda M, Sugimoto K (2010) Auxin modulates the transition from the mitotic cycle to the endocycle in Arabidopsis. **137**: 63–71

Jenkins GI (2017) Photomorphogenic responses to ultraviolet-B light. doi: 10.1111/PCE.12934

Jin J, He K, Tang X, Li Z, Lv L, Zhao Y, Luo J, Gao G (2015) An Arabidopsis Transcriptional Regulatory Map Reveals Distinct Functional and Evolutionary Features of Novel Transcription Factors. Molecular Biology and Evolution **32**: 1767–1773

Jin J, Tian F, Yang DC, Meng YQ, Kong L, Luo J, Gao G (2017) PlantTFDB 4.0: toward a central hub for transcription factors and regulatory interactions in plants. Nucleic Acids Research **45**: D1040–D1045

Kajala K, Gouran M, Shaar-Moshe L, Mason GA, Rodriguez-Medina J, Kawa D, Pauluzzi G, Reynoso M, Canto-Pastor A, Manzano C, et al (2021) Innovation, conservation, and repurposing of gene function in root cell type development. Cell **184**: 3333-3348.e19

Kakei Y, Yamazaki C, Suzuki M, Nakamura A, Sato A, Ishida Y, Kikuchi R, Higashi S, Kokudo Y, Ishii T, et al (2015) Small-molecule auxin inhibitors that target YUCCA are powerful tools for studying auxin function. Plant Journal **84**: 827–837

Kamoutsis AP, Chronopoulou-Sereli AG, Paspatis EA (1999) Paclobutrazol affects growth and flower bud production in Gardenia under different light regimes. HortScience **34**: 674–675

Kang C (2018) Light control of root system architecture (reading version).

Kasperbauer MJ (1971) Spectral Distribution of Light in a Tobacco Canopy and Effects of End-of-Day Light Quality on Growth and Development. Plant Physiology **47**: 775–778

Keiller D, Smith H (1989) Control of carbon partitioning by light quality mediated by phytochrome. Plant Science **63**: 25–29

Kepinski S, Leyser O (2005) The Arabidopsis F-box protein TIR1 is an auxin receptor. Nature **435**: 446–451

Keuskamp DH, Keller MM, Ballaré CL, Pierik R (2012) Blue light regulated shade avoidance. Plant signaling & behavior **7**: 514–517

Keuskamp DH, Pollmann S, Voesenek LACJ, Peeters AJM, Pierik R (2010a) Auxin transport through PIN-FORMED 3 (PIN3) controls shade avoidance and fitness during competition. Proceedings of the National Academy of Sciences of the United States of America **107**: 22740–22744

Keuskamp DH, Sasidharan R, Pierik R (2010b) Physiological regulation and functional significance of shade avoidance responses to neighbors. Plant Signaling and Behavior **5**: 655–662

Keuskamp DH, Sasidharan R, Vos I, Peeters AJM, Voesenek LACJ, Pierik R (2011) Blue-light-mediated shade avoidance requires combined auxin and brassinosteroid action in Arabidopsis seedlings. Plant Journal **67**: 208–217

Kim H, Park PJ, Hwang HJ, Lee SY, Oh MH, Kim SG (2006) Brassinosteroid signals control expression of the AXR3/IAA17 gene in the cross-talk point with auxin in root development. Bioscience, Biotechnology and Biochemistry **70**: 768–773

Kim W-C, Kim J-Y, Ko J-H, Kang H, Han K-H (2014) Identification of direct targets of transcription factor MYB46 provides insights into the transcriptional regulation of secondary wall biosynthesis. Plant Mol Biol **85**: 589–599

Kiss JZ, Mullen JL, Correll MJ, Hangarter RP (2003) Phytochromes A and B mediate red-light-induced positive phototropism in roots. Plant Physiology **131**: 1411–1417

Knauss S, Rohrmeier T, Lehle L (2003) The auxin-induced maize gene ZmSAUR2 encodes a short-lived nuclear protein expressed in elongating tissues. Journal of Biological Chemistry **278**: 23936–23943

Ko JH, Han KH, Park S, Yang J (2004) Plant body weight-induced secondary growth in Arabidopsis and its transcription phenotype revealed by whole-transcriptome profiling. Plant Physiology **135**: 1069–1083

Kohnen M V., Schmid-Siegert E, Trevisan M, Petrolati LA, Sénéchal F, Müller-Moulé P, Maloof J, Xenarios I, Fankhauser C (2016a) Neighbor detection induces organ-specific transcriptomes, revealing patterns underlying hypocotyl-specific growth. Plant Cell **28**: 2889–2904

Kohnen M V., Schmid-Siegert E, Trevisan M, Petrolati LA, Sénéchal F, Müller-Moulé P, Maloof JN, Xenarios I, Fankhauser C, van Roekel JSC, et al (2016b) Neighbor detection induces organ-specific transcriptomes, revealing patterns underlying hypocotyl-specific growth. Plant Cell **28**: 2889–2904

Kong E, Liu D, Guo X, Yang W, Sun J, Li X, Zhan K, Cui D, Lin J, Zhang A (2013) Anatomical and chemical characteristics associated with lodging resistance in wheat. The Crop Journal **1**: 43–49

Kozuka T, Kobayashi J, Horiguchi G, Demura T, Sakakibara H, Tsukaya H, Nagatani A (2010) Involvement of Auxin and Brassinosteroid in the Regulation of Petiole Elongation under the Shade. Plant Physiology **153**: 1608–1618

Kraus G (1867) Die Gewebespannung des Stammes und ihre Folgen.

Kraus G (1869) Über die Ursachen der Formänderungen etiolirender Pflanzen.

Křeček P, Skůpa P, Libus J, Naramoto S, Tejos R, Friml J, Zažímalová E (2009) The PIN-FORMED (PIN) protein family of auxin transporters. Genome Biology **10**: 249

Kumar S, Stecher G, Tamura K (2016) MEGA7: Molecular Evolutionary Genetics Analysis Version 7.0 for Bigger Datasets. Molecular Biology and Evolution **33**: 1870–1874

Küpers JJ, van Gelderen K, Pierik R (2018) Location Matters: Canopy Light Responses over Spatial Scales. Trends in Plant Science **23**: 865–873

Küpers JJ, Snoek BL, Oskam L, Pantazopoulou CK, Matton SEA, Reinen E, Liao CY, Eggermont EDC, Weekamp H, Biddanda-Devaiah M, et al (2023) Local light signaling at the leaf tip drives remote differential petiole growth through auxin-gibberellin dynamics. Current Biology **33**: 75-85.e5

Kurepin L V., Emery RJN, Pharis RP, Reid DM (2007) Uncoupling light quality from light irradiance effects in Helianthus annuus shoots: putative roles for plant hormones in leaf and internode growth. Journal of Experimental Botany **58**: 2145–2157

Kutschera U (2001) Stem elongation and cell wall proteins in flowering plants. Plant Biology **3**: 466–480

Kutschera U (1992) The Role of the Epidermis in the Control of Elongation Growth in Stems and Coleoptiles. Botanica Acta **105**: 246–252

Kutschera U, Köhiler K (1992) Turgor and longitudinal tissue 12Helianthus annuus. Journal of Experimental Botany **43**: 1577–1581

Kutschera U, Niklas KJ (2007) The epidermal-growth-control theory of stem elongation: An old and a new perspective. Journal of Plant Physiology **164**: 1395–1409

Lachaud S, Catesson AM, Bonnemain JL (1999) Structure and functions of the vascular cambium. Comptes Rendus de l'Academie des Sciences - Serie III **322**: 633–650

Lamesch P, Berardini TZ, Li D, Swarbreck D, Wilks C, Sasidharan R, Muller R, Dreher K, Alexander DL, Garcia-Hernandez M, et al (2012) The Arabidopsis Information Resource (TAIR): Improved gene annotation and new tools. Nucleic Acids Research. doi: 10.1093/NAR/GKR1090

Lanza M, Garcia-Ponce B, Castrillo G, Catarecha P, Sauer M, Rodriguez-Serrano M, Páez-García A, Sánchez-Bermejo E, Tc M, Leo del Puerto Y, et al (2012) Role of actin cytoskeleton in brassinosteroid signaling and in its integration with the auxin response in plants. Developmental cell **22**: 1275–1285

Law CW, Chen Y, Shi W, Smyth GK (2014) Voom: Precision weights unlock linear model analysis tools for RNA-seq read counts. Genome Biology **15**: 1–17

Lee J, Han S, Lee HY, Jeong B, Heo TY, Hyun TK, Kim K, Je B Il, Lee H, Shim D, et al (2019) Brassinosteroids facilitate xylem differentiation and wood formation in tomato. Planta **249**: 1391–1403

Leivar P, Monte E (2014) PIFs: Systems Integrators in Plant Development. The Plant Cell **26**: 56

Li J, Chory J (1999) Brassinosteroid actions in plants. Journal of Experimental Botany **50**: 275–282

Li L, Ljung K, Breton G, Schmitz RJ, Pruneda-Paz J, Cowing-Zitron C, Cole BJ, Ivans LJ, Pedmale U V., Jung HS, et al (2012) Linking photoreceptor excitation to changes in plant architecture. Genes & development **26**: 785–790

Li SB, Xie ZZ, Hu CG, Zhang JZ (2016) A review of auxin response factors (*ARF*s) in plants. Frontiers in Plant Science **7**: 175431

Li Y, Strabala TJ, Hagen G, Guilfoyle TJ (1994) The soybean SAUR open reading frame contains a cis element responsible for cycloheximide-induced mRNA accumulation. Plant Molecular Biology **24**: 715–723

Liao Y, Smyth GK, Shi W (2014) featureCounts: an efficient general purpose program for assigning sequence reads to genomic features. Bioinformatics **30**: 923–930

Lichtenthaler HK, Buschmann C, Döll M, Fietz HJ, Bach T, Kozel U, Meier D, Rahmsdorf U (1981) Photosynthetic activity, chloroplast ultrastructure, and leaf characteristics of high-light and low-light plants and of sun and shade leaves. Photosynthesis Research **2**: 115–141

Lim GH, Singhal R, Kachroo A, Kachroo P (2017) Fatty Acid- and Lipid-Mediated Signaling in Plant Defense. Annual Review of Phytopathology **55**: 505–536

Lin C (2002) Blue Light Receptors and Signal Transduction. The Plant Cell **14**: s207

Liu H, Tang X, Zhang N, Li S, Si H (2023a) Role of bZIP Transcription Factors in Plant Salt Stress. International Journal of Molecular Sciences. doi: 10.3390/IJMS24097893

Liu M, Yu H, Zhao G, Huang Q, Lu Y, Ouyang B (2018) Identification of drought-responsive microRNAs in tomato using high-throughput sequencing. Functional and Integrative Genomics **18**: 67–78

Liu Q, Zhao Y, Rahman S, She M, Zhang J, Yang R, Islam S, O'Hara G, Varshney RK, Liu H, et al (2023b) The putative vacuolar processing enzyme gene TaVPE3cB is a candidate gene for wheat stem pith-thickness. Theoretical and Applied Genetics **136**: 138

Liu Y, Jafari F, Wang H (2021) Integration of light and hormone signaling pathways in the regulation of plant shade avoidance syndrome. aBIOTECH **2**: 131–145

Lobet G, Pagès L, Draye X (2011) A Novel Image-Analysis Toolbox Enabling Quantitative Analysis of Root System Architecture. Plant Physiology **157**: 29–39

Long L, Minghui Y, Wenjing Y, Yulong D, Shuyan L (2023) Research advance in growth and development of bamboo organs. Industrial Crops and Products **205**: 117428

Lovell PH, Raven PH, Curtis H (1971) Biology of Plants. The Journal of Ecology. doi: 10.2307/2258156

Lu R, Zhang J, Wu YW, Wang Y, Zhang J, Zheng Y, Li Y, Li XB (2021) bHLH transcription factors LP1 and LP2 regulate longitudinal cell elongation. Plant Physiology **187**: 2577–2591

De Lucas M, Davière JM, Rodríguez-Falcón M, Pontin M, Iglesias-Pedraz JM, Lorrain S, Fankhauser C, Blázquez MA, Titarenko E, Prat S (2008) A molecular framework for light and gibberellin control of cell elongation. Nature **451**: 480–484

Luccioni LG, Oliverio KA, Yanovsky MJ, Boccalandro HE, Casal JJ (2002) Brassinosteroid mutants uncover fine tuning of phytochrome signaling. Plant Physiology **128**: 173–181

Lundeen C V., Wood HN, Braun AC (1973) Intracellular Levels of Cyclic Nucleotides during Cell Enlargement and Cell Division in Excised Tobacco Pith Tissues. Differentiation **1**: 255–260

Lunn JE, Delorge I, Figueroa CM, Van Dijck P, Stitt M (2014) Trehalose metabolism in plants. Plant journal **79**: 544–567

Luo J, Zhou JJ, Zhang JZ (2018) Aux/IAA Gene Family in Plants: Molecular Structure, Regulation, and Function. International Journal of Molecular Sciences **19**: 86–113

Luscombe NM, Austin SE, Berman HM, Thornton JM (2000) An overview of the structures of protein-DNA complexes. Genome biology **1**: 1–37

Lyu X, Cheng Q, Qin C, Li Y, Xu X, Ji R, Mu R, Li H, Zhao T, Liu J, et al (2021) GmCRY1s modulate gibberellin metabolism to regulate soybean shade avoidance in response to reduced blue light. Molecular Plant **14**: 298–314

Ma L, Li G (2019) Auxin-Dependent Cell Elongation During the Shade Avoidance Response. Frontiers in Plant Science **10**: 914

Mack JK, Davis AR (2015) The relationship between cell division and elongation during development of the nectar-yielding petal spur in Centranthus ruber (Valerianaceae). 641–649

Markakis MN, Boron AK, Van Loock B, Saini K, Cirera S, Verbelen JP, Vissenberg K (2013) Characterization of a Small Auxin-Up RNA (SAUR)-Like Gene Involved in Arabidopsis thaliana Development. PLOS ONE **8**: e82596

Marks D (2010) Growing notes and review of MoneyMaker tomatoes. GardenFocused.co.uk, https://www.gardenfocused.co.uk/vegetable/tomato-outdoor/variety-moneymaker.php

Mashiguchi K, Tanaka K, Sakai T, Sugawara S, Kawaide H, Natsume M, Hanada A, Yaeno T, Shirasu K, Yao H, et al (2011) The main auxin biosynthesis pathway in Arabidopsis. Proceedings of the National Academy of Sciences of the United States of America **108**: 18512–18517

Matsui A, Todaka D, Tanaka M, Mizunashi K, Takahashi S, Sunaoshi Y, Tsuboi Y, Ishida J, Bashir K, Kikuchi J, et al (2022) Ethanol induces heat tolerance in plants by stimulating unfolded protein response. Plant molecular biology **110**: 131–145

Maughan T, Drost D, Black B, Day S (2017) Using Shade for Fruit and Vegetable Production. Horticulture

Mauseth JD (2003) Botany : an introduction to plant biology. Jones and Bartlett Publishers

Mayor C, Brudno M, Schwartz JR, Poliakov A, Rubin EM, Frazer KA, Pachter LS, Dubchak I (2000) VISTA : visualizing global DNA sequence alignments of arbitrary length. Bioinformatics (Oxford, England) **16**: 1046–1047

Mazur E, Kurczyńska EU, Friml J (2014) Cellular events during interfascicular cambium ontogenesis in inflorescence stems of Arabidopsis. **251**: 1125–1139

McCommis KS, Finck BN (2015) Mitochondrial pyruvate transport: A historical perspective and future research directions. Biochemical Journal **466**: 443–454

Melzer S, Lens F, Gennen J, Vanneste S, Rohde A, Beeckman T (2008) Flowering-time genes modulate meristem determinacy and growth form in Arabidopsis thaliana. Nature genetics **40**: 1489–1492

Meng Y, Shuai H, Lu X, Chen F, Zhou W, Yang W, Shu K (2017) Karrikins: Regulators involved in phytohormone signaling networks during seed germination and seedling development. Frontiers in Plant Science **7**: 2021

Michaelson MJ, Price HJ, Ellison JR, Johnston JS (1991) COMPARISON OF PLANT DNA CONTENTS DETERMINED BY FEULGEN MICROSPECTROPHOTOMETRY AND LASER FLOW CYTOMETRY. American Journal of Botany **78**: 183–188

Michaud O, Fiorucci A-SS, Xenarios I, Fankhauser C (2017) Local auxin production underlies a spatially restricted neighbor-detection response in Arabidopsis. Proceedings of the National Academy of Sciences of the United States of America **114**: 7444–7449

Mierziak J, Kostyn K, Kulma A (2014) Flavonoids as Important Molecules of Plant Interactions with the Environment. Molecules **19**: 16240

Miller Coyle H (2004) Plant Cell Structure and Function. Forensic Botany. doi: 10.1201/9780203484593.ch3

Miyazawa Y, Manythong C, Fukuda S, Ogata K (2014) Comparison of the growth traits of a commercial pioneer tree species, paper mulberry (Broussonetia papyrifera L. vent.), with those of shade-tolerant tree species: Investigation of the ecophysiological mechanisms underlying shade-intolerance. Agroforestry Systems **88**: 907–919

Mizukami Y, Fischer RL (2000) Plant organ size control: AINTEGUMENTA regulates growth and cell numbers during organogenesis. Proceedings of the National Academy of Sciences of the United States of America **97**: 942–947

Moazzeni H, Zarre S, Pfeil BE, Bertrand YJK, German DA, Al-Shehbaz IA, Mummenhoff K, Oxelman B (2014) Phylogenetic perspectives on diversification and character evolution in the species-rich genus Erysimum (Erysimeae; Brassicaceae) based on a densely sampled ITS approach. Botanical Journal of the Linnean Society **175**: 497–522

Molina-Contreras MJ, Paulišić S, Then C, Moreno-Romero J, Pastor-Andreu P, Morelli L, Roig-Villanova I, Jenkins H, Hallab A, Gan X, et al (2019) Photoreceptor Activity Contributes to Contrasting Responses to Shade in Cardamine and Arabidopsis Seedlings. The Plant Cell **31**: 2649–2663

Montavon M, Horwitz BA, Greppin H (1983) Far-Red Light-Induced Changes in Intracellular Potentials of Spinach Mesophyll Cells. Plant Physiology **73**: 671–676

Morón-García O, Garzón-Martínez GA, Martínez-Martín MJP, Brook J, Corke FMK, Doonan JH, Camargo Rodríguez A V (2022) Genetic architecture of variation in Arabidopsis thaliana rosettes. PLoS ONE. doi: 10.1371/journal.pone.0263985

van Mourik H, van Dijk ADJ, Stortenbeker N, Angenent GC, Bemer M (2017) Divergent regulation of Arabidopsis SAUR genes: A focus on the SAUR10-clade. BMC Plant Biology **17**: 245

Moustafa E, Wong E (1967) Purification and properties of chalcone-flavanone isomerase from soya bean seed. Phytochemistry **6**: 625–632

Mueller LA, Lankhorst RK, Tanksley SD, Giovannoni JJ, White R, Vrebalov J, Fei Z, Eck J van, Buels R, Mills AA, et al (2009) A Snapshot of the Emerging Tomato Genome Sequence. The Plant Genome. doi: 10.3835/PLANTGENOME2008.08.0005

Mueller LA, Solow TH, Taylor N, Skwarecki B, Buels R, Binns J, Lin C, Wright MH, Ahrens R, Wang Y, et al (2005) The SOL Genomics Network. A comparative resource for Solanaceae biology and beyond. Plant Physiology **138**: 1310–1317

Müller-Moulé P, Nozue K, Pytlak ML, Palmer CM, Covington MF, Wallace AD, Harmer SL, Maloof JN (2016) YUCCA auxin biosynthetic genes are required for Arabidopsis shade avoidance. PeerJ. doi: 10.7717/peerj.2574

Murase K, Hirano Y, Sun TP, Hakoshima T (2008) Gibberellin-induced DELLA recognition by the gibberellin receptor GID1. Nature **456**: 459–463

Murray TD (1983) Role of the Hypodermis and Secondary Cell Wall Thickening in Basal Stem Internodes in Resistance to Strawbreaker Foot Rot in Winter Wheat. Phytopathology **73**: 261

Musselman LJ (2002) The Tomato in American Early History, Culture, and Cookery. Economic Botany **56**: 406–406

Nagao K, Tominaga R (2020) Localization of tomato (Solanum lycopersicum) R3 MYB protein encoded by SlTRY in Arabidopsis roots. Plant Signaling and Behavior. doi: 10.1080/15592324.2020.1800198

Nagata T, Todoriki S, Kikuchi S (2004) Radial expansion of root cells and elongation of root hairs of Arabidopsis thaliana induced by massive doses of gamma irradiation. Plant and Cell Physiology **45**: 1557–1565

Naika S, Jeude J van L de, Goffau M de, Hilmi M, Dam B Van (2005) Cultivation of tomato.

Nakabayashi K, Okamoto M, Koshiba T, Kamiya Y, Nambara E (2005) Genome-wide profiling of stored mRNA in Arabidopsis thaliana seed germination: epigenetic and genetic regulation of transcription in seed. The Plant journal : for cell and molecular biology **41**: 697–709

Narsai R, Law SR, Carrie C, Xu L, Whelan J (2011) In-depth temporal transcriptome profiling reveals a crucial developmental switch with roles for RNA processing and organelle metabolism that are essential for germination in Arabidopsis. Plant physiology **157**: 1342–1362

Ndoli A (2018) Farming with Trees : A Balancing Act in the Shade.

Nemhauser JL, Torii KU (2016) HHS Public Access. 1–16

Nor Diana MI, Zulkepli NA, Siwar C, Zainol MR (2022) Farmers' Adaptation Strategies to Climate Change in Southeast Asia: A Systematic Literature Review. Sustainability (Switzerland) **14**: 3639

Nozue K, Tat A V., Kumar Devisetty U, Robinson M, Mumbach MR, Ichihashi Y, Lekkala S, Maloof JN (2015) Shade Avoidance Components and Pathways in Adult Plants Revealed by Phenotypic Profiling. PLoS Genetics **11**: 1–26

O'Malley RC, Huang SSC, Song L, Lewsey MG, Bartlett A, Nery JR, Galli M, Gallavotti A, Ecker JR (2016) Cistrome and Epicistrome Features Shape the Regulatory DNA Landscape. Cell **165**: 1280–1292

Oh E, Zhu JY, Bai MY, Arenhart RA, Sun Y, Wang ZY (2014) Cell elongation is regulated through a central circuit of interacting transcription factors in the Arabidopsis hypocotyl. eLife **3**: 3031

Oh E, Zhu JY, Wang ZY (2012) Interaction between BZR1 and PIF4 integrates brassinosteroid and environmental responses. Nature Cell Biology **14**: 802–809

Oh MH, Honey SH, Tax FE (2020) The control of cell expansion, cell division, and vascular development by brassinosteroids: A historical perspective. International Journal of Molecular Sciences. doi: 10.3390/ijms21051743

Oh S, Park S, Han K-HH (2003) Transcriptional regulation of secondary growth in Arabidopsis thaliana. Journal of Experimental Botany **54**: 2709–2722

Okushima Y, Fukaki H, Onoda M, Theologis A, Tasaka M (2007) *ARF7* and *ARF19* regulate lateral root formation via direct activation of LBD/ASL genes in Arabidopsis. Plant Cell **19**: 118–130

Osborne DJ (1991) Light and plant responses. A study of plant photophysiology and the natural environment. Endeavour **15**: 37

Padmanabhan C, Zheng Y, Shamimuzzaman M, Wilson JR, Gilliard A, Fei Z, Ling K-S (2022) The tomato yellow leaf curl virus C4 protein alters the expression of plant developmental genes correlating to leaf upward cupping phenotype in tomato. Plos One **17**: e0257936

Page ER, Liu W, Cerrudo D, Lee EA, Swanton CJ (2011) Shade Avoidance Influences Stress Tolerance in Maize. Weed Science **59**: 326–334

Page ER, Tollenaar M, Lee EA, Lukens L, Swanton CJ (2009) Does the shade avoidance response contribute to the critical period for weed control in maize (Zea mays)? Weed Research **49**: 563–571

Pantazopoulou CK, Bongers FJ, Küpers JJ, Reinen E, Das D, Evers JB, Anten NPRR, Pierik R (2017) Neighbor detection at the leaf tip adaptively regulates upward leaf movement through spatial auxin dynamics. Proceedings of the National Academy of Sciences **114**: 7450–7455

Parapunova V, Busscher M, Busscher-Lange J, Lammers M, Karlova R, Bovy AG, Angenent GC, De Maagd RA (2014) Identification, cloning and characterization of the tomato TCP transcription factor family. BMC Plant Biology **14**: 1–17

Park JE, Kim YS, Yoon HK, Park CM (2007) Functional characterization of a small auxin-up RNA gene in apical hook development in Arabidopsis. Plant Science **172**: 150–157

Parra JL, Graham CC, Freile JF, Hewitt N, Setiyawan, Domenici V, Ancora D, Cifelli M, Serani A, Veracini CA, et al (2010) Evolution of development of vascular cambia and secondary growth. New Phytologist **186**: 577–592

Paul-Victor C, Rowe N (2011) Effect of mechanical perturbation on the biomechanics, primary growth and secondary tissue development of inflorescence stems of Arabidopsis thaliana. Annals of Botany **107**: 209–218

Paul MJ, Jhurreea D, Zhang Y, Primavesi LF, Delatte T, Schluepmann H, Wingler A (2010) Upregulation of biosynthetic processes associated with growth by trehalose 6-phosphate. Plant Signaling and Behavior **5**: 386–392

Perrot-Rechenmann C (2010) Cellular responses to auxin: division versus expansion. Cold Spring Harbor perspectives in biology. doi: 10.1101/cshperspect.a001446

Peter J, Wang N, Bagdassarian KS, Doherty RE, Kroon JT, Connor KA, Wang XY, Wang W, Jermyn IH, Turner SR, et al (2019) Organ-specific genetic interactions between paralogues of the PXY and ER receptor kinases enforce radial patterning in Arabidopsis vascular tissue. Development (Cambridge) 146:

Pierik R, Cuppens MLC, Voesenek LACJ, Visser EJW (2004) Interactions between ethylene and gibberellins in phytochrome-mediated shade avoidance responses in tobacco. Plant Physiology **136**: 2928–2936

Pierik R, Djakovic-Petrovic T, Keuskamp DH, De Wit M, Voesenek LACJ (2009) Auxin and Ethylene Regulate Elongation Responses to Neighbor Proximity Signals Independent of Gibberellin and DELLA Proteins in Arabidopsis. Plant Physiology **149**: 1701–1712

Pierik R, De Wit M (2014) Shade avoidance: Phytochrome signalling and other aboveground neighbour detection cues. Journal of Experimental Botany **65**: 2815–2824

Pradhan Mitra P, Loqué D (2014) Histochemical staining of Arabidopsis thaliana secondary cell wall elements. Journal of Visualized Experiments. doi: 10.3791/51381

Procko C, Burko Y, Jaillais Y, Ljung K, Long JA, Chory J (2016) The epidermis coordinates auxin-induced stem growth in response to shade. Genes and Development **30**: 1529–1541

Procko C, Crenshaw CM, Ljung K, Noel JP, Chory J (2014) Cotyledon-Generated Auxin Is Required for Shade-Induced Hypocotyl Growth in Brassica rapa. Plant Physiology **165**: 1285–1301

Pucciariello O, Legris M, Rojas CC, Iglesias MJ, Hernando CE, Dezar C, Vazquez M, Yanovsky MJ, Finlayson SA, Prat S, et al (2018) Rewiring of auxin signaling under persistent shade. Proceedings of the National Academy of Sciences of the United States of America **115**: 5612–5617

Qiu T, Chen Y, Li M, Kong Y, Zhu Y, Han N, Bian H, Zhu M, Wang J (2013) The tissue-specific and developmentally regulated expression patterns of the SAUR41 subfamily of SMALL AUXIN UP RNA genes: Potential implications. Plant Signaling and Behavior. doi: 10.4161/psb.25283

R Development Core Team (2010) R: A language and environment for statistical computing. R Foundation for Statistical Computing., Vienna, Austria

Ragheb AY, Kassem MES, El-Sherei MM, Marzouk MM, Mosharrafa SA, Saleh NAM (2019) Morphological, phytochemical and anti-hyperglycemic evaluation of Brachychiton populneus. Revista Brasileira de Farmacognosia **29**: 559–569

Ragni L, Greb T (2018) Secondary growth as a determinant of plant shape and form. Seminars in Cell and Developmental Biology **79**: 58–67

Rambaut A (2012) FigTree v1. 4. and epidemiology. Edinburgh, UK: University of Edinburgh

Ranade SS, Delhomme N, García-Gil MR (2019) Transcriptome analysis of shade avoidance and shade tolerance in conifers. Planta **250**: 299–318

Randall RS, Miyashima S, Blomster T, Zhang J, Elo A, Karlberg A, Immanen J, Nieminen K, Lee JY, Kakimoto T, et al (2015) AINTEGUMENTA and the D-type cyclin CYCD3;1 regulate root secondary growth and respond to cytokinins. Biology Open **4**: 1229–1236

Rayle DL, Cleland R (1970) Enhancement of Wall Loosening and Elongation by Acid Solutions. Plant Physiology **46**: 250

Rayle DL, Cleland RE (1992) The Acid Growth Theory of auxin-induced cell elongation is alive and well. Plant Physiology **99**: 1271

Reed JW, Nagatani A, Elich TD, Fagan M, Chory J (1994) Phytochrome A and Phytochrome B Have Overlapping but Distinct Functions in Arabidopsis Development'. Plant Physiol

Reed JW, Nagpal P, Poole DS, Furuya M, Chory J, Poo1e DS, Furuya M, Chorya9 J, Poole DS, Furuya M, et al (1993) Mutations in the gene for the red/far-red light receptor phytochrome B alter cell elongation and physiological responses throughout Arabidopsis development. The Plant cell **5**: 147–157

Ren H, Gray WM (2015) SAUR Proteins as Effectors of Hormonal and Environmental Signals in Plant Growth. Molecular Plant **8**: 1153–1164

Reynoso MA, Kajala K, Bajic M, West DA, Pauluzzi G, Yao AI, Hatch K, Zumstein K, Woodhouse M, Rodriguez-Medina J, et al (2019) Evolutionary flexibility in flooding response circuitry in angiosperms. Science **365**: 1291–1295

Ritchie ME, Phipson B, Wu D, Hu Y, Law CW, Shi W, Smyth GK (2015) limma powers differential expression analyses for RNA-sequencing and microarray studies. Nucleic acids research **43**: e47

Robinson MD, McCarthy DJ, Smyth GK (2009) edgeR: A Bioconductor package for differential expression analysis of digital gene expression data. Bioinformatics **26**: 139–140

Robinson S, Kuhlemeier C (2018) Global Compression Reorients Cortical Microtubules in Arabidopsis Hypocotyl Epidermis and Promotes Growth. Current Biology **28**: 1794-1802.e2

Robson PRH, Whitelam GC, Smith H (1993) Selected Components of the Shade-Avoidance Syndrome Are Displayed in a Normal Manner in Mutants of Arabidopsis thaliana and Brassica rapa Deficient in Phytochrome B. Plant Physiology **102**: 1179–1184

Roig-Villanova I, Bou-Torrent J, Galstyan A, Carretero-Paulet L, Portolés S, Rodríguez-Concepción M, Martínez-García JF (2007) Interaction of shade avoidance and auxin responses: A role for two novel atypical bHLH proteins. EMBO Journal **26**: 4756–4767

Ruberti I, Sessa G, Ciolfi A, Possenti M, Carabelli M, Morelli G (2012) Plant adaptation to dynamically changing environment: The shade avoidance response. Biotechnology Advances **30**: 1047–1058

Ryan KG, Swinny EE, Markham KR, Winefield C (2002) Flavonoid gene expression and UV photoprotection in transgenic and mutant Petunia leaves. Phytochemistry **59**: 23–32

Sakaoka S, Mabuchi K, Morikami A, Tsukagoshi H (2018) MYB30 regulates root cell elongation under abscisic acid signaling. Communicative and Integrative Biology **11**: 1–8

Salisbury FJ, Hall A, Grierson CS, Halliday KJ (2007) Phytochrome coordinates Arabidopsis shoot and root development. The Plant journal : for cell and molecular biology **50**: 429–438

Sanchez P, Nehlin L, Greb T (2012) From thin to thick: major transitions during stem development. Cell **17**: 113–121

Sasidharan R, Chinnappa CC, Staal M, Elzenga JTM, Yokoyama R, Nishitani K, Voesenek LACJ, Pierik R (2010) Light quality-mediated petiole elongation in Arabidopsis during shade avoidance involves cell wall modification by xyloglucan endotransglucosylase/hydrolases. Plant Physiology **154**: 978–990

Sasidharan R, Chinnappa CC, Voesenek LACJ, Pierik R (2008) The Regulation of Cell Wall Extensibility during Shade Avoidance: A Study Using Two Contrasting Ecotypes of Stellaria longipes. Plant Physiology **148**: 1557–1569

Sasidharan R, Keuskamp DH, Kooke R, Voesenek LACJ, Pierik R (2014) Interactions between auxin, microtubules and XTHs mediate green shade- induced petiole elongation in Arabidopsis. PLoS ONE. doi: 10.1371/journal.pone.0090587

Sato S, Tabata S, Hirakawa H, Asamizu E, Shirasawa K, Isobe S, Kaneko T, Nakamura Y, Shibata D, Aoki K, et al (2012) The tomato genome sequence provides insights into fleshy fruit evolution. **485**: 635–641

Savaldi-Goldstein S, Chory J (2008) Growth coordination and the shoot epidermis. Current Opinion in Plant Biology **11**: 42–48

Savaldi-Goldstein S, Peto C, Chory J (2007) The epidermis both drives and restricts plant shoot growth. Nature **446**: 199–202

Savidge RA (1983) The role of plant hormones in higher plant cellular differentiation. II. Experiments with the vascular cambium, and sclereid and tracheid differentiation in the pine, Pinus contorta. The Histochemical Journal **15**: 447–466

Scarpella E, Meijer AH (2004) Pattern formation in the vascular system of monocot and dicot plant species. New Phytologist. doi: 10.1111/j.1469-8137.2004.01191.x

Schindelin J, Arganda-Carreras I, Frise E, Kaynig V, Longair M, Pietzsch T, Preibisch S, Rueden C, Saalfeld S, Schmid B, et al (2012) Fiji: an open-source platform for biological-image analysis. Nature methods **9**: 676–682

Schmid M, Davison TS, Henz SR, Pape UJ, Demar M, Vingron M, Schölkopf B, Weigel D, Lohmann JU (2005) A gene expression map of Arabidopsis thaliana development. Nature genetics **37**: 501–506

Schmitt J (1997) Is photomorphogenic shade avoidance adaptive? Perspectives from population biology. Plant, Cell and Environment **20**: 826–830

Schrager-Lavelle A, Gath NN, Devisetty UK, Carrera E, López-Díaz I, Blázquez MA, Maloof JN (2019) The role of a class III gibberellin 2-oxidase in tomato internode elongation. Plant Journal **97**: 603–615

Sehr EM, Agusti J, Lehner R, Farmer EE, Schwarz M, Greb T, Mendel G (2010) Analysis of secondary growth in the Arabidopsis shoot reveals a positive role of jasmonate signalling in cambium formation. Plant Journal **63**: 811–822

Šenkyřík JB, Křivánková T, Kaczorová D, Štefelová N (2023) Investigation of the Effect of the Auxin Antagonist PEO-IAA on Cannabinoid Gene Expression and Content in Cannabis sativa L. Plants under In Vitro Conditions. Plants 2023, Vol 12, Page 1664 **12**: 1664

Sheerin DJ, Hiltbrunner A (2017) Molecular mechanisms and ecological function of far-red light signalling. doi: 10.1111/pce.12915

Shen H, Zhu L, Bu QY, Huq E (2012) MAX2 affects multiple hormones to promote photomorphogenesis. Molecular Plant **5**: 750–762

Sherman JD, Stack SM (1995) Two-dimensional spreads of synaptonemal complexes from solanaceous plants. VI. High-resolution recombination nodule map for tomato (Lycopersicon esculentum). Genetics **141**: 683–708

Shi D, Jouannet V, Agustí J, Kaul V, Levitsky V, Mironova V V, Sanchez P, Greb T (2020) Tissue-specific transcriptome profiling of the Arabidopsis thaliana inflorescence stem reveals local cellular signatures. bioRxiv. doi: 10.1101/2020.02.10.941492

Shin J, Park E, Choi G, Yu-shuai P, Ru-feng W, Lu-jun Z, Kerckhoffs LHJ, Schreuder MEL, Van Tuinen A, Koornneef M, et al (1997) Phytochrome control of anthocyanin biosynthesis in tomato seedlings: Analysis using photomorphogenic mutants. Photochemistry and Photobiology **65**: 374–381

Siddiqi KS, Husen A (2017) Plant response to strigolactones: Current developments and emerging trends. Applied Soil Ecology **120**: 247–253

Sieburth LE, Deyholos MK (2006) Vascular development: the long and winding road. Current Opinion in Plant Biology **9**: 48–54

Skubisz G, Kravtsova TI, Velikanov LP (2007) Analysis of the strength properties of pea stems. International Agrophysics **21**: 189–197

Smith H, Whitelam GC (1997) The shade avoidance syndrome: Multiple responses mediated by multiple phytochromes. Plant, Cell and Environment **20**: 840–844

Sottosanti K (2023) Pioneer species | Definition, Examples, Ecology, & Facts | Britannica. Encyclopedia Britannica, https://www.britannica.com/science/pioneer-species

Spaninks K, Lamers G, Lieshout J van, Offringa R (2023) Light quality regulates apical and primary radial growth of Arabidopsis thaliana and Solanum lycopersicum. Scientia Horticulturae **317**: 112082

Spartz AK, Ren H, Park MY, Grandt KN, Lee SH, Murphy AS, Sussman MR, Overvoorde PJ, Gray WM (2014) SAUR Inhibition of PP2C-D Phosphatases Activates Plasma Membrane H+-ATPases to Promote Cell Expansion in Arabidopsis. The Plant cell **26**: 2129–2142

Stacey G, ˇ Fendrych M, Leung J, Friml J (2016) TIR1/AFB-Aux/IAA auxin perception mediates rapid cell wall acidification and growth of Arabidopsis hypocotyls. doi: 10.7554/eLife.19048.001

Stamm P, Kumar PP, Prakash •, Kumar PP (2013) Auxin and gibberellin responsive Arabidopsis SMALL AUXIN UP RNA36 regulates hypocotyl elongation in the light. Plant Cell Reports **32**: 759–769

Stortenbeker N, Bemer M (2019) The SAUR gene family: the plant's toolbox for adaptation of growth and development. Journal of Experimental Botany **70**: 17–27

Su H, Abernathy SD, White RH, Finlayson SA (2011) Photosynthetic photon flux density and phytochrome B interact to regulate branching in Arabidopsis. Plant, Cell & Environment **34**: 1986–1998

Sun Y, Fan XY, Cao DM, Tang W, He K, Zhu JY, He JX, Bai MY, Zhu S, Oh E, et al (2010) Integration of Brassinosteroid Signal Transduction with the Transcription Network for Plant Growth Regulation in Arabidopsis. Developmental Cell **19**: 765–777

Taiz L, Zeiger E, Møller IM, Murphy A (2010) Plant Physiology and Development, Fifth Edition, 6th ed. Sunderland

Tang Y jia, Liesche J (2017) The molecular mechanism of shade avoidance in crops – How data from Arabidopsis can help to identify targets for increasing yield and biomass production. Journal of Integrative Agriculture **16**: 1244–1255

Tao Y, Ferrer JL, Ljung K, Pojer F, Hong F, Long JA, Li L, Moreno JE, Bowman ME, Ivans LJ, et al (2008) Rapid synthesis of auxin via a new tryptophan-dependent pathway is required for shade avoidance in plants. Cell **133**: 164

Tarasov A, Vilella AJ, Cuppen E, Nijman IJ, Prins P (2015) Sambamba: fast processing of NGS alignment formats. Bioinformatics **31**: 2032–2034

The Arabidopsis Information Resource (2015) TAIR - Home Page. https://www.arabidopsis.org/index.jsp

Thompson NP, Heimsch C (1964) Stem Anatomy and Aspects of Development in Tomato. American Journal of Botany **51**: 7

Thompson NP, Jacobs WP (1966) Polarity of IAA Effect on Sieve-Tube and Xylem Regeneration in Coleus and Tomato Stems. Plant Physiology **41**: 673–682

Todesco S, Campagna D, Levorin F, D'Angelo M, Schiavon R, Valle G, Vezzi A (2008) PABS: an online platform to assist BAC-by-BAC sequencing projects. BioTechniques **44**: 60–64

Tomescu AMF, Mcqueen CR (2022) A protoxylem pathway to evolution of pith? An hypothesis based on the Early Devonian euphyllophyte Leptocentroxyla. Annals of Botany **130**: 785–798

Tonn N, Greb T (2017) Radial plant growth. Current Biology. doi: 10.1016/j.cub.2017.03.056

Townsley BT, Covington MF, Ichihashi Y, Zumstein K, Sinha NR (2015) BrAD-seq: Breath Adapter Directional sequencing: a streamlined, ultra-simple and fast library preparation protocol for strand specific mRNA library construction. Frontiers in Plant Science **6**: 1–11

Turnerag1 SR, Somervilleb CR (1997) Collapsed Xylem Phenotype of Arabidopsis Identifies Mutants Deficient in Cellulose Deposition in the Secondary Cell Wall. American Society of Plant Physiologists

Ueguchi-Tanaka M, Nakajima M, Katoh E, Ohmiya H, Asano K, Saji S, Hongyu X, Ashikari M, Kitano H, Yamaguchi I, et al (2007) Molecular interactions of a soluble gibberellin receptor, GID1, with a rice DELLA protein, SLR1, and gibberellin. Plant Cell **19**: 2140–2155

Ueoka-Nakanishi H, Hori N, Ishida K, Ono N, Yamashino T, Nakamichi N, Mizuno T (2011) Characterization of Shade Avoidance Responses in Lotus japonicus. Biosci Biotechnol Biochem **75**: 110442–110443

Vandenbussche F, Habricot Y, Condiff AS, Maldiney R, Van Der Straeten D, Ahmad M (2007) HY5 is a point of convergence between cryptochrome and cytokinin signalling pathways in Arabidopsis thaliana. Plant Journal **49**: 428–441

Venning FD (1949) Investigations on the Morphology, Anatomy, and Secondary Growth in the Main Axis of Marglobe Tomato (Lycopersicon Esculentum Mill.). American Journal of Botany **36**: 559

Vert G, Walcher CL, Chory J, Nemhauser JL (2008) Integration of auxin and brassinosteroid pathways by Auxin Response Factor 2. Proceedings of the National Academy of Sciences of the United States of America **105**: 9829–9834

Wada T, Tachibana T, Shimura Y, Okada K, Nagao K, Tominaga R, Wada T, Tachibana T, Shimura Y, Okada K (1997) Epidermal cell differentiation in Arabidopsis determined by a Myb homolog, CPC. Science **277**: 1113–1116

Walcher CL, Nemhauser JL (2012) Bipartite promoter element required for auxin response. Plant Physiology **158**: 273–282

Walter A, Scharr H, Gilmer F, Zierer R, Nagel KA, Ernst M, Wiese A, Virnich O, Christ MM, Uhlig B, et al (2007) Dynamics of seedling growth acclimation towards altered light conditions can be quantified via GROWSCREEN: a setup and procedure designed for rapid optical phenotyping of different plant species. New Phytologist **174**: 447–455

Wang L, Wang S, Li W (2012) RSeQC: quality control of RNA-seq experiments. Bioinformatics (Oxford, England) **28**: 2184–2185

Wang MM, Liu MM, Ran F, Guo PC, Ke YZ, Wu YW, Wen J, Li PF, Li JN, Du H (2018) Global Analysis of WOX Transcription Factor Gene Family in Brassica napus Reveals Their Stress- and Hormone-Responsive Patterns. International journal of molecular sciences **19**: 1–21

Wang W, Bai MY, Wang ZY (2014) The brassinosteroid signaling network-a paradigm of signal integration. Current Opinion in Plant Biology **21**: 147–153

Wang X, Gao X, Liu Y, Fan S, Ma Q (2020) Progress of Research on the Regulatory Pathway of the Plant Shade-Avoidance Syndrome. Frontiers in Plant Science **11**: 1–12

Wang X, Wang X, Hu Q, Dai X, Tian H, Zheng K, Wang X, Mao T, Chen JG, Wang S (2015) Characterization of an activation-tagged mutant uncovers a role of GLABRA2 in anthocyanin biosynthesis in Arabidopsis. The Plant journal : for cell and molecular biology **83**: 300–311

Wang X, Zhang S, Chen L, Huang B, Fang C, Ma X, Liu H, Sun F, Fei B (2022) Effects of pith ring on the hygroscopicity and dimensional stability of bamboo. Industrial Crops and Products. doi: 10.1016/j.indcrop.2022.115027

Wang Y, Liu H, Wang S, Li H (2017) Genome-wide identification and expression analysis of the YUCCA gene family in soybean (Glycine max L.). Plant Growth Regulation **81**: 265–275

Watanabe T, Tomizaki R, Watanabe R, Maruyama H, Shinano T, Urayama M, Kanayama Y (2021) Ionomic differences between tomato introgression line IL8–3 and its parent cultivar M82 with different trends to the incidence of blossom-end rot. Scientia Horticulturae **287**: 110266

Waters MT, Smith SM (2013) KAI2- and MAX2-mediated responses to karrikins and strigolactones are largely independent of HY5 in arabidopsis seedlings. Molecular Plant **6**: 63–75

Wei Q, Jiao C, Guo L, Ding Y, Cao J, Feng J, Dong X, Mao L, Sun H, Yu F, et al (2017) Exploring key cellular processes and candidate genes regulating the primary thickening growth of Moso underground shoots. The New phytologist **214**: 81–96

Weijschedé J, Antonise K, De Caluwe H, De Kroon H, Huber H (2008) Effects of cell number and cell size on petiole length variation in a stoloniferous herb. American Journal of Botany **95**: 41–49

Weijschedé J, Martínková J, De Kroon H, Huber H (2006) Shade avoidance in Trifolium repens: costs and benefits of plasticity in petiole length and leaf size. New Phytologist **172**: 655–666

Went FW (1944) Plant Growth Under Controlled Conditions. III. Correlation Between Various Physiological Processes and Growth in the Tomato Plant. American Journal of Botany **31**: 597

Winter D, Vinegar B, Nahal H, Ammar R, Wilson G V., Provart NJ (2007) An "Electronic Fluorescent Pictograph" browser for exploring and analyzing large-scale biological data sets. PloS one. doi: 10.1371/JOURNAL.PONE.0000718

de Wit M, Keuskamp DH, Bongers FJ, Hornitschek P, Gommers CMM, Reinen E, Martínez-Cerón C, Fankhauser C, Pierik R (2016) Integration of Phytochrome and Cryptochrome Signals Determines Plant Growth during Competition for Light. Current Biology **26**: 3320–3326

de Wit M, Ljung K, Fankhauser C (2015) Contrasting growth responses in lamina and petiole during neighbor detection depend on differential auxin responsiveness rather than different auxin levels. New Phytologist **208**: 198–209

Woodward AW, Bartel B (2005) Auxin: Regulation, action, and interaction. Annals of Botany **95**: 707–735

Wu J, Liu S, He Y, Guan X, Zhu X, Cheng L, Wang J, Lu G (2012) Genome-wide analysis of SAUR gene family in Solanaceae species. Gene **509**: 38–50

Xiang Y, Sapir T, Rouillard P, Ferrand M, Jiménez-Gómez JM (2022) Interaction between photoperiod and variation in circadian rhythms in tomato. BMC Plant Biology **22**: 1–12

Xie Y, Liu Y, Ma M, Zhou Q, Zhao Y, Zhao B, Wang B, Wei H, Wang H (2020) Arabidopsis FHY3 and FAR1 integrate light and strigolactone signaling to regulate branching. Nature Communications. doi: 10.1038/s41467-020-15893-7

Xu C, Liberatore KL, Macalister CA, Huang Z, Chu YH, Jiang K, Brooks C, Ogawa-Ohnishi M, Xiong G, Pauly M, et al (2015) A cascade of arabinosyltransferases controls shoot meristem size in tomato. Nature Genetics **47**: 784–792

Xu F, He S, Zhang J, Mao Z, Wang W, Li T, Hua J, Du S, Xu P, Li L, et al (2018) Photoactivated CRY1 and phyB Interact Directly with AUX/IAA Proteins to Inhibit Auxin Signaling in Arabidopsis. Molecular Plant **11**: 523–541

Xu H, Liu Q, Yao T, Fu X (2014) Shedding light on integrative GA signaling. Current opinion in plant biology **21**: 89–95

Xu HL, Gauthier L, Desjardins Y, Gosselin A (1997) Photosynthesis in leaves, fruits, stem and petioles of greenhouse-grown tomato plants. Photosynthetica 1997 33:1 **33**: 113–123

Yang C, Li L (2017) Hormonal regulation in shade avoidance. Frontiers in Plant Science **8**: 290176

Yang D, Seaton DD, Krahmer J, Halliday KJ Photoreceptor effects on plant biomass, resource allocation, and metabolic state. doi: 10.1073/pnas.1601309113

Yang L, Zhao X, Yang F, Fan D, Jiang Y, Luo K (2016) PtrWRKY19, a novel WRKY transcription factor, contributes to the regulation of pith secondary wall formation in Populus trichocarpa. Scientific Reports **6**: 1–12

Yang T, Davies PJ, Reid JB (1996) Genetic dissection of the relative roles of auxin and gibberellin in the regulation of stem elongation in intact light-grown peas. Plant Physiology **110**: 1029–1034

Yang X, Kundariya H, Xu YZ, Sandhu A, Yu J, Hutton SF, Zhang M, Mackenzie SA (2015) MutS HOMOLOG1-Derived Epigenetic Breeding Potential in Tomato. Plant Physiology **168**: 222–232

Ye L, Wang X, Lyu M, Siligato R, Eswaran G, Vainio L, Blomster T, Zhang J, Mähönen AP (2021) Cytokinins initiate secondary growth in the Arabidopsis root through a set of LBD genes. Current Biology **31**: 3365-3373.e7

Yin Y, Vafeados D, Tao Y, Yoshida S, Asami T, Chory J (2005) A new class of transcription factors mediates brassinosteroid-regulated gene expression in Arabidopsis. Cell **120**: 249–259

Young MD, Wakefield MJ, Smyth GK, Oshlack A (2010) Gene ontology analysis for RNA-seq: accounting for selection bias. Genome Biology. doi: 10.1186/gb-2010-11-2-r14

Zabel RA, Morrell JJ (2020) The decay setting: Some structural, chemical, and moisture features of wood features of wood in relation to decay development. Wood Microbiology. Elsevier, pp 149–183

Zha M, Zhao Y, Wang Y, Chen B, Tan Z (2022) Strigolactones and Cytokinin Interaction in Buds in the Control of Rice Tillering. Frontiers in Plant Science **13**: 837136

Zhang KX, Xu HH, Yuan TT, Zhang L, Lu YT (2013) Blue-light-induced PIN3 polarization for root negative phototropic response in Arabidopsis. The Plant journal : for cell and molecular biology **76**: 308–321

Zhang Y, Pfeiffer A, Tepperman JM, Dalton-Roesler J, Leivar P, Grandio EG, Quail PH (2020) Central clock components modulate plant shade avoidance by directly repressing transcriptional activation activity of PIF proteins. Proceedings of the National Academy of Sciences of the United States of America **117**: 3261–3269

Zhang Z, Gao L, Ke M, Gao Z, Tu T, Huang L, Chen J, Guan Y, Huang X, Chen X (2022) GmPIN1-mediated auxin asymmetry regulates leaf petiole angle and plant architecture in soybean. Journal of integrative plant biology **64**: 1325–1338

Zhao H, Li X, Ma L (2012) Basic helix-loop-helix transcription factors and epidermal cell fate determination in Arabidopsis. Plant Signaling and Behavior **7**: 1556–1560

Zhao Y, Christensen SK, Fankhauser C, Cashman JR, Cohen JD, Weigel D, Chory J (2001) A role for flavin monooxygenase-like enzymes in auxin biosynthesis. Science (New York, NY) **291**: 306–309

Zheng Z, Guo Y, Novák O, Dai X, Zhao Y, Ljung K, Noel JP, Chory J (2013) Coordination of auxin and ethylene biosynthesis by the aminotransferase VAS1. Nature Chemical Biology **9**: 244–246

(2005) Tomato History | A Brief History Lesson about the Tomato. 2

Preseq | The Smith Lab. https://smithlabresearch.org/software/preseq/

GENERAL SUMMARY

In a quest to unravel the intricate dance of plants with light, our journey begins with the pivotal role of light and plant growth general introduction. The competition among neighboring vegetation sparks the phenomenon of shade avoidance syndrome (SAS), driven by far-red light enrichment. Armed with a foundation of molecular insights from prior research on shade avoidance syndrome, our thesis sets sail into uncharted territory.

Chapter 1 delves into the shade avoidance syndrome (SAs) in tomato cultivars M82 and Moneymaker, dissecting cellular developmental plasticity under white light and far-red supplemented conditions. Microscopy-based quantification zooms into the first internode, revealing significant cellular anatomy responses, setting the stage for deeper exploration in subsequent chapters.

Chapter 2 explores the molecular mechanism with tissue specific signally in SAS. A time series RNAseq sheds light on auxin's early role in internode elongation and identification of transcription factors, paving the way for Chapter 4's exploration of hormones, identifying potential key regulators.

The hormonal dynamics take center stage in Chapter 4, as we probe into auxin, gibberellins, and brassinosteroids during SAS. The study unveils complex interactions governing stem elongation, highlighting the nuanced influence of auxin, while GA and BR emerge as potent players. The intricate interplay of these hormones shapes plant responses to shade, emphasizing their crucial roles.

Chapter 5 encapsulates a multidimensional exploration, examining cell expansion, the regulatory roles of transcription factors, and the dynamics of shade avoidance responses across 8 dicots. Pith elongation patterns, transcriptional regulation, and motif distribution offer a nuanced understanding of conserved regions, showcasing the interdisciplinary nature of plant biology.Our journey concludes with a spotlight on the distribution of dissimilar transcription factors across plant families, paving the way for future investigations.

In the final chapter, we cast a broad perspective on the constraints of RNAseq analysis, hormone analysis, and evolutionary considerations. The discovery of a general conservation pattern between pith-specific expression in far-red across diverse species and transcription factor conservation opens avenues for deeper research. While our proposed linkage model awaits further confirmation, this ongoing exploration promises to unveil the molecular intricacies of plant responses to light, enriching our understanding of adaptation strategies.

GENERAL SUMMARY (DUTCH)

In een zoektocht om de ingewikkelde dans van planten met licht te ontrafelen, begint onze reis met de cruciale rol van licht en de algemene introductie van plantengroei. De concurrentie tussen naburige vegetatie veroorzaakt het fenomeen van het schaduwontwijkingssyndroom (SAS), aangewakkerd door verrijking met verrood licht. Gewapend met een basis van moleculaire inzichten uit eerdere onderzoeken naar het schaduwontwijkingssyndroom, zet onze scriptie koers naar onontgonnen gebied.

Hoofdstuk 2 duikt diep in het schaduwontwijkingssyndroom (SAS) bij tomatencultivars M82 en Moneymaker, waarbij de cellulaire ontwikkelingsplasticiteit onder wit licht en verrood aangevulde omstandigheden wordt ontleed. Microscopie-gebaseerde kwantificatie zoomt in op het eerste internode en onthult significante reacties in de cellulaire anatomie, wat een opmaat vormt voor verdere verkenning in de daaropvolgende hoofdstukken.

Hoofdstuk 3 onderzoekt het moleculaire mechanisme met weefselspecifieke signalering in SAS. Een RNA-seq op verschillende tijdsstippen werpt licht op de vroege rol van auxine in de internode elongatie en de identificatie van transcriptiefactoren, waarmee de weg wordt bereid voor de verkenning van hormonen in hoofdstuk 4, waar potentiële sleutelregulatoren worden geïdentificeerd.

De hormonale dynamiek staat centraal in hoofdstuk 4, waarin we dieper ingaan op auxine, gibberellines en brassinosteroïden tijdens SAS. De studie onthult complexe interacties die de stengelongatie reguleren, waarbij de genuanceerde invloed van auxine naar voren komt, terwijl GA en BR als sterke spelers opkomen. Het gecompliceerde samenspel van deze hormonen vormt de plantenreacties op schaduw en benadrukt hun cruciale rollen.

Hoofdstuk 5 omvat een multidimensionale verkenning, waarbij celuitbreiding, de regulerende rollen van transcriptiefactoren en de dynamiek van reacties op schaduw worden onderzocht bij 8 dicotyllen. Patronen van pithelongatie, transcriptieregulatie en de conservatie-analyse bieden een genuanceerd begrip van geconserveerde regio's, waarbij de interdisciplinaire aard van plantenbiologie wordt benadrukt. Onze reis eindigt met de verdeling van verschillende transcriptiefactoren binnen plantenfamilies in de schijnwerpers, wat de weg opent voor toekomstige onderzoeken.

In het laatste hoofdstuk werpen we een brede blik op de beperkingen van RNA-seq-analyse, hormoonanalyse en evolutionaire overwegingen. De ontdekking van een algemeen geconserveerd patroon tussen pith-specifieke expressie in verrood over diverse

soorten en de conservatie van transcriptiefactoren opent deuren voor diepgaander onderzoek. Terwijl ons voorgestelde koppelingsmodel wacht op verdere bevestiging, belooft dit voortdurende onderzoek de moleculaire complexiteit van plantenreacties op licht te onthullen en ons begrip van aanpassingsstrategieën te verrijken.

GENERAL SUMMARY (CHINESE)

为了解开植物与光之间错综复杂的关系，我们的旅程从光对植物生长的关键促进作用介绍开始。种植相近的植物之间的对于光的竞争引发了避荫综合症（SAS）的现象，这一现象由远红光在此条件下富集产生。我们的论文以前人对避荫综合症的分子研究为基础，并展开对于未知领域的探索。

第一章深入探讨番茄品种M82和Moneymaker中的避荫综合症（SAS）表型变化，剖析在白光和远红光补充条件下的细胞发育可塑性。我们基于显微镜的定量分析聚焦于第一个节间的木髓细胞伸长，这一细胞解剖学响应在众多变化中最为显著，基于此我们深入探索后续章节。

第二章探索了SAS中的组织特异性信号的分子机制。我们基于表型确定了一系列时间序列RNA测序，揭示了生长素在节间伸长q潜在作用，鉴定出几个可能的关键转录因子，为对激素的探索和潜在关键调节因子的识别铺平道路。

第四章中，激素动态变化控制细胞伸长成为重点，我们探讨了避荫综合症中的生长素、赤霉素和油菜素内酯。研究揭示了控制茎伸长的复杂相互作用，　赤霉素和油菜素内酯重要的作用开始显现，而生长素的作用比较微妙。这些激素之间的复杂相互作用塑造了植物对遮荫的反应，强调了它们的关键作用。

第五章进行了一个多维度的探索，检验了细胞伸长与转录因子的调节表达，在8种双子叶植物中避荫反应的保守性。木髓伸长模式、转录调提供了关于保守区域的细致理解，我们的旅程以植物科间不同转录因子表达方式结束，为未来的研究铺平了道路。

在最后一章中，我们对RNA测序分析、激素分析和进化考虑方面的限制进行了广泛的观点阐述。在远红光下特定于木髓部表达的普遍保守模式和不同物种中转录因子保守性的发现为更深入的研究开辟了途径。虽然我们提出的联系模型还待进一步确认，但这一持续的探索有望揭示植物对光反应的分子细节，丰富我们对适应策略的理解。

ABOUT THE AUTHOR

Linge Li, originating from the Yitong Manchu Autonomous County in Jilin Province grew up in the coastal city of Dalian, Liaoning Province. She is the daughter of a food chemistry professor and a governor. Her interest in biology was kindled early on when collecting shells on the beaches of her hometown. This budding passion was nurtured and amplified in high school, thanks to the inspiring influence of her teacher, Ms. Yanhua Gao, who encouraged her to delve deeper into the world of biology.

Linge's academic journey took a significant turn during her Bachelor's studies at Northeastern Forestry University. Here, she embarked on an internship that involved identifying plant species in the vast expanses of the Maoer Mountain campus, the largest in Asia. This experience brought her into a close relationship with the wild plants, transforming them from mere study subjects into friends and companions in her quest for knowledge.

Her passion for plant biology led her to pursue a Master's degree at Leiden University, fully funded by a CSC scholarship and this period marked a significant transition in her life, as she was introduced to Dr. Kaisa Kajala by Professor Dr. Ren Voesenek. Seizing this opportunity, Linge began her PhD study, delving into the intriguing world of tomato plants and their shade avoidance behavior, under the guidance of both Kaisa and Professor Dr. Ronald Pierik.

Linge's journey was not just confined to the lab; she also played an active role in the Utrecht University council for two years, contributing her insights and experiences to the broader academic community. Her PhD journey was marked by unique challenges, including navigating through the maternity leaves of Dr. Kajala, a lab breakdown, and the global impact of COVID-19. Despite these hurdles, she persevered and completed her PhD in November 2023.

ACKNOWLEDGEMENTS

In a quaint coastal city Dalian, China, where I was born, the call of nature was a part of my childhood. Surrounded by the magnificence of the sea and the mountains, my passion for biology took root. This passion led me on an academic journey, starting at a university nestled amongst welcoming trees, where the foundations of my future were laid.

First and foremost, I must express my profound gratitude to **Prof. Dr. Ronald Pierik** and **Dr. Kaisa Kajala**. I was fortunate to have avoided difficulties, thanks to the introduction by Prof. Dr. Rens Voesenek. Their guidance and support have been cornerstones of my journey. Their help extended far beyond the scientific realm, offering wisdom and insights that have profoundly shaped both my professional and personal life. Their mentorship, especially Kaisa's, is something I will never forget, and the lessons learned under their tutelage are invaluable. Despite the challenges – the birth of Kaisa's children, the shadow of Covid, the breakdown of the phytotron, and numerous group changes – the support and camaraderie here were unwavering.

I extend my deepest gratitude to **Yorrit**, **Chrysa**, **Sara**, **Muthanna**, **Tuğba**, **Emilie**, and **Ankie**. Your wisdom and support have been invaluable to me. The lessons I've learned from each of you have been integral to my journey. A special acknowledgment to Yorrit, whose assistance was crucial in bringing this book to fruition.

Reflecting on my past, my thoughts often wander back to my high school days. While I don't miss every aspect of that time, I am immensely grateful for the resilience and determination I found in myself. It's a period of my life that shaped me in more ways than one. Special thanks go to my high school friends – **Xiyuan**, **Ze**, and **Zhoudong**. Their presence at my defense ceremony was a poignant reminder of our 15 years of friendship. Though our paths have diverged, their support, both in person and online, has been a source of comfort and joy.

The Netherlands, with its inspiring landscapes and academic excellence, was my next destination. Here, in the hallowed halls of Leiden, I pursued my dreams, fueled by the wisdom and guidance of my mentors, **Dr. Frederic Lens** and **Prof. Dr. Remko Offinga**. In my master's study, I had friends like **Jerry**, **Chao**, and **Huihen** who understood me, and together, we formed a close-knit team. Additionally, I was fortunate to have exceptional mentors in the lab, namely **Yao**, **Ivo**, and **Xiaoyu**, who generously guided and supported me as I completed my degree there.

Destiny then guided me to Utrecht, a place that soon felt like a second home. Kaisa's team, which initially comprised just **Mariana** and me, was a small but ambitious endeavor. We spent countless hours building up our research, it was a time of learning and adaptation, especially as we encountered unexpected challenges like not knowing the presence of chemical manure while we navigated the nutrient solution of Arabidopsis to the greenhouse for tomatoes.

These early days with Kaisa's team were foundational. The experience taught us resilience and adaptability, qualities that were vital in our scientific journey. The larger group at Utrecht, including Sara, Chrysa, Sjon, Kasper, Sarah, Diederik, Hans, and Zeguang, provided a supportive and collaborative environment, fostering both professional growth and personal connections.

As I embarked on my PhD, the environment at Z304 became my sanctuary. This was where I, alongside **Sjon**, **Chrysa**, **Angelica**, **Gabriel**, **Muthanna**, and **Dani**, delved deeper into the mysteries of great food and unzipped the escape room, bonding over culinary delights and the shared thrill of solving puzzles together. With many of you, we developed a valuable relationship I will cherish for ever.

The Shady Group and Kaisa Weits Group have been instrumental in shaping my academic path, serving as dynamic centers of innovation and fellowship. In these groups, I have been blessed with the opportunity to forge deep connections with many friends, engaging in meaningful dialogues and inspiring a multitude of ideas. The vibrancy of these groups is largely due to the contributions of remarkable individuals such as Lisa, Nicole, Sanne, Kyra, Pierre, Kasper, Sarah, Martina, Sara, Valerie, Andres and Shahram in the **Shady Team,** and Leo, Rianne, Sara, Chrysa, Mariana, Yaron, Lucila in **Kaisa's Team**, not to forget Viktoriia, Gaberiel, and Liao in the **Weits Group**.

A heartfelt thanks is especially owed to **Nicole, Lisa** and **Diederik**. Your assistance with the Dutch language aspects of the PhD graduation system has been vital. Without your guidance and help, navigating this process would have been a daunting challenge.

My academic endeavors were not confined to laboratories and lecture halls. The entire campus was a canvas for learning and friendship. From the Botanic Garden to the David de Wied Building, from UMC to the Bestuurgebouw, every corner of Utrecht resonated with the spirit of friendship and scholarship. My experience with **Romy** and **Bridget** in the University Council was exceptionally enriching. It taught me not only about academia but also about the broader aspects of life. Together, we endeavored to assist our colleagues and effect change. While working with many great colleagues, we saw some of our efforts come to fruition and

others not, but from each experience, I learned invaluable lessons. I have no regrets about the efforts we made, and I am deeply grateful for everything our team taught me.

Over the past two years, my involvement with **Network (No ing): PROUT (Utrecht PhD Network)** has been a source of enrichment, balancing the rigors of PhD life with meaningful support and camaraderie. This group's dedication to easing the lives of fellow PhD students extended beyond academics, incorporating fun activities, shared meals, and outings. Moments spent with Ellen, Jelmer, Deborah, Daphne, Melissa, and Rianne, were filled with great memories. These experiences, fostering a sense of community and well-being, were integral to my journey, working together to achieve a common goal and sharing our successes and challenges was an incredibly fulfilling experience.

The Institute of Environmental Biology (IEB) was a melting pot of brilliant minds from various fields – Ecology, Plant-Microbe Interactions, and Microbiology. Here, I had the fortune of meeting incredible friends like **Violeta**, **Peter**, **Zhilei**, and **Jie** from Ecology, and **Hao**, **Run**, **Dharani,** and **Giannis** from PMI. Their genuine support and camaraderie were invaluable. Each one of them, with their unique perspectives and insights, contributed significantly to my journey. Their willingness to help, share knowledge, and engage in thought-provoking discussions played a pivotal role in my academic and personal growth.

I also want to extend my heartfelt thanks to my dear friends **JZ** and **Xuanxuan**, who are here today as my paranymphs. I began my PhD journey with JZ, and we finished it together. JZ knows me better than anyone else and has been a genuine friend. My friendship with Xuanxuan spans more than 11 years since university, I feel lucky to have you here and in the past. Having both of you here, in this defining moment, means the world to me.

Last but not least, my deepest gratitude goes to my husband **Song Guo**, and my parents, **Prof. Dr. Wei Li** and **Mrs. Xiaofeng Ma**. Their unwavering support and love have been the bedrock of my journey. Growing up in such a warm and nurturing family has been a blessing. To all my family members, your encouragement and belief in me have been my greatest strength. Your love and support have been the guiding lights of my life, and I am eternally grateful for having you all in my life.

As I stand at the threshold of a new chapter, ready to embark on another adventure, I carry with me the lessons, the memories, and the relationships that have shaped me in this incredible academic odyssey.

Writing this acknowledgment has been a challenge, as I am keenly aware of the many names and contributions I must remember. If by any chance I have overlooked someone, please accept my sincerest apologies.

Education Statement of the Graduate School Experimental Plant Sciences

Issued to: **Linge Li**
Date: **27 March 2024**
Group: **Experimental Computional Plant Development**
University: **Utrecht University**

1) Start-Up Phase	*date*	*cp*
► **First presentation of your project**		
Fighting shade: tomato stem emongation in SAS	Oct 12 2018	1.5
► **Writing or rewriting a project proposal**		
► **MSc courses**		
Subtotal Start-Up Phase		1.5

2) Scientific Exposure	*date*	*cp*
► **EPS PhD days**		
EPS Get2Gether 2021, Online	Febr 1, 2 2021	0.4
EPS Get2Gether 2022, Soest (NL)	May 3, 4 2022	0.6
► **EPS theme symposia**		
EPS theme 1 symposium 'Developmental Biology of Plants', Wageningen (NL)	Feb 5 2020	0.3
EPS theme 3 symposium 'Metabolism and Adaptation', Online	Oct 30 2020	0.2
EPS theme 3 symposium 'Metabolism and Adaptation', Nijmegen (NL)	Nov 1 2022	0.3
EPS theme 1 symposium 'Developmental Biology of Plants', Wageningen (NL)	Oct 3 2023	0.3
► **National platform meetings**		
Annual Meeting Experimental Plant Sciences, Lunteren (NL)	Apr 8, 9 2019	0.6
Annual Meeting Experimental Plant Sciences, Online	Apr 12,13 2021	0.5
Annual Meeting Experimental Plant Sciences, Lunteren (NL)	Apr 11,12 2022	0.6
Annual Meeting Experimental Plant Sciences, Lunteren (NL)	Apr 17,18 2023	0.6
► **Seminars (series), workshops and symposia**		
IEB Seminar: Fluxes of carbon through photorespiration.	Jul 8 2020	0.1
IEB Seminar: Does conservation work and how do we know?	Oct 21 2021	0.1
IEB Seminar: Chlorophyll and carotenoid pigments as indicators of long-term dynamics in aquatic ecosystems	Nov 25 2021	0.1
IEB Seminar: Desert microbes for boosting sustainable agriculture in extreme environments.	Mar 24 2022	0.1
IEB Seminar: Reaching out for the sun - Molecular mechanism underlying growth adaptation in Arabidopsis thaliana	Mar 28 2022	0.1
IEB Seminar: Molecular responses of Arabidopsis to insect eggs	Jun 28 2022	0.1
IEB/ UU Plants Seminar: The function of plant specialized metabolites in the assemblage of plant root microbiota	Jul 25 2022	0.1
IEB Seminar: Be my guest - How legumes host endosymbiotic rhizobia	Jul 26 2022	0.1
IEB/ UU Plants Seminar: "TENURE TRACK SELECTION"	Sep 12 2022	0.1

	IEB Seminar: How can plants stay in this world while their pathogens can evolve much faster than plants?	Sep 27 2022	0.1
	IEB/ UU Plants Seminar: Bioinformatics approaches to approach tandem gene breeding in solanaceae crops	Jun 23 2023	0.1
	IEB/ UU Plants Seminar: Regulation of vascular development by light and more	Jun 29 2023	0.1
	IEB/ UU Plants Seminar: Learning the grammar of crop regulatory dna for precise engineering of gene expression	Jul 11 2023	0.1
	IEB/ UU Plants Seminar: Surface receptor signaling in plant immunity	Jul 29 2022	0.1
	IEB Seminar - On the occasion of the PhD defense of Violeta Angulo Fernandez	Sep 20 2023	0.1
►	**Seminar plus**		
►	**International symposia and congresses**		
	Plant Biology Europe Virtual Conference (PBE), Online	Jun 29-Jul 1 2021	0.9
	CSHL - International Symposium on Plant Photobiology (ISPP), Online	Jul 22-25 2021	1.2
	The 21st International Conference on Systems Biology (ICSB), Berlin (DE)	Oct 8-12 2022	1.2
►	**Presentations**		
	Poster presentation - Cell type view into tomato shade avoidance response, ICSB	Oct 8-12 2022	1.0
	Presentation - Shed a light on SAR: Cell type view into tomato stem shade avoidance response, EPS theme 3	Nov 1 2022	1.0
	Presentation - Unraveling the hormonal tango: How tomato stems dance to avoid shade, EPS theme 1	Oct 3 2023	1.0
	Presentation - Shed a light on SAR: Cell type view into tomato stem shade avoidance response, Annual Meeting EPS	Apr 18 2023	1.0
►	**Interviews**		
	Annual meetings with mentor first year	May 21 2019	0.1
	Annual meeting with mentor second year	Jun 10 2020	0.1
	Annual meetings with mentor third year	Jul 5 2021	0.1
	Annual meeting with mentor fourth year	May 11 2022	0.1
►	**Excursions**		
	BASF-Nunhems company visit by EPS PhD council	Nov 23 2023	0.3
	Subtotal Scientific Exposure		13.9

3) In-Depth Studies		*date*	*cp*
►	**Advanced scientific courses & workshops**		
	Transcription factors and transcriptional regulation, Wageningen (NL)	Dec 10-12 2018	1.0
	Microscopy and spectroscopy in food and plant science, Wageningen (NL)	May 7-9 2019	0.9
	Gentle hands-on introduction to Python programming, Online	Jul 2, 3 2020	0.6
►	**Journal club**		
	Weekly journal club (Shady Group of Plant Environmental Signalling)	2020-2023	1.0
►	**Individual research training**		
	Subtotal In-Depth Studies		3.5

4) Personal Development	date	cp
► **General skill training courses**		
Mindfulness and stress reduction, Utrecht (NL)	May 2019	3.0
Integrity in the workplace: how to do good research?, Utrecht (NL)	Feb 2020	0.2
Illustrator, Utrecht (NL)	Mar 2020	0.6
Digital Pictures: Data Integrity and Display, Utrecht (NL)	May 7-8 2020	1.0
The Art of Presenting Science, Online	Jun 23-26 2020	1.0
Supervising Research of MSc students at the Graduate School of Life Sciences, Utrecht (NL)/Online	Sep 2- Dec 2 2020	1.2
How to make a movie about your research, Online	Mar 2, 30 2021	0.6
Introduction to Python for Life Sciences (6 days), Utrecht (NL)	May 2023	3.0
► **Organisation of scientific meetings, PhD courses or outreach activities**		
► **Membership of EPS PhD Council**		
Subtotal Personal Development		10.6

5) Teaching & Supervision Duties	date	cp
► **Courses**		
► **Supervision of BSc/MSc projects**		3.0
BSc project"Growing thick:The relation of hormonal regulation to abiotic stress-induced cambial responses"	May-Jul 2021	
BSc project "Investigation of the effect of Gibberellin 3 on Arabidopsis thaliana inflorescence response"	Oct-Nov 2021	
BSc project "Effect of the shade avoidance response on pith diameter in multiple dicot families"	Feb-Jul 2022	
BSc project"Investigation of auxin function in tomato stem elongation of shade avoidance response"	Apr-May 2022	
BSc project"Understanding the Hormonal Dynamics and Regulatory Mechanisms in Shade Avoidance Responses of Dicot Species"	May-Jul 2023	
Msc mini project "Understanding hormonal trigger cell elongation in tomato shade avoidance syndrome"	Jul 2023	
Msc mini project "Understanding brassinosteroid function in tomato shade avoidance syndrome"	Jul 2023	
Subtotal Teaching & Supervision Duties		3.0

TOTAL NUMBER OF CREDIT POINTS*	32.5

Herewith the Graduate School declares that the PhD candidate has complied with the educational requirements set by the Educational Committee of EPS with a minimum total of 30 ECTS credits.

** A credit represents a normative study load of 28 hours of study.*

LIST OF PUBLICATIONS

Li, L., Wonder, J., Helming, T., Van Asselt, G., Pantazopoulou, K., Van de Kaa, Y., Kohlen, W., Pierik, R., & Kajala, K. (submitting). Brassinosteroid and gibberellin signaling are required for tomato internode elongation in response to low red: far-red light. Journal of Experimental Botanys.

Courbier, S., Snoek, B. L., Kajala, K., Li, L., Van Wees, S. C. M. M., & Pierik, R. (2021). Mechanisms of far-red light-mediated dampening of defense against Botrytis cinerea in tomato leaves. Plant Physiology, 187(3), 1250–1266. https://doi.org/10.1093/plphys/kiab354

A